SPATIAL AND TEMPORAL VARIABILITY OF EXCHANGE BETWEEN STREAM WATERS AND THE HYPORHEIC ZONE USING LABORATORY FLUME EXPERIMENTS, FIELD TRACERS, AND TRANSIENT STORAGE MODELING

Kaylyn S. Gootman

A dissertation submitted to the faculty at the University of North Carolina at Chapel Hill in partial fulfillment of the requirements for the degree of Doctor of Philosophy in the Environment, Ecology and Energy Program.

Chapel Hill
2019

Approved by

Jaye E. Cable,

Ricardo González-Pinzón,

Jonathan M. Lees,

Michael F. Piehler,

Diego Riveros-Iregui

ABSTRACT

Kaylyn S. Gootman: Spatial and Temporal Variability of Exchange Between Stream Waters and the Hyporheic Zone Using Laboratory Flume Experiments, Field Tracers, and Transient Storage Modeling
(Under the direction of Jaye E. Cable)

Groundwater-surface water interactions play a major role in regulating global water quality because they integrate diverse fluxes of water and its constituents within and beyond drainage basin boundaries. The hyporheic zone is the top portion of the unconfined, near-stream aquifer beneath and adjacent to streambed environments and facilitates riverine groundwater-surface water interactions. This continual transfer of water, dissolved constituents, particulate matter, and energy throughout the streambed is termed hyporheic exchange. As such, hyporheic exchange has the potential to influence a suite of critical riverine functions.

While hydrologic research over the past century has improved our understanding of complex riverine processes at many spatial scales, ranging from individual plots and river reaches to entire catchments, there is still demand for improved predictions and understanding of hyporheic functions at larger spatial scales. Within the field of hyporheic zone research, there is a tendency to focus on smaller spatial scales because they are easier to characterize and relatively reduced in complexity. However, scaling up hyporheic exchange and its associated riverine processing is challenging because of increasing spatiotemporal complexity and heterogeneity associated with larger spatial scales. Thus, the field of hyporheic zone research is out of phase with hyporheic exchange prediction demands.

The goal of this dissertation is to improve our understanding of hyporheic exchange spatiotemporal variability, through three independent manuscripts, to better meet demand for riverine processing predictions. Chapter 2 details experimental work focusing on hyporheic exchange at the sediment water interface in a recirculating laboratory flume. Chapters 3 and 4 employ reactive tracers to study hyporheic exchange from different spatiotemporal perspectives, downwelling flowpaths in the same season and stream reaches across two seasons, throughout different portions of the Jemez River, New Mexico. The results of this research provide a foundation for further study and development of hyporheic exchange scaling relationships as they pertain to riverine materials processing and water quality controls.

To Ben, for his patience, support, and laughter when it matters most.

ACKNOWLEDGMENTS

This dissertation was supported by a number of individuals and institutions who deserve many thanks. First and foremost, I would like to thank my advisor, Dr. Jaye Cable, for her guidance, support, and mentorship over these past six years. Jaye took a chance on a young scientist who wanted to study the watersheds of the world and write about them with far too many words. I do not know where I would be today without her challenging me to think critically, learn the philosophy of "word economy," and discover my passions for smaller-scale hydrology and science education. I know I can always count on Jaye for dynamic conversations about science, teaching, and life outside of academia. Jaye's encouragement for me to explore things outside of my comfort zone have made me a better scientist, mentor, and person.

I am also grateful to my committee members for their support throughout the course of my Ph.D. education. Dr. Mike Piehler gave me my first big break as an undergraduate researcher and has always supported me throughout each stage of my scientific and professional career. Thank you to Dr. Ricardo González-Pinzón for hosting me at the University of New Mexico for my field research, in addition to teaching me about "smart tracers," tracer studies, modeling, and science communication. Most of this dissertation would not have been possible without your laboratory and research support in person and over the phone. Thank you to Dr. Jonathan Lees for always being willing to discuss data analysis and statistics, while instilling an appreciation of the many uses of R through your teaching. And thank you to Dr. Diego Riveros-Iregui for your

support and encouragement along the way, in addition to introducing me to with Ricardo when I was looking for a new way to study groundwater-surface water interactions.

Dr. Julia Knapp is not technically a member of my Ph.D. committee, but she has nonetheless provided indispensable guidance and support throughout my graduate studies. Julia has graciously shared her expertise in modeling with me, helped me adapt two of her transient storage models, made time in her busy schedule to troubleshoot MATLAB code, and has been a wonderful co-author to work with. I thank her for her guidance and careful attention to detail.

I would not be where I am today without the training and support from my many mentors throughout my scientific journey. Members of the Piehler lab, including Dr. Scott Ensign, Suzanne Thompson, Rebecca Schwartz, Dr. Ashely Smyth, and Dr. Teri O'Meara, helped shape me as a scientist and always encouraged my growth and curiosity. Thank you to my mentor from the US EPA, Dr. Jennifer Richmond-Bryant, for encouraging me to apply to graduate school. And to Christine Lippy, thank you for letting me practice communicating my science with your students every year and discover that the purpose of my research is "to help water."

I am grateful to the following individuals for providing field, laboratory, and data analysis assistance in North Carolina and New Mexico: Rachel Housego, Nuvan Rathnayaka, Dr. Pierre Passaggia, Nadia Cohen, Elsemarie DeVries, Alexis Racioppi, Betsy Summers, James Fluke, Vanessa Garayburu-Caruso, Fabian Carbajal, Kathryn Bebe, Justin Nichols, Dr. Harvey Siem, Alexander Smith, and Drew Hoag. To Charlotte Hopson and Savannah Swinea, thank you for allowing me to mentor you as we worked on answering scientific questions together. Each of you has taught me so much about the power of mentorship and taught me to be better scientist. I would also like to thank Dr. Laura Moore for the use laboratory equipment in the sediments lab. Thank you to Dr. Rich McLaughlin, Dr. Brian White, James Mahaney, and the members of the

Joint Fluids Laboratory at UNC for inviting me to your group meetings and allowing me to using the recirculating laboratory flume. Thank you to my fellow Coloradan and lab mate, Jill Arriola. I cannot imagine graduate school without our many dinner conversations. Not everyone is willing to road trip for over 24 hours with a friend from graduate school, their husband, and dog in a small sedan. I am so lucky to have you as a colleague and life-long friend.

Funding for this research was provided by a number for sources. Chapter 2 was supported by a GSA Grant-in-Aid (RG 1407-17), a UNC-Chapel Hill Graduate School Summer Research Fellowship, and a UNC-Chapel Hill Dissertation Completion Fellowship; and student support funding from the NSF (IUSE: GEOPATHS-IMPACT) for the UNC-Chapel Hill Increasing Diversity and Enhancing Academia Program. Chapters 3 and 4 were supported by NSF (HRD-1345169) to Dr. Ricardo González-Pinzón; CUASHI Pathfinder Fellowship and a GSA Grant-in-Aid (RG 1407-16); the University of North Carolina at Chapel Hill; the University of New Mexico; the Pueblo of Jemez Department of Natural Resources; and funding from the European Union's Seventh Framework Program (Grant Agreement 608881) through an ETH Zurich Postdoctoral Fellowship to Dr. Julia Knapp. Additionally, I would like to thank the Environment, Ecology and Energy Program for their support, financially and otherwise.

Lastly, I would like to thank my family and friends. Without their love and support over the years, this part of my scientific journey would not have been possible. My parents have always been supportive of my pursuit of scientific knowledge and encouraged my study of the environment. Ariana, you have always been my biggest cheerleader. Your strength and courage inspire me to be better every day. And to my husband, Ben, thank you for always being there to lift me up and showing me how to go forward during the times that I could not clearly see the end of this journey or the exciting start of the next adventure.

PREFACE

Parts of this work were done in collaboration with other talented scientists. Three of the chapters are in the process of being prepared for submission to different journal publications. Chapter 2 is being prepared for *Hydrological Processes* with Dr. Jaye Cable. Chapters 3 is being prepared for *Water Resources Research*. Chapter 4 will be submitted to *Water Resources Research* by May 30, 2019. Chapters 3 and 4 are being prepared with the same co-authors including, Dr. Ricardo González-Pinzón, Dr. Julia Knapp, Vanessa Garayburu-Caruso, and Dr. Jaye Cable.

TABLE OF CONTENTS

LIST OF TABLES xii

LIST OF FIGURES xiii

LIST OF ABBREVIATIONS AND SYMBOLS xvi

CHAPTER 1 - INTRODUCTION 1

The Hyporheic Zone: An Overview 1

Hyporheic Zone Research Challenges 8

Meeting Hyporheic Zone Research Challenges 11

Dissertation Goal and Structure 14

REFERENCES 16

CHAPTER 2. – CUMULATIVE IMPACTS OF RECURSVIE FINE PARTICLE LOADING ON STREAMBED HYPORHEIC EXCHANGE USING A RECIRCULATING LABORATORY FLUME. 25

Introduction 25

Methods 28

Results 40

Discussion 49

Conclusions 57

Acknowledgements 58

REFERENCES 59

CHAPTER 3. – HYPORHEIC ZONE PROCESSING CONTROLS VARY WITH DEPTH AND STREAM ORDER THROUGHOUT A 4TH ORDER FLUVIAL NETWORK. 69

Introduction 69

Methods 73

Results and Discussion 87

Conclusions 104

Acknowledgements 107

REFERENCES 108

CHAPTER 4. – SPATIOTEMPORAL VARAIBLITY IN TRANSPORT AND REACTIVE PROCESSES ACROSS A 1^{ST}-5^{TH} ORDER FLUVIAL NETWORK. 117

Introduction 117

Methods 125

Results and Discussion 134

Conclusions 151

Acknowledgements 153

REFERENCES 154

CHAPTER 5. - CONCLUSION. 163

Overall Conclusions 163

Future Research Directions 164

Final Thoughts 167

REFERENCES 168

APPENDIX A: CHAPTER 3 SUPPLEMENTAL INFORMATION. 172

APPENDIX B: CHAPTER 4 SUPPLEMENTAL INFORMATION 195

LIST OF TABLES

Table 2.1. Experimental Parameters (mean ± 1σ) for Flume Experiments 29

Table 2.2. Experiment Model Fits 44

Table 2.3. Sediment core analysis data 48

Table 3.1. Site and Injection Characteristics 76

Table 3.2. USGS MINIPOINT Sampler locations and depths 79

Table 3.3. Sediment sample results 88

Table 3.4. Benthic biolayer contributions to hyporheic zone depth 99

Table 4.1. Study site characteristics 127

Table 4.2. Tracer masses, travel times, and recoveries 129

Table 4.3. Model parameter variability 143

Table 4.4. Hyporheic zone metrics 147

Appendix 3.1: Table of model parameters 172

Appendix 3.18: Table of hyporheic zone metrics 194

Appendix 4.22: Model parameters 219

Appendix 4.23: Study comparison metrics 221

LIST OF FIGURES

Figure 1.1. Hyporheic zone schematic 3

Figure 1.2. Hyporheic zone conceptual diagrams 5

Figure 1.3. Hyporheic zone scale dependency 10

Figure 2.1. Flume conceptual diagram 31

Figure 2.2. Flume experiment photos 34

Figure 2.3. Values of average vertical water flux 42

Figure 2.4. Water column total suspended sediment concentrations 45

Figure 3.1. Site map, sampling set up, model conceptualization, and field photo 77

Figure 3.2. Sampling depth versus model parameters 93

Figure 3.3. Sampling stations metrics 103

Figure 4.1. Stream orders of hydrologic studies published in the last 30 years 120

Figure 4.2. Map of field sites, study set up, model conceptualization, and field photo 124

Figure 4.3. Model parameter outputs 138

Figure 4.4. Breakthrough curves for the 2015 and 2016 4th order stream reach 140

Figure 4.5. Damköhler scaling of bulk hyporheic zone activity 149

Appendix 3.2: Breakthrough curves for the 2nd order stream 175

Appendix 3.3: Breakthrough curves for the 3rd order stream 177

Appendix 3.4: Breakthrough curves for the 4th order stream 179

Appendix 3.5: Simulated breakthrough curve zeroth temporal moments 180

Appendix 3.6: Simulated breakthrough curve fraction of tracer recovery 181

Appendix 3.7: Density plots for the 2nd order stream Site A depth 1 182

Appendix 3.8: Density plots for the 2nd order stream Site A depth 2 183

Appendix 3.9: Density plots for the 2nd order stream Site B depth 1 184

Appendix 3.10: Density plots for the 2nd order stream Site B depth 2 185

Appendix 3.11: Density plots for the 3rd order stream Site A depth 1 186
Appendix 3.12: Density plots for the 3rd order stream Site A depth 2 187
Appendix 3.13: Density plots for the 3rd order stream Site B depth 1 188
Appendix 3.14: Density plots for the 3rd order stream Site B depth 2 189
Appendix 3.15: Density plots for the 3rd order stream Site B depth 3 190
Appendix 3.16: Density plots for the 4th order stream Site A depth 1 191
Appendix 3.17: Density plots for the 4th order stream Site A depth 2 192
Appendix 3.18: Density plots for the 4th order stream Site B depth 1 193
Appendix 4.3: Measured and simulated results for the 1st order stream 200
Appendix 4.4: Measured and simulated results for the 2nd order stream 201
Appendix 4.5: Measured and simulated results for the 3rd order stream 202
Appendix 4.6: Measured and simulated results for the 5th order stream 203
Appendix 4.7: Density plots for the 2015 1st order stream 204
Appendix 4.8: Density plots for the 2015 2nd order stream 205
Appendix 4.9: Density plots for the 2015 3rd order stream 206
Appendix 4.10: Density plots for the 2015 4th order stream 207
Appendix 4.11: Density plots for the 2015 5th order stream 208
Appendix 4.12: Density plots for the 2016 2nd order stream 209
Appendix 4.13: Density plots for the 2016 3rd order stream 210
Appendix 4.14: Density plots for the 2016 4th order stream 211
Appendix 4.15: 2015 3rd order stream sensitivity analysis for velocity 212
Appendix 4.16: 2015 3rd order stream sensitivity analysis for dispersion 213
Appendix 4.17: 2015 3rd order stream sensitivity analysis for the mass transfer rate 214
Appendix 4.18: 2015 3rd order stream sensitivity analysis for the size of the storage zone 215
Appendix 4.19: 2015 3rd order stream sensitivity analysis for the Raz retardation factor 216

Appendix 4.20: 2015 3rd order stream sensitivity analysis for the Raz transformation 217

Appendix 4.21: 2015 3rd order stream sensitivity analysis for groundwater dilution 218

LIST OF ABBREVIATIONS AND SYMBOLS

A – Sample Cross-Sectional Area (cm^2) (Chapter 2)

A – Stream Cross-Sectional Area (m^2) (Chapter 4)

A_{meas} – Measured Cross Sectional Stream Area (cm^2) (Chapter 4)

A_s – Storage Zone Cross-Sectional Area (m^2) (Chapter 4)

A_s/A – Ratio of the Cross-Sectional Area of the Storage Zone to the Area of the Stream $(-)$

ADV – Acoustic Doppler Velocimeter

Br^- – Bromide

BTC – Breakthrough Curve

c_i – Compound Concentration in the Main Channel $(mol\ m^{-3})$ or $(mol\ L^{-1})$

$C_{i,hz}$ – Hyporheic Zone Tracer Concentration $(mol\ m^{-3})$ or $(mol\ L^{-1})$

$c_{in,i}$ – Groundwater Inflow $(m\ s^{-1})$ (Chapter 4)

$\overline{C}(0)$ – Concentration of the Flume Water at Baseline Conditions (mg/L)

$\overline{C}(t_{core})$ – Concentration of the Flume Surface water at Sediment Core Collection (mg/L)

$c_{i,GW}$ – Concentration of Compound i in the Groundwater $(mol\ m^{-3})$

Da – Reach Scale Damköhler Number $(-)$

DREAM (ZS) – *Differential Evolution Adaptive Metropolis* algorithm (Vrugt et al., 2009)

D – Dispersion Coefficient $(m^2\ s^{-1})$

D_z – Dispersion with Depth $(m^2\ s^{-1})$

d_{50} – Mean Grain Size (μm)

d_{hz} – Apparent Hyporheic Zone Depth (cm) (Chapter 4)

$\tilde{d}_{hz}$ – Average Hyporehic Zone Depth of Bromide (cm) (Chapter 3)

$\tilde{d}_{reac}$ – Average Hyporehic Zone Depth of Resazurin (cm) (Chapter 3)

GPS – Global Positioning System

K – Hydraulic Conductivity (cm/s)

k – First Order Mass-Transfer Rate Coefficient (s^{-1})

h – Hydraulic Head (cm)

i – Compound where $i = 0 = Br^{-}; i = 1 = Raz; i = 2 = Rru$

λ_1 – Total Resazurin Transformation Rate Coefficient (s^{-1})

$\lambda_{1\,max}$ – Maximum Total Resazurin Transformation Rate Coefficient (s^{-1})

λ_{12} – Total Resazurin to Resorufin Transformation Rate Coefficient (s^{-1})

λ_2 – Total Resorufin Transformation Rate Coefficient (s^{-1})

L – Sample Length (cm) (Chapter 2)

LOD – Limit of Detection $(-)$

LOQ – Limit of Quantification $(-)$

$\mu_{0,i}$ – Zeorth Temporal Moment of compound i $(mol.s.m^{-3})$ (Chapter 3)

$\mu_0(x_A)$ – Zeorth Temporal Moment of compound i at Site A $(mol.s.m^{-3})$ (Chapter 4)

$\mu_0(x_B)$ – Zeorth Temporal Moment of compound i at Site B $(mol.s.m^{-3})$ (Chapter 4)

M – Total Core Mass, Where Subscripts "pre" and "post" Denote Core Collection Time (g)

M_i – Injected Tracer Mass for tracer i (mol)

MCMC – Markov Chain Monte Carlo algorithm

m – Core Particle Mass (g)

$m_1(x_A)$ – Normalized 1st Temporal Moment of Bromide at Site A (h)

$m_1(x_B)$ – Normalized 1st Temporal Moment of Bromide at Site B (h)

m_c – Mass Deposited Per Core (g)

m_{loss} – Total Mass Loss from the Water column to the Streambed (%)

n – Porosity $(-)$ (Chapter 2)

NaBr – Sodium Bromide

$nRSS_i$ – Normalized Residual Sum of Squares for compound i $(-)$

Q – Discharge $(m^3\ s)$

Q_{HEF} – Hyporheic Exchange Flow from Wondzell (2011) $(m^3\ s)$

q_{he} – Hyporehic Exchange Rate (s^{-1}) (Chapter 3)

q_{he} – Reach-Scale Hyporehic Exchange Rate Coefficient (s^{-1}) (Chapter 4)

q_{in} – Rate Coefficient Accounting for Groundwater Mixing (s^{-1})

ρ – Average *Ex Situ* Dry Bulk Density $(g\ cm^3)$

R_1 – Equlibrium Sorption Coefficient of Resazurin in the Hyporheic Zone $(-)$

R_2 – Equlibrium Sorption Coefficient of Resorufin in the Hyporheic Zone $(-)$

R_i – Equlibrium Sorption Coefficient of Tracer *i* in the Hyporheic Zone $(-)$

$\hat{R}$ – Gelman and Rubin (1992) Statistic to Assess Sampled Chain Convergence $(-)$

Raz – Resazurin

Rru – Resorufin

$r_{hz,i}$ – Reaction Rate of compound *i* in the Hyporheic Zone $(mol\ m^3\ s^{-1})$

r_i – Tracer Mass Recovery $(-)$ (Chapter 4)

σ – Standard Deviation

θ – Porosity $(-)$ (Chapters 3 and 4)

TSS – Total Suspended Solids (mg/L)

τ – Mean Reach Travel Time (h) (Chapter 4)

$\tau(z)$ – Hyporheic Zone Residence Time (s) (Chapter 3)

τ_{hz} – Mean Hyporheic Zone Residence Time (s) (Chapter 4)

$\tilde{\tau}_{hz}$ – Mean Hyporheic Zone Residence Time of Downwelling Stream Water (s) (Chapter 3)

$\tilde{\tau}_{reac}$ – Mean Hyporheic Zone Residence Time of the Reactive Tracer (s) (Chapter 3)

V – Volume discharging over time (cm^3) (Chapter 2)

v_{0*} – Celerity of Bromide in the Subsurface Depth Compartments $(m\ s^{-1})$

v_{1*} – Celerity of Reazurin in the Subsurface Depth Compartments $(m\ s^{-1})$

V_c – Volume of the Sediment Core Earth Material, Including Both Voids and Solids (cm^3)

V_f – Volume of the Flume (L)

V_v – Volume of the Sediment core Void Space (cm^3)

v – In-Stream Advective Velocity $(m\ s^{-1})$

v_z – Apparent Vertical Transport Velocity with Depth $(m\ s^{-1})$

VFLUX – Vertical Fluid [Heat] Transport Solver

w_{hz} – Width of the Hyporheic Zone (m)

X_{rec}^{br} – Ingtegrated Conservative Tracer Recovery $(-)$

X_{rec}^{raz} – Ingtegrated Reactive Tracer Recovery $(-)$

z – Sampling Depth (m)

CHAPTER 1 - INTRODUCTION

The Hyporheic Zone: An Overview

Rivers and streams have traditionally been defined as the active channels in which water and its constituents are transported downstream (Woessner, 2000; Sophocleous, 2002; Wohl et al., 2015). However, surface water bodies are not isolated components of the hydrologic system; their interactions with underlying groundwater environments influence biogeochemistry and ecology across spatial scales ranging from the sediment-water interface to entire drainage basins (Stanford & Ward, 1993; Brunke & Gonser, 1997; Thorp et al., 2006; Reisinger et al., 2015). Groundwater-surface water interactions facilitate the exchange of water and its constituents across surface and subsurface riverine ecotones (Baron et al., 2002; Hancock et al., 2008; Gooseff, 2010; Ormerod et al., 2010). These exchanges occur over a wide range of spatiotemporal scales and benefit surrounding ecosystems by regulating water, nutrient, and energy exchange flows while improving water quality (Hancock, 2002; Gerecht et al., 2011; Nowinski et al., 2012). Thus, improved understanding of riverine groundwater-surface water interactions is needed for effective stream ecosystem management in the face of anthropogenic pressures and climatic uncertainties (Poole & Berman, 2000; Wagener et al., 2010; Oelkers et al., 2011).

One major pathway for streams to interact with underlying groundwater reservoirs is through the hyporheic zone, which is the area within the shallow streambed sediments and banks where water, nutrients, and energy are exchanged via vertical, lateral, and longitudinal flows

(Orghidan, 1959; Brunke & Gonser, 1997; Boulton & Hancock, 2006). Hyporheic pore spaces serve as the connecting ecotone between surface and groundwater environments and consequently reflect characteristics of both environments (Fig. 1.1). Streambed permeability, and the resulting hydraulic conductivity, governs multi-scale, dynamic hyporheic zone flow paths (Brunke, 1999; Boulton et al., 2010; Cardenas, 2015). Over time, shifts in water contributions and permeability alter hyporheic flow paths and the magnitude of water that is pumped through the streambed.

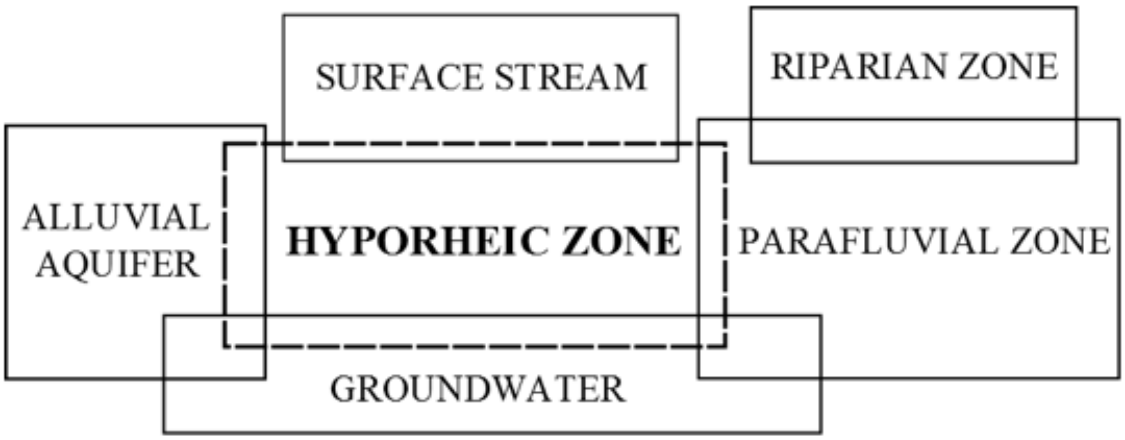

Figure 1.1. Hyporheic Zone Schematic. A simplified schematic of the hydrological compartments that can interact with the hyporheic zone (modified from Boulton et al., 1998).

The hyporheic zone can extend vertically from the streambed surface into the deeper sediments of the alluvial aquifer and laterally into the parafluvial zone (Gerecht et al., 2011; Boano et al., 2014; Cranswick & Cook, 2015). During hyporheic exchange, upwelling groundwater provides the benthic zone with nutrients while downwelling stream water brings dissolved oxygen and organic matter into the streambed (Boulton et al., 1998; Hunt et al., 2006). This multi-directional water exchange (> 0.01 $m^3/s/km$ to < 100 $m^3/s/km$) is regulated by streambed energy gradients and provides a vector for dissolved constituents (e.g. solutes, oxygen, nutrients, pollutants) to come into direct contact with entrained carbon sources, streambed microbial communities, and anoxic sediments (Fig. 1.2) (Boulton & Hancock, 2006; Hester & Gooseff, 2011; Harvey, 2016). As such, the hyporheic zone is a dynamic ecotone that has the potential to filter stream water during the transit downstream while serving as transient storage zone, reactor bed, temperature regulator, and refuge for both benthic and hyporheic organisms (Grimm & Fisher, 1984; Nogaro et al., 2010; Harvey et al., 2018).

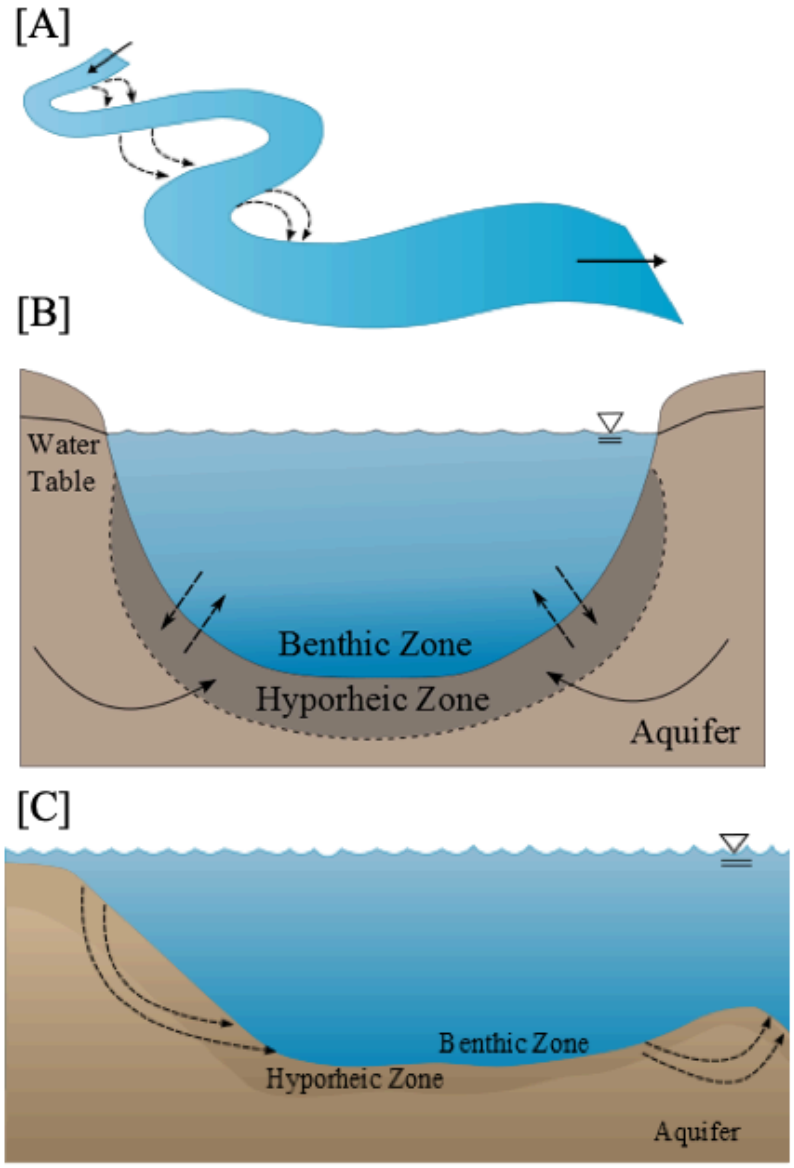

Figure 1.2. Hyporheic zone conceptual diagrams. Conceptual diagrams of the hyporheic zone in (a) plan view, (b) lateral cross-section, and (c) longitudinal cross-section views (modified from Gooseff, 2010). The dashed arrows indicate flow paths where hyporheic exchange can occur. The solid arrows in (a) and (b) indicate stream flow and groundwater flow direction.

Although the hyporheic zone is relatively small in size when compared to other riverine ecotones, it connects surrounding hydrologic reservoirs and is considered highly significant to riverine physical, biogeochemical, and ecological functioning (Stanford & Ward, 1993; Fischer et al., 2005; Krause et al., 2011). This significance has been documented at several spatial and temporal scales, ranging from sediment surfaces to entire catchments and minutes to days, using a variety of metrics including laboratory studies, direct field measurements, and modeling of streambed reactivity (Gooseff et al., 2005; Ensign & Doyle, 2006; Wondzell, 2006; Heathwaite, 2010; Harvey & Gooseff, 2015). Previous researchers have determined that hyporheic zone significance, at any spatiotemporal scale, is a function of its activity and connectivity between stream surface water and groundwater (Boulton et al., 1998; Bencala, 2000; Harvey et al., 2018).

Interest in the hyporheic zone and its impact on riverine ecosystem functions has steadily increased over the past four decades (Robertson & Wood, 2010; Cardenas, 2015; Ward, 2016). The growth of hyporheic zone research from its early description by Orghidan (1959) coincided with a paradigm shift from defining rivers and aquifers as distinct entities to interconnected hydrologic components (Bencala, 1993; Gooseff, 2010). The recognition of hyporheic exchange as a driver of ecosystem processes began with the study of baseflow streambed fauna and dissolved oxygen contributions to streams (Harvey & Gooseff, 2015). Modern hyporheic zone studies have expanded to include process- and function-based research within the context of the broader riverine ecosystem (Boulton et al., 2010; Marmonier et al., 2010).

Recent work has focused on the continued pursuit of hyporheic zone research as an evolving and interdisciplinary field. In a recent review, Boano et al. (2014), noted that the exploration of hyporheic zone properties and their functional significance has led to a greater appreciation of their consequences for water quality and stream ecology. Hyporheic zone studies

provide opportunities to employ methodologies that advance our understating of streambed functions and interactions with the stream ecosystem at a number of spatiotemporal scales (Sophocleous, 2002; Wondzell, 2011; Ward; 2016;). A diverse combination of laboratory, field, and modeling studies have provided new insight into individual and related processes that occur throughout hyporheic zones. Modern hyporheic zone research aims towards a unified approach where understanding hyporheic zone processes and how they scale throughout fluvial networks are paramount for the continual appreciation, appropriate management, and continued restoration of the entire riverine environment (O'Connor & Harvey, 2008; Stonedahl et al., 2010).

Advances in technology and the development of new methodologies, including *in situ* measures of streambed respiration and metabolism; tracer applications; and transient storage modeling, have paved the way for the development of hyporheic zone research as a viable and dynamic field of study. The application of techniques from multiple scientific disciplines has allowed researchers to make clearer connections between hyporheic exchange mechanics and ecosystem functions (White, 1993; Wondzell & Swanson, 1996; Wroblicky et al., 1998; ; Wainwright et al., 2011; Bhaskar et al., 2012). Subsequent studies have shifted hyporheic zone research towards its modern emergence as an interdisciplinary field that employs advanced tools and multiple perspectives to answer complex questions (Lawrence et al., 2013; Fox et al., 2014; Kaufman et al., 2017). Efforts to understand hyporheic zone dynamics and how they scale across entire watersheds have resulted from the development of multi-scale conceptual frameworks, interdisciplinary approaches, numerical modeling, and cross system comparisons (Harvey et al., 2013; Abbott et al., 2016; Pinay et al., 2015; Magliozzi et al., 2018).

Hyporheic Zone Research Challenges

As an inherently dynamic ecotone, the hyporheic zone spatial extent is highly variable over time and exhibits regional diversity (Ward & Tockner, 2001; Boulton et al., 2010; Ward et al., 2018). Diel and seasonal hydrologic patterns may exert additional variability on hyporheic contributions to overall riverine materials processing. Alterations in contributing groundwater and surface water volumes may change the streambed biogeochemistry and rates of hyporheic exchange, in addition to the hyporheic zone areal extent and functionality (Cranswick et al., 2014; Harvey et al., 2018). Additionally, natural and anthropogenic perturbations, such as large storm events and landscape development, can alter hyporheic exchange capacities over relatively short time scales (Karwan & Saiers, 2009; Hartwig & Borchardt, 2014; Jones et al., 2015). These irregular periods of disturbance and response add to the dynamic nature and functionality of hyporheic zone environments.

Spatial heterogeneity also presents additional research challenges when it comes to scaling up hyporheic exchange estimates from individual streams to entire catchments (McDonnell et al., 2007; Magliozzi et al., 2018). Heterogeneity, from a hydrologic perspective, varies at multiple spatial scales, ranging from within a single stream to across an entire catchment, and temporal scales, ranging from individual storm events to varying climatic inputs (Groffman et al., 2009; Bencala et al., 2011). Results from a single reach, with its own unique hydrogeomorphic characteristics, may not always be applicable throughout a single fluvial network or across various site locations. These challenges surrounding data transferability are exacerbated when modeling and experimental data are scaled up and contribute to interpretation uncertainties (O'Connor et al., 2010; Marmonier et al., 2012; González-Pinzón et al., 2013).

Furthermore, hyporheic zone baseline data coverage is incomplete at many spatial and temporal scales (Boulton et al., 1998; Sophocleous, 2002; Krause et al., 2011). Catchment managers need predictions based on comprehensive data from a range of temporal and spatial scales when making water quality management decisions. However, however high-resolution hyporheic zone data do not exist at all spatial scales (Fig. 1.3). For example, there is a known preference for studying hyporheic zones in smaller, low-order streams which may bias our understanding of hyporheic processing dynamics throughout fluvial networks (Doyle, 2005; Heathwaite, 2010; Xie et al., 2016). The shortage of comprehensive field data is reflected in studies that extrapolate smaller-scale measurements to larger reach and catchment scales (Xie & Zhang, 2010; Boano et al., 2014). Additionally, there are unclear conclusions regarding the relative proportion of hyporheic contributions to catchment-scale processing throughout the entire fluvial network. For example, recent work by Gomez-Velez et al. (2015) has shown from an extensive modeling study of the Mississippi River network that hyporheic contributions to overall riverine processing are excepted to decrease as stream order increases but these conclusions have rarely been tested in the field. As a result, the uncertainty in conclusions surrounding how hyporheic zone contributions scale may lead to a misrepresentation of hyporheic processing contributions across fluvial networks and how those contributions influence local and regional water quality outcomes.

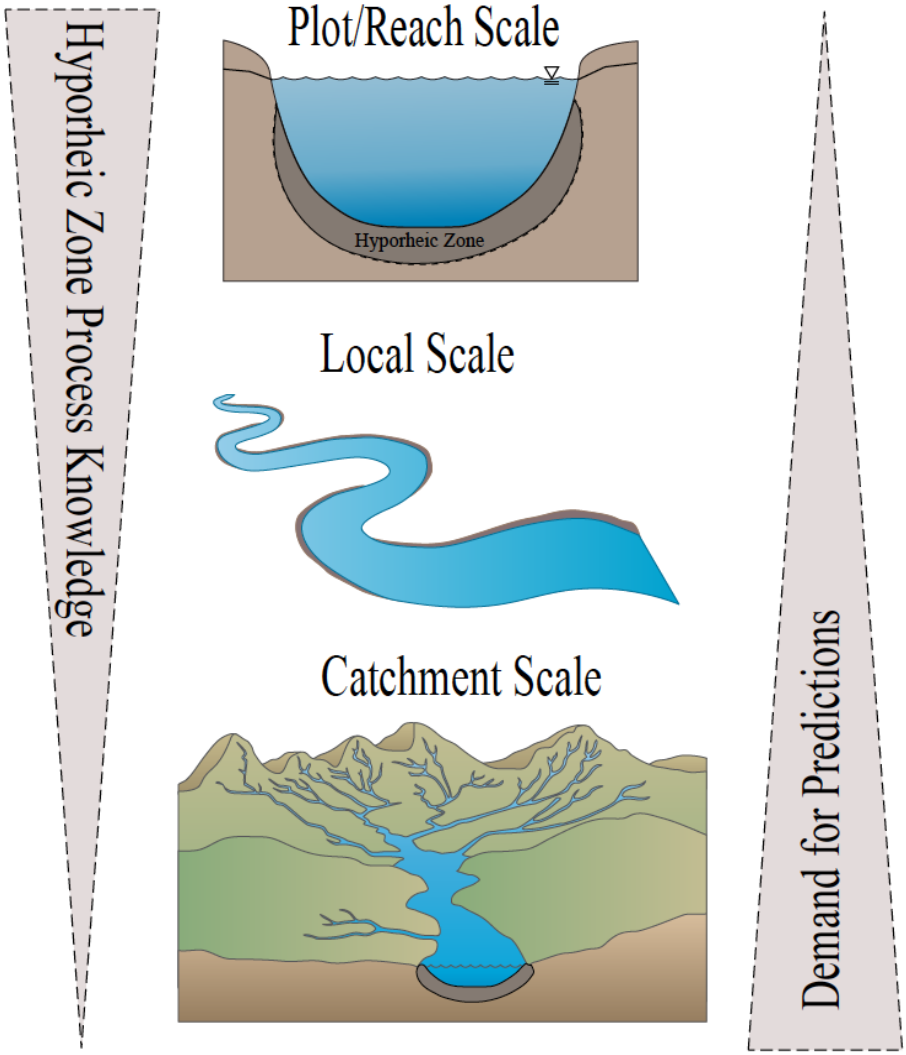

Figure 1.3. Hyporheic zone scale dependency. Scale dependency of hyporheic zone process knowledge and understanding in contrast to demand for predictions from decision makers and environmental regulators (Adapted from Krause et al., 2011). Delineated hyporheic zones are represented by the dark brown regions.

Another challenge for the field of hyporheic zone research is that scientists and decision makers tend to disagree about the relative importance of variables influencing hyporheic activity at spatial scales and temporal scales of interest (Fig. 1.3). This is further complicated by a lack of uniform hyporheic zone metrics and study techniques (Brunke & Gonser, 1997; Lawrence et al., 2013). The absence of a unified conceptual model may also add to hyporheic zone research challenges (Stream Solute Workshop, 1990; Descloux et al., 2010; Ward, 2016). Packman and Bencala (2000) and Krause et al. (2011) cite the perspective and background of the researcher as a major barrier to hyporheic zone interdisciplinary research approaches. Oftentimes, the observation scale and perspective of the researcher often drive result applicability (Hartwig & Borchardt, 2014; Datry et al., 2015).

Meeting Hyporheic Zone Research Challenges

While hydrologic research over the past century has improved our understanding of complex processes at multiple spatial scales, ranging from individual plots and stream reaches to entire catchments, there is still demand for improved predictions and understanding of varied water quality outcomes at larger spatial scales of interest (Krause et al., 2011). Within the field of hyporheic zone research, there is a tendency to focus on smaller spatial scales because they are easier to characterize and reduced in complexity counterparts (Ensign & Doyle, 2006; Dodds et al., 2008; Gooseff et al., 2013; Ward, 2016). However, scaling up hyporheic zone process knowledge from smaller to larger spatial scales is challenging because of the increasing spatiotemporal complexity and heterogeneity at these larger scales (Xie & Zhang, 2010; González-Pinzón et al., 2015). Thus, the current state of hyporheic zone scientific research is out of phase with prediction demands (Fig. 1.3)

Efforts to close knowledge gaps between conceptual and experimental studies are being made by modern hyporheic zone researchers. Boulton et al. (1998) recommended the development of a conceptual framework to improve hyporheic zone models and address future research challenges. The development of riverine ecosystem frameworks that emphasize the relative importance of the hyporheic zone will be useful from research, educational, management, and restoration perspectives (Pinay et al., 2015). Experimental methodologies will directly benefit from a comprehensive understanding of major processes that impact riverine hyporheic exchange and the role of streambed ecotones in the riverine ecosystem. In a recent review, Ward (2016) noted that many hyporheic researchers tend to focus on similar processes, thus further limiting our ability to characterize the interaction or independence of hyporheic processes. Well-organized frameworks that simplify intersystem comparisons can be used to illuminate cross-system generalities and provide predictions for environmental managers and regulators (Findlay, 1995; Hancock, 2002; Boulton, 2007; McDonnell et al., 2007).

Additional hyporheic zone data at multiple spatiotemporal scales are needed to calibrate conceptual models, test frameworks, and meet current research demands. Closing the knowledge gaps surrounding heterogeneity with comprehensive data sets, common metadata, and consistent methodologies, will help advance the field of hyporheic zone research (Findlay, 1995; Boulton et al., 2010; Ward, 2016). Further consolidation hyporheic zone metrics can lead to cross-site comparisons of results and uncertainties across various riverine ecosystems. González-Pinzón et al. (2015) recommended selecting techniques based on the research question perspective (i.e. physical, biological, or chemical processes) and identifying the spatial/temporal scales of study. New techniques and approaches, including “smart” tracers, distributed temperature sensing, electrical resistivity, and anesthetizing substances, may also provide additional insights to

quantifying spatial and temporal heterogeneity in hyporheic functions (Fleckenstein et al., 2010; Lautz et al., 2010; Briggs et al., 2013; Knapp et al., 2018).

Further experimental work is still needed to address these known hyporheic zone challenges and enable multi-scale assessment and prediction of hyporheic processes (Boano et al., 2014; Cardenas, 2015; Ward, 2016). Krause et al. (2011) argued that adapting current monitoring technology to detect spatially and temporally dynamic processes could lead to better hyporheic zone data resolution. Additionally, Marmonier et al. (2012) recognized the importance of scaling hyporheic zone processing up to larger scales but acknowledged that data coverage is still lacking. Confirmations of theoretical and modeling results are needed to advance hyporheic zone research at many spatial and temporal scales.

Interdisciplinary hyporheic zone research may provide a key role in strengthening interdisciplinary cooperation between hydrologists, biologists, ecologists, and biogeochemists (Boano et al., 2014; González-Pinzón et al., 2015). This type of collaborative work better equips researchers to address linkages between hyporheic zone hydrology, biogeochemistry, and ecology that are nested across temporal and spatial scales (Fleckenstein et al., 2010; Gomez-Velez et al., 2014; Covino, 2017). In a recent review, Krause et al. (2011) cited interdisciplinary approaches as a tool to advance our understanding of hyporheic zone processes and ecosystem functions while fostering greater dialogue between scientific disciplines. González-Pinzón et al. (2015) determined that collaborative hyporheic zone research efforts have the potential maximize our mechanistic understanding and reduce research costs associated with using multiple techniques. Additionally, the development of successful riverine management and restoration strategies can benefit from collaborative hyporheic research efforts (Sophocleous, 2002). As such, the benefits of future cross-disciplinary hyporheic zone research can generate a

better understanding of hyporheic dynamics and heterogeneity, strengthen the scientific community, reduce costs for individual researchers, and improve riverine management techniques.

Dissertation Goal and Structure

This dissertation seeks to quantify hyporheic zone spatial and temporal heterogeneity using field, laboratory, and modeling approaches. Chapter 1 is a literature review with the background and significance for this research. Chapter 2 experimentally shows how streambed filtration is influenced by fine particle disturbance events with the use of a recirculating laboratory flume. The additive effect of successive disturbance events was shown to amplify the model river system variability and suggests that streambed filtration and clogging are dynamic processes. Better understanding of streambed clogging dynamics improves disturbance-response predictions and can improve water resource management in natural systems. Chapter 3 answers how hyporheic contributions from the streambed to the stream vary with depth and stream order across the same fluvial network. I used a series of tracer injections and stream sampling experiments in the field to calibrate a model for streambed interactions with the hyporheic zone. I found that streambed reactivity potential does not always scale as expected with increasing stream order. Our model approach to quantify hyporheic exchange within and between stream reaches improves riverine processing scaling predictions. Chapter 4 details hyporheic zone processing changes with space and time. I used a transient storage model calibrated with data from field experiments to examine hyporheic exchange across a ranges of stream orders (1^{st}-5^{th}). I found that the fluvial network did not consistently follow scaling expectations from the literature and demonstrate that hyporheic zone behavior throughout the fluvial network remains

an elusive contribution. My findings improve network-scale predictions of streambed spatiotemporal variability and the impact on water quality and quantity. Chapters 3 and 4 are currently in preparation for submission as companion papers to *Water Rescources Research*. Finally, Chapter 5 provides an overall conclusion and future directions for addressing remaining hyporheic exchange spatiotemporal variability challenges.

REFERENCES

Abbott, B. W., Baranov, V., Mendoza-Lera, C., Nikolakopoulou, M., Harjung, A., Kolbe, T., et al. (2016). Using multi-tracer inference to move beyond single-catchment ecohydrology. *Earth-Science Reviews*, *160*, 19–42. https://doi.org/10.1016/j.earscirev.2016.06.014

Baron, J. S., LeRoy Poff, N., Angermeier, P. L., Dahm, C. N., Gleick, P. H., Hairston, N. G., et al. (2002). Meeting ecological and societal needs for freshwater. *Ecological Applications*, *12*(5), 1247–1260. https://doi.org/10.1890/1051-0761(2002)012[1247:MEASNF]2.0.CO;2

Bencala, K. E. (1993). A perspective on stream-catchment connections. *Journal of the North American Benthological Society*, *12*(1), 44–47.

Bencala, K. E. (2000). Hyporheic zone hydrological processes. *Hydrological Processes*, *14*, 2797–2798. https://doi.org/10.1002/1099-1085(20001030)14:15<2797::AID-HYP402>3.0.CO;2-6

Bencala, K. E., Gooseff, M. N., & Kimball, B. a. (2011). Rethinking hyporheic flow and transient storage to advance understanding of stream-catchment connections. *Water Resources Research*, *47*(3), n/a-n/a. https://doi.org/10.1029/2010WR010066

Bhaskar, A. S., Harvey, J. W., & Henry, E. J. (2012). Resolving hyporheic and groundwater components of streambed water flux using heat as a tracer. *Water Resources Research*, *48*(8), 1–16. https://doi.org/10.1029/2011WR011784

Boano, F., Harvey, J. W., Marion, A., Packman, A. I., Revelli, R., Ridolfi, L., & Wörman, A. (2014). Hyporheic flow and transport processes: Mechanisms, models, and biogeochemical implications. *Reviews of Geophysics*, *52*, 603–679. https://doi.org/10.1002/2012RG000417

Boulton, A. J. (2007). Hyporheic rehabilitation in rivers: Restoring vertical connectivity. *Freshwater Biology*, *52*(4), 632–650. https://doi.org/10.1111/j.1365-2427.2006.01710.x

Boulton, A. J., & Hancock, P. J. (2006). Rivers as groundwater-dependent ecosystems: a review of degrees of dependency, riverine processes and management implications. *Australian Journal of Botany*, *54*(2), 133. https://doi.org/10.1071/BT05074

Boulton, A. J., Findlay, S., Marmonier, P., Stanley, E. H., & Valett, H. M. (1998). The Functional Significance of the Hyporheic Zone in Streams and Rivers. *Annual Review of Ecology and Systematics*, *29*(1), 59–81. https://doi.org/10.1146/annurev.ecolsys.29.1.59

Boulton, A. J., Datry, T., Kasahara, T., Mutz, M., & Stanford, J. A. (2010). Ecology and management of the hyporheic zone: stream–groundwater interactions of running waters and their floodplains. *Journal of the North American Benthological Society*, *29*(1), 26–40. https://doi.org/10.1899/08-017.1

Briggs, M. a., Lautz, L. K., & Hare, D. K. (2013). Residence time control on hot moments of net

nitrate production and uptake in the hyporheic zone. *Hydrological Processes*, *3751*(June 2013), 3741–3751. https://doi.org/10.1002/hyp.9921

Brunke, M. (1999). Colmation and depth filtration within streambeds: Retention of particles in hypoheic interstices. *International Review of Hydrobiology*, *84*(2), 99–117. https://doi.org/10.1002/iroh.199900014

Brunke, M., & Gonser, T. (1997). The ecological significance of exchange processes between rivers and groundwater. *Freshwater Biology*, *37*, 1–33. https://doi.org/https://doi.org/10.1046/j.1365-2427.1997.00143.x

Cardenas, M. B. (2015). Hyporheic zone hydrologic science: A historical account of its emergence and a prospectus. *Water Resources Research*, *6*(4), 446. https://doi.org/10.1016/0022-1694(68)90080-2

Covino, T. (2017). Hydrologic connectivity as a framework for understanding biogeochemical flux through watersheds and along fluvial networks. *Geomorphology*, *277*, 133–144. https://doi.org/10.1016/j.geomorph.2016.09.030

Cranswick, R. H., & Cook, P. G. (2015). Scales and magnitude of hyporheic, river-aquifer and bank storage exchange fluxes. *Hydrological Processes*, *29*(14), 3084–3097. https://doi.org/10.1002/hyp.10421

Cranswick, R. H., Cook, P. G., & Lamontagne, S. (2014). Hyporheic zone exchange fluxes and residence times inferred from riverbed temperature and radon data. *Journal of Hydrology*, *519*(PB), 1870–1881. https://doi.org/10.1016/j.jhydrol.2014.09.059

Datry, T., Lamouroux, N., Thivin, G., Descloux, S., & Baudoin, J. M. (2015). Estimation of sediment hydraulic conductivity in river reaches and its potential use to evaluate streambed clogging. *River Research and Applications*, *31*, 880–891. https://doi.org/10.1002/rra

Descloux, S., Datry, T., Philippe, M., & Marmonier, P. (2010). Comparison of different techniques to assess surface and subsurface streambed colmation with fine sediments. *International Review of Hydrobiology*, *95*(6), 520–540. https://doi.org/10.1002/iroh.201011250

Dodds, W. K., Beaulieu, J. J., Eichmilier, J. J., Fischer, J. R., Franssen, N. R., Gudder, D. a., et al. (2008). Nitrogen cycling and metabolism in the thalweg of a prairie river. *Journal of Geophysical Research: Biogeosciences*, *113*(4), 1–11. https://doi.org/10.1029/2008JG000696

Doyle, M. W. (2005). Incorporating hydrologic variability into nutrient spiraling. *Journal of Geophysical Research*, *110*(G1), G01003. https://doi.org/10.1029/2005JG000015

Ensign, S. H., & Doyle, M. W. (2006). Nutrient spiraling in streams and river networks. *Journal of Geophysical Research*, *111*(G4). https://doi.org/10.1029/2005JG000114

Findlay, S. (1995). Importance of surface-subsurface exchange in stream ecosystems: The hyporheic zone. *Limnology and Oceanography*, *40*(1), 159–164. https://doi.org/10.4319/lo.1995.40.1.0159

Fischer, H., Kloep, F., Wilzcek, S., & Pusch, M. T. . (2005). A River's Liver : Microbial Processes within the Hyporheic Zone of a Large Lowland River. *Biogeochemistry*, *76*(2), 349–371. https://doi.org/10.1007/sl0533-005-6896-y

Fleckenstein, J. H., Krause, S., Hannah, D. M., & Boano, F. (2010). Groundwater-surface water interactions: New methods and models to improve understanding of processes and dynamics. *Advances in Water Resources*, *33*(11), 1291–1295. https://doi.org/http://dx.doi.org/10.1016/j.advwatres.2010.09.011

Fox, A., Boano, F., & Arnon, S. (2014). Impact of losing and gaining streamflow conditions on hyporheic exchange fluxes induced by dune-shaped bed forms. *Water Resources Research*, *50*, 1895–1907. https://doi.org/10.1002/2013WR014668.Received

Gerecht, K. E., Cardenas, M. B., Guswa, A. J., Sawyer, A. H., Nowinski, J. D., & Swanson, T. E. (2011). Dynamics of hyporheic flow and heat transport across a bed-to-bank continuum in a large regulated river. *Water Resources Research*, *47*(3), n/a-n/a. https://doi.org/10.1029/2010WR009794

Gomez-Velez, J. D., Krause, S., & Wilson, J. L. (2014). Effect of low-permeability layers on spatial patterns of hyporheic exchange and groundwater upwelling. *Water Resources Research*, *50*(6), 5196–5215. https://doi.org/10.1002/2013WR015054

Gomez-Velez, J. D., Harvey, J. W., Cardenas, M. B., & Kiel, B. (2015). Denitrification in the Mississippi River network controlled by flow through river bedforms. *Nature Geoscience*, *8*(October). https://doi.org/10.1038/ngeo2567

González-Pinzón, R., Haggerty, R., & Dentz, M. (2013). Scaling and predicting solute transport processes in streams. *Water Resources Research*, *49*(7), 4071–4088. https://doi.org/10.1002/wrcr.20280

González-Pinzón, R., Ward, A. S., Hatch, C. E., Wlostowski, A. N., Singha, K., Gooseff, M. N., et al. (2015). A field comparison of multiple techniques to quantify groundwater – surface-water interactions. *Freshwater Science*, *34*(August 2014), 139–160. https://doi.org/10.1086/679738.

González-Pinzón, R., Mortensen, J., & Van Horn, D. (2015). Comment on "solute-specific scaling of inorganic nitrogen and phosphorus uptake in streams" by Hall et al. (2013). *Biogeosciences*, *12*(18), 5365–5369. https://doi.org/10.5194/bg-12-5365-2015

Gooseff, M. N. (2010). Defining Hyporheic Zones - Advancing Our Conceptual and Operational Definitions of Where Stream Water and Groundwater Meet. *Geography Compass*, *4*(8), 945–955. https://doi.org/10.1111/j.1749-8198.2010.00364.x

Gooseff, M. N., LaNier, J., Haggerty, R., & Kokkeler, K. (2005). Determining in-channel (dead zone) transient storage by comparing solute transport in a bedrock channel-alluvial channel sequence, Oregon. *Water Resources Research*, *41*(6), 1–7. https://doi.org/10.1029/2004WR003513

Gooseff, M. N., Briggs, M. A., Bencala, K. E., McGlynn, B. L., & Scott, D. T. (2013). Do transient storage parameters directly scale in longer, combined stream reaches? Reach length dependence of transient storage interpretations. *Journal of Hydrology*, *483*(0), 16–25. https://doi.org/http://dx.doi.org/10.1016/j.jhydrol.2012.12.046

Grimm, N. B., & Fisher, S. G. (1984). Exchange between interstitial and surface water: Implications for stream metabolism and nutrient cycling. *Hydrobiologia*, *111*(3), 219–228. https://doi.org/10.1007/BF00007202

Groffman, P. M., Butterbach-Bahl, K., Fulweiler, R. W., Gold, A. J., Morse, J. L., Stander, E. K., et al. (2009). Challenges to incorporating spatially and temporally explicit phenomena (hotspots and hot moments) in denitrification models. *Biogeochemistry*, *93*(1–2), 49–77. https://doi.org/10.1007/s10533-008-9277-5

Hancock, P. J. (2002). Human impacts on the stream-groundwater exchange zone. *Environmental Management*, *29*(6), 763–81. https://doi.org/10.1007/s00267-001-0064-5

Hancock, P. J., Hunt, R. J., & Boulton, A. J. (2008). Preface: hydrogeoecology, the interdisciplinary study of groundwater dependent ecosystems. *Hydrogeology Journal*, *17*(1), 1–3. https://doi.org/10.1007/s10040-008-0409-8

Hartwig, M., & Borchardt, D. (2014). Alteration of key hyporheic functions through biological and physical clogging along a nutrient and fine-sediment gradient. *Ecohydrology*, n/a-n/a. https://doi.org/10.1002/eco.1571

Harvey, J., Gomez-Velez, J., Schmadel, N., Scott, D., Boyer, E., Alexander, R., et al. (2018). How Hydrologic Connectivity Regulates Water Quality in River Corridors. *Journal of the American Water Resources Association*, *55*(2), 369–381. https://doi.org/10.1111/1752-1688.12691

Harvey, J. W. (2016). Hydrologic Exchange Flows and Their Ecological Consequences in River Corridors. In B. Jones, Jeremy & E. Stanley (Eds.), *Stream Ecosytems in a Changing Environment* (pp. 1–83). Academic Press.

Harvey, J. W., & Gooseff, M. N. (2015). River corridor science: Hydrologic exchange and ecological consequences from bedforms to basins. *Water Resources Research*, *51*, 6893–6922. https://doi.org/10.1002/2015WR017617

Harvey, J. W., Böhlke, J. K., Voytek, M. A., Scott, D., & Tobias, C. R. (2013). Hyporheic zone denitrification: Controls on effective reaction depth and contribution to whole-stream mass balance. *Water Resources Research*, *49*(10), 6298–6316.

https://doi.org/10.1002/wrcr.20492

Heathwaite, A. L. (2010). Multiple stressors on water availability at global to catchment scales: Understanding human impact on nutrient cycles to protect water quality and water availability in the long term. *Freshwater Biology*, *55*(SUPPL. 1), 241–257. https://doi.org/10.1111/j.1365-2427.2009.02368.x

Hester, E. T., & Gooseff, M. N. (2011). Hyporheic Restoration in Streams and Rivers. *Stream Restoration in Dynamic Fluvial Systems: Scientific Approaches, Analyses, and Tools*, *194*, 167–187. https://doi.org/10.1029/2010GM000966

Hunt, R. J., Strand, M., & Walker, J. F. (2006). Measuring groundwater–surface water interaction and its effect on wetland stream benthic productivity, Trout Lake watershed, northern Wisconsin, USA. *Journal of Hydrology*, *320*(3–4), 370–384. https://doi.org/10.1016/j.jhydrol.2005.07.029

Jones, I., Growns, I., Arnold, A., McCall, S., & Bowes, M. (2015). The effects of increased flow and fine sediment on hyporheic invertebrates and nutrients in stream mesocosms. *Freshwater Biology*, 813–826. https://doi.org/10.1111/fwb.12536

Karwan, D. L., & Saiers, J. E. (2009). Influences of seasonal flow regime on the fate and transport of fine particles and a dissolved solute in a New England stream. *Water Resources Research*, *45*(11), 1–9. https://doi.org/10.1029/2009WR008077

Kaufman, M. H., Cardenas, M. B., Buttles, J., Kessler, A. J., & Cook, P. L. M. (2017). Hyporheic hot moments: Dissolved oxygen dynamics in the hyporheic zone in response to surface flow perturbations. *Water Resources Research*, *53*(8), 6642–6662. https://doi.org/10.1002/2016WR020296

Knapp, J. L. A., González-Pinzón, R., & Haggerty, R. (2018). The Resazurin-Resorufin System: Insights From a Decade of "Smart" Tracer Development for Hydrologic Applications. *Water Resources Research*, *54*(9), 6877–6889. https://doi.org/10.1029/2018WR023103

Krause, S., Hannah, D. M., Fleckenstein, J. H., Heppell, C. M., Kaeser, D., Pickup, R., et al. (2011). Inter-disciplinary perspectives on processes in the hyporheic zone. *Ecohydrology*, *4*, 481–499. https://doi.org/10.1002/eco

Lautz, L. K., Kranes, N. T., & Siegel, D. I. (2010). Heat tracing of heterogeneous hyporheic exchange adjacent to in-stream geomorphic features. *Hydrological Processes*, *24*(21), 3074–3086. https://doi.org/10.1002/hyp.7723

Lawrence, J. E., Skold, M. ., Hussain, F. A., Silverman, D. R., Resh, V. H., Sedlak, D. L., et al. (2013). Hyporheic Zone in Urban Streams: A Review and Opportunities for Enchancing Water Quality and Improving Aquatic Habiat by Active Managment. *Environmental Engineering Science*, *30*(8), 480–501.

Magliozzi, C., Grabowski, R., Packman, A. I., & Krause, S. (2018). Toward a conceptual framework of hyporheic exchange across spatial scales. *Hydrology and Earth System Sciences*, *22*(May), 6163–6185. https://doi.org/10.5194/hess-2018-268

Marmonier, P., Luczyszyn, H., des Châtelliers, M. C., Landon, N., Claret, C., & Dole-Olivier, M.-J. (2010). Hyporheic flowpaths and interstitial invertebrates associated with stable and eroded river sections: interactions between micro- and meso-scales. *Fundamental and Applied Limnology / Archiv Für Hydrobiologie*, *176*(4), 303–317. https://doi.org/10.1127/1863-9135/2010/0176-0303

Marmonier, P., Archambaud, G., Belaidi, N., Bougon, N., Breil, P., Chauvet, E., et al. (2012). The role of organisms in hyporheic processes: gaps in current knowledge, needs for future research and applications. *Annales de Limnologie - International Journal of Limnology*, *48*(3), 253–266. https://doi.org/10.1051/limn/2012009

McDonnell, J. J., Sivapalan, M., Vaché, K., Dunn, S., Grant, G., Haggerty, R., et al. (2007). Moving beyond heterogeneity and process complexity: A new vision for watershed hydrology. *Water Resources Research*, *43*(7). https://doi.org/10.1029/2006WR005467

Nogaro, G., Datry, T., Mermillod-Blondin, F., Descloux, S., & Montuelle, B. (2010). Influence of streambed sediment clogging on microbial processes in the hyporheic zone. *Freshwater Biology*, *55*(6), 1288–1302. https://doi.org/10.1111/j.1365-2427.2009.02352.x

Nowinski, J. D., Cardenas, M. B., Lightbody, A. F., Swanson, T. E., & Sawyer, A. H. (2012). Hydraulic and thermal response of groundwater–surface water exchange to flooding in an experimental aquifer. *Journal of Hydrology*, *472–473*(0), 184–192. https://doi.org/http://dx.doi.org/10.1016/j.jhydrol.2012.09.018

O'Connor, B. L., & Harvey, J. W. (2008). Scaling hyporheic exchange and its influence on biogeochemical reactions in aquatic ecosystems. *Water Resources Research*, *44*(12), 1–17. https://doi.org/10.1029/2008WR007160

O'Connor, B. L., Hondzo, M., & Harvey, J. W. (2010). Predictive Modeling of Transient Storage and Nutrient Uptake: Implications for Stream Restoration, (December), 1018–1032. https://doi.org/10.1061/ASCE̊HY.1943-7900.0000180

Oelkers, E. H., Hering, J. G., & Zhu, C. (2011). Water: Is There a Global Crisis? *Elements*, *7*(3), 157–162. https://doi.org/10.2113/gselements.7.3.157

Orghidan, T. (1959). A new habitat of subsurface waters: the hyporheic biotope. *Fundamental and Applied Limnology / Archiv Für Hydrobiologie*, *176*(4), 291–302. https://doi.org/10.1127/1863-9135/2010/0176-0291

Ormerod, S. J., Dobson, M., Hildrew, A. G., & Townsend, C. R. (2010). Multiple stressors in freshwater ecosystems. *Freshwater Biology*, *55*(SUPPL. 1), 1–4. https://doi.org/10.1111/j.1365-2427.2009.02395.x

Packman, A. I., & Bencala, K. E. (2000). Modeling methods in study of surface-subsurface

hydrological interactions. In J. B. Jones & P. J. Mulholland (Eds.), *Streams and Ground Waters* (pp. 45–80). Academic Press.

Pinay, G., Peiffer, S., De Dreuzy, J. R., Krause, S., Hannah, D. M., Fleckenstein, J. H., et al. (2015). Upscaling Nitrogen Removal Capacity from Local Hotspots to Low Stream Orders' Drainage Basins. *Ecosystems*, *18*(6), 1101–1120. https://doi.org/10.1007/s10021-015-9878-5

Poole, G. C., & Berman, C. H. (2000). Pathways of Human Influence on Water Temperature Dynamics in Stream Channels. U.S. Environmental Protection Agency, Region 10. Seattle, WA, 20.

Reisinger, A. J., Tank, J. L., Rosi-Marshall, E. J., Hall, R. O., & Baker, M. A. (2015). The varying role of water column nutrient uptake along river continua in contrasting landscapes. *Biogeochemistry*, *125*(1), 115–131. https://doi.org/10.1007/s10533-015-0118-z

Robertson, A. L., & Wood, P. J. (2010). Ecology of the hyporheic zone: origins, current knowledge and future directions. *Fundamental and Applied Limnology / Archiv Für Hydrobiologie*, *176*(4), 279–289. https://doi.org/10.1127/1863-9135/2010/0176-0279

Sophocleous, M. (2002). Interactions between groundwater and surface water: the state of the science. *Hydrogeology Journal*, *10*(1), 52–67. https://doi.org/10.1007/s10040-001-0170-8

Stanford, J. A., & Ward, J. V. (1993). An Ecosystem Perspective of Alluvial Rivers : Connectivity and the Hyporheic Corridor An ecosystem perspective of alluvial rivers : connectivity and the hyporheic corridor. *Journal of North American Benthological Society*, *12*(1), 48–60.

Stonedahl, S. H., Harvey, J. W., Wörman, A., Salehin, M., & Packman, A. I. (2010). A multiscale model for integrating hyporheic exchange from ripples to meanders. *Water Resources Research*, *46*(12), 1–14. https://doi.org/10.1029/2009WR008865

Thorp, J. H., Thoms, M. C., & Delong, M. D. (2006). The riverine ecosystem synthesis: biocomplexity in river networks across space and time. *River Research and Applications*, *22*(2), 123–147. https://doi.org/10.1002/rra.901

Wagener, T., Sivapalan, M., Troch, P. a., McGlynn, B. L., Harman, C. J., Gupta, H. V., et al. (2010). The future of hydrology: An evolving science for a changing world. *Water Resources Research*, *46*(5), n/a-n/a. https://doi.org/10.1029/2009WR008906

Wainwright, J., Turnbull, L., Ibrahim, T. G., Lexartza-Artza, I., Thornton, S. F., & Brazier, R. E. (2011). Linking environmental régimes, space and time: Interpretations of structural and functional connectivity. *Geomorphology*, *126*(3–4), 387–404. https://doi.org/http://dx.doi.org/10.1016/j.geomorph.2010.07.027

Ward, A. S. (2016). The evolution and state of interdisciplinary hyporheic research. *Wiley*

Interdisciplinary Reviews: Water, *3*(January/February), 83–103. https://doi.org/10.1002/wat2.1120

Ward, A. S., Schmadel, N. M., & Wondzell, S. M. (2018). Simulation of dynamic expansion, contraction, and connectivity in a mountain stream network. *Advances in Water Resources*, *114*, 64–82. https://doi.org/10.1016/j.advwatres.2018.01.018

Ward, J. V., & Tockner, K. (2001). Biodiversity: towards a unifying theme for river ecology. *Freshwater Biology*, *46*(6), 807–819. https://doi.org/10.1046/j.1365-2427.2001.00713.x

White, D. S. (1993). Perspectives on Defining and Delineating Hyporehic Zones. *Journal of the North American Benthological Society*, *12*(1), 61–69.

Woessner, W. W. (2000). Stream and fluvial plain ground water interactions: Rescaling hydrogeologic thought. *Ground Water*, *38*(3), 423–429. https://doi.org/https://doi.org/10.1111/j.1745-6584.2000.tb00228.x

Wohl, E., Bledsoe, B. P., Jacobson, R. B., Poff, N. L., Rathburn, S. L., Walters, D. M., & Wilcox, A. C. (2015). The Natural Sediment Regime in Rivers: Broadening the Foundation for Ecosystem Management. *BioScience*, *65*(4), 358–371. https://doi.org/10.1093/biosci/biv002

Wondzell, S. M. (2006). Effect of morphology and discharge on hyporheic exchange flows in two small streams in the Cascade Mountains of Oregon, USA. *Hydrological Processes*, *20*(2), 267–287. https://doi.org/10.1002/hyp.5902

Wondzell, S. M. (2011). The role of the hyporheic zone across stream networks. *Hydrological Processes*, *25*(22), 3525–3532. https://doi.org/10.1002/hyp.8119

Wondzell, S. M., & Swanson, F. J. (1996). Seasonal and Storm Dynamics of the Hyporheic Zone of a 4th-Order Mountain Stream . I : Hydrologic Processes. *Journal of North American Benthological Society*, *15*(1), 3–19.

Stream Solute Workshop. (1990). Concepts and Methods for Assessing Solute Dynamics in Stream Ecosystems. *Journal of the North American Benthological Society*, *9*(2), 95–119.

Wroblicky, G. J., Campana, M. E., Valett, H. M., & Dahm, N. (1998). Seasonal variation in surface-subsurface water exchnage and lateral hyporheic area of two stream-aquifer systems. *Water Resources Research*, *34*(3), 317–328. https://doi.org/https://doi.org/10.1029/97WR03285

Xie, X., & Zhang, D. (2010). Data assimilation for distributed hydrological catchment modeling via ensemble Kalman filter. *Advances in Water Resources*, *33*(6), 678–690. https://doi.org/10.1016/j.advwatres.2010.03.012

Xie, Y., Cook, P. G., Shanafield, M., Simmons, C. T., & Zheng, C. (2016). Uncertainty of

natural tracer methods for quantifying river-aquifer interaction in a large river. *Journal of Hydrology*, *535*, 135–147. https://doi.org/10.1016/j.jhydrol.2016.01.071

CHAPTER 2. – CUMULATIVE IMPACTS OF RECURSVIE FINE PARTICLE LOADING ON STREAMBED HYPORHEIC EXCHANGE USING A RECIRCULATING LABORATORY FLUME.

Introduction

Fine particles encompass a class of inorganic (e.g. sand, silt, and clay) and organic (e.g. biofilms and particulate pollutants) particles that are < 2mm ID (Battin & Sengschmitt, 1999; Brunke, 1999; Karwan & Saiers, 2009; Mathers et al., 2014). Mechanisms that deliver these particles to streams include bank erosion, upstream sediment erosion and transport, pollution events such as coal ash spills, urban stormwater runoff, and microbial mat growth. Fine particles may settle on the top of the streambeds and form an armor layer throughout various stream reach sections (Brunke, 1999; Rehg et al., 2005; Marmonier et al., 2010). The buildup of external fine particles can reduce external streambed permeability and is defined as streambed clogging (Brunke & Gonser, 1997; Heppell et al., 2009; Pacioglu et al., 2012). Streambed clogging can develop during periods of low current velocity and can also be induced by microbial biofilms in eutrophic streams (Battin & Sengschmitt, 1999; Packman & McKay, 2003). Fine particles that pass through the streambed surface and accumulate below the armor layer can work their way deeper into the streambed sediments while experiencing phases of resuspension and deposition (Chen et al., 2010; Descloux et al., 2013).

One benefit of fine particle loading is that excess nutrients and pollutants that sorb onto fine particles can remain lodged in the streambed for extended periods of time (Brunke, 1999; Arnon et al., 2010; Nogaro et al., 2010). For example, Drummond et al., (2017) quantified fine

particle immobilization rates and found that fine particle retention had the potential to serve as sources of carbon and nutrients to downstream environments throughout various flow conditions, different streambed environments, and across a wide range of temporal scales. Therefore, fine particle loading can increase the streambed processing potential by increasing the amount of time available for streambed primary production (Kimball et al., 1995; Medema et al., 1998; Nagorski & Moore, 1999; Searcy et al., 2005; Ren & Packman, 2007). When the fine particle loading events are temporary, resulting cycles of streambed clogging and scouring can actually benefit streambed activity by altering head gradients that encourage deeper hyporheic flowpaths (Brunke & Gonser, 1997; Sophocleous, 2002; Foster & Chilton, 2003).

In contrast, when fine particle delivery to the streambed is persistent, prolonged periods of streambed clogging that limit streambed water exchange and filtration can occur (Descloux et al., 2014; Mathers et al., 2014; Datry et al., 2015; Harper et al., 2017). Streambed clogging impairs vertical connectivity between the stream and its underlying aquifer by reducing hydraulic conductivity, interstitial pore spaces, habitat heterogeneity (Jones et al., 2015). Impaired vertical connectivity has the potential to limit the groundwater-surface water interactions and reduce hyporheic exchange rates (Packman & Brooks, 2001; Rehg et al., 2005; Fetzer et al., 2017). Additional consequences of streambed clogging can lead to stagnation of hyporheic water, streambed siltation, loss of habitat space, and modification of in-stream biogeochemical cycling, which can result in worsening water quality and environmental degradation through the growth of biofilms (Maridet et al., 1996; Fisher et al., 1998; Hartwig & Borchardt, 2015). Consequently, streambed clogging is currently recognized as one of the largest threats to water quality around the world (Marmonier et al., 2010; Descloux et al., 2014; Mathers et al., 2014; Cardenas, 2015).

Predicting the impacts of streambed clogging as episodic events, that includes cycles of disturbance and recovery, can be challenging due to landscape heterogeneity, unknowns related to watershed scaling, and temporal variability (Ward & Tockner, 2001; Boulton et al., 2010; Marmonier et al., 2012). The study of disturbance and response in hydrology is a well-recognized challenge because the distribution of water throughout the hydrology cycle is constantly disrupted over distinct time intervals (Lake, 2000; Ebel & Mirus, 2014). Ebel and Mirus (2014) point to the additional complications of disturbance impact assessments that arise from small scale changes, such as perturbations to an individual plot, that readily impact relevant hydrologic function and water resources at larger spatial scales.

Defining disturbance and response criteria from a systems perspective is challenging because it is difficult to define "baseline" conditions in the environment and separate overlapping disturbances from one another in both space and time (Wagener et al., 2010). Furthermore, forecasting streambed responses to successive fine particle mediated clogging are difficult to characterize because they often require extensive pre- and post-event monitoring, in addition to monitoring the actual disturbance events in real time (Peters et al., 2006; Cloern & Jassby, 2012). Although predicting impacts of hydrologic disturbances remains challenging, the ability to predict future hydrologic impacts, such as runoff and discharge, is highly valued for the management and development of water resources (Foufoula-Georgiou & Georgakakos, 1991; Serban & Askew, 1991). This study examines fine particle disturbances in a controlled environment where we are able to measure pre- and post-disturbance conditions in response to multiple fine particle loading events and quantify the impacts of streambed clogging on hyporheic exchange.

The purpose of this paper is (1) to quantify water column and streambed responses to fine particle loading, and (2) to understand how streambed hyporheic exchange is influenced by individual and successive disturbance events. The intention is to utilize artificially created thermal gradients to calculate hyporheic exchange rates before and after three unique fine particle additions to our laboratory stream environment. As such, we focus on quantifying water column and streambed sediment fine particle loading, in addition to using water flux as a proxy for hyporheic exchange at the sediment water interface and within the streambed. To meet our objectives, we combined in-situ measurements of water column clay concentration and temperature time series with ex-situ measurements of streambed grain size, hydraulic conductivity, and porosity. We found that streambed hyporheic exchange was variably affected by individual disturbances and eventually new baseline conditions were maintained after the cumulative impacts of three disturbance events.

Methods

We constructed a series of experiments to observe streambed clogging events in a homogenous silica sand streambed using a recirculating laboratory flume (Packman et al., 1997; Packman & McKay, 2003; Rehg et al., 2005). Three sequential kaolinite clay injections served as fine particle disturbances that were proxies for riverine erosional events. Each disturbance was evaluated individually and also considered as a series of sequential disturbance events (Table 2.1). This set of experiments allowed the examination of streambed responses to clogging events under controlled flow and streambed conditions using direct measurements and streambed heat flux modeling (Gordon et al., 2012; Lautz, 2012).

Table 2.1. Experimental Parameters (mean ± 1σ) for Flume Experiments[a]

Experiment Number	Discharge ($L\ s^{-1}$)	Water Depth (cm)	Velocity ($cm\ s^{-1}$)	Bed Depth (cm)	Temp. (°C)	Kaolinite Mass Injected (g)	Time Run (h)
Baseline	1.4 ± 1.1	21.7 ± 1.2	1.7 ± 1.3	7.5 ± 0.5	22.4 ± 0.1	n.d.	4.5
I	2.3 ± 1.4	21.7 ± 1.2	2.9 ± 1.7	7.5 ± 0.5	22.4 ± 0.5	29.6 ± 1e-4	146.8
II	2.5 ± 1.2	21.7 ± 1.2	3.0 ± 1.6	7.5 ± 0.5	22.2 ± 0.5	31.3 ± 1e-4	127.4
III	1.6 ± 0.9	21.7 ± 1.2	2.0 ± 1.1	7.5± 0.5	22.3 ± 0.5	50.4 ± 1e-4	131.8

[a]n.d. indicates that mass was not injected for the baseline conditions before the Experiment I.

Recirculating flumes are useful tools to create model streambeds and evaluate hyporheic exchange because they simplify the system by reducing the main exchange mechanism to a vertical flux that operates within a closed loop (Packman & Bencala, 2000; Stonedahl et al., 2010). The use of recirculating flumes to study hyporheic responses to variable conditions is well documented (Einstein, 1968; Ren & Packman, 2004a). For example, Packman and Brooks (1995) investigated the effects of streambed exchange on the transport and retention of clay particles in a sand streambed and found that relatively finer particles do not remain in the surface flow but can be trapped, due to particle sedimentation and deposition, and released from the streambed due to bed load resuspension. Fries and Trowbridge (2003) utilized a recirculating flume to study fine particle deposition rates and observed enhanced deposition to permeable sediment beds. Rehg et al. (2005) studied the effects of fine particle characteristics and moving bedforms on streambed clogging. This study found that fine sediment loads can have different impacts on hyporheic exchange depending on the stream flow conditions, streambed sediment transport rate, and the extent of fine particle and bed sediment interactions (Rehg et al., 2005).

Additionally, recirculating laboratory flumes have been used to study the effects of temperature on hyporheic exchange. Hyporheic zone heat transport is critical for many temperature-sensitive physical, chemical, and biological processes (Stanford & Ward, 1988; Stanford et al., 1996; Norman & Cardenas, 2014). Sawyer et al. (2011, 2012) utilized recirculating flumes in conjunction with heat transport to better under the impacts of channel-spanning logs on hyporheic temperature dynamics. Norman and Cardenas (2014) investigated the effects of bed topography on hyporheic thermal dynamics with a series of flume experiments.

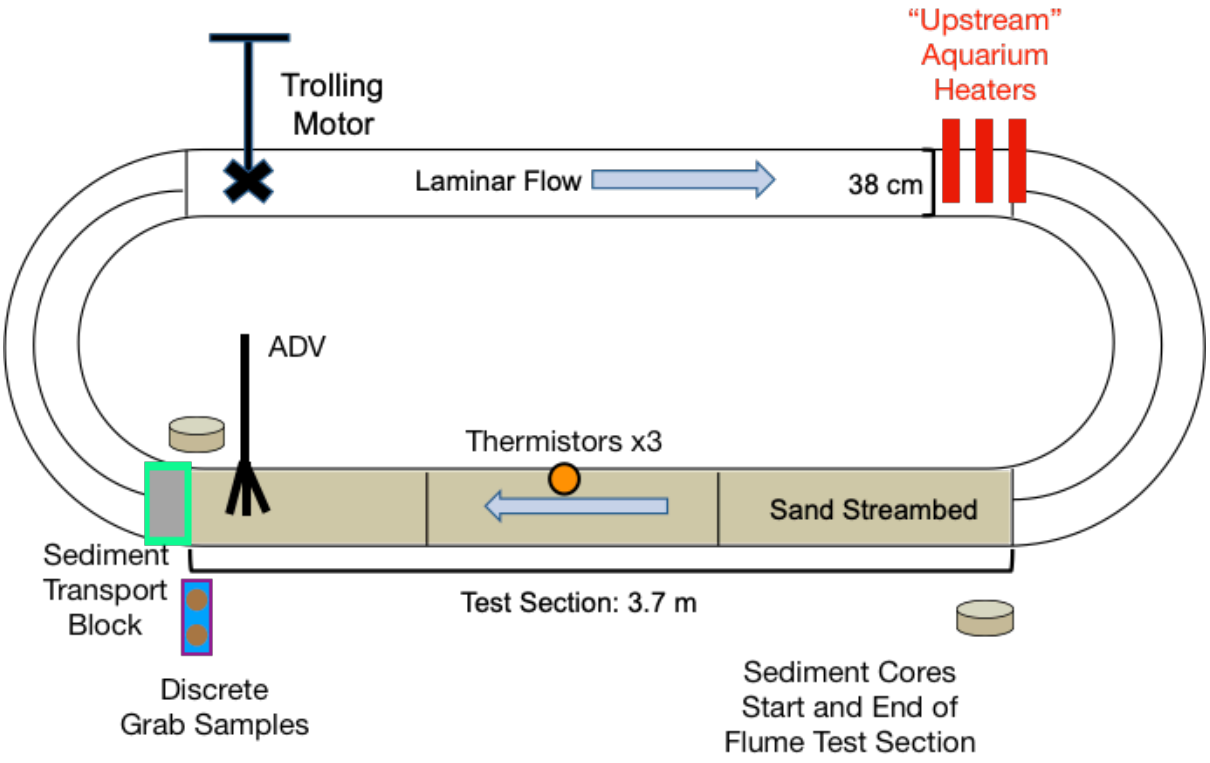

Figure 2.1. Flume conceptual diagram. A conceptual diagram of the recirculating laboratory flume used for this experiment along with the sampling and data collections methods, which are referred to throughout the text.

The flume used in this particular study was a recirculating, elliptical, "racetrack" flume, located in the Joint Applied Math and Marine Sciences Fluids Laboratory at the University of North Carolina at Chapel Hill (Fig. 2.1). This particular flume has the capacity to hold approximately 1640 L of water and is completely uncovered. We utilized an AC-powered trolling motor (MotorGuide, Machete II) to create surface water flow. The average flow rate from each experiment can be found in Table 2.1. Throughout each experiment, flow velocity was monitored with an acoustic Doppler velocimeter (ADV; Sontek) located immediately downstream from the tail of the test section (Fries & Trowbridge, 2003). The ADV sensor was 15 cm above the streambed surface. Each curved section of the flume contained two turning vanes designed to reduce water turbulence. The flume test section was located on the opposite side of the trolling motor and has a length of 365.76 cm, width of 37.80 cm, and depth of 24.39 cm. The outer wall of the flume test section had a series of three observation windows, which allowed for visual inspection and monitoring of streambed clogging. All flume experiments discussed utilized freshwater.

Prior to the first experiment, the flume test section was packed by hand with 0.11 m^3 of loose, silica sand to an average depth of 7.5 ± 0.5 cm. The sand used in these experiments had a with a mean grain size of 254.10 ± 12.28 μm, determined by laser particle size analysis (LS 13 320 Particle Size Analyzer, Beckman-Coulter) and mean ex-situ saturated hydraulic conductivity of 1.95e-2 ± 6.77e-3 cm/s, determined with a constant head permeameter (KSAT, Meter Environment).

The sand streambed was flattened and the flume was filled with water until the water depth was approximately 22 cm. Once the desired water depth was reached, the trolling motor was set to a speed that created a water velocity previously found to create ripples throughout the

test section streambed of this particular laboratory flume (Elliott & Brooks, 1997; Packman et al., 2000; Rehg et al., 2005). A weighted foam block was placed downstream of the test section tail to ensure sediments did not get transported outside of the test section during the ripple creation process.

After ripples were created throughout the entire test section length, the trolling motor speed was reduced until there was no observable sediment bed transport for a period of 4 h. Next, bedform geometry and streambed characteristics were measured using a ruler along three transects running the length of the test section sediment bed (Fries & Taghon, 2010) (Fig. 2.2).

Powdered kaolinite clay (Twigg County Georgia, Ward's Scientific), with a particle diameter of <2 μm, was used as a proxy for individual and successive erosional streambed disturbances (Packman et al., 1997; Ren & Packman, 2004b, 2007). Multiple dilute kaolinite clay suspensions were used to successively clog the test section stream bed over a period of approximately five to six days for each clay injection (Table 2.1). Each individual clay injection was evaluated as an individual disturbance in addition to the entire time series of successive disturbance events. The procedure for adding clay particle suspensions to the flume water was designed to provide well-mixed initial conditions. For each clay injection, fine particles, in addition to 10 g of sodium metaphosphate to ensure that clay particles did not form larger particle conglomerates, were mixed in 2 L of flume surface water and added back to the flume over the previously found period of time required for one complete transit time around the flume (Fries & Trowbridge, 2003; Fries & Taghon, 2010; Drummond et al., 2018).

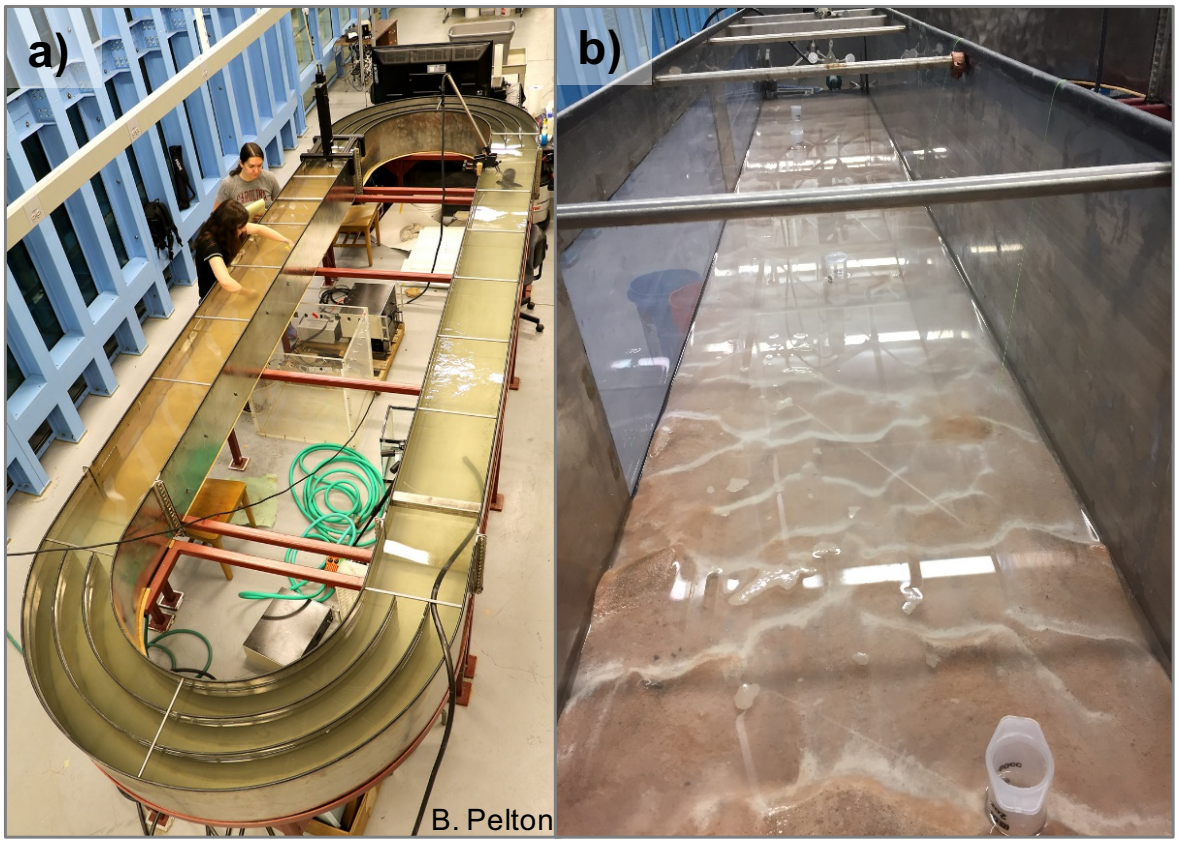

Figure 2.2. Flume experiment photos. A) Recirculating racetrack flume at UNC-Chapel Hill; (B) Flume streambed sediments show kaolinite deposited on the surface post Experiment III, white striations on the streambed ripples.

As sand was being added, a series of thermistors (Tidbit, Hobo) were installed in the middle of the test section at three different depths (i.e., 0 cm, 3.5 cm, and 7 cm). Each thermistor was set to record the water temperature every minute for the duration of all three experiments. Three standard aquarium heaters with a capacity of 300 watts/110-120 volts per unit were installed on the opposite side of the test section to create a heat differential that was used to calculate vertical flux over time as a proxy for hyporheic exchange in our flume environment (Sawyer et al., 2011, 2012; Norman & Cardenas, 2014). Prior experiments informed the number of heaters needed to create an adequate heat differential in flume environment.

Throughout the course of each experiment the heaters were turned on in the morning and off in the evening to mimic diurnal temperature fluctuations that occur in natural streams (Briggs et al., 2012; Briggs et al., 2014; Irvine et al., 2017). Temperature time series were recorded using the three thermistors at a sampling interval of one measurement per minute. The Vertical Fluid [Heat] Transport Solver (VFLUX) program was used to analyze the data and calculate water fluxes as a proxy for hyporheic exchange (Gordon et al., 2012; Irvine et al., 2015; Caissie & Luce, 2017). VFLUX provides a robust, inexpensive method to calculate hyporheic exchange from paired diel temperature time series.

VFLUX calculates the one-dimensional vertical fluid flow, or seepage flux, through saturated porous media, using heat transport equations (Lautz, 2012; Gordon et al., 2013; Lautz et al., 2010). To use VFLUX, temperature time series data, measured by multiple temperature sensor pairs, are collected in a vertical profile to calculate vertical flux for all specified sensor pairs at specific times and depths using the diurnal temperature signal and a variety of amplitude methods. Vertical flux estimates were calculated using the Luce flux method every 2 h for each sensor pair using the artificially imposed diurnal temperature signal throughout our series of

experiments (Luce et al., 2013). For more details of the heat transport modeling, signal processing, and error analysis, please see Hatch et al. (2006), Keery et al. (2007), Lautz et al. (2012), Gordon et al. (2013), and Luce et al. (2013).

Although may studies have used streambed water temperature as a tracer for hyporheic exchange in the field, the use of streambed water temperature as a tracer of fine particle disturbance and streambed response is less well utilized, especially in the laboratory environment. While other studies have utilized temperature variations (e.g. Sawyer et al., 2011; Norman and Cardenas, 2014) to study hyporheic thermal dynamics in a flume environment, to our knowledge, no other studies have used heat transport as a proxy measurement of fine particle disturbance responses in a recirculating laboratory flume. Utilizing heat transport in the context of disturbance response provides a number of experimental advantages including *in-situ* time series data that can be collected without disturbing the experimental streambed and the high degree of sampling resolution and precision that can be obtained with relatively inexpensive sensors.

Surface water grab samples of 500 mL were used to quantify the mass of fine particles in suspension over time using total suspended solids (TSS) (Meybeck et al., 2003). The first surface water grab sample was collected 10 minutes after each injection to ensure full mixing with the flume water. Subsequent water grab samples were collected at 15-minute intervals during the first two hours for the duration of the falling limb of the water column clay concentration. At each sampling time point, water samples were collected from the tail of the test section. After each grab sample was collected, the removed volume of water was replaced in the flume to ensure our total flume water volume remained constant. All grab samples were stored until they could be vigorously shaken by hand to break up flocs and vacuum filtered through a 0.7 μm

GF/F filter (Packman & McKay, 2003; Rehg et al., 2005; Karwan et al., 2007; Rossi et al., 2013). TSS values were used to quantify the percent of added clay deposition from the water column to the streambed throughout each experiment, while considering changes to each experiment baseline conditions, via gravitational settling and streambed pumping by calculating the areas under each TSS curve.

Once the water column clay concentration reached either the prior or new baseline condition, based on the TSS data, the trolling motor was stopped and sediment cores were collected from the head and tail of the test section. Additionally, multiple swabs were taken throughout the flume to better approximate the error in the clay particle mass that was lost to due to adherence to the flume sides outside of the test section after the conclusion of each experiment. This error term was improved by quantifying the collected mass by rinsing the wipes with a known volume of water and filtering the suspended sediment using vacuum filtration.

Multiple sediment cores were collected from the sand bed before and after each experiment to quantify permeability and verify clay particle deposition and infiltration (Fries & Trowbridge, 2003; Fries & Taghon, 2010). Two cores were taken, one from the head and one from the tail of the test section, prior to the first disturbance to measure baseline streambed permeability and grain size fractions (Fig. 2.1). Once each experiment appeared to return to steady state conditions, as approximated from the clarity of the water column and TSS calculations, two more sediment cores were extracted, one from the head and one from the tail of the test section. After each core was removed, additional sand was used to replace the extracted bed sediments. Subsequent cores were carefully sampled in areas that had no sand replacement. Cores were collected with cut acrylic tubes (7 cm in diameter) in one upstream and one downstream position in the test section. Measures of *ex situ* hydraulic conductivity, K, were

quantified for each sediment core using a constant head permeameter that was modeled after a design posted online by Dr. Martin Stute (Stute, 2005). K (cm/s) was calculated using a version of Darcy's Law (Darcy, 1856):

$$K = \frac{VL}{Ath} \tag{1}$$

where V is the volume of water discharging in time (cm^3), L is the length of the sample (cm), A is the cross-sectional area of the sample (cm^2), and h is the hydraulic head (cm). Three K measurements were made for each sediment core and averaged for each experiment. Additionally, porosity, n $(-)$, was calculated using the following equation (Fetter, 2001):

$$n = \frac{V_v}{V} \tag{2}$$

where V_v is the volume of the sediment core void space (cm^3) and V is the volume of the sediment core earth material, including both voids and solids (cm^3).

All sediment cores were kept intact and used to determine the bulk core mass and approximate deposited clay over time. Each core was dried and weighed to estimate the total mass deposited during each experiment (Fries & Trowbridge, 2003) . Calculation of the total mass deposited per core (m_c) was calculated using the method describe in Fries and Trowbridge (2003). m_c (g) was the difference between pre-experiment and post-experiment cores, adjusted by the core weights:

$$m_c = m_{post} - m_{pre}\frac{M_{post}}{M_{pre}} \tag{3}$$

where m is the core particle mass (g), M is the total core mass (g) and the subscripts "pre" and "post" denote the time of core collection, before and after each fine particle disturbance experiment. The total mass loss from the water column to the streambed, m_{loss} (%),was

calculated from the start and end of the concentration time series for each experiment (Fries & Trowbridge, 2003):

$$m_{loss} = \frac{V_f[\overline{C}(0) - \overline{C}(t_{core})]}{m_{injected}} \quad (4)$$

where V_f is the volume of the flume (L), $\overline{C}(0)$ is the concentration of the flume surface water at the baseline conditions, and $\overline{C}(t_{core})$ is the concentration of the flume surface water at the time of the sediment core collection.

Additionally, each core was analyzed using a laser particle size analyzer (LS 13 320 Particle Size Analyzer, Beckman-Coulter) to estimate the change in streambed sediment mean grain size in response to each individual clay addition and the cumulative effect of the three disturbance events (Fox et al., 2016; Fries, 2007). Pre-injection cores were used as a baseline for the background particle size distribution in undisturbed sand cores and used to correct our measurements.

Results

The artificial diel temperature signal was observed at all temperature sensors throughout each experiment. Therefore, it was possible to calculate vertical water flux for all functioning sensor pairs before our fine particle disturbances and throughout the course of each experiment. The resulting temperature time series had a detectable, moderate difference in amplitude, meaning that our sensor spacing of 3.5 cm apart was within the sensitivity of the model (Hatch et al., 2006; Keery et al., 2007; Gordon et al., 2012). We chose to calculate vertical water flux between the flume surface water and sediment bed using the amplitudes and phases of the filtered temperature signals according to the Luce method (Luce et al., 2013). The largest vertical flux variation throughout the time series collected at each sampling depth was one order of magnitude, which occurred at the 3.5 cm depth of all three disturbance experiments and the 7 cm depth of Experiment III. This indicates that the largest change in vertical flux typically occurred at the middle depth. All of our resulting flux values were within the range expected from studies that utilized VFLUX in natural streams (Lautz et al., 2010; Gordon et al., 2013).

Before the start of our disturbance experiments, the sediment-water interface had the highest flux value while vertical flux slightly decreased with increasing depth (Fig. 2.3). After the first disturbance experiment, the 3.5 cm depth displayed the highest vertical flux values and the flux at the sediment-water interface was the smallest. After the second and third disturbance experiments, the vertical flux increased with increasing depth. When we compare the response of vertical flux to the individual disturbance experiments, vertical flux decreased from baseline conditions after the first and second disturbance before slightly increasing after the third disturbance experiment (Fig. 2.3). The gradually decrease in vertical water flux at the sediment-water interface and at the two studied depths indicate that the disturbances created in

Experiments I and II resulted in streambed clogging. The largest difference in vertical flux occurred between the baseline and Experiment II. This indicates that two ~30 g additions of fine particles resulted in streambed clogging. However, after Experiment III, there was a slight increase in vertical flux at each measured depth, including the sediment-water interface. This increase shows that particles were resuspended and added back to the water column. However, the vertical flux did not return to the baseline levels or those observed after Experiment I.

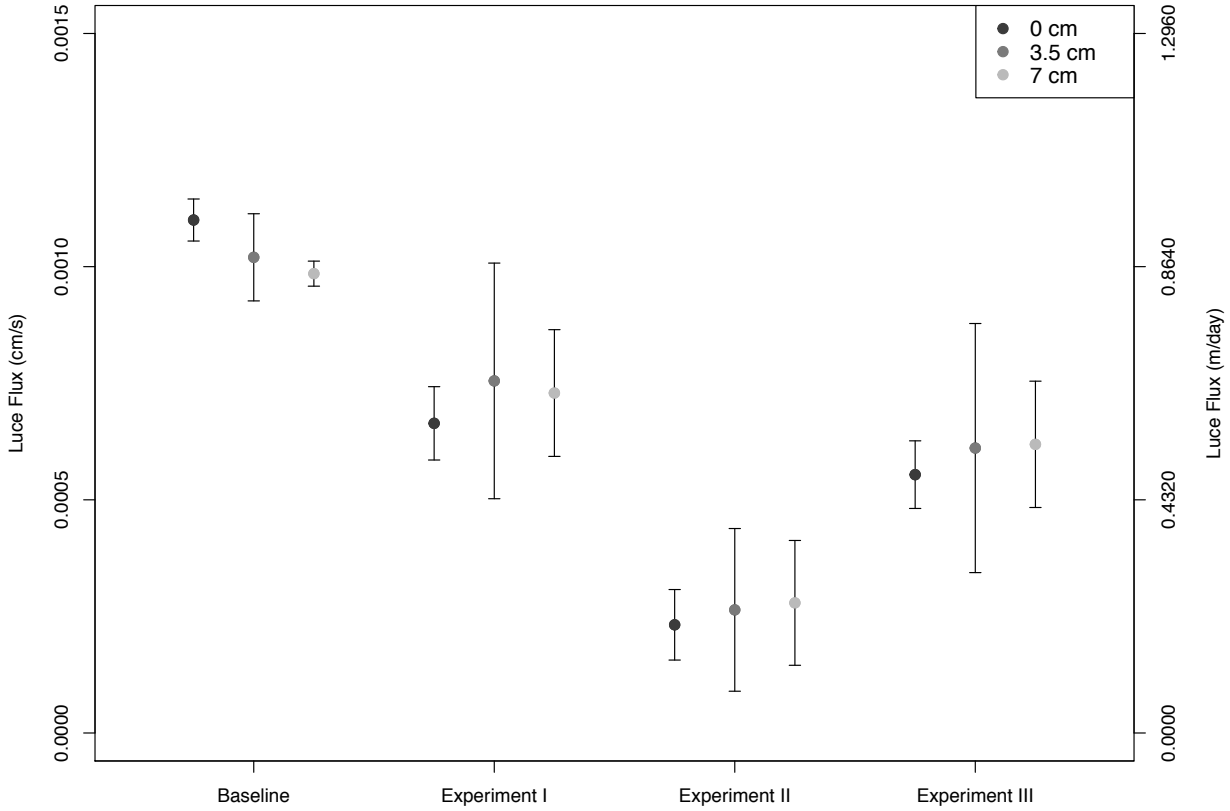

Figure 2.3. Values of average vertical water flux. Average vertical water flux values (cm/s) quantified over the course of each experimental condition using the Luce et al. (2013) amplitude method the sediment-water interface (0 cm), a mid-depth (3.5 cm), and a deeper depth (7 cm). The error bars represent one standard deviation from the mean.

Figure 2.4 and Table 2.2 show the total suspended solids results, TSS, with standard error for each measurement and best fit models with 95% confidence intervals from each disturbance experiment. Background samples were measured prior to each experiment to quantify the baseline conditions represented by the dashed black line in Figure 2.4. Models of TSS over time were fit using non-linear regression models with varying numbers of parameters. The best model fit was determined with Akaike Information Criteria (Cavanaugh, 1997). Experiment I and III, as indicated by the dashed black line in Figure 2.4, resulted in baseline conditions that were higher than the baseline conditions prior to the disturbance associated with that particular experiment. Experiment II returned to the prior baseline conditions that were present after Experiment I.

The behavior of the TSS concentration over time throughout each experiment was best described by exponential model fits with varying numbers of model parameters. TSS models from Experiments I and II resulted in similar model fits with the same number of parameters while the model from Experiment II had one fewer parameter (Table 2.2). The Experiment II model parameters were an order of magnitude smaller than their analogs from the other experiment model fits. This demonstrates that the streambed clogging dynamics were similar in Experiment I and III but different during Experiment II. Area under the curve predictions of fine particle deposition to the streambed from each clay addition varied across the three experiments. Experiments I and III resulted in over half of the fine particles added being deposited on the streambed while less than one third of the fine particles added during Experiment II resulted in streambed deposition (Table 2.2).

Table 2.2. Experiment Model Fits. Experiment TSS model fits, model parameter terms, and the predicted fine particle deposition to the streambed from the baseline and clay addition.

Experiment #	TSS Model Fit	a	b	c	Fine Particle Deposition (%)
I	$TSS = a * e^{(b*time)} + c$	13.5989	-0.0027	8.335	51
II	$TSS = e^{(a+b*time)}$	3.2933	-0.0002	n.d.	29
II	$TSS = a * e^{(b*time)} + c$	29.7109	-0.0021	16.1541	64

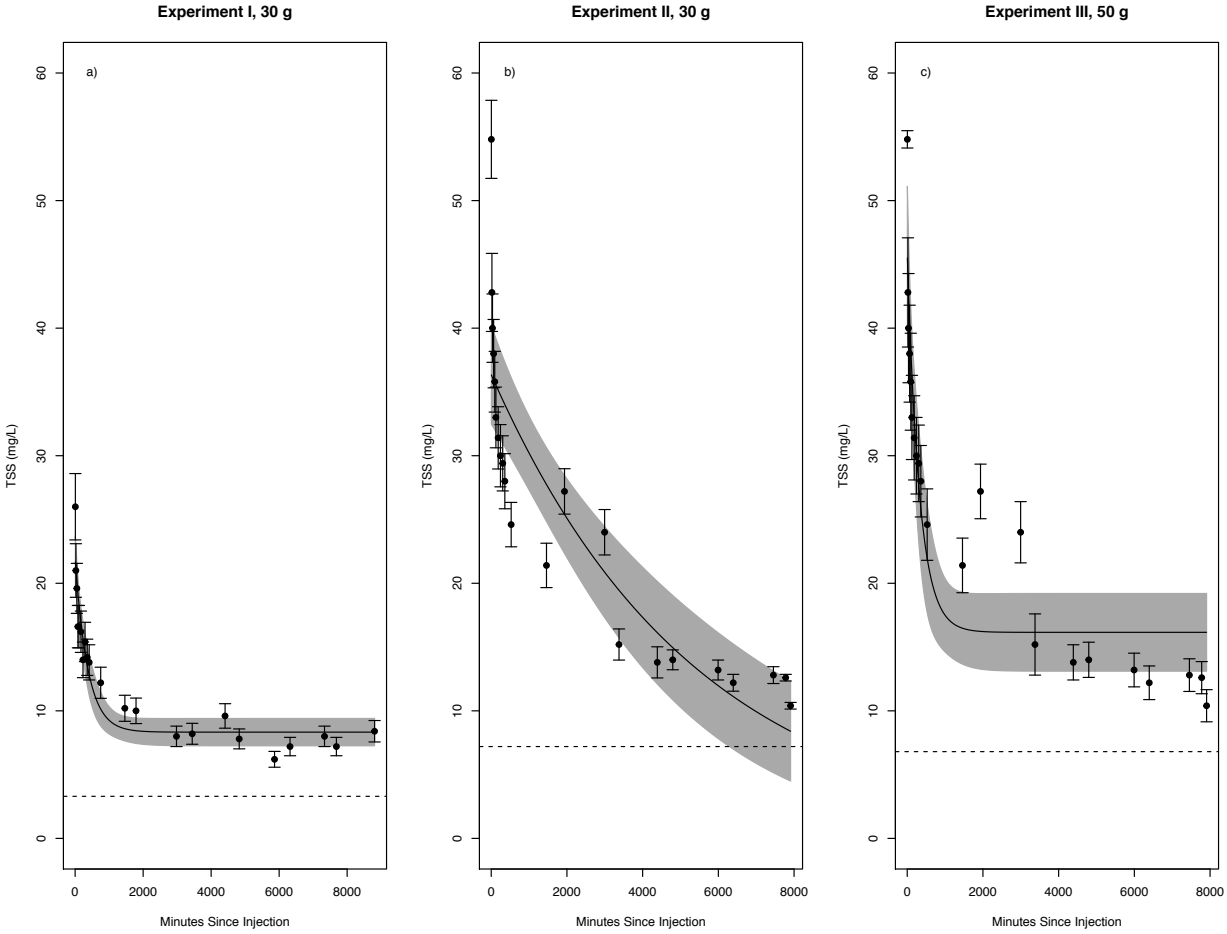

Figure 2.4. Water column total suspended sediment concentrations. Water column total suspended sediment concentration (TSS) (mg/(l)) over time after each fine particle addition where the error bars represent measurement standard error. The solid black line represents the modeled TSS behavior over time with a 95% confidence interval, noted by the gray polygon, and the dashed line represents the baseline from the prior experimental condition.

Sediment core results that were measured as a response to each disturbance can be found in Table 2.3. Bulk *ex situ* hydraulic conductivity, K, and porosity, n, slightly increased from the baseline conditions to the end of Experiment I, decreased after Experiment II, and increased after Experiment III. These two parameters were expected to follow a similar pattern, as they were directly measured from the same sediment cores. The variability in the trend of our K values could be due to the formation of additional flow paths throughout the sediment cores during the repeated constant head permeameter measurements. The bulk mean grain size, d_{50}, increased from the baseline conditions after Experiment I before steadily decreasing after each following experiment. This increase in d_{50} may have been due to error in the streambed sediment coring procedure or the length of time allowed for the initial sand streambed to settle to steady state conditions with flowing surface water.

The calculation of the mass deposited per core, m_c, confirmed the deposition of fine particles that was predicted from the water column data, as mass was added to each sediment core in response to the fine particle additions. Values of m_c were higher than expected for our sediment cores. Our higher than expected values of m_c could be an artifact of using unique pre- and post-disturbance cores to calculate our baseline conditions before the added mass was calculated. However, following the method of Fries and Trowbridge (2003), we believe that the trend in m_c helps explain the streambed response to the successive fine particle disturbances. m_c after Experiment II was higher than the other experiments indicating that conditions after the second disturbance had the highest streambed clogging potential. Predicted mass loss from the water column, m_{loss}, accounted for the cumulative mass added at each experiment and steadily decreased with disturbance as the streambed surface was likely saturated with fine particles by the end of Experiment III (see Fig. 2.2A for a photograph). Experiment III also had more mass in

the water column and by the conclusion of this experiment, there may not have been enough time for more of the fine particles to be deposited on or infiltrate the streambed. This lower m_{loss} value may also indicate fine particle resuspension occurred during Experiment III.

Table 2.3. Sediment core analysis data. Data ± 1σ from sediment core analysis after each fine particle addition experiment including *ex situ* hydraulic conductivity, $K\ (cm/s)$, porosity, $n\ (-)$, mean grain size, $d_{50}(\mu m)$, the mass deposited per core, $m_c\ (g)$, and predicted mass loss from the water column to the sediment bed $m_{loss}\ (\%)$.[a]

Experiment #	$K\ (cm/s)$	$n\ (-)$	$d_{50}(\mu m)$	$m_c\ (g)$	$m_{loss}\ (\%)$.
Baseline	0.032 ± 0.001	0.32 ± 0.06	254 ± 17	n.d.	n.d.
I	0.039 ± 0.004	0.34 ± 0.07	265 ± 14	5.77 ± 0.18	97
II	0.028 ± 0.005	0.46 ± 0.09	243 ± 2	6.21 ± 0.17	89
III	0.036 ± 0.002	0.40 ± 0.08	179 ± 5	4.07 ± 0.13	65

[a] n.d. indicates that mass was not injected for the baseline conditions before the Experiment I.

Discussion

Water column total suspended solid concentrations, TSS, displayed varying behavior in response to the disturbances over the course of each experiment (Fig. 2.4). The exponential decrease in TSS throughout each experiment and fine particle deposition estimates demonstrate vertical fine particle deposition from the water column to the streambed (Table 2.2). The new baseline conditions at the conclusion of Experiments I and III indicated that each of these disturbances increased the water column clay concentration and delivered fine particles to the streambed that could contribute to building a clay armor layer and eventually infiltrate the streambed sediments (Marmonier et al., 2010). The TSS values from Experiment III that were outside the 95% confidence interval did not seem to alter the overall exponential water column TSS concentration decline but could indicate some fine particle resuspension occurred after the initial disturbance had time to influence the experimental environment.

The possibility of fine resuspension from the streambed surface to the water column was supported by the increase in vertical flux when comparing Experiment II to Experiment III (Fig. 2.3). Fine particle resuspension has been measured in other flume (Packman & Brooks, 1995; Rehg et al., 2005) and field studies (Sophocleous, 2002; Foster & Chilton, 2003; Navel et al., 2012). Our results show that the settling, infiltration, and resuspension of fine particles are possible when considering the range of fine particle disturbance responses.

Experiment II demonstrated a fine particle disturbance response that was different than the other experiments. While Experiments I and II resulted in new baseline conditions, the TSS concentration at the end of Experiment II returned to the conditions at the end of Experiment I. This indicates that there was a high potential for fine particles added to this surface water from the first two experiments to deposit on the streambed surface and contribute to streambed

clogging. The lowest vertical flux values from Experiment II support this higher potential for streambed clogging. Thus, when we consider the cumulative impacts of the first and second disturbances, the additive effect of Experiment I and II had the greatest influence on lowering the streambed hyporheic exchange rate. To better understand the additive effects of fine particle disturbances on hyporheic exchange in natural environments, longer term pre- and post-disturbance data are needed to better quantify individual and cumulative disturbance effects (Harding et al., 1998; Allan, 2004; Ormerod et al., 2010; Feld et al., 2011).

Heat tracing methods using VFLUX were successfully used to measure vertical water flux as a proxy for hyporheic exchange at the sediment water interface and at depth throughout the course of our study. Differences in our average flux rates indicated that hyporheic exchange responded to each of our fine particle disturbances throughout the course of each experiment. The addition of fine particles from Experiment I and II clearly limited hyporheic exchange when compared to the baseline conditions (Fig. 2.3). Vertical flux showed the greatest variability between the baseline conditions and Experiment II. This indicates that cumulative effects of the first and second fine particle disturbances resulted in reduced hyporheic exchange at the sediment-water interface and within the streambed sediments. The lower vertical flux values at the streambed surface show that a clay armor layer formed and limited hyporheic exchange at the sediment-water interface (Brunke, 1999; Heppell et al., 2009; Nowinski et al., 2011; Pacioglu et al., 2012). The formation of a fine particle armor layer at the streambed surface may have contributed to the lower vertical flux values at depth however this cannot bed isolated from the role of fine particle infiltration in lowering rates of hyporheic exchange at depth.

The vertical flux results from Experiment III present an interesting situation. We expected this third disturbance to result in even lower hyporheic exchange rates because the

addition of a third fine particle disturbance was thought to have an additive effect on reducing hyporheic exchange and increasing streambed clogging through the further retention of fine particles in the streambed (Brunke, 1999; Lake, 2000; Marmonier et al., 2010; Descloux et al., 2013; Datry et al., 2015). However, our results indicate that Experiment III actually increased the vertical exchange flux and resulted in conditions similar to the conclusion of Experiment I (Fig. 2.3). This increase in hyporheic exchange may have resulted from gradual removal, or scouring, and re-suspension of fine particles from the armor layer by surface water. Re-suspension was deemed possible since the critical diameter of kaolinite clay is small enough to be eroded by our surface water flow rates (Dingman, 1984; Brunke & Gonser, 1997).

Prolonged periods of streambed clogging throughout the duration of Experiment I and II may have resulted in a clay particle armor layer that was eventually eroded given enough time with continuous surface flow (Schälchli, 1992; Brunke, 1999). The measured *ex situ* hydraulic conductivity after Experiment III (Table 2.3) supports this conclusion, as the average K increased from Experiment II to Experiment III, indicating that hyporheic exchange increased in response to the third disturbance event.

The results of our bulk streambed core analysis also show variable fine particle disturbance response throughout the course of each experiment (Table 2.3). Average ex-situ hydraulic conductivity, K, and bulk core porosity, n, and sediment core mean grain size, d_{50}, increased slightly between the measured baseline conditions and the conclusion of Experiment I. These increases indicate that sediment conditions became less favorable to streambed clogging after the first disturbance experiment. However, the uncertainties reported in Table 2.3 for n and d_{50} show that there is not much difference between baseline streambed sediment conditions and conditions at the conclusion of Experiment I. The trends in the mass deposited per sediment core,

m_c, and mass loss, m_{loss}, from the water column, show that there was fine particle accumulation at and within the sediment bed, as fine particles were undergoing deposition (Fries & Trowbridge, 2003).

Streambed sediment results at the conclusion of Experiment II, which represented the cumulative impacts of the first and second disturbance event, decreased in K and d_{50}, while increasing in n. Thus, after the second disturbance there appeared to be a fining of the sediment bed that contributed to additional streambed clogging and the lower value of hydraulic conductivity (Hancock, 2002; Boulton et al., 2010). These results are supported by the water column clay concentration and vertical flux measurements, as the second disturbance resulted in fine sediment loading to the streambed that contributed to streambed clogging. The increase in m_c and high m_{loss} value show that more fine particles were deposited on the sediment bed and there was still some remaining fine particle mass in the water column at the end of the experiment.

At the conclusion of Experiment III, K increased to a level similar to the first disturbance experiment. This followed a similar trend as the increase in hyporheic exchange between Experiment II and III. This increase in K and the vertical flux demonstrate that streambed clogging and its influence on hyporheic exchange are variable in response to different disturbance events. The continued decrease in d_{50} and n decreased showed that there was a continued fining of the sediment bed from the cumulative response to the three separate fine particle additions. The m_c results showed slightly less mass deposited per core than the previous disturbance experiments, however there was a greater percentage of the added clay particle mass that remained in suspension.

When we consider each individual disturbance event, we can understand how the water column, streambed sediments, and hyporheic exchange may respond to unique disturbance events. Similar size disturbance events (i.e. Experiment I and II) had variable responses in the water column and streambed sediments. Both disturbances lowered the vertical flux throughout the streambed but the initial disturbance event from Experiment I was the only disturbance that resulted in the creation of a new baseline condition, as indicated by the static water column fine particle concentration (Packman & Brooks, 1995; Rehg et al., 2005). After the disturbance from Experiment II, the water column clay concentration experienced a continual loss of fine particles to the streambed, as seen in Figure 2.4b and the sediment analysis results in Table 2.3. This fining of the streambed continued for the duration of the experiment, as indicated by the decrease in the mean grain size (Smith & Nicholas, 2005; Ren & Packman, 2007; Pizzuto et al., 2014). Thus, similar types of disturbances may have markedly different responses, depending on how that response is measured and the prior conditions to the selected disturbance event.

The larger disturbance from Experiment III resulted in water column conditions that were similar to Experiment I, as indicated by the similar shape exponential models in Figure 2.4a and 2.4b. Since this was a larger disturbance event, we excepted the water column to retain a greater number of clay particles. This was confirmed by the higher steady state conditions at the end of Experiment III, which resulted in a new baseline for total suspended solids concentration. Interestingly, while the fining of the streambed sediments continued, hyporheic exchange increased from the rate calculated for Experiment II. This, along with the increase in total suspended solids early in the water column time series data (Fig. 2.4c), indicates that there was a breakup of the clay armor layer and some resuspension of the previously deposited fine particles or the newly added particles from the Experiment III disturbance.

In reality, each disturbance response cannot just be considered as an individual event, as the results from each experiment are the cumulative responses to the prior conditions and disturbances. In the case of our study, Experiment I was representative of a single change from the original baseline conditions, while Experiments II and II represented the cumulative effects of two or three disturbances, respectively, from the original baseline conditions. When we consider the additive effect of successive disturbance events, we see how multiple fine particle loading events amplify the system variability, as hyporheic exchange rates decrease and increase in response to systemwide perturbations. Inconsistencies in how the experimental stream reach responded to each fine particle disturbance event support the idea that both episodic and chronic disturbances, in addition to their additive effects, can have variable effects on hyporheic exchange and broader riverine environments (Sarriquet et al., 2006; O'Connor & Harvey, 2008; Marmonier et al., 2010). Much of what we know about streambed responses to fine particle loading events depends on the timescale of our observations. While this bias is inherent in any observational study, perhaps considering prior and post-experimental conditions can better place streambed responses in the context of what is a true baseline condition versus disturbance response. Integrating frameworks from other disciplines, such as those developed for ecological sciences, may provide a path forward for how to characterize hydrologic baseline conditions, series of disturbances, how systems respond, and if new baseline conditions are created (Clark, 1989; Lake et al., 2000; Robertson & Wood, 2010; Ebel & Mirus, 2014).

Observations of variable hyporheic exchange response to fine particle loading events led to the conclusion that streambed responses to disturbances are dynamic and may not always result in persistent streambed clogging. The results of this laboratory flume study and other experimental fine particle studies show a range of how fine particle disturbances may influence

river systems, suggesting that streambed filtration and clogging are dynamic processes that deserve further study in controlled and natural environments (Packman et al., 2000; Rehg et al., 2005; Datry et al., 2007; Ren & Packman, 2007; Fox et al., 2018; Ward et al., 2018). These findings are also supported by variable observational and experimental data from previous studies that examined fine particle interactions with hydrologic properties. For example, Drummond et al. (2017; 2018) found that fine particle retention rates were a function of flow condition, location in the streambed, and the stream condition. Ren and Packman (2007) explored the influence of fine particle size distributions on streambed clogging and found that particle sedimentation and filtration contribute variably to hyporheic exchange rates. Further work is needed to better account for the variability of streambed responses to fine particle disturbances (Resh et al., 1988). Thus, accounting for the range of fine particle disturbance responses when describing and predicting the impacts of riverine sedimentation will improve our understanding of how fine particles variably influence hyporheic exchange.

Previous researchers have noted that the sedimentation and clogging of streambed sediments will continue to be a problem for water quality, and potentially water quantity, as we continue to develop the natural landscape (Young & Huryn, 1999; Poole & Berman, 2001; Mason et al., 2012). Therefore, we can improve our understanding of how streambed functions are related to hyporheic exchange, including streambed filtration rates, change in response to disturbances by applying simple, inexpensive data collection to studies before and after data are collected. Using temperature time series and heat differentials with a program such as VFLUX, may provide a path forward towards a better understanding how hyporheic exchange capacities change in response to individual and successive disturbance events. The added cost of collecting longer streambed temperature time series data is minimal and has the potential to improve our

predictions of how hyporheic exchange is influenced by disturbance events (Mathers et al., 2014; Hartwig & Borchardt, 2015; Wohl, 2015). By collecting temperature data before, during, and after planned field experiments we can ultimately get a clearer picture of how natural conditions and disturbances influence water quality, water quantity, and streambed materials processing. Knowing more about riverine disturbance and response to fine particle loading events and other disturbances can help improve water resource management.

Conclusions

This study presents observations of fine particle disturbance responses in a recirculating laboratory flume environment. Measurements of changes in fine particle water column concentration, vertical water fluxes throughout the streambed, and clay deposition show variable responses from baseline conditions when each disturbance was considered individually and as a series of cumulative events. Hyporheic exchange decreased with each successive disturbance before increasing during the larger fine particle disturbance, even though there was continued streambed fining and a higher water column clay concentration. Possible explanations for this increase in hyporheic exchange were the eventual scouring of the clay armor layer and fine particle resuspension after the third disturbance event. The use of VFLUX to measure streambed temperature time series data at depth allowed us to monitor the individual and cumulative streambed responses to a series of fine particle disturbance events. These results support expanding the application of streamed temperature time series data to improve our understanding of hydrologic responses to streambed clogging in model laboratory systems, while informing possible functional outcomes in stream environments.

Acknowledgements

Funding for this work was supported by the following: a GSA Grant-in-Aid (RG 1407-17), a UNC-Chapel Hill Graduate School Summer Research Fellowship, and a UNC-Chapel Hill Dissertation Completion Fellowship to KSG; and student support funding from the NSF (IUSE: GEOPATHS-IMPACT) for the UNC-Chapel Hill Increasing Diversity and Enhancing Academia Program. The authors wish to thank Savannah Swinea for her work and intellectual contributions to this project. The authors also wish to thank Charlotte Hopson, Rachel Housego, James Mahaney, Dr. Rich McLaughlin, Nuvan Rathnayaka, Dr. Brian White, Dr. Pierre Passaggia, Nadia Cohen, Elsemarie DeVries, Dr. Laura Moore, Dr. Johnathan Lees, Brian Pelton, Alexis Racioppi, and Jill Arriola for their laboratory and analysis assistance.

REFERENCES

Allan, J. D. (2004). Landscapes and Riverscapes : The Influence of Land Use on Stream Ecosystems. *Annual Review of Ecology, Evolution, and Systematics*, *35*, 257–284.

Arnon, S., Marx, L. P., Searcy, K. E., & Packman, A. I. (2010). Effects of overlying velocity, particle size, and biofilm growth on stream-subsurface exchange of particles. *Hydrological Processes*, *24*, 108–114. https://doi.org/10.1002/hyp

Battin, T. J., & Sengschmitt, D. (1999). Linking sediment biofilms, hydrodynamics, and river bed clogging: Evidence from a large river. *Microbial Ecology*, *37*(3), 185–196. https://doi.org/10.1007/s002489900142

Boulton, A. J., Datry, T., Kasahara, T., Mutz, M., & Stanford, J. A. (2010). Ecology and management of the hyporheic zone: stream–groundwater interactions of running waters and their floodplains. *Journal of the North American Benthological Society*, *29*(1), 26–40. https://doi.org/10.1899/08-017.1

Briggs, M. a., Lautz, L. K., McKenzie, J. M., Gordon, R. P., & Hare, D. K. (2012). Using high-resolution distributed temperature sensing to quantify spatial and temporal variability in vertical hyporheic flux. *Water Resources Research*, *48*(2), 1–16. https://doi.org/10.1029/2011WR011227

Briggs, M. A., Lautz, L. K., Buckley, S. F., & Lane, J. W. (2014). Practical limitations on the use of diurnal temperature signals to quantify groundwater upwelling. *Journal of Hydrology*, *519*(PB), 1739–1751. https://doi.org/10.1016/j.jhydrol.2014.09.030

Brunke, M. (1999). Colmation and depth filtration within streambeds: Retention of particles in hypoheic interstices. *International Review of Hydrobiology*, *84*(2), 99–117. https://doi.org/10.1002/iroh.199900014

Brunke, M., & Gonser, T. (1997). The ecological significance of exchange processes between rivers and groundwater. *Freshwater Biology*, *37*, 1–33. https://doi.org/https://doi.org/10.1046/j.1365-2427.1997.00143.x

Caissie, D., & Luce, C. H. (2017). Quantifying streambed advection and conduction heat fluxes. *Water Resources Research*, *53*(2), 1595–1624. https://doi.org/10.1002/2016WR019813

Cardenas, M. B. (2015). Hyporheic zone hydrologic science: A historical account of its emergence and a prospectus. *Water Resources Research*, *6*(4), 446. https://doi.org/10.1016/0022-1694(68)90080-2

Cavanaugh, J. E. (1997). Unifying the Derivations for the Akaike and Corrected Akaike Information Criteria from Statistics & Probability Letters. *Statistics & Probability Letters*, *33*, 201–208.

Chen, C., Packman, A. I., Zhang, D., & Gaillard, J. F. (2010). A multi-scale investigation of interfacial transport, pore fluid flow, and fine particle deposition in a sediment bed. *Water Resources Research*, *46*(11), 1–12. https://doi.org/10.1029/2009WR009018

Clark, J. S. (1989). Ecological Disturbance as a Renewal Process: Theory and Application to Fire History. *Oikos*, *56*(1), 17–30. https://doi.org/10.2307/3566083

Cloern, J. E., & Jassby, A. D. (2012). Drivers of change in estuarine-coastal ecosystems: Discoveries from four decades of study in San Francisco Bay. *Reviews of Geophysics*, *50*(4), 1–34. https://doi.org/10.1029/2012rg000397

Darcy, H. (1856). Les fontaines publiques de la ville d Dijon. In V. Dalmont (Ed.), *Les fontaines publiques de la ville d Dijon*. Paris.

Datry, T., Lamouroux, N., Thivin, G., Descloux, S., & Baudoin, J. M. (2007). Not:Estimation fo sediment hydraulic conductivity in river reaches and its potential use to evaluate streambed clogging, *7*(4), 189. https://doi.org/10.1002/rra

Datry, T., Lamouroux, N., Thivin, G., Descloux, S., & Baudoin, J. M. (2015). Estimation of sediment hydraulic conductivity in river reaches and its potential use to evaluate streambed clogging. *River Research and Applications*, *31*, 880–891. https://doi.org/10.1002/rra

Descloux, S., Datry, T., & Marmonier, P. (2013). Benthic and hyporheic invertebrate assemblages along a gradient of increasing streambed colmation by fine sediment. *Aquatic Sciences*, *75*(4), 493–507. https://doi.org/10.1007/s00027-013-0295-6

Descloux, S., Datry, T., & Usseglio-Polatera, P. (2014). Trait-based structure of invertebrates along a gradient of sediment colmation: Benthos versus hyporheos responses. *Science of the Total Environment*, *466–467*, 265–276. https://doi.org/10.1016/j.scitotenv.2013.06.082

Dingman, S. L. (1984). *Fluvial Hydrology*. New York: W. H. Freeman and Company.

Drummond, J. D., Larsen, L. G., Gonzalez-Pinzon, R., Packman, A. I., & Harvey, J. W. (2017). Fine particle retention within streamstorage areas at base flow and in response to a storm event. *Water Resources Research*, *53*, 5690–5705. https://doi.org/10.1002/2016WR020202

Drummond, J. D., Boano, F., Atwill, E. R., Li, X., Harter, T., & Packman, A. I. (2018). Cryptosporidium oocyst persistence in agricultural streams -a mobile-immobile model framework assessment. *Scientific Reports*, *8*(1), 1–9. https://doi.org/10.1038/s41598-018-22784-x

Drummond, J. D., Larsen, L. G., González-Pinzón, R., Packman, A. I., & Harvey, J. W. (2018). Less fine particle retention in a restored versus unrestored urban stream: balance between hyporheic exchange, resuspension and immobilization. *Journal of Geophysical Research: Biogeosciences*, 1–15. https://doi.org/10.1029/2017JG004212

Ebel, B. A., & Mirus, B. B. (2014). Disturbance hydrology: Challenges and opportunities. *Hydrological Processes*, *28*(19), 5140–5148. https://doi.org/10.1002/hyp.10256

Einstein, H. A. (1968). Deposition of Suspended Particles in a Gravel Bed. *Journal of the Hydraulics Division*, *5*, 1197–1205.

Elliott, H., & Brooks, N. H. (1997). Transfer of nonsorbing solutes to a streambed with bed forms: Laboratory experiments, *33*(JANUARY 1997), 137–151.

Feld, C. K., Birk, S., Bradley, D. C., Hering, D., Kail, J., Marzin, A., et al. (2011). *From Natural to Degraded Rivers and Back Again*. *Advances in Ecological Research* (1st ed., Vol. 44). Elsevier Ltd. https://doi.org/10.1016/B978-0-12-374794-5.00003-1

Fetter, C. W. (2001). *Applied Hydrogeology*. (P. Lynch, Ed.) (4th ed.). Upper Saddle River, New Jersey: Prentice-Hall, Inc.

Fetzer, J., Holzner, M., Plötze, M., & Furrer, G. (2017). Clogging of an Alpine streambed by silt-sized particles – Insights from laboratory and field experiments. *Water Research*, *126*, 60–69. https://doi.org/10.1016/j.watres.2017.09.015

Fisher, S. G., Grimm, N. B., Martí, E., Holmes, R. M., & Jones, J. B. (1998). Material spiraling in stream corridors: A telescoping ecosystem model. *Ecosystems*, *1*(1), 19–34. https://doi.org/10.1007/s100219900003

Foster, S. S. D., & Chilton, P. J. (2003). Groundwater: the processes and global significance of aquifer degradation. *Philosophical Transactions of the Royal Society of London. Series B, Biological Sciences*, *358*(1440), 1957–72. https://doi.org/10.1098/rstb.2003.1380

Foufoula-Georgiou, E., & Georgakakos, K. P. (1991). Hydrologogic Advances in Space-Time Precipitation Modeling and Forecasting.

Fox, A., Laube, G., Schmidt, C., Fleckenstein, J. H., & Arnon, S. (2016). The effect of losing and gaining flow conditions on hyporheic exchange in heterogeneous streambeds. *Water Resources Research*, *52*(9), 7460–7477. https://doi.org/10.1002/2016WR018677

Fox, A., Packman, A. I., Boano, F., Phillips, C. B., & Arnon, S. (2018). Interactions Between Suspended Kaolinite Deposition and Hyporheic Exchange Flux Under Losing and Gaining Flow Conditions. *Geophysical Research Letters*, *45*(9), 4077–4085. https://doi.org/10.1029/2018GL077951

Fries, J. S. (2007). Predicting Interfacial Diffusion Coefficients for Fluxes across the Sediment-Water Interface. *Journal of Hydraulic Engineering*, *133*(March), 267–272. https://doi.org/10.1061/(ASCE)0733-9429(2007)133:3(267)

Fries, J. S., & Taghon, G. L. (2010). Particle Fluxes into Permeable Sediments: Comparison of Mechanisms Mediating Deposition. *Journal of Hydraulic Engineering*, *136*(4), 214–221.

https://doi.org/10.1061/(ASCE)HY.1943-7900.0000169

Fries, J. S., & Trowbridge, J. H. (2003). Flume observations of enhanced fine-particle deposition to permeable sediment beds. *Limnology and Oceanography*, *48*(2), 802–812. https://doi.org/10.4319/lo.2003.48.2.0802

Gordon, R. P., Lautz, L. K., Briggs, M. A., & McKenzie, J. M. (2012). Automated calculation of vertical pore-water flux from field temperature time series using the VFLUX method and computer program. *Journal of Hydrology*, *420–421*(0), 142–158. https://doi.org/http://dx.doi.org/10.1016/j.jhydrol.2011.11.053

Gordon, R. P., Lautz, L. K., & Daniluk, T. L. (2013). Spatial patterns of hyporheic exchange and biogeochemical cycling around cross-vane restoration structures: Implications for stream restoration design. *Water Resources Research*, *49*(4), 2040–2055. https://doi.org/10.1002/wrcr.20185

Hancock, P. J. (2002). Human impacts on the stream-groundwater exchange zone. *Environmental Management*, *29*(6), 763–81. https://doi.org/10.1007/s00267-001-0064-5

Harding, J. S., Benfield, E. F., Bolstad, P. V, Helfman, G. S., & Jones, E. B. (1998). Stream biodiversity: the ghost of land use past. *Proceedings of the National Academy of Sciences of the United States of America*, *95*(25), 14843–7.

Harper, S. E., Foster, I. D. L., Lawler, D. M., Mathers, K. L., McKenzie, M., & Petts, G. E. (2017). The complexities of measuring fine sediment accumulation within gravel-bed rivers. *River Research and Applications*, *33*(10), 1575–1584. https://doi.org/10.1002/rra.3198

Hartwig, M., & Borchardt, D. (2015). Alteration of key hyporheic functions through biological and physical clogging along a nutrient and fine-sediment gradient. *Ecohydrology*, *975*(November 2014), n/a-n/a. https://doi.org/10.1002/eco.1571

Hatch, C. E., Fisher, A. T., Revenaugh, J. S., Constantz, J., & Ruehl, C. (2006). Quantifying surface water-groundwater interactions using time series analysis of streambed thermal records: Method development. *Water Resources Research*, *42*(10), 1–14. https://doi.org/10.1029/2005WR004787

Heppell, C. M., Wharton, G., Cotton, J. A. C., Bass, J. A. B., & Robers, S. E. (2009). Sediment storage in the shallow hyporheic of lowland vegetated river reaches. *Hydrological Processes*, *23*, 2239–2251. https://doi.org/10.1002/hyp

Irvine, D., Lautz, L., Briggs, M., Gordon, R., & McKenzie, J. (2015). Experimental evaluation of the applicability of phase, amplitude, and combined methods to determine water flux rates from temperature time series using VFLUX 2. *Journal of Hydrology*, *531*, 728–737. https://doi.org/10.1016/j.jhydrol.2015.10.054

Irvine, D. J., Briggs, M. A., Cartwright, I., Scruggs, C. R., & Lautz, L. K. (2017). Improved Vertical Streambed Flux Estimation Using Multiple Diurnal Temperature Methods in

Series. *Groundwater*, *55*(1), 73–80. https://doi.org/10.1111/gwat.12436

Jones, I., Growns, I., Arnold, A., McCall, S., & Bowes, M. (2015). The effects of increased flow and fine sediment on hyporheic invertebrates and nutrients in stream mesocosms. *Freshwater Biology*, 813–826. https://doi.org/10.1111/fwb.12536

Karwan, D. L., & Saiers, J. E. (2009). Influences of seasonal flow regime on the fate and transport of fine particles and a dissolved solute in a New England stream. *Water Resources Research*, *45*(11), 1–9. https://doi.org/10.1029/2009WR008077

Karwan, D. L., Gravelle, J. a., & Hubbart, J. a. (2007). Effects of timber harvest on suspended sediment loads in Mica Creek, Idaho. *Forest Science*, *53*(2), 181–188.

Keery, J., Binley, A., Crook, N., & Smith, J. W. N. (2007). Temporal and spatial variability of groundwater–surface water fluxes: Development and application of an analytical method using temperature time series. *Journal of Hydrology*, *336*(1–2), 1–16. https://doi.org/http://dx.doi.org/10.1016/j.jhydrol.2006.12.003

Kimball, B. A., Callender, E., & Axtmann, E. V. (1995). Effects of colloids on metal transport in a river receiving acid mine drainage, upper Arkansas River, Colorado, U.S.A. *Applied Geochemistry*, *10*(3), 285–306. https://doi.org/10.1016/0883-2927(95)00011-8

Lake, P. S. (2000). Disturbance , patchiness , and diversity in streams. *Journal of the North American Benthological Society*, *19*(4), 573–592. https://doi.org/10.1043/0887-3593(2000)019<0573:DPADIS>2.0.CO;2

Lake, P. S., Palmer, M. a., Biro, P., Cole, J., Covich, A. P., Dahm, C., et al. (2000). Global Change and the Biodiversity of Freshwater Ecosystems: Impacts on Linkages between Above-Sediment and Sediment Biota. *BioScience*, *50*(12), 1099. https://doi.org/10.1641/0006-3568(2000)050[1099:GCATBO]2.0.CO;2

Lautz, L. K. (2012). Observing temporal patterns of vertical flux through streambed sediments using time-series analysis of temperature records. *Journal of Hydrology*, *464–465*(0), 199–215. https://doi.org/http://dx.doi.org/10.1016/j.jhydrol.2012.07.006

Lautz, L. K., Kranes, N. T., & Siegel, D. I. (2010). Heat tracing of heterogeneous hyporheic exchange adjacent to in-stream geomorphic features. *Hydrological Processes*, *24*(21), 3074–3086. https://doi.org/10.1002/hyp.7723

Luce, C. H., Tonina, D., Gariglio, F., & Applebee, R. (2013). Solutions for the diurnally forced advection-diffusion equation to estimate bulk fluid velocity and diffusivity in streambeds from temperature time series. *Water Resources Research*, *49*(1), 488–506. https://doi.org/10.1029/2012WR012380

Maridet, L., Philippe, M., Wasson, J. G., & Mathieu, J. (1996). Spatial and temporal distribution of macroinvertebrates and trophic variables within the bed sediment of three streams

differing by their morphology and riparian vegetation. *Archiv Für Hydrobiologie*, *136*(1), 41–64.

Marmonier, P., Luczyszyn, H., des Châtelliers, M. C., Landon, N., Claret, C., & Dole-Olivier, M.-J. (2010). Hyporheic flowpaths and interstitial invertebrates associated with stable and eroded river sections: interactions between micro- and meso-scales. *Fundamental and Applied Limnology / Archiv Für Hydrobiologie*, *176*(4), 303–317. https://doi.org/10.1127/1863-9135/2010/0176-0303

Marmonier, P., Archambaud, G., Belaidi, N., Bougon, N., Breil, P., Chauvet, E., et al. (2012). The role of organisms in hyporheic processes: gaps in current knowledge, needs for future research and applications. *Annales de Limnologie - International Journal of Limnology*, *48*(3), 253–266. https://doi.org/10.1051/limn/2012009

Mason, S. J. K., McGlynn, B. L., & Poole, G. C. (2012). Hydrologic response to channel reconfiguration on Silver Bow Creek, Montana. *Journal of Hydrology*, *438–439*(0), 125–136. https://doi.org/http://dx.doi.org/10.1016/j.jhydrol.2012.03.010

Mathers, K. L., Millett, J., Robertson, A. L., Stubbington, R., & Wood, P. J. (2014). Faunal response to benthic and hyporheic sedimentation varies with direction of vertical hydrological exchange. *Freshwater Biology*, *59*, 2278–2289. https://doi.org/10.1111/fwb.12430

Medema, G. J., Schets, F. M., Teunis, P. F. M., & Havelaar, A. H. (1998). Sedimentation of free and attached Cryptosporidium oocysts and Giardia cysts in water. *Applied and Environmental Microbiology*, *64*(11), 4460–4466.

Meybeck, M., Laroche, L., Dürr, H. ., & Syvitski, J. P. . (2003). Global variability of daily total suspended solids and their fluxes in rivers. *Global and Planetary Change*, *39*(1–2), 65–93. https://doi.org/10.1016/S0921-8181(03)00018-3

Nagorski, S. A., & Moore, J. N. (1999). Arsenic mobilization in the hyporheic zone of a contaminated stream. *Water Resources Research*, *35*(11), 3441–3450.

Navel, S., Mermillod-Blondin, F., Montuelle, B., Chauvet, E., & Marmonier, P. (2012). Sedimentary context controls the influence of ecosystem engineering by bioturbators on microbial processes in river sediments. *Oikos*, *121*(7), 1134–1144. https://doi.org/10.1111/j.1600-0706.2011.19742.x

Nogaro, G., Datry, T., Mermillod-Blondin, F., Descloux, S., & Montuelle, B. (2010). Influence of streambed sediment clogging on microbial processes in the hyporheic zone. *Freshwater Biology*, *55*(6), 1288–1302. https://doi.org/10.1111/j.1365-2427.2009.02352.x

Norman, F. A., & Cardenas, M. B. (2014). Heat transport in hyporheic zones due to bedforms: An experimental study. *Water Resources Research*, *50*(4), 3568–3582. https://doi.org/10.1002/2013WR014673

Nowinski, J. D., Cardenas, M. B., & Lightbody, A. F. (2011). Evolution of hydraulic conductivity in the floodplain of a meandering river due to hyporheic transport of fine materials. *Geophysical Research Letters*, *38*(1), n/a-n/a. https://doi.org/10.1029/2010GL045819

O'Connor, B. L., & Harvey, J. W. (2008). Scaling hyporheic exchange and its influence on biogeochemical reactions in aquatic ecosystems. *Water Resources Research*, *44*(12), 1–17. https://doi.org/10.1029/2008WR007160

Ormerod, S. J., Dobson, M., Hildrew, A. G., & Townsend, C. R. (2010). Multiple stressors in freshwater ecosystems. *Freshwater Biology*, *55*(SUPPL. 1), 1–4. https://doi.org/10.1111/j.1365-2427.2009.02395.x

Pacioglu, O., Shaw, P., & Robertson, A. (2012). Patch scale response of hyporheic invertebrates to fine sediment removal in two chalk rivers. *Fundamental and Applied Limnology / Archiv Für Hydrobiologie*, *181*(4), 283–288. https://doi.org/10.1127/1863-9135/2012/0388

Packman, A. I., & Bencala, K. E. (2000). Modeling methods in study of surface-subsurface hydrological interactions. In J. B. Jones & P. J. Mulholland (Eds.), *Streams and Ground Waters* (pp. 45–80). Academic Press.

Packman, A. I., & Brooks, N. H. (1995). Colloidal Particle Exchange Between Stream and Stream Bed in a Laboratory Flume. *Marine and Freshwater Research*, *46*(1), 233–236.

Packman, A. I., & Brooks, N. H. (2001). Hyporheic exchange of solutes and colloids with moving bed forms. *Water Resources Research*, *37*(10), 2591–2605. https://doi.org/10.1029/2001WR000477

Packman, A. I., & McKay, J. S. (2003). Interplay of stream-subsurface exchange, clay particle deposition, and streambed evolution. *Water Resources Research*, *39*(4), 1–10. https://doi.org/10.1029/2002WR001432

Packman, A. I., Brooks, N. H., & Morgan, J. J. (1997). Experimental techniques for laboratory investigation of clay colloid transport and filtration in a stream with a sand bed. *Water, Air, and Soil Pollution*. https://doi.org/10.1023/A:1018380231521

Packman, A. I., Brooks, N. H., & Morgan, J. J. (2000). A physicochemical model for colloid exchange between a stream and a sand streambed with bed forms. *Water Resources Research*, *36*(8), 2351. https://doi.org/10.1029/2000WR900059

Peters, D. P. C., Bestlemeyer, B., Herrick, J. E., Fredricson, E. L., Monger, H. C., & Havstad, K. M. (2006). Disentangling Complex Landscapes: New Insights into Arid and Semiarid System Dynamics. *BioScience*, *56*(6), 491. https://doi.org/10.1641/0006-3568(2006)56[491:dclnii]2.0.co;2

Pizzuto, J., Schenk, E. R., Hupp, C. R., Gellis, A., Noe, G., Williamson, E., et al. (2014). Characteristic length scales and time-averaged transport velocities of suspended sediment in

the mid-Atlantic Region, USA. *Water Resources Research*, (1), 790–805. https://doi.org/10.1002/2013WR014485.Received

Poole, G. C., & Berman, C. H. (2001). An ecological perspective on in-stream temperature: Natural heat dynamics and mechanisms of human-caused thermal degradation. *Environmental Management*, *27*(6), 787–802. https://doi.org/10.1007/s002670010188

Rehg, K. J., Packman, A. I., & Ren, J. (2005). Effects of suspended sediment characteristics and bed sediment transport on streambed clogging. *Hydrological Processes*, *19*(2), 413–427. https://doi.org/10.1002/hyp.5540

Ren, J., & Packman, A. I. (2004a). Modeling of Simultaneous Exchange of Colloids and Sorbing Contaminants between Streams and Streambeds. *Environmental Science & Technology*, *38*(10), 2901–2911. https://doi.org/10.1021/es034852l

Ren, J., & Packman, A. I. (2004b). Stream-subsurface exchange of zinc in the presence of silica and kaolinite colloids. *Environmental Science and Technology*, *38*(24), 6571–6581. https://doi.org/10.1021/es035090x

Ren, J., & Packman, A. I. (2007). Changes in fine sediment size distributions due to interactions with streambed sediments. *Sedimentary Geology*, *202*(3), 529–537. https://doi.org/http://dx.doi.org/10.1016/j.sedgeo.2007.03.021

Resh, V. H., Brown, A. V, Covich, A. P., Gurtz, M. E., Li, H. W., Minshall, G. W., et al. (1988). The Role of Disturbance in Stream Ecology The role of disturbance in stream ecology. *Journal N. Am. Benthol Soc.*, *7*(4).

Robertson, A. L., & Wood, P. J. (2010). Ecology of the hyporheic zone: origins, current knowledge and future directions. *Fundamental and Applied Limnology / Archiv Für Hydrobiologie*, *176*(4), 279–289. https://doi.org/10.1127/1863-9135/2010/0176-0279

Rossi, L., Chèvre, N., Fankhauser, R., Margot, J., Curdy, R., Babut, M., & Barry, D. A. (2013). Sediment contamination assessment in urban areas based on total suspended solids. *Water Research*, *47*(1), 339–350. https://doi.org/10.1016/j.watres.2012.10.011

Sarriquet, P. E., Delettre, Y. R., & Marmonier, P. (2006). Effects of catchment disturbance on stream invertebrates: comparison of different habitats (vegetation, benthic and interstitial) using bio-ecological groups. *Annales de Limnologie - International Journal of Limnology*, *42*(4), 205–219. https://doi.org/10.1051/limn/2006022

Sawyer, A. H., Bayani Cardenas, M., & Buttles, J. (2011). Hyporheic exchange due to channel-spanning logs. *Water Resources Research*, *47*(8), 1–12. https://doi.org/10.1029/2011WR010484

Sawyer, A. H., Bayani Cardenas, M., & Buttles, J. (2012). Hyporheic temperature dynamics and heat exchange near channel-spanning logs. *Water Resources Research*, *48*(1), W01529. https://doi.org/10.1029/2011WR011200

Schälchli, U. (1992). The clogging of coarse gravel river beds by fine sediment. *Hydrobiologia*, *235–236*(1), 189–197. https://doi.org/10.1007/BF00026211

Searcy, K. E., Packman, A. I., Atwill, E. R., & Harter, T. (2005). The association of Cryptosporidium parvum with suspended sediments and impact on oocyst deposition. *Applied and Environmental Microbiology*, *71*(2), 1072–1078. https://doi.org/10.1128/AEM.71.2.1072

Serban, P., & Askew, A. J. (1991). Hydrological forecasting and updating procedures. *IAHS Pub.No.201*, (201), 357–369.

Smith, G. H. S., & Nicholas, A. P. (2005). Effect on flow structure of sand deposition on a gravel bed: Results from a two-dimensional flume experiment. *Water Resources Research*, *41*(10), 1–12. https://doi.org/10.1029/2004WR003817

Sophocleous, M. (2002). Interactions between groundwater and surface water: the state of the science. *Hydrogeology Journal*, *10*(1), 52–67. https://doi.org/10.1007/s10040-001-0170-8

Stanford, J. A., & Ward, J. V. (1988). The hyporheic habitat of river ecosystems. *Nature*, *335*(6185), 64–66. https://doi.org/10.1038/335064a0

Stanford, J. A., Ward, J. V., Liss, W. J., Frissell, C. A., Williams, R. N., Lichatowich, J. A., & Coutant, C. C. (1996). a General Protocol for Restoration of Regulated Rivers. *Regulated Rivers: Research & Management*, *12*(45), 391–413. https://doi.org/10.1002/(sici)1099-1646(199607)12:4/5<391::aid-rrr436>3.3.co;2-w

Stonedahl, S. H., Harvey, J. W., Worman, A., Salehin, M., & Packman, A. I. (2010). A multiscale model for integrating hyporheic exchange from ripples to meanders. *Water Resources Research*, *46*(12), 1–14. https://doi.org/10.1029/2009WR008865

Stute, M. (2005). Design for a Cheap Permeameter. Retrieved from https://d32ogoqmya1dw8.cloudfront.net/files/NAGTWorkshops/hydrogeo/cheap_permeameter.jpg

Wagener, T., Sivapalan, M., Troch, P. a., McGlynn, B. L., Harman, C. J., Gupta, H. V., et al. (2010). The future of hydrology: An evolving science for a changing world. *Water Resources Research*, *46*(5), n/a-n/a. https://doi.org/10.1029/2009WR008906

Ward, A. S., Morgan, J. A., White, J. R., & Royer, T. V. (2018). Streambed restoration to remove fine sediment alters reach-scale transient storage in a low-gradient fifth-order river, Indiana, USA. *Hydrological Processes*, (March), 1–15. https://doi.org/10.1002/hyp.11518

Ward, J. V., & Tockner, K. (2001). Biodiversity: towards a unifying theme for river ecology. *Freshwater Biology*, *46*(6), 807–819. https://doi.org/10.1046/j.1365-2427.2001.00713.x

Wohl, E. (2015). Legacy Effects on Sediments in River Corridors. *Earth-Science Reviews*, *147*, 30–53. https://doi.org/10.1016/j.earscirev.2015.05.001

Young, R. G., & Huryn, A. D. (1999). Effects of land use on stream metabolism and organic matter turnover. *Ecological Applications*, *9*(4), 1359–1376. https://doi.org/10.1890/1051-0761(1999)009[1359:EOLUOS]2.0.CO;2

CHAPTER 3. – HYPORHEIC ZONE PROCESSING CONTROLS VARY WITH DEPTH AND STREAM ORDER THROUGHOUT A 4TH ORDER FLUVIAL NETWORK.

Introduction

In freshwater ecosystems, surface and ground waters interact across multiple spatial and temporal scales throughout the river continuum (Battin et al., 2003; Krause et al., 2011; Magliozzi et al., 2018). One such interaction is the exchange of riverine surface water and groundwater within the hyporheic zone, which is defined as the top portion of the unconfined, near-stream aquifer with flow paths that originate and terminate in the active stream channel (Orghidan, 1959; Gooseff, 2010; Ward, 2016). Although the size of the hyporheic zone is relatively small when compared to other riverine ecotones, it is highly connected to groundwater and surface water environments and has the potential to significantly influence riverine water quality (Brunke & Gonser, 1997; Woessner, 2000; Cardenas, 2015; Harvey et al., 2018). Hyporheic exchange, or the bidirectional transfer of water and its constituents through the hyporheic zone, creates a de facto filtration system that moderates streambed-water column interactions, regulates in-stream processing rates, attenuates contaminants, drives reach-scale biogeochemical dynamics, and governs streambed metabolic activity (Bencala, 2000; Argerich et al., 2011; Fischer et al., 2005; Boano et al., 2014).

Hyporheic zone reactivity depends on several physical and chemical factors including hydraulic head gradients; suspended and bedload particle size distributions; streambed morphology and hydraulic conductivity; pore water velocity and chemical makeup; pH; ionic

strength; biofilm density; and the relative abundance of macroinvertebrates (Stream Solute Workshop, 1990; Ren & Packman, 2007; Karwan & Saiers, 2012; Aubeneau et al., 2015; Mathers et al., 2017). Therefore, the combination of these abiotic and biotic characteristics dictates the potential of the hyporheic zone to filter stream water, transform dissolved constituents, and substantially improve water quality during the transit downstream (Boulton et al., 1998; Faulkner et al., 2012; Lawrence et al., 2013). This significance has been documented at several scales, ranging from streambed sediment surfaces to entire catchments, using a variety of physical, chemical, and biological metrics (Harvey & Fuller, 1998; Woessner, 2000; Findlay et al., 2003; Heathwaite, 2010; Gomez-Velez & Harvey, 2014; González-Pinzón, et al., 2015; Hartwig & Borchardt, 2015).

Although the hyporheic zone is widely recognized as an important regulator of riverine water quality, not all portions of the streambed contribute equally to riverine materials processing via hyporheic exchange. For instance, the presence of a shallow, benthic biolayer at the uppermost potions of streambed hyporheic zones has been documented as an active area for abiotic and biotic biogeochemical transformations (Battin, et al., 2003; Arnon et al., 2013; Knapp et al., 2017). The benthic biolayer has been described as an extension of a surficial streambed biofilm that extends deeper into the hyporheic zone depending on flow rates, solute transport, streambed sediment particle size, redox chemistry, *in-situ* biogeochemistry, carbon pools, nutrient sources, and the degree of hydrologic connectivity between the stream and hyporheic sediments (Hagerthey & Kerfoot, 2005; Knapp et al., 2017; Harvey et al., 2018).

Consequently, the combination of enhanced biotic and abiotic transformations in the shallow hyporheic zone sediments may result in areas of higher reactivity. For example, Schaper et al. (2019) found that the shallowest hyporheic zone depths were associated with oxic

conditions that encouraged the highest microbial activity along short, vertical flowpaths. The authors proposed that the benthic biolayer may be relatively more important to reach-scale reactivity that long, lateral flowpaths through deeper hyporheic zone depths, which agrees with the findings of Gomez-Velez et al. (2015). Additionally, Haggerty et al. (2014) found that the presence of biofilms contributed to hyporheic zone processing, regardless of bed form type. Thus, benthic biolayers may significantly contribute to overall riverine reactivity when compared to contributions from deeper hyporheic zone depths.

One difficulty associated with predicting and scaling riverine reactivity is our ability to characterize variable hyporheic zone contributions across fluvial networks along various depth profiles and how those contributions change with increasing stream order (O'Connor et al., 2010; González-Pinzón et al., 2013). A combination of modeling and field studies that assessed hyporheic zone processes have provided some answers about reactivity variability at the pore-scale (O'Conner & Hondzo, 2008; Day-Lewis et al., 2017), centimeter-scale (Harvey et al., 2013;Larsen et al., 2014; Knapp et al., 2017), reach-scale (Grimm & Fisher, 1984; ; Zarnetske et al., 2015; Knapp et al., 2017), and catchment scale (Stewart et al., 2011; Gomez-Velez & Harvey, 2014) but to our knowledge, there are few studies that directly measure variable streamed reactivity contributions across multiple stream order reaches. Additionally, the added challenges of increasing spatial heterogeneity and streambed processing complexity with increasing stream order, make it even more difficult to scale up variable contributions to hyporheic zone reactivity (McDonnell et al., 2007; O'Connor & Harvey, 2008). Knowing more about how reactivity changes with hyporheic zone depth throughout the same fluvial network may provide insight to how benthic biolayer and deeper hyporheic zone contributions to riverine materials processing scale.

Field tracer studies may provide an answer to improve variable reactivity predictions across multiple stream networks (McGuire & McDonnell, 2015; Abbott et al., 2016). The development of reactive tracer studies provides a possible path forward to better characterize variable hyporheic zone contributions to overall riverine processing from shallow and deeper depths. Biogeochemical processes have been previously been quantified using chemically reactive tracers and their application provides an *in situ* measurement of hyporheic zone reactivity (Haggerty et al., 2008; González-Pinzón & Haggerty, 2013; Lemke, et al., 2013; Knapp & Cirpka, 2018;). The addition of multi-depth sampling to reactive tracer tests allows for the direct quantification of variable hyporheic zone contributions from the benthic biolayer and deeper hyporheic zone depths without disturbing the naturally occurring range of flowpath variability and travel time distributions (González-Pinzón, et al., 2015; Knapp et al., 2017, 2018). Additionally, the combination of these two techniques can support the direct measurement of variable streamed reactivity contributions and be easily applied across a variety of fluvial networks so long as the recommendations of González-Pinzón et al. (2015) to have clearly defined questions and identified spatiotemporal scales of interest are carefully considered.

In this study we performed three reactive tracer tests in three unique stream order reaches from the same 4th order fluvial network to address the following questions: (1) how variable are subsurface contributions to hyporheic exchange along shallow, downwelling flowpaths; and (2) how does hyporheic zone reactivity vary within and between different stream orders of the same fluvial network? The goal of this study was to (a) quantify contributions of the shallow subsurface to streambed reactivity and (b) identify hyporheic exchange variability within and between different stream order sections from a 4th order fluvial network. This paper presents results from three reactive tracer tests that were completed in three sequential stream orders of

the Jemez River, New Mexico. Tracer breakthrough curves (BTCs) were collected directly from the pore waters at two sampling locations that were variable distances from our tracer injection location in each studied stream order. We chose to study subsurface-scale hyporheic zone processing at two locations within each stream order to better capture inter- and intra-spatial variability within and between different stream order reaches.

We analyzed the BTCs using previously a published subsurface transient storage model that reflects the internal structure of the hyporheic zone through the analysis of BTC depth profiles (Knapp et al., 2017). The subsurface model presented by Knapp et al. (2017) considers vertical advective-dispersive-reactive transport and compartmentalizes the hyporheic zone as a series individual layers with distinct reactivity and groundwater inflows. Thus, this particular model conceptualization represents the vertical component of dowelling hyporheic flow paths but does not make assumptions about hyporheic water returning to the stream. We demonstrate that hyporheic exchange contributions vary with depth within the same stream order and subsurface reactivity does not always scale as expected with increasing stream order. This study advances our understanding of streambed reactivity spatial variability and can be used to improve predictions of watershed function as they pertain to making basin-wide water quality management decisions.

Methods

We completed our tracer tests in unique three stream orders located in the Jemez River watershed during May 2016 (Fig 3.1a). The Jemez River is located in northern New Mexico and drains an area of approximately 2,678 km^2 before joining the main stem of the Rio Grande. The upper portion of the watershed is comprised of forests and riparian zone grasslands (Coop &

Givnish, 2007; Small & McConnell, 2008). The region is characterized by a semi-arid continental climate with temperatures ranging from 5.4 °C in January to 15 °C in July (New Mexico Climate Center, 2018). At higher elevations in this region, precipitation, including rain and snowfall, averages 639 mm yr^{-1} (New Mexico Climate Center, 2018). During our study, observed Jemez River streambed substrates comprised of poorly sorted small boulders, gravel, sand, and included a range of silt and clay size fractions.

Our three tracer experiments took place between 16 May and 21 May 2016 in the 2nd, 3rd, and 4th order reaches of the Jemez River (Fig. 3.1a; Table 3.1). All study sites were located north of Jemez Pueblo, New Mexico. Reach travel distances between the injection location and our two sampling stations, upstream station at Site A and downstream station at Site B (Fig. 3.1b), were determined using recorded GPS coordinates and Google Earth imagery (Google Earth, Google, Mountainview, California, USA). In-stream discharge was measured at the injection and at both downstream sampling stations with an acoustic Doppler velocimeter (SonTek/YSI FlowTracker ADV; SonTek, San Diego, California, USA). Our experiments took place during the annual spring snowmelt period and resulted in wetter hydrologic conditions with relatively higher values of surface water discharge than summer baseflow in the region. *In situ* surface water temperature was monitored with multiparameter water quality sondes (EXO2 Sonde, YSI Incorporated, Yellow Springs, Ohio, USA). Reach travel distances, measured discharge, and mean water temperature can be found in Table 3.1.

To assess intra- and inter-reach spatial variability of hydraulic conductivity, K (cm/s), 15 measures of *in situ K* were carried out along each stream reach following methods detailed by Datry et al. (2015). For each reach, we performed a simplified falling head slug test to estimate *in situ K* (Lee & Cherry, 1979; Butler, 1998; Baxter et al., 2003Genereux et al., 2008). We

constructed a set of PVC, minipiezometers to use for our slug tests following the specifications and procedure noted in Datry et al. (2015) and integrated the slug test equation between different water levels in the stream and inside the minipiezometer (Hvorslev, 1951; Chapuis, 1989). In addition to our simplified falling head slug tests, five streambed sediment grab samples of ~300 g were collected from each sampling location to determine dry bulk density, porosity, and grain size for each stream order sampling location. For more information on the methods used for the sediment analysis please see work by Vomocil (1965), Cui et al. (1996), Wroblicky et al. (1998), and Fetter, (2001).

Table 3.1. Site and Injection Characteristics. Study sampling date, stream order, discharge at the upstream site A and downstream site B (m^3/s), distance from the injection location to upstream Site A and downstream Site B (m), mean water temperature ($°C$), elevation above sea level (km), and the injected tracer masses (g).

Sampling Date	Stream Order	Q at A (m^3/s)	Q at B (m^3/s)	Distance Inj. to A (m)	Distance Inj. to B (m)	Mean Water Temp. (C°)	Elevation (km)	Mass Injected NaBr (g)	Mass Injected Raz (g)
16-May	2	0.11	0.12	1459	3548	21.00	2.68	152	28
20-May	3	0.50	0.51	1770	6340	14.20	2.45	500	30
21-May	4	0.78	0.70	2225	8215	19.18	1.81	1400	133

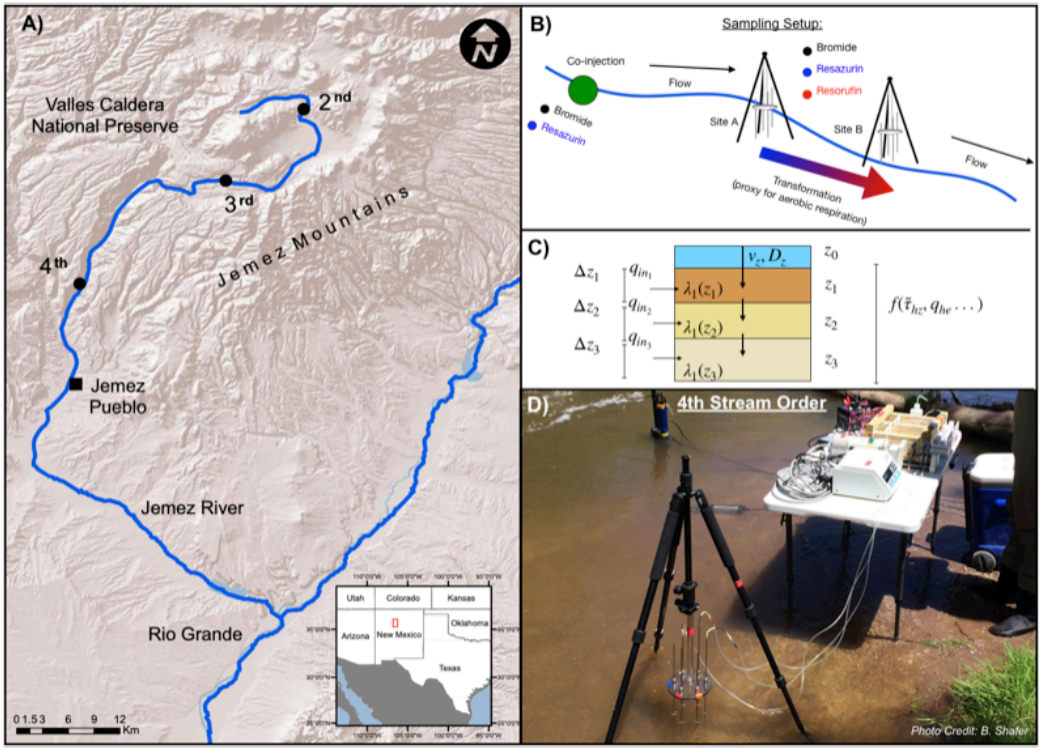

Figure 3.1. Site map, sampling set up, model conceptualization, and field photo. A map of the Jemez River with **(a)** our stream order reaches noted with black circles; **(b)** diagram detailing the field sampling set up at each study reach where bromide and resazurin were co-injected upstream of two sampling stations, Site A and Site B, that were instrumented with a single USGS MINIPOINT sampler at each site location; **(c)** the transient storage model conceptualization (parameters are defined in the text below) used for our analysis at each site location, considering in-stream transport to the sampler (blue box) and downwelling flowpaths through various layers of the hyporheic zone (brown boxes); **(d)** photo of the field sampling setup featuring a USGS MINIPOINT sampler from the 4th order stream reach.

Our tracer experiment was conducted in each stream order with a co-injection of bromide (Br^-) and resazurin (Raz) at the injection location (Fig. 3.1b and Table 3.1). Raz is a redox-sensitive phenoxazine dye that can be used as a reactive, "smart" tracer to estimate microbiological activity associated with stream water-sediment interactions, which make it an ideal tracer for hyporheic zone reactivity (Haggerty et al., 2008; González-Pinzón et al., 2012; Knapp et al., 2018). Under mildly reducing conditions, Raz, which is weakly fluorescent, undergoes an irreversible reduction to its highly fluorescent daughter product, resorufin (Rru). The transformation from Raz to Rru can be used to investigate metabolic processes and hyporheic exchange because it is a function of oxygen turnover in the presence of living cells and serves as a proxy of streambed respiration (Argerich et al., 2011; González-Pinzón et al., 2012, 2014, 2015; Knapp & Cirpka, 2018). Throughout our three tracer tests, we sampled depth profile breakthrough curves (BTCs) of Br^-, Raz and Rru at each of our two stream sampling stations and used them as inputs for our subsurface transient storage model (Fig. 3.1c).

Table 3.2. USGS MINIPOINT Sampler locations and depths. USGS MINIPOINT sampler locations where Site A denotes the upstream location and Site B denotes the downstream location, sampling depths (cm), and a brief description of the surrounding sampler geomorphology.

Sampling Date	Stream Order	Sampling Station Site	Sampling Depths (cm)	Sampler Location Geomorphology
16-May	2	A	3, 6	Pool Margin
16-May	2	B	3, 5	Pool Margin
20-May	3	A	4, 10	Long Run
20-May	3	B	3, 7, 11	Riffle
21-May	4	A	3, 9	Long Run
21-May	4	B	3	Pool

During our tracer tests, water samples from the shallow sub-surface were collected. simultaneously from several depths at upstream, Site A, and downstream, Site B, locations in our three studied stream orders using USGS MINIPOINT samplers (Fig. 3.1d) (Duff et al., 1998; Harvey & Fuller, 1998; Harvey et al., 2013). The samplers were located across variety of geomorphic features and water samples were collected from depths that ranged from 3 to 11 cm in the streambed (Table 3.2). Water samples were collected from additional depths that did not have Br^- BTC signals that were discernable from background noise were dropped from the subsequent analysis.

Small diameter (1/8" nominal outside diameter), stainless steel tubes, with three 1 cm pore water sampling slots, were positioned in the streambed by gently pushing each tube into the streambed until the desired sampling depth was reached. Small-volume (15 mL) water samples were pumped at low rates (< 2 mL min^{-1}). Using USGS MINIPOINT samplers allowed for hyporheic flow path sampling at multiple depths without disturbing natural subsurface solute gradients at two locations within each of our stream order reaches (Harvey & Fuller, 1998; Knapp et al., 2017).

Each USGS MINIPOINT sampler was used to collect pore waters at multiple sampling depths below the streambed surface, where possible, that were determined based on the underlaying streambed geomorphology (Table 3.2). Surface water samples were collected with 60 mL plastic syringes. Please see the Methods section in Chapter 4 for more information about our surface water sampling procedure. A simultaneous co-injection of $NaNO_3^-$ allowed us to monitor the tracer signal in real-time using a multiparameter water quality sensor connected to a field laptop (EXO2 Sonde, YSI Incorporated, Yellow Springs, Ohio, USA) and allowed us to adjust our sample collection times accordingly. Simultaneous water samples from all depths

were collected at 8 min intervals throughout the rising and falling limbs of our tracer co-injections. During the tails of the tracer injections, the sample collection intervals were decreased to every 16-60 min. Subsurface water samples were pumped from the streambed at each site using a multi-head DC variable speed pump and pumped through size 13 Masterflex Noprene/tygon tubing before inline filtration. All pump lines terminated at press-on luer fittings that were fitted with filter holders that contained nylon membrane filters (0.45 μm pore size, 25-mm diameter). All water samples were filtered directly into 20-mL polyethylene plastic scintillation vials with polypropylene caps and stored on ice and in the dark until they could be analyzed in the laboratory within 48 h after sampling.

Each collected water sample was aliquoted (~1 mL) and buffered to a pH 8.5 before fluorescence was read (Haggerty et al., 2008, 2009). All water samples were analyzed for Raz and Rru fluorescence signals with a spectroflurometer (Varian Cary Eclipse; Santa Clara, California) at excitation/emission wavelengths of 602/632 nm for Raz and 571/584 nm for Rru. Fluorescence readings were converted to concentrations with the help of calibration standards. The limit of quantification (LOQ) for Raz was 1.01 x 10^{-1} $mol\ L^{-1}$ and 1.67 x 10^{-3} $mol\ L^{-1}$ for Rru. The remaining sample portions were frozen at -20 °C and stored in the dark until they could be thawed and analyzed for Br^- with ion chromatography using a Dionex ICS-1000 Ion Chromatograph with AS23/AG23 analytical and guard columns, and a 1000-μl injection loop with a Br^- analytical limit of detection (LOD) of 1.67 x 10^{-3} $mol\ L^{-3}$ (Thermo Fisher Scientific Inc.; Sunnyvale, California).

The transient storage model used for this analysis describes reactive transport within the subsurface as water moves vertically from the stream into the streambed hyporheic zone, developed by Knapp et al. (2017). This model was adapted for an admixture of groundwater that

occurs during surface water downwelling through the hyporheic zone and describes shallow vertical subsurface transport as a function of streambed sampling depth (Fig. 3.1c). Results were derived from modeled hyporheic zone that was compartmentalized into layers of varying reactivity during downwelling. For this model, we assume that hyporheic waters are not fully mixed with the surface waters and therefore cannot provide information about upwelling hyporheic water. We simulated tracer BTCs using the tracer data collected from the surface water and with USGS MINIPOINT samplers at each of our two downstream sampling locations (Duff et al., 1998; Harvey et al., 2013). The governing equations for each hyporheic zone tracer concentration, $C_{i,hz}$ (where $i = 0 = Br^{-}; i = 1 = Raz; i = 2 = Rru$), include:

$$\frac{\partial c_{0,hz}}{\partial t} + v_z \frac{\partial c_{0,hz}}{\partial z} - D_z \frac{\partial^2 c_{0,hz}}{\partial z^2} = q_{in}\left(c_{0,GW} - c_{0,hz}\right) \quad (1)$$

$$R_{1z} \frac{\partial c_{1,hz}}{\partial t} + v_z \frac{\partial c_{1,hz}}{\partial z} - D_z \frac{\partial^2 c_{1,hz}}{\partial z^2} = -\lambda_1 c_{1,hz} + q_{in}\left(c_{1,GW} - c_{1,hz}\right) \quad (2)$$

$$R_{2z} \frac{\partial c_{2,hz}}{\partial t} + v_z \frac{\partial c_{2,hz}}{\partial z} - D_z \frac{\partial^2 c_{2,hz}}{\partial z^2} = -\lambda_2 c_{2,hz} + \lambda_{12} c_{1,hz} + q_{in}\left(c_{2,GW} - c_{2,hz}\right) \quad (3)$$

where z $[cm]$ represents the vertical spatial coordinate along the hyporheic zone flow path, simplified as sampling depth; and q_{in} $[s^{-1}]$ denotes a rate coefficient accounting for groundwater mixing, which can be interpreted as added groundwater discharge to the stream water per volume of pore space. The transport parameters, v_z and D_z, characterize apparent vertical transport as velocity $[m\ s^{-1}]$ and dispersion $[m^2\ s^{-1}]$ with depth. The transformation rate coefficients are represented by λ_1 $[s^{-1}]$, the total Raz transformation rate coefficient; λ_{12} $[s^{-1}]$, the transformation of Raz to Rru rate coefficient; and λ_2 $[s^{-1}]$ is the Rru transformation rate coefficient. The equilibrium sorption coefficients of Raz and Rru in the hyporheic zone are represented by R_1 and R_2 $[-]$, respectively. Both coefficients assume linear sorption at local equilibrium. The concentration of compound i in the groundwater is represented by

$c_{i,GW}$ $[mol\ m^{-3}]$, where all admixed groundwater has an initial $c_{i,GW} = 0$ for all tracer compounds added to the stream. Thus, the net effect of groundwater mixing is dilution, which is equivalent to a first-order transformation with the rate coefficient, q_{in} $[s^{-1}]$. Groundwater dilution in our transient storage model is represented as lateral inflow that influences all tracer concentrations at every sampled hyporheic zone depth section. Additionally, the effects of the transformation rate coefficients $[s^{-1}]$ for Raz, λ_1, and Rru, λ_2, are exclusive to the non-conservative compounds Raz and Rru.

All hyporheic transport equations were solved between two consecutive hyporheic zone layers where the shallower BTC depth becomes the fixed-concentration upstream boundary condition for the subsequent BTC depth. To solve these equations, we assumed a semi-infinite domain and solved the system of equations analytically in the Laplace domain, followed by a numerical back-transform into the time domain (Hollenbeck, 1998; Knapp et al., 2017). All estimated parameters were calculated as a function of depth z $[cm]$ and allowed to differ between depth compartments. A depth compartment is defined as the depth section between two consecutive USGS MINIPOINT sampling ports.

Model parameter estimation was completed using the *Differential Evolution Adaptive Metropolis* (DREAM (ZS)) algorithm (Vrugt et al., 2009). DREAM (ZS) is a self-adaptive Markov chain Monte Carlo (MCMC) algorithm that automatically updates the scale and orientation of the parameter distribution during sampling (Vrugt et al., 2008; Laloy & Vrugt, 2012; Vrugt, 2016). DREAM (ZS) samples from an archive of past model parameter states to generate new parameters sets and provide correlated parameter uncertainties (Knapp et al., 2017; Knapp & Cirpka, 2017). All parameters were guided by previously published values and constrained to be non-negative (Haggerty et al. 2008; Haggerty et al. 2009; Lemke et al. 2013;

Knapp et al. 2017; Knapp and Cirpka 2017). The Raz and Rru retardation coefficients parameter lower limits were set to 1. Our parameter estimation procedure was completed in two steps. First, parameters for Br^- and Raz were jointly estimated, followed by an estimation of the Rru-specific parameters. Simulated BTCs represented the best fitting parameters obtained from a forward run after the burn-in period evaluations were discarded. Model goodness of fit was assessed using a normalized residual sum of squares (*nRSS*) $[-]$, where the sum of squared residuals was normalized by the squared theoretical peak tracer concentrations of each tracer BTC. A thinning rate of 10 was applied to the estimated parameter sets during all optimization runs to reduce autocorrelation between successively stored parameter chains. Sampled chain convergence was monitored using the Gelman and Rubin (1992) $\hat{R}$ statistic with a desired threshold of 1.2. For further details on the model parameter estimation procedure, please see Knapp et al. (2017).

To better evaluate and compare hyporheic exchange contributions within and across our different stream orders, we decide to evaluate a number hyporheic zone metrics based on equations presented in Knapp et al. (2017) using the model results at each sampling station. Our first analysis step was to evaluate the tracer mass recoveries using the zeroth temporal moments of our simulated BTCs at each sampling depth (Harvey & Gorelick, 1995; Lemke et al., 2013; Liao et al., 2013). The zeroth temporal moments, $\mu_{0,i}$ $[mol.s.m^{-3}]$, over time t $[s]$ for Br^- $(i = 0)$ and Raz $(i = 1)$ were defined at each sampling depth, z (cm), were defined as:

$$\mu_{0,i} = \int_0^\infty c_i(z,t)dt. \tag{4}$$

The recovery of the conservative and reactive tracers along the subsurface depth profiles were used to determine the average hyporheic zone depth at the different stream sampling locations (Knapp et al., 2017). The values of the tracer recoveries were exponentially interpolated layer-wise and exponentially extrapolated. Average hyporheic zone depth, $\tilde{d}_{hz}$ $[cm]$,

of Br^- and average hyporheic zone depth, $\tilde{d}_{reac}\ [cm]$, of Raz were quantified by calculating the depth integral of each tracer recovery:

$$\tilde{d}_{hz} = \int_{z=0}^{\infty} X_{rec}^{br}(z)dz \tag{5}$$

$$\tilde{d}_{reac} = \int_{0}^{\infty} X_{rec}^{raz}(z)dz \tag{6}$$

where detailed derivations of the integrated conservative tracer recovery, $X_{rec}^{br}\ [-]$, and reactive tracer recovery, $X_{rec}^{raz}\ [-]$, as functions of depth from the simulated BTCs for each depth sampled with a USGS MINIPOINT sampler can be found in Knapp et al. (2017).

Hyporheic zone residence time, $\tau(z)\ [s]$, for the subsurface BTCs were then calculated based on an analysis from Knapp et al. (2017) that used the first temporal moments of the conservative tracer as a function of depth:

$$\tau(z) = \int_{0}^{z} \frac{1}{v_{0*}(\zeta)} d\zeta \tag{7}$$

where $z\ [cm]$ represents the sampling depth and $v_{0*}\ [m\ s^{-1}]$ is the celerity of Br^- in the subsurface depth compartments.

Additionally, the mean hyporheic zone residence time of the downwelling stream water at each sampling station was estimated using the recovery-weighted average of $\tau(z)$:

$$\tilde{\tau}_{hz} = \frac{1}{\tilde{d}_{hz}} \int_{0}^{\infty} \tau(z) X_{rec}^{br}(z)dz \tag{8}$$

where $\tilde{d}_{hz}\ [m]$ is the equivalent hyporheic zone depth from the depth-integral of the conservative tracer recovery profile and $X_{rec}^{br}(z)[-]$ is the conservative tracer recovery at depth. The mean hyporheic zone residence time of the reactive tracer was calculated similarly to equation (7), where $v_{1*}\ [m\ s^{-1}]$ is the celerity of the Raz in the subsurface:

$$\tilde{\tau}_{reac} = \int_{0}^{z} \frac{R_1}{v_{1*}(\zeta)} d\zeta \tag{9}$$

Since the subsurface model simulates water entering the hyporheic zone, no assumptions were made about the remaining stream channel water (Knapp et al., 2017). Thus, the exchange rate $q_{he}[s^{-1}]$ between the stream and the hyporheic zone at the sediment water interface was calculated from the uppermost layer with:

$$q_{he} = \frac{v_z}{\theta w_{hz}} \tag{10}$$

where v_z $[m\ s^{-1}]$ is downwelling water velocity, $\theta[-]$ is streambed porosity, and w_{hz} $[m]$ is the hyporheic zone width approximated from the measured active channel width.

Results and Discussion

Measured stream water discharge ranged from 0.11-0.79 $m^3 s^{-1}$ (Table 3.1). Discharge increased with increasing stream order and increased between the upstream sampling station, Site A, and downstream sampling station, Site B, expect in the 4th stream order where discharge decreased between Site A and Site B (Table 3.1). This decrease in measured discharge can be explained by the geomorphology differences at the 4th order sampling locations, as the Site B was located in a pool with slower moving waters (Table 3.2). *In situ* hydraulic conductivity (0.04 ± 0.05 - 0.07 ± 0.03 $m\ s^{-1}$) and porosity (24-50 %) were similar between the pairs of sampling stations within each stream order (Table 3.3). Values of dry bulk density, which ranged from 0.79 ± 0.32 - 1.59 ± 0.26 $g\ cm^3$ across all sites, were similar between Site A and Site B in the 3rd and 4th stream orders, whereas dry bulk densities from the 2nd stream order were almost twice as high at Site B when compared to Site A (Table 3.3). The lower dry bulk density at the 2nd stream order Site A indicated that the upper reach sediments at this site were less compacted than the other stream order sediments. Porosity ranged from 0.27 in the 3rd stream order to 0.52 in the 2nd stream order and was most variable between sampling sites in the 2nd stream order.

Average grain size proportions revealed similar gravel and sand size particle percentages across most stream order sites, except at Site B in the 4th stream order, where sand sized particles were the dominant size class. This increase in sand size particles was expected due to the arid landscape surrounding this stream reach (Table 3.3). The sites sampled in the 2nd order stream reach had relatively more fine particles that the other studied stream order continuum (Vannote et al., 1980; Sedell et al., 1989; Magliozzi et al., 2018;). The higher fine particle percentage and lower hydraulic conductivity values from the 2nd stream order, suggest that as finer particles fill pore spaces, exchange flows between the surface water and hyporheic zone are reduced.

Table 3.3. Sediment sample results. Sampling date, stream order, sampling station where A indicates upstream and B indicates downstream, average *in situ* hydraulic conductivity, K, $(cm/s) \pm 1\sigma$, average *ex situ* dry bulk density, ρ, $(g/cm^3) \pm 1\sigma$, porosity, θ $(-)$, sample percent gravel, sand, and fines.

Sampling Date	Stream Order	Sampling Station	K (cm/s)	ρ (g/cm^3)	θ (-)	Gravel (%)	Sand (%)	Fines (%)
16-May	2	A	0.04 ± 0.05	0.79 ± 0.32	0.52	52.90	46.28	1.25
16-May	2	B	0.04 ± 0.06	1.10 ± 0.15	0.49	40.94	54.28	4.99
20-May	3	A	0.06 ± 0.03	1.59 ± 0.26	0.27	54.94	44.52	0.68
20-May	3	B	0.06 ± 0.04	1.45 ± 0.28	0.27	49.78	50.15	0.13
21-May	4	A	0.07 ± 0.02	1.47 ± 0.44	0.31	56.49	45.56	0.83
21-May	4	B	0.07 ± 0.03	1.41 ± 0.47	0.38	19.70	80.16	0.23

We obtained eight unique, best-fit transient storage model parameters for sampling location from the analysis of 36 subsurface BTCs in total. All simulated model parameters were within the expected ranges given the differences in hydrology for three studied stream orders (Appendix 3.1). The upper boundary condition for each depth profile was bounded by the simulated surface water BTCs from 18 measured BTCs at each sampling location. Plots of the surface and subsurface BTCs can be found in Appendix 3.2, Appendix 3.3, and Appendix 3.4.

Measured tracer concentrations were generally higher in the surface water and decreased with increasing sampling depth and study site distance from the injection location. The measured zeroth temporal moments and tracer mass recoveries also decreased with depth, indicating increasing Br^- dilution with depth due to the admixture of groundwater in the subsurface (Appendix 3.5 and Appendix 3.6). Successively less tracer mass recovery, and thus less clearly defined BTCs, along our depth profiles can be attributed to the higher transformation potential of the upper hyporheic zone layers and increasing groundwater dilution with depth. This was expected as reactivity is higher in the benthic biolayer and is consistent with other studies (Boulton, 2007; Arnon et al., 2013; Knapp et al., 2017).

For both tracers, the upstream sampling location at Site A typically, had better subsurface tracer recovery, which was expected due to the shorter travel length between the injection and Site A. The largest groundwater dilution of ~76% occurred between depth 1 (3 cm) and depth 2 (7 cm) at Site B in the 3rd stream order (Appendix 3.6). For Raz, the decrease in the zeroth temporal moments and tracer mass recoveries were likely due to a combination dilution and transformation to its daughter product, Rru (Appendix 3.5 and Appendix 3.6). The largest Raz dilution and transformation of ~78% occurred between depth 1 (3 cm) and depth 2 (7 cm) at Site B in the 3rd stream order.

Each of our model parameter estimates from the joint fit of Br^- and Raz resulted in an $\hat{R}$ statistic (Gelman and Rubin 1992) that confirmed good parameter convergence. The quality of the model simulations, as indicated by the *nRSS* values in Appendix 3.1, were fairly robust for most Br^- fits and all Raz fits. Model fits did not always increase in *nRSS* with sampling depth, as was the case for Knapp et al. (2017). Thus, our tracer signals were more variable with depth than expected. This was confirmed with by the additional signal noise and poorer tracer mass recovery in the measured subsurface BTCs. Notably, sampling depth 2 (10 cm) from Site A in the 3rd order stream and sampling depth 1 from Site A (3 cm) in the 4th order stream had higher $nRSS_{br}$ values, indicating greater uncertainties in these Br^- model fits. The higher uncertainty at Site A in the 3rd order stream is due to the underestimation of the Br^- and could be due the larger distance between this and the prior sampling depth. Uncertainty at Site A in the 4th order stream was also due to a slight Br^- BTC peak underestimate. However, since the parameter convergence values were acceptable at these sites we chose to keep these sampling depths in the analysis to better capture possible reactivity scenarios at these two locations.

The second estimation for the Rru-specific parameters did not always result in acceptable parameter convergence and generally higher parameter uncertainties, as indicated by larger $nRSS_{rru}$ values when compared to the *nRSS* value for the other tracers. These Rru-specific uncertainties are likely related to error propagation from the Br^- and Raz joint fit and the low concentrations of Rru in the subsurface sampling depths. Thus, we elected to interpret hyporheic processes based on the transformation of Raz alone due to the higher Rru-related parameter uncertainties. Rru measurements were used to confirm that the measured Rru BTCs could be simulated with the estimated model parameters (Knapp et al., 2017). Model parameter interactions were analyzed with the DREAM(ZS) postprocessing toolbox to determine parameter

correlations from the joint-fit of Br^- and Raz (Vrugt et al., 2009). The resulting marginal distributions and two-dimensional correlations of the posterior parameter samples of can be found in the Appendix 3.7 – Appendix 3.18.

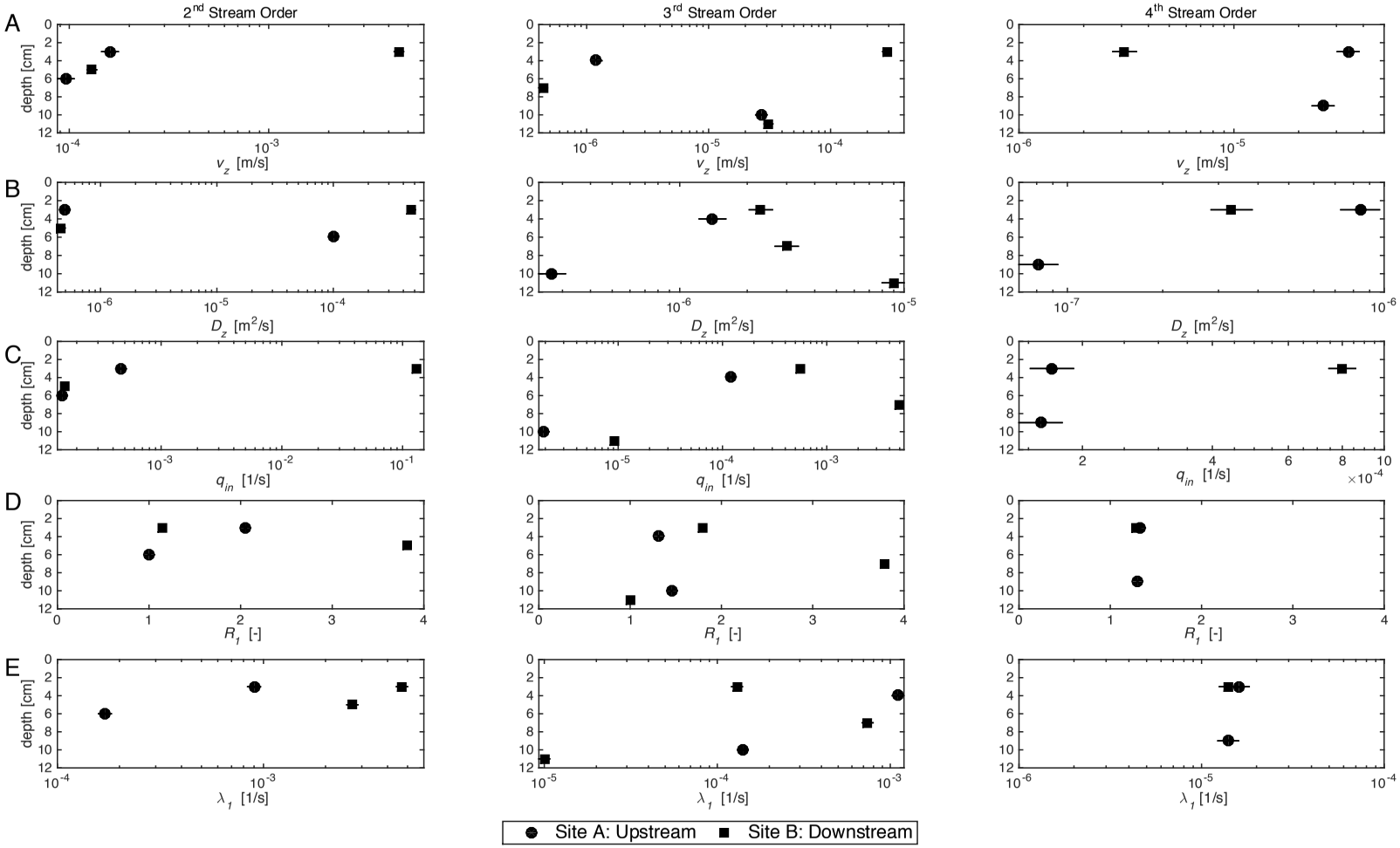
A
B
C
D
E
2nd Stream Order
3rd Stream Order
4th Stream Order
depth [cm]
v_z [m/s]
D_z [m^2/s]
q_{in} [1/s]
R_1 [-]
λ_1 [1/s]
Site A: Upstream
Site B: Downstream

Figure 3.2. Sampling depth versus model parameters. Sampling depth versus model parameters from the subsurface model fits along the downwelling flowpaths, where the circles indicate the upstream location, Site A, and the squares indicate the downstream location, Site B, and the horizontal bars represent ± 1 σ. v_z $[m\ s^{-1}]$ is apparent velocity; D_z $[m^2\ s^{-1}]$ represents the dispersion coefficient; q_{in} $[s^{-1}]$ represents the dilution factor; R_1 $[-]$ is the retardation factor of resazurin; and λ_1 $[s^{-1}]$ is the total resazurin transformation rate coefficient.

The model parameters from the joint-fit estimate are plotted with depth in Figure 3.2 for each stream order sampling station. Within the 2nd order stream, most parameters decreased with depth at each sampling station as was expected with increasing vertical distance away from the surface waters due to increasing dilution and anoxic conditions. However, dispersion, D_z, increased with depth at Site A and the total Raz transformation rate coefficient, R_1, increased with depth at Site B, indicating that the spreading of both conservative and reactive tracer fronts was influenced by different geomorphic and hydrologic factors within the 2nd order stream. The shallowest sampling depth (3 cm) at Site B had parameter values that were higher by at least one order of magnitude than the other sampled depths, indicating unique processing dynamics at this downstream location. This same sampling depth at Site B, had the highest level of groundwater influence, q_{in}, and reactivity, inferred from the total Raz transformation rate, λ_1, suggesting that this region of the streambed had the greatest potential for hyporheic exchange. Additionally, both sampling stations from the 2nd stream order had higher potential reactivity at the shallower sampling depths, supporting the benthic biolayer concept where reactivity is highest in the benthos when compared to the hyporheic zone.

Parameter estimates from the 3rd order stream did not follow the expected pattern of decreasing with increasing sampling depth at both sites. Apparent velocity, v_z, increased with depth at Site A and was more variable at Site B, while D_z decreased with depth at Site A and increased with depth at Site B. q_{in} and λ_1 followed similar patterns of decreasing with depth at Site A and at Site B both parameter values were higher at depth 2 (7 cm). This unexpected pattern at Site B demonstrates that the admixture of groundwater, in addition to the slowing of v_z and increase in R_1 at this middle depth, increased the potential for reactivity relatively deeper into the hyporheic zone. The differences in the potential reactivity between the 3rd stream order

sites reflect the differences in geomorphology, as Site A was located in a long run and Site B was located in a riffle environment. Values of λ_1 were highest in the shallowest sampling depths, further demonstrating that the benthic biolayer has a higher reactivity potential. However, at Site A the shallowest sampling depth (4 cm), λ_1 was higher than λ_1 at the shallowest depth from Site B (3 cm), indicating that potential reactivity along downwelling flowpaths is influenced by factors related to spatial heterogeneity including streambed geomorphology and groundwater inflows.

The 4th order stream upstream location at Site A followed expected patterns of decreasing parameter values with increasing depth, further supporting the existence of a potential benthic biolayer at this site. However, the differences in most parameter values, except for D_z, were within the same order of magnitude indicating that there was not very much difference in transport and reactive process controls between the two sampling depths of 3 cm and 9 cm. Since Site B only had one sampling depth that was analyzed (3 cm), we cannot infer how reactivity may change with deeper hyporheic zone depths. Interestingly, Site B had a much higher q_{in} value than Site A, which was expected because the downstream site was located in a pool environment while the upstream site was located in a longer run. However, values of R_1 and λ_1 were similar at the shallowest sampling depths from Site A and Site B, demonstrating that factors influencing Raz behavior were similar across two different geomorphic features in the 3rd order stream.

When we compare our parameter estimates across our sampling locations, several patterns were evident from the threes studied stream orders. First, the parameters of apparent vertical transport, v_z and D_z, did not always decrease with depth as expected in the 3rd stream order. This may be explained by groundwater inflow, as indicated by increases in q_{in} with depth

at both sampling locations in this stream order. More variable q_{in} in the 3rd stream order may also explain why these model parameters differ than the 2nd and 4th stream order parameter depth profiles. Second, our λ_1 results from each sampling station were typically higher at the shallowest sampling depth, with the exception of depth 2 (7 cm) of the Site B in the 3rd stream order, suggesting the presence of a benthic biolayer with a higher reactivity potential than the deeper hyporheic zone sediments across most studied stream order locations, similar to the findings of Knapp et al. (2017) and Schaper et al. (2019).

And lastly, our transient storage model parameter ranges were generally highest in the 2nd order stream, followed by the 3rd and 4th stream orders, respectively, indicating that we can reasonably expect transient storage parameters to decrease when scaling up hyporheic exchange parameters related to downwelling flowpaths. However, this was not always the case, as values of q_{in} from the 3rd order stream were on the lower end of the study range and smaller than the 4th stream order. This suggests that parameters influencing hyporheic exchange may not always scale as expected, especially with variable groundwater inflows. We except that if the same tracer studies were performed under different flow conditions, such as baseflow or extreme drought, we would find different parameter relationships with increasing stream order. Thus, caution is needed to avoid overinterpreting a noted pattern or trend as the standard hyporheic exchange scaling relationships, especially when they are closely linked to prior and current hydrologic conditions (Kurz et al., 2017; Rana et al., 2017).

A suite of metrics was calculated to better compare hyporheic exchange variability within and across our studied stream orders (Appendix 3.18; Fig. 3.4). Each metric was calculated for the hyporheic zone where each sampler was located within each stream order. These calculations allow for a direct comparison between sampling stations, regardless of the number of available

sampling depths. Mean residence times based on the conservative, $\tilde{\tau}_{hz}$, and reactive, $\tilde{\tau}_{reac}$, tracers differed within and across all studied stream orders and were throughout the 3rd order stream (Appendix 3.18; Fig. 3.4a and Fig 3.4b). $\tilde{\tau}_{reac}$ values represented the residence time of the Raz and were lower than $\tilde{\tau}_{hz}$ because the reactive tracer residence time was influenced by conservative transport and *in situ* reactions throughout the hyporheic zone. Both residence time values were consistently longer at the upstream sampling locations which was a function of how hydrologic conditions, including in-stream velocity and groundwater dilution, local geomorphology, and sampling distance from the injection location influence downwelling hyporheic flowpaths.

The sampled depth profiles allowed us to quantify the mean hyporheic zone depth, $\tilde{d}_{hz}$, at each of our study locations (Appendix 3.18; Fig. 3.4c). $\tilde{d}_{hz}$ ranged from 2. cm at Site B in the 4th stream order to 65 cm in at Site A in the 3rd stream order. The wide range of $\tilde{d}_{hz}$ are reflected by the maximum sampling depths and underlying streambed conditions, in addition to the conservative tracer mass recovery. Our range of $\tilde{d}_{hz}$ was larger than the hyporheic zone sampling depths found in Knapp et al. (2017). Thus, the $\tilde{d}_{hz}$ results from Site A in the 3rd stream order may reflect an even higher influence from less groundwater contributions on the conservative tracer recovery, as the mean residence times were the longest at this location.

The mean hyporheic zone depth of Raz, $\tilde{d}_{reac}$, reflects the active portion of the hyporheic zone that contributes to the streambed reactivity potential at each sampling location and serves as proxy for the depth extent of the benthic biolayer (Appendix 3.18; Fig. 3.4d). Values of $\tilde{d}_{reac}$ were always smaller than $\tilde{d}_{hz}$ because they represent the highly reactive benthic biolayer portion of the streambed and also explain why $\tilde{\tau}_{reac}$ was smaller than $\tilde{\tau}_{hz}$ (Knapp et al., 2017). $\tilde{d}_{reac}$ ranged from ranged from 2 cm at Site B in the 4th stream order to 16 cm in at Site A in the 2nd

stream order, which reflects a range of reactive depths across our studied stream orders. $\tilde{d}_{reac}$ at Site B was shallower than Site A in the 2nd and 4th stream orders, while $\tilde{d}_{reac}$ was deeper at the Site A in the 3rd order stream. This supports the unique behavior of the 3rd order stream relative to the connecting stream order reaches.

When we compare $\tilde{d}_{reac}$ as a fraction of $\tilde{d}_{hz}$, we can see the relative contributions of the benthic biolayer to the overall hyporheic zone depth (Table 3.4). The reactive portion of the hyporheic zone made up a smaller fraction of the overall hyporheic zone depth at Site A in the 3rd and 4th stream orders, whereas Site A had a larger reactive hyporheic zone contribution than Site B in the 2nd stream order. These results further demonstrate intra- and inter-reach variability in the proportion of the benthic biolayer to hyporheic exchange and agree with similar studies that directly compared zones of high reactivity to overall hyporheic zone depth (Harvey et al., 2013; Knapp et al., 2017; Schaper et al., 2019).

Table 3.4. Benthic biolayer contributions to hyporheic zone depth. Relative contributions of the high reactivity benthic biolayer to overall hyporheic zone depth at each study location throughout the studied portion of the Jemez River fluvial network.

Sampling Date	Stream Order	Sampling Station	$\widetilde{d}_{reac}/\widetilde{d}_{hz}$ (%)
16-May	2	A	63
16-May	2	B	31
20-May	3	A	14
20-May	3	B	66
21-May	4	A	53
21-May	4	B	96

The transformation rate coefficients, determined from the maximum Raz transformation rate, $\lambda_{1\,max}$, provided insight into the variability in reactivity potential within the same stream order and across different stream orders (Appendix 3.18; Fig. 3.4e). In terms of inter-reach variability, $\lambda_{1\,max}$ consistently decreased with increasing stream order, indicating that when scaling the hyporheic exchange across the Jemez River fluvial network, potential reactivity decreases as streams get larger. This finding is supported by other fluvial network studies which found that the relative importance of the hyporheic zone decreases in larger order streams (e.g., Gomez-Velez et al., 2015). The decrease in $\lambda_{1\,max}$ may be due to the decrease in stream water contact time with hyporheic sediments and increasing surface water contributions (Wondzell, 2011; Harvey & Gooseff, 2015). However, this study was completed during spring snowmelt conditions and these findings are only applicable under higher water level conditions. Baseflow conditions may result in a more variable pattern of streambed reactivity potential.

Interestingly, intra-reach values of $\lambda_{1\,max}$ were more variable than their inter-reach counterparts, as the upstream sampling stations did not always have higher $\lambda_{1\,max}$ values. The 2nd stream order downstream $\lambda_{1\,max}$ value was higher than the upstream site, even though both were sampled at pool margins. Conversely, the opposite was true in the 4th stream order where the sampled long run at Site A had a higher $\lambda_{1\,max}$ value than the sample riffle at Site B. The 3rd order reach $\lambda_{1\,max}$ values were similar at Site A and Site B and demonstrate how different geomorphologies within the same reach can have similar reactivity potentials.

Hyporheic exchange rates at the sediment-water interface, q_{he}, also varied within and across our studied stream orders supporting the concept of intra- and inter-reach variability. As stream order increased, q_{he} generally decreased. q_{he} between Site A and Site B were only one order of magnitude different in the 2nd and 4th stream orders. This indicates that the upstream and

downstream locations had similar hyporheic exchange values within each stream reach. However, q_{he} varied by two orders of magnitude in the 3rd stream order, indicating greater intra-reach variability within this particular stream order.

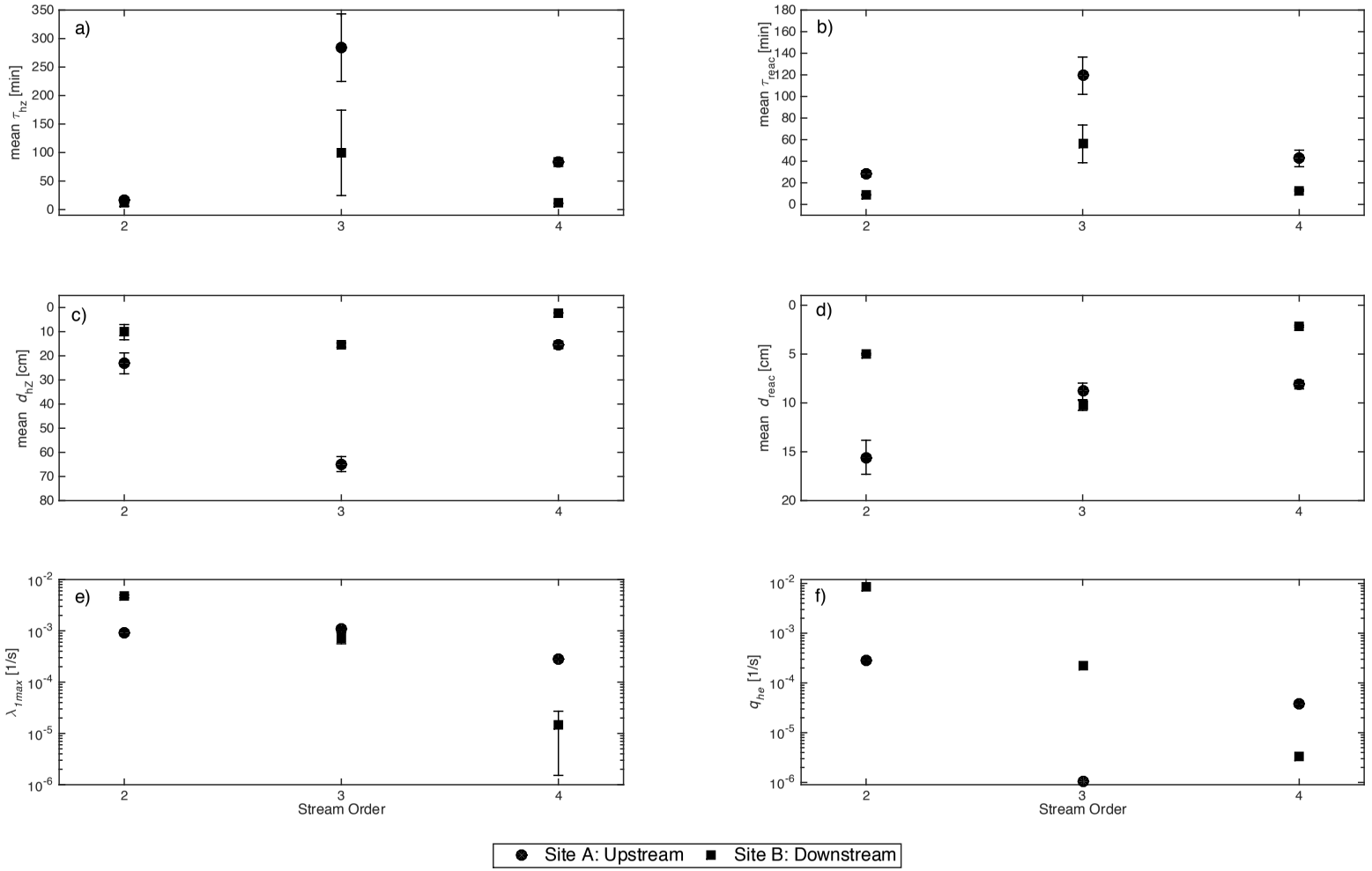
a)
mean τ_{hz} [min]
b)
mean τ_{reac} [min]
c)
mean d_{hZ} [cm]
d)
mean d_{reac} [cm]
e)
λ_{1max} [1/s]
f)
q_{he} [1/s]
Stream Order
Stream Order
Site A: Upstream
Site B: Downstream

Figure 3.3. Sampling stations metrics. Calculated hyporheic exchange metrics for each sampling station within each studied stream order including mean water age of the conservative and reactive tracer, $\tilde{\tau}_{hz}$ and $\tilde{\tau}_{reac}$, mean hyporheic zone, $\tilde{d}_{hz}$, mean reactive depth, $\tilde{d}_{reac}$, the highest decay coefficient from the given sampling station, $\lambda_{1\,max}$, and hyporheic exchange rates at the sediment water interface, q_{he}.

Conclusions

Our simulations of conservative and reactive solute transport along downwelling flowpaths were completed to provide a detailed look at the vertical, centimeter-scale resolution of hyporheic processes, which enabled us to differentiate reactivity potential from a range of hyporheic zone depths. The simulated BTCs of our measured subsurface observations, in addition to a suite of hyporheic exchange metrics, allowed us to quantify variable hyporheic exchange contributions with depth within a single stream order and across multiple stream orders from the same 4th order fluvial network. We found that hyporheic exchange contributions vary throughout the same stream order and reactivity potential along downwelling flowpaths does not always scale as expected with increasing stream order. As such, we can conclude that in the Jemez River there is a high degree of variability along hyporheic flowpaths and reactivity potential quantified for one location may not be applicable across multiple stream order reaches. Altogether, these data suggest that intra-reach and inter-reach heterogeneity play variable roles in hyporheic contributions to overall fluvial network processing.

These results demonstrate that subsurface contributions to overall hyporheic exchange vary within the same stream order and throughout a single fluvial network. The inconsistent patterns between upstream and downstream sampling locations within each Jemez River stream order displays the variability that exists along downwelling flowpaths when evaluating hyporheic zones from different geomorphic features. Our site-specific results reflect the role of streambed heterogeneity in factors controlling hyporheic exchange throughout a single stream reach. When we compare the results from three consecutive stream orders, we generally found the presence of a higher reactivity benthic biolayer but there were not always consistent patterns of decreasing hyporheic contributions with increasing stream order.

This analysis revealed that reactivity potential may not always follow longitudinal scaling expectations due to overlying surface water levels, variable groundwater dilution contributions, and the relative contribution of the benthic biolayer compared to the larger hyporheic zone extent. For example, Harvey et al. (2013) found that different geomorphic units had variable contributions to hyporheic zone reactions and water fluxes. They found that zones of higher reactivity potential had unequal contributions to overall stream denitrification due to variable controls on reaction rate constants including hyporheic exchange rate, substrate nutrient concentrations, microbe abundance, granular surface area, and the presence of anoxic microzones. Although we did not differentiate the role of individual streambed conditions on overall hyporheic zone depth and exchange, we believe that our depth profile bulk reactivity measurements derived from the use of the Raz-Rru system support the concept of variable reactivity potential throughout the benthic biolayer versus deeper hyporheic sediments. Thus, increasing our understanding of how intra- and inter-reach variably contribute to hyporheic exchange will improve our scaling predictions of streambed subsurface reactivity potential.

Variability in streambed processing at either the subsurface- (e.g. Harvey and Fuller 1998; O'Connor and Harvey 2008; Briggs et al. 2013) or reach-scale (e.g. Hall et al. 2002; Wright et al. 2005; Gooseff et al. 2013; Lemke et al. 2013) is well documented in the literature but few studies (e.g., González-Pinzón et al. 2015; Knapp et al. 2017) directly examine subsurface hyporheic exchange variability from multiple perspectives. Studies that take a multi-perspective approach, such as subsurface evaluations throughout a single fluvial network, add value by providing more information on where and when hyporheic exchange variability exists. Consequently, these results from different stream orders expand our ability to discover potential patterns in processing controls at differing spatial perspective. Many studies that approach

hyporheic exchange processing from different spatial scales generally conclude that further study and river network model development is needed to support broader applications of riverine scaling relationships. However, approaching hyporheic exchange from the from an intra- and inter-reach perspective within the same study, can help to fill processing knowledge gaps while further advancing the potential for improving predictions of hyporheic exchange scaling without the need for additional site characterization.

Furthermore, our use of a reactive tracer study from two spatial scales of interest, including groups of subsurface flow paths and by stream order, provides two spatial perspectives of hyporheic zone processing variability that exists along the river continuum (McClain et al., 2003; Abbott et al., 2016; Bernhardt et al., 2017). We also note that temporal variability is also important to understand the complex interactions between hydrological and biogeochemical processes in different stream orders and across catchments (Ocampo et al., 2006; Bernot et al., 2010). The inconsistencies spatial variability demonstrated by our results supports the need for dynamic processing control considerations when making larger-scale predictions and building scaling relationships that are transferable to other river systems (Harvey & Gooseff, 2015; Ward et al., in review, 2019). Using reactive tracer tests from multiple different locations in the same river system allows us to approach hyporheic exchange from two different spatial perspectives and is an important step towards understanding how processing controls vary in different stream order sections and how these relationships may scale across fluvial networks to better predict water quality outcomes for larger spatial scales of interest.

Acknowledgements

Funding for this work was supported by the following: NSF (HRD-1345169) to RGP; CUASHI Pathfinder Fellowship and a GSA Grant-in-Aid (RG 1407-16) to KSG; the University of North Carolina at Chapel Hill; the University of New Mexico; and the Pueblo of Jemez Department of Natural Resources. The authors wish to thank Betsy Summers, James S. Fluke, Fabian Carbajal, Kathryn Bebe, and Justin Nichols, for their assistance in New Mexico, and Charlotte Hopson, Alexander Smith, Drew Hoag, Taylor Asher, Dr. Harvey Siem, and Savannah Swinea for their assistance in North Carolina.

REFERENCES

Abbott, B. W., Baranov, V., Mendoza-Lera, C., Nikolakopoulou, M., Harjung, A., Kolbe, T., et al. (2016). Using multi-tracer inference to move beyond single-catchment ecohydrology. *Earth-Science Reviews*, *160*, 19–42. https://doi.org/10.1016/j.earscirev.2016.06.014

Argerich, A., Haggerty, R., Martí, E., Sabater, F., & Zarnetske, J. (2011). Quantification of metabolically active transient storage (MATS) in two reaches with contrasting transient storage and ecosystem respiration. *Journal of Geophysical Research: Biogeosciences*, *116*(3), 1–14. https://doi.org/10.1029/2010JG001379

Arnon, S., Yanuka, K., & Nejidat, A. (2013). Impact of overlying water velocity on ammonium uptake by benthic biofilms. *Hydrological Processes*, *27*(4), 570–578. https://doi.org/10.1002/hyp.9239

Aubeneau, A. F., Drummond, J. D., Schumer, R., Bolster, D., Tank, J. L., & Packman, A. I. (2015). Effects of benthic and hyporheic reactive transport on breakthrough curves. *Freshwater Science*, *34*(1), 301–315. https://doi.org/10.1086/680037

Battin, T. J., Kaplan, L. A., Newbold, J. D., & Hendricks, S. P. (2003). A mixing model analysis of stream solute dynamics and the contribution of a hyporheic zone to ecosystem function. *Freshwater Biology*, *48*(6), 995–1014. https://doi.org/10.1046/j.1365-2427.2003.01062.x

Battin, T. J., Kaplan, L. A., Newbold, J. D., & Hansen, C. M. (2003). Contributions of microbial biofilms to ecosystem processes in stream mesocosms. *Nature*, *426*, 439–442.

Baxter, C., Hauer, F. R., & Woessner, W. W. (2003). Measuring Groundwater–Stream Water Exchange: New Techniques for Installing Minipiezometers and Estimating Hydraulic Conductivity. *Transactions of the American Fisheries Society*, *132*(3), 493–502. https://doi.org/10.1577/1548-8659(2003)132<0493:MGWENT>2.0.CO;2

Bencala, K. E. (2000). Hyporheic zone hydrological processes. *Hydrological Processes*, *14*, 2797–2798. https://doi.org/10.1002/1099-1085(20001030)14:15<2797::AID-HYP402>3.0.CO;2-6

Bernhardt, E. S., Blaszczak, J. R., Ficken, C. D., Fork, M. L., Kaiser, K. E., & Seybold, E. C. (2017). Control Points in Ecosystems: Moving Beyond the Hot Spot Hot Moment Concept. *Ecosystems*, *20*(4), 665–682. https://doi.org/10.1007/s10021-016-0103-y

Bernot, M. J., Sobota, D. J., Hall, R. O., Mulholland, P. J., Dodds, W. K., Webster, J. R., et al. (2010). Inter-regional comparison of land-use effects on stream metabolism. *Freshwater Biology*, *55*(9), 1874–1890. https://doi.org/10.1111/j.1365-2427.2010.02422.x

Boano, F., Harvey, J. W., Marion, A., Packman, A. I., Revelli, R., Ridolfi, L., & Wörman, A. (2014). Hyporheic flow and transport processes: Mechanisms, models, and biogeochemical implications. *Reviews of Geophysics*, *52*, 603–679. https://doi.org/10.1002/2012RG000417

Boulton, A. J. (2007). Hyporheic rehabilitation in rivers: Restoring vertical connectivity. *Freshwater Biology*, *52*(4), 632–650. https://doi.org/10.1111/j.1365-2427.2006.01710.x

Boulton, A. J., Findlay, S., Marmonier, P., Stanley, E. H., & Valett, H. M. (1998). The Functional Significance of the Hyporheic Zone in Streams and Rivers. *Annual Review of Ecology and Systematics*, *29*(1), 59–81. https://doi.org/10.1146/annurev.ecolsys.29.1.59

Briggs, M. a., Lautz, L. K., & Hare, D. K. (2013). Residence time control on hot moments of net nitrate production and uptake in the hyporheic zone. *Hydrological Processes*, *3751*(June 2013), 3741–3751. https://doi.org/10.1002/hyp.9921

Brunke, M., & Gonser, T. (1997). The ecological significance of exchange processes between rivers and groundwater. *Freshwater Biology*, *37*, 1–33. https://doi.org/https://doi.org/10.1046/j.1365-2427.1997.00143.x

Butler, J. J. J. (1998). *The Design, Performance, and Analysis of Slug Tests*. Boca Raton, Florida: CRC Press.

Cardenas, M. B. (2015). Hyporheic zone hydrologic science: A historical account of its emergence and a prospectus. *Water Resources Research*, *6*(4), 446. https://doi.org/10.1016/0022-1694(68)90080-2

Chapuis, R. P. (1989). Shape Factors for Permeability Tests in Boreholes and Piezometers. *Ground Water*, *27*, 647–653.

Coop, J. D., & Givnish, T. J. (2007). Gradient analysis of reversed treelines and grasslands of the Valles Caldera, New Mexico. *Journal of Vegetation Science*, *18*(1), 43–54. https://doi.org/https://doi.org/10.1111/j.1654-1103.2007.tb02514.x

Cui, Y., Paola, C., & Parker, G. (1996). Numerical simulation of aggradation and downstream fining. *Journal of Hydraulic Research*, *34*(2), 185–204. https://doi.org/10.1080/00221689609498496

Datry, T., Lamouroux, N., Thivin, G., Descloux, S., & Baudoin, J. M. (2015). Estimation of sediment hydraulic conductivity in river reaches and its potential use to evaluate streambed clogging. *River Research and Applications*, *31*, 880–891. https://doi.org/10.1002/rra

Day-Lewis, F. D., Linde, N., Haggerty, R., Singha, K., & Briggs, M. A. (2017). Pore network modeling of the electrical signature of solute transport in dual-domain media. *Geophysical Research Letters*, *44*(10), 4908–4916. https://doi.org/10.1002/2017GL073326

Duff, J. H., Murphy, F., Fuller, C. C., Triska, F. J., Harvey, J. W., & Jackman, A. P. (1998). A mini drivepoint sampler for measuring pore-water solute concentrations in the hyporheic zone of sand-bottom streams. *Limnology and Oceanography*, *43*(6), 1378–1383. https://doi.org/10.4319/lo.1998.43.6.1378

Faulkner, B. R., Renée Brooks, J., Forshay, K. J., & Cline, S. P. (2012). Hyporheic flow patterns in relation to large river floodplain attributes. *Journal of Hydrology*, *448–449*(0), 161–173. https://doi.org/http://dx.doi.org/10.1016/j.jhydrol.2012.04.039

Fetter, C. W. (2001). *Applied Hydrogeology*. (P. Lynch, Ed.) (4th ed.). Upper Saddle River, New Jersey: Prentice-Hall, Inc.

Findlay, S. E. G., Sinsabaugh, R. L., Sobczak, W. V., & Hoostal, M. (2003). Metabolic and structural response of hyporheic microbial communities to variations in supply of dissolved organic matter. *Limnology and Oceanography*, *48*(4), 1608–1617. https://doi.org/10.4319/lo.2003.48.4.1608

Fischer, H., Kloep, F., Wilzcek, S., & Pusch, M. T. . (2005). A River's Liver : Microbial Processes within the Hyporheic Zone of a Large Lowland River. *Biogeochemistry*, *76*(2), 349–371. https://doi.org/10.1007/sl0533-005-6896-y

Gelman, A., Rubin, D. B., Gelman, A., & Rubin, D. B. (1992). Inference from Iterative Simulation Using Multiple Sequences Linked references are available on JSTOR for this article : Inference from Iterative Simulation Using Multiple Sequences. *Statistical Science*, *7*(4), 457–472. https://doi.org/10.1214/ss/1177011136

Genereux, D. P., Leahy, S., Mitasova, H., Kennedy, C. D., & Corbett, D. R. (2008). Spatial and temporal variability of streambed hydraulic conductivity in West Bear Creek, North Carolina, USA. *Journal of Hydrology*, *358*(3–4), 332–353. https://doi.org/http://dx.doi.org/10.1016/j.jhydrol.2008.06.017

Gomez-Velez, J. D., & Harvey, J. W. (2014). A hydrogeomorphic river network model predicts where and why hyporheic exchange is important in large basins. *Geophysical Research Letters*, *41*(18), 6403–6412. https://doi.org/10.1002/2014GL061099

Gomez-Velez, J. D., Harvey, J. W., Cardenas, M. B., & Kiel, B. (2015). Denitrification in the Mississippi River network controlled by flow through river bedforms. *Nature Geoscience*, *8*(October). https://doi.org/10.1038/ngeo2567

González-Pinzón, R., & Haggerty, R. (2013). An efficient method to estimate processing rates in streams. *Water Resources Research*, *49*, 6096–6099. https://doi.org/10.1002/wrcr.20446

González-Pinzón, R., Haggerty, R., & Myrold, D. D. (2012). Measuring aerobic respiration in stream ecosystems using the resazurin-resorufin system. *Journal of Geophysical Research*, *117*(January), G00N06. https://doi.org/10.1029/2012JG001965

González-Pinzón, R., Haggerty, R., & Dentz, M. (2013). Scaling and predicting solute transport processes in streams. *Water Resources Research*, *49*(7), 4071–4088. https://doi.org/10.1002/wrcr.20280

González-Pinzón, R., Haggerty, R., & Argerich, A. (2014). Quantifying spatial di ff erences in

metabolism in headwater streams. *Freshwater Science*, *33*(3), 798–811. https://doi.org/10.1086/677555.

González-Pinzón, R., Ward, A. S., Hatch, C. E., Wlostowski, A. N., Singha, K., Gooseff, M. N., et al. (2015). A field comparison of multiple techniques to quantify groundwater – surface-water interactions. *Freshwater Science*, *34*(August 2014), 139–160. https://doi.org/10.1086/679738.

González-Pinzón, R., Peipoch, M., Haggerty, R., Martí, E., & Fleckenstein, J. H. (2015). Nighttime and daytime respiration in a headwater stream. *Ecohydrology*, n/a-n/a. https://doi.org/10.1002/eco.1615

Gooseff, M. N. (2010). Defining Hyporheic Zones - Advancing Our Conceptual and Operational Definitions of Where Stream Water and Groundwater Meet. *Geography Compass*, *4*(8), 945–955. https://doi.org/10.1111/j.1749-8198.2010.00364.x

Gooseff, M. N., Briggs, M. A., Bencala, K. E., McGlynn, B. L., & Scott, D. T. (2013). Do transient storage parameters directly scale in longer, combined stream reaches? Reach length dependence of transient storage interpretations. *Journal of Hydrology*, *483*(0), 16–25. https://doi.org/http://dx.doi.org/10.1016/j.jhydrol.2012.12.046

Grimm, N. B., & Fisher, S. G. (1984). Exchange between interstitial and surface water: Implications for stream metabolism and nutrient cycling. *Hydrobiologia*, *111*(3), 219–228. https://doi.org/10.1007/BF00007202

Hagerthey, S. E., & Kerfoot, W. C. (2005). Spatial variation in groundwater-related resource supply influences freshwater benthic algal assemblage composition. *Journal of the North American Benthological Society*, *24*(4), 807–819. https://doi.org/10.1899/04-004.1

Haggerty, R., Argerich, A., & Martí, E. (2008). Development of a "smart" tracer for the assessment of microbiological activity and sediment-water interaction in natural waters: The resazurin-resorufin system. *Water Resources Research*, *44*(4), n/a-n/a. https://doi.org/10.1029/2007WR006670

Haggerty, R., Martí, E., Argerich, A., von Schiller, D., & Grimm, N. B. (2009). Resazurin as a "smart" tracer for quantifying metabolically active transient storage in stream ecosystems. *Journal of Geophysical Research*, *114*(G3), G03014. https://doi.org/10.1029/2008JG000942

Haggerty, R., Ribot, M., Singer, G. A., Marti, E., Argerich, A., Agell, G., & Battin, T. J. (2014). Ecosytem respiration increase with biofilm growth and bed forms: Flume measurements with resazurin. *Journal of Geophysical Research: Biogeosciences*, *119*(2), 487–507. https://doi.org/10.1002/2013JG002552.Received

Hall, R. O., Bernhardt, E. S., & Likens, G. E. (2002). Relating nutrient uptake with transient storage in forested mountain streams. *Limnology and Oceanography*, *47*(1), 255–265.

https://doi.org/10.4319/lo.2002.47.1.0255

Hartwig, M., & Borchardt, D. (2015). Alteration of key hyporheic functions through biological and physical clogging along a nutrient and fine-sediment gradient. *Ecohydrology*, *975*(November 2014), n/a-n/a. https://doi.org/10.1002/eco.1571

Harvey, C. F., & Gorelick, S. M. (1995). Mapping hydraulic conductivity: Sequential conditioning with measurements of solute arrival time, hydraulic head, and local conductivity. *Water Resources Research*, *31*(7), 1615–1626. https://doi.org/10.1029/95WR00547

Harvey, J., Gomez-Velez, J., Schmadel, N., Scott, D., Boyer, E., Alexander, R., et al. (2018). How Hydrologic Connectivity Regulates Water Quality in River Corridors. *Journal of the American Water Resources Association*, *55*(2), 369–381. https://doi.org/10.1111/1752-1688.12691

Harvey, J. W., & Fuller, C. C. (1998). Effect of enhanced manganese oxidation in the hyporheic zone on basin-scale geochemical mass balance. *Water Resources Research*, *34*(4), 623. https://doi.org/10.1029/97WR03606

Harvey, J. W., & Gooseff, M. N. (2015). River corridor science: Hydrologic exchange and ecological consequences from bedforms to basins. *Water Resources Research*, *51*, 6893–6922. https://doi.org/10.1002/2015WR017617

Harvey, J. W., Böhlke, J. K., Voytek, M. A., Scott, D., & Tobias, C. R. (2013). Hyporheic zone denitrification: Controls on effective reaction depth and contribution to whole-stream mass balance. *Water Resources Research*, *49*(10), 6298–6316. https://doi.org/10.1002/wrcr.20492

Heathwaite, A. L. (2010). Multiple stressors on water availability at global to catchment scales: Understanding human impact on nutrient cycles to protect water quality and water availability in the long term. *Freshwater Biology*, *55*(SUPPL. 1), 241–257. https://doi.org/10.1111/j.1365-2427.2009.02368.x

Hollenbeck, K. (1998). INVLAP. M: A matlab function for numerical inversion of Laplace transforms by the de Hoog algorithm. Retrieved from https://www.mathworks.com/matlabcentral/answers/uploaded_files/1034/invlap.m

Hvorslev, M. J. (1951). Time Lag and Soil Permeability in Ground-Water Observations. *Bulletin n. 36*. https://doi.org/Bulletin no. 36

Karwan, D. L., & Saiers, J. E. (2012). Hyporheic exchange and streambed filtration of suspended particles. *Water Resources Research*, *48*(1), 1–12. https://doi.org/10.1029/2011WR011173

Knapp, J. L. A., & Cirpka, O. A. (2017). Determination of Hyporheic Travel-Time Distributions and other Parameters from Concurrent Conservative and Reactive Tracer Tests by Local-in-

Global Optimization. *Water Resources Research*, *53*. https://doi.org/10.1002/2017WR020734

Knapp, J. L. A., & Cirpka, O. A. (2018). A Critical Assessment of Relating Resazurin-Resorufin Experiments to Stream Metabolism in Lowland Streams, 1–35. https://doi.org/10.1029/2018JG004797

Knapp, J. L. A., González-Pinzón, R., Drummond, J. D., Larsen, L. G., Cirpka, O. A., & Harvey, J. W. (2017). Tracer-based characterization of hyporheic exchange and benthic biolayers in streams. *Water Resources Research*, *53*. https://doi.org/10.1002/2013WR014979

Knapp, J. L. A., González-Pinzón, R., & Haggerty, R. (2018). The Resazurin-Resorufin System: Insights From a Decade of "Smart" Tracer Development for Hydrologic Applications. *Water Resources Research*, *54*(9), 6877–6889. https://doi.org/10.1029/2018WR023103

Krause, S., Hannah, D. M., Fleckenstein, J. H., Heppell, C. M., Kaeser, D., Pickup, R., et al. (2011). Inter-disciplinary perspectives on processes in the hyporheic zone. *Ecohydrology*, *4*, 481–499. https://doi.org/10.1002/eco

Kurz, M. J., Drummond, J. D., Martí, E., Zarnetske, J. P., Lee-Cullin, J., Klaar, M. J., et al. (2017). Impacts of water level on metabolism and transient storage in vegetated lowland rivers: Insights from a mesocosm study. *Journal of Geophysical Research: Biogeosciences*, *122*(3), 628–644. https://doi.org/10.1002/2016JG003695

Laloy, E., & Vrugt, J. A. (2012). High-dimensional posterior exploration of hydrologic models using multiple-try DREAM(ZS) and high-performance computing. *Water Resources Research*, *48*(1), 1–18. https://doi.org/10.1029/2011WR010608

Larsen, L. G., Harvey, J. W., & Maglio, M. M. (2014). Dynamic hyporheic exchange at intermediate timescales: Testing the relative importance of evapotranspiration and flood pulses. *Water Resources Research*, *50*(1), 318–335. https://doi.org/10.1002/2013WR014195

Lawrence, J. E., Skold, M. E., Hussain, F. a., Silverman, D. R., Resh, V. H., Sedlak, D. L., et al. (2013). Hyporheic Zone in Urban Streams: A Review and Opportunities for Enhancing Water Quality and Improving Aquatic Habitat by Active Management. *Environmental Engineering Science*, *30*(8), 480–501. https://doi.org/10.1089/ees.2012.0235

Lee, D., & Cherry, J. (1979). A Field Exercise on Groundwater Flow Using Seepage Meters and Mini-piezometers. *Journal of Geological Education*, *27*(1), 6–10.

Lemke, D., Liao, Z., Wöhling, T., Osenbrück, K., & Cirpka, O. A. (2013). Concurrent conservative and reactive tracer tests in a stream undergoing hyporheic exchange. *Water Resources Research*, *49*(5), 3024–3037. https://doi.org/10.1002/wrcr.20277

Lemke, D., Schnegg, P.-A., Schwientek, M., Osenbrück, K., & Cirpka, O. A. (2013). On-line fluorometry of multiple reactive and conservative tracers in streams. *Environmental Earth*

Sciences, *69*(2), 349–358. https://doi.org/10.1007/s12665-013-2305-3

Liao, Z., Lemke, D., Osenbrück, K., & Cirpka, O. A. (2013). Modeling and inverting reactive stream tracers undergoing two-site sorption and decay in the hyporheic zone. *Water Resources Research*, *49*(6), 3406–3422. https://doi.org/10.1002/wrcr.20276

Magliozzi, C., Grabowski, R., Packman, A. I., & Krause, S. (2018). Toward a conceptual framework of hyporheic exchange across spatial scales. *Hydrology and Earth System Sciences*, *22*(May), 6163–6185. https://doi.org/10.5194/hess-2018-268

Mathers, K. L., Hill, M. J., & Wood, P. J. (2017). Benthic and hyporheic macroinvertebrate distribution within the heads and tails of riffles during baseflow conditions. *Hydrobiologia*. https://doi.org/10.1007/s10750-017-3092-8

McClain, M. E., Boyer, E. W., Dent, C. L., Gergel, S. E., Grimm, N. B., Groffman, P. M., et al. (2003). Biogeochemical Hot Spots and Hot Moments at the Interface of Terrestrial and Aquatic Ecosystems. *Ecosystems*, *6*(4), 301–312. https://doi.org/10.1007/s10021-003-0161-9

McDonnell, J. J., Sivapalan, M., Vaché, K., Dunn, S., Grant, G., Haggerty, R., et al. (2007). Moving beyond heterogeneity and process complexity: A new vision for watershed hydrology. *Water Resources Research*, *43*(7). https://doi.org/10.1029/2006WR005467

McGuire, K. J., & Mcdonnell, J. J. (2015). Tracer advances in catchment hydrology. *Hydrological Processes*, *29*(25), 5135–5138. https://doi.org/10.1002/hyp.10740

New Mexico Climate Center. Cooperative Observer Program Stations. 2018 Jul [accessed 2018 Jul]. https://weather.nmsu.edu/coop

O'Conner, B. L., & Hondzo, M. (2008). Enhancement and inhibition of denitrification by fluid-flow and dissolved oxygen flux to stream sediments. *Environmental Science and Technology*, *42*, 119–125. https://doi.org/10.1021/es801841c

O'Connor, B. L., & Harvey, J. W. (2008). Scaling hyporheic exchange and its influence on biogeochemical reactions in aquatic ecosystems. *Water Resources Research*, *44*(12), 1–17. https://doi.org/10.1029/2008WR007160

O'Connor, B. L., Hondzo, M., & Harvey, J. W. (2010). Predictive Modeling of Transient Storage and Nutrient Uptake: Implications for Stream Restoration, (December), 1018–1032. https://doi.org/10.1061/ASCÊHY.1943-7900.0000180

Ocampo, C. J., Oldham, C. E., & Sivapalan, M. (2006). Nitrate attenuation in agricultural catchments: Shifting balances between transport and reaction. *Water Resources Research*, *42*(1), 1–16. https://doi.org/10.1029/2004WR003773

Orghidan, T. (1959). A new habitat of subsurface waters: the hyporheic biotope. *Fundamental and Applied Limnology / Archiv Für Hydrobiologie*, *176*(4), 291–302.

https://doi.org/10.1127/1863-9135/2010/0176-0291

Rana, S. M. M., Scott, D. T., & Hester, E. T. (2017). Effects of in-stream structures and channel flow rate variation on transient storage. *Journal of Hydrology*, *548*, 157–169. https://doi.org/10.1016/j.jhydrol.2017.02.049

Ren, J., & Packman, A. I. (2007). Changes in fine sediment size distributions due to interactions with streambed sediments. *Sedimentary Geology*, *202*(3), 529–537. https://doi.org/http://dx.doi.org/10.1016/j.sedgeo.2007.03.021

Schaper, J., Posselt, M., Bouchez, C., Jaeger, A., Nützmann, G., Putschew, A., et al. (2019). Fate of trace organic compounds in the hyporheic zone: influence of retardation, the benthic bio-layer and organic carbon. *Environmental Science & Technology*, acs.est.8b06231. https://doi.org/10.1021/acs.est.8b06231

Sedell, J. R., Richey, J. E., & Swanson, F. J. (1989). The River Continuum Concept: A Basis for th Expected Ecosystem Behavior of Very Large Rivers? In D. P. Dodge (Ed.), *Proceedings of the International Large River Symposium* (pp. 49–55). Canadian Journal of Fisheries and Aquatic Sciences.

Small, E. E., & McConnell, J. R. (2008). Comparison of soil moisture and meteorological controls on pine and spruce transpiration. *Ecohydrology*, *1*, 205–214. https://doi.org/10.1002/eco

Stewart, R. J., Wollheim, W. M., Gooseff, M. N., Briggs, M. A., Jacobs, J. M., Peterson, B. J., & Hopkinson, C. S. (2011). Separation of river network-scale nitrogen removal among the main channel and two transient storage compartments. *Water Resources Research*, *47*(8), 1–19. https://doi.org/10.1029/2010WR009896

Stream Solute Workshop. (1990). Concepts and Methods for Assessing Solute Dynamics in Stream Ecosystems. *Journal of the North American Benthological Society*, *9*(2), 95–119.

Vannote, R. L., Minshall, G. W., Cummins, K. W., Sedell, J. R., & Cushing, C. E. (1980). The River Continuum Concept. *Canadian Journal of Fisheries and Aquatic Sciences*, *37*(1), 130–137. https://doi.org/10.1139/f80-017

Vomocil, J. A. (1965). Porosity. In C. A. Black (Ed.), *Methods of Soil Analysis* (pp. 299–314). Madison, Wisconsin: American Society of Argronomy.

Vrugt, J. A. (2016). Markov chain Monte Carlo simulation using the DREAM software package: Theory, concepts, and MATLAB implementation. *Environmental Modelling and Software*, *75*(January), 273–316. https://doi.org/10.1016/j.envsoft.2015.08.013

Vrugt, J. A., ter Braak, C. J. F., Clark, M. P., Hyman, J. M., & Robinson, B. A. (2008). Treatment of input uncertainty in hydrologic modeling: Doing hydrology backward with Markov chain Monte Carlo simulation. *Water Resources Research*, *44*(12), 1–15.

https://doi.org/10.1029/2007WR006720

Vrugt, J. A., ter Braak, C. J. F., Diks, C. G. H., Robinson, B. A., Hyman, J. M., & Higdon, D. (2009). Accelerating Markov Chain Monte Carlo Simulation by Differential Evolution with Self-Adaptive Randomized Subspace Sampling. *International Journal of Nonlinear Sciences and Numerical Simulation*, *10*(3). https://doi.org/10.1515/IJNSNS.2009.10.3.273

Ward, A. S. (2016). The evolution and state of interdisciplinary hyporheic research. *Wiley Interdisciplinary Reviews: Water*, *3*(January/February), 83–103. https://doi.org/10.1002/wat2.1120

Ward, A. S., Wondzell, B. S. M., Schmadel, N. M., Herzog, S., Zarnetske, J. P., Baranov, V., et al. (in review, 2019). Spatial and temporal variation in river corridor exchange across a 5th order mountain stream network. *Hydrology and Earth System Sciences*, (April), 1–39. https://doi.org/https://doi.org/10.5194/hess-2019-108

Woessner, W. W. (2000). Stream and fluvial plain ground water interactions: Rescaling hydrogeologic thought. *Ground Water*, *38*(3), 423–429. https://doi.org/https://doi.org/10.1111/j.1745-6584.2000.tb00228.x

Wondzell, S. M. (2011). The role of the hyporheic zone across stream networks. *Hydrological Processes*, *25*(22), 3525–3532. https://doi.org/10.1002/hyp.8119

Wright, K. K., Baxter, C. V., & Li, J. L. (2005). Restricted hyporheic exchange in an alluvial river system: implications for theory and management. *Journal of the North American Benthological Society*, *24*(3), 447. https://doi.org/10.1899/0887-3593(2005)024\[0447:RHEIAA\]2.0.CO;2

Wroblicky, G. J., Campana, M. E., Valett, H. M., & Dahm, N. (1998). Seasonal variation in surface-subsurface water exchnage and lateral hyporheic area of two stream-aquifer systems. *Water Resources Research*, *34*(3), 317–328. https://doi.org/https://doi.org/10.1029/97WR03285

Zarnetske, J. P., Haggerty, R., & Wondzell, S. M. (2015). Coupling multiscale observations to evaluate hyporheic nitrate removal at the reach scale. *Freshwater Science*, *34*(1), 172–186. https://doi.org/10.1086/680011

CHAPTER 4. – SPATIOTEMPORAL VARAIBLITY IN TRANSPORT AND REACTIVE PROCESSES ACROSS A 1ST-5TH ORDER FLUVIAL NETWORK.

Introduction

Streams and rivers transport fundamental resources for terrestrial and aquatic life (Woessner, 2000; Krause et al., 2011; Wohl, 2015). In these fluvial systems, key biogeochemical constituents are transformed in regions of rapid turnover such as riparian, benthic, and hyporheic zones. The hyporheic zone plays an important role in small-to-large-scale riverine ecological functioning due to the transfer of mass and energy between two contrasting but complementary environments, i.e., surface and ground waters (Orghidan 1959; Fischer et al. 2005; Nowinski et al. 2011; Boano et al. 2014; Hester et al. 2017; Magliozzi et al. 2018). This dynamic and spatially varying mixing zone provides an ideal physical habitat for microbial communities, which benefit from increased resources and contact times under a range of redox conditions (Woessner, 2000; Brunke and Gonser, 1997; Gooseff, 2010).

Research interest in the hyporheic zone, and its functional significance has steadily grown in recent years (Ward, 2016). However, most studies focus on hyporheic exchange in small, easily construed headwater streams rather than in large rivers (Tank et al. 2008; Hall et al. 2013; González-Pinzón et al. 2015; Ward et al., in review, 2019). Over the past three decades, more than 90% of hyporheic zone studies have been conducted in headwater streams with the majority of those studies taking place in low order (i.e., 1st, 2nd, and 3rd) streams, as defined by Strahler (1952) (Fig. 4.1). Studying hyporheic exchange in low-order streams offer research advantages because they are small, abundant, tractable, easily constrained, and more accessible

than their larger-order counterparts (Ensign and Doyle, 2006; Tank et al., 2008; Gooseff et al., 2013; Ward, 2016). Low-order streams also make up a large proportion of reach lengths throughout many fluvial networks, highly influencing regional water quality and ecological functioning (Alexander et al., 2007; Freeman et al., 2007; Gomez-Velez and Harvey, 2014).

Furthermore, in addition to making up a larger proportion of catchment reach lengths, low-order streams are thought to have greater influence over hyporheic zone processing than their high-order counterparts throughout various fluvial networks. For example, Gomez-Velez et al. (2015) found that vertical hyporheic excursions into the streambed generally decreased with increasing stream order in the Mississippi River network, meaning that watershed hyporheic contributions are expected to decrease with increasing stream order. Additionally, shallower stream depths, typically found in low-order streams, maintain closer contact between surface water and reactive bed sediments and may encourage higher streambed reaction rates (Harvey and Gooseff, 2015). The expectation of hyporheic zone contributions decreasing with increasing stream order is in line with hydrologic and geomorphic assumptions underlying upscaling approaches, due to shorter residence times, finer streambed sediment that results in a lower hydraulic conductivity, and a greater river depth in higher order streams (Wondzell, 2011; Harvey and Gooseff, 2015).

This, however, has rarely been tested across different stream orders in the field, as studying hyporheic exchange in studying larger rivers involves many experimental challenges. As river size and flow rates increase, it can become impractical or difficult to apply methods traditionally used in small stream orders due to reduced stream accessibility associated with geographic and anthropogenic complexity, increased tracer costs, and increased distances

required to have comparable residence times (Tank et al. 2008; Xie and Zhang 2010; González-Pinzón, et al. 2015).

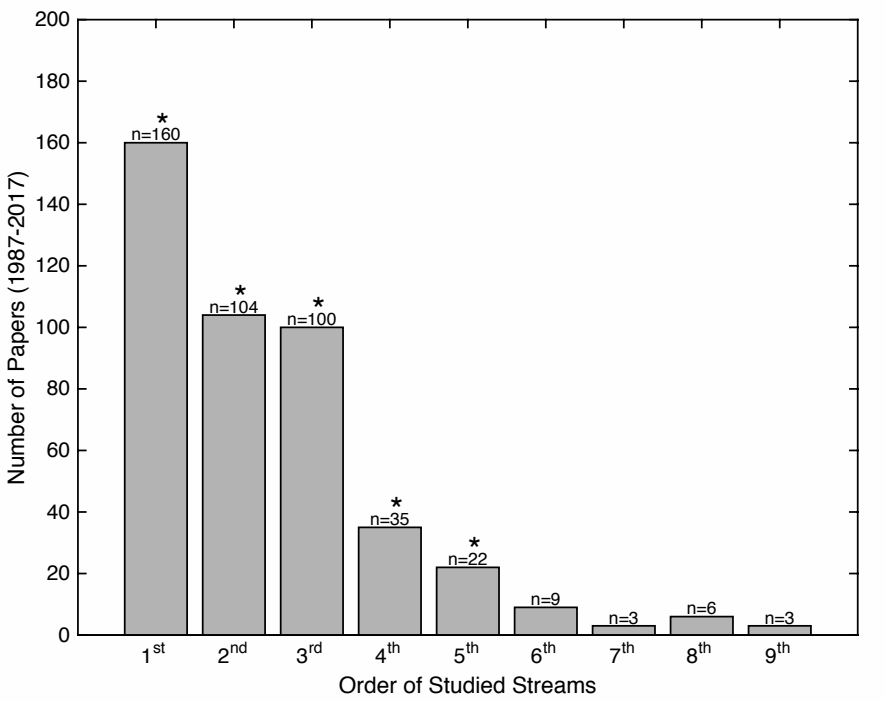

Figure 4.1. Stream orders of hydrologic studies published in the last 30 years. The number of hydrologic studies published in 1st through 9th order streams from 1987-2017 years via a comprehensive literature search completed on 21 November 2017 using Elsevier's Scopus search engine. The considered journal articles were found using a targeted search query in an online search engine. Search terms included "transient storage" or "hyporheic" in addition to "stream order" from article titles, abstracts, and key words. Study stream orders were manually extracted and recorded from the resulting 703 articles if provided by the authors or inferable from publication figures. Asterisks (∗) indicate the stream orders that were targeted in this study.

The preference for studying low-order streams may thus bias our understanding of hyporheic exchange processes and how they operate along fluvial networks (Doyle, 2005; Heathwaite, 2010; Xie et al., 2016). This bias originates with the lack of data collection on hyporheic zone processing in larger systems. Bias is then amplified through data-limited models used to infer hyporheic processing in rivers of different geomorphology, streambed substrates, shear stresses, and flow regimes (Beven, 2000; Wollheim et al., 2006; Harvey and Gooseff, 2015; Abbott et al., 2016; Hester et al., 2017). As a result, predicting the influence of hyporheic exchange on solute transport, microbial activity, and biogeochemical transformations at the watershed scale remains elusive (Wondzell, 2011; Boano et al. 2014; Pinay et al. 2015). The uncertainty in how hyporheic exchange contributions scale with increasing stream order may result in a misrepresentation of hyporheic zone processing for high-order streams. For example, having limited data on the hyporheic zone area in high-order streams could result in an underestimate of processing contributions in these larger stream reaches and result in an underestimation of hyporheic zone contributions at the catchment-scale. Without further exploration of hyporheic exchange in large-order streams, the reliance on data from headwater streams may mask contributions from larger stream order reaches and how those contributions vary throughout the year (McClain et al., 2003; Groffman et al., 2009; Harvey and Gooseff, 2015). Ultimately, understanding the drivers behind hyporheic exchange across a range of stream orders and flow regimes is important for predicting catchment-wide water quality outcomes and their influence on water resource management (Graf, 2001; Stream Solute Workshop, 1990; Stonedahl et al., 2013; Ward, 2016; Magliozzi et al., 2018).

The few field studies available with data from larger rivers suggest that they play an important role in nutrient spiraling and that the fluxes between aquatic and terrestrial

environments in those systems may be equally significant and comparable to their smaller-order counterparts (Ensign and Doyle 2006; Tank et al. 2008; Hall et al. 2013; González-Pinzón, et al. 2015). The field-based evidence seems to contradict the results from modeling studies suggesting that small-order streams have twice as much biogeochemical potential as large-order streams when they are compared on a per kilometer basis (Gomez-Velez and Harvey, 2014). While these differences in stream order hyporheic contributions between field and modeling studies have been identified throughout different catchments, variability has not been fully explained for the underlying drivers of hyporheic exchange dynamics across fluvial networks. Data-based analyses are needed as an effort to support inter-stream order hyporheic zone processing comparisons and determine if the paradigm of expected changes in hyporheic zone contributions throughout the fluvial network holds true.

In this study we explored hyporheic exchange dynamics from spatial and temporal perspectives using *in situ* measurements from within the same river system to address the questions: (1) how do hyporheic zone contributions to riverine processing change with space and time? And, (2) does the spatiotemporal variability of hyporheic exchange scale across fluvial networks? We present and discuss the results of nine reactive tracer tests using the resazurin-resorufin (Raz-Rru) system (Haggerty et al., 2008, Knapp et al., 2018). These tests were done in five different stream orders along the Jemez River, New Mexico (Fig. 2a), during two different flow regimes (i.e., summer baseflow and spring receding water conditions). The Raz-Rru system was chosen for this study because the irreversible transformation of Raz to Rru is considered a proxy for aerobic respiration and provides an *in situ* estimation of hyporheic zone processing due to metabolic activity (Haggerty et al., 2008; González-Pinzón et al., 2012; González-Pinzón, et al., 2015; Knapp and Cirpka, 2018). We found that our studied fluvial network did not

consistently follow the expectations of decreasing hyporheic exchange contributions with increasing stream order and demonstrate that the scaling of hyporheic zone processing is not fully understood.

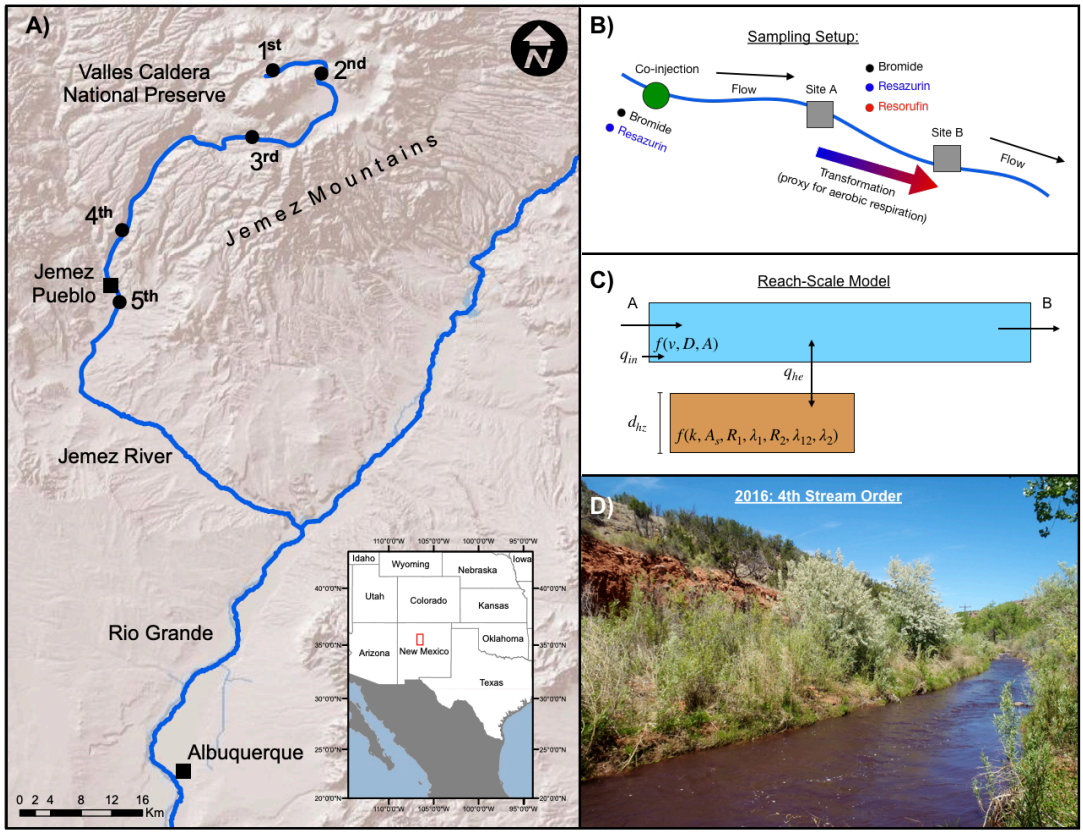

Figure 4.2. Map of field sites, study set up, model conceptualization, and field photo. A map of the Jemez River shows **(a)** our study reaches highlighted along the river with black circles; **(b)** diagram detailing the field sampling setup for each stream order reach where bromide and resazurin were injected and analyzed with samples from two downstream sampling stations; **(c)** the transient storage model conceptualization used for the reach-scale analysis, with two downstream sampling stations A and B, considering in-stream (blue box) and hyporheic zone (brown box) parameters; **(d)** photo taken during a tracer injection at the 4th order stream reach in 2016.

Methods

We completed nine tracer tests in five different stream orders of the Jemez River watershed during June 2015 and May/June 2016. The Jemez River is located in northern New Mexico (Fig. 4.2a) and drains an area of 2,678 km^2 before becoming a tributary to the Rio Grande (USGS, 2018). The upper portion of the watershed is forested with a mix of subalpine balds, aspen groves, mixed conifer, spruce, ponderosa, and riparian zone grasslands (Coop and Givnish, 2007; Small and McConnell, 2008). This region is characterized by a semi-arid, continental climate with temperatures ranging from -5.4 °C in January to 15 °C in July (Los Alamos 13 W, Cooperative Observer Program Stations, New Mexico Climate Center, New Mexico State University). The lower portion of the Jemez River watershed contains shrub/grassland vegetation and has an arid climate with temperatures ranging from 1.0°C in January to 26°C in July (Homer et al., 2015; New Mexico Climate Center, 2018).

Local precipitation averages 639 mm yr^{-1} at higher elevations and 210 mm yr^{-1} at lower elevations including rain and snowfall (New Mexico Climate Center, 2018). Annual stream high flows occur during the peak spring snowmelt period, and annual stream low flows occur during the summer season (USGS, 2018). Historical river basin geology consists of igneous and metamorphic complexes, along with sedimentary, and volcanic deposits (Smith et al. 1970; Craig, 1992; Coop and Givnish 2007; Cibils et al. 2008). Streambed substrates sampled during our experiments along the Jemez River continuum consisted of poorly sorted small boulders, gravel, sand, and included a range of fine particle fractions.

The tracer experiments took place between 23 June and 27 June in 2015 and 16 May and 4 June 2016 (Table 4.1). We selected representative site locations for each of our five stream orders (Fig. 4.2a). Reach length was measured as the distance between each pair of sampling

stations of the respective stream order using Google Earth imagery (Google Earth, Google, Mountainview, California, USA). Discharge was measured during the tracer tests with an acoustic Doppler velocimeter (SonTek/YSI FlowTracker ADV; SonTek, San Diego, California, USA). In 2015, study reach lengths and discharge varied from 0.57 km to 2.75 km and 0.014 m^3s^{-1} to 0.180 m^3s^{-1}, respectively (Table 4.1). In 2016, study reach lengths and measured discharge varied from 0.01 km to 3.77 km and 0.001 m^3s^{-1} to 0.790 m^3s^{-1}, respectively (Table 4.1). The differences in discharge between the two sampling years represent seasonal differences in flow between dry, baseflow conditions in the summer months and wet, snowmelt conditions in the spring season. *In situ* surface water temperature was monitored with multiparameter water quality sondes (EXO2 Sonde, YSI Incorporated, Yellow Springs, Ohio, USA) and ranged from 18.50-25.17 °C in 2015 and from 14.20-21.00 °C in 2016.

Streambed sediment grab samples of approximately 300 g were collected for representative stream order porosity measurements from the 1st through 5th order stream during the 2016 sampling campaign (Table 4.1) (Vomocil, 1965; Wroblicky et al., 1998). Porosity was determined from measured sediment particle and dry bulk densities (Fetter, 2001). We assumed the 2016 porosity measurements were representative of our studied stream orders in both sampling periods. Porosity was generally higher at the lower stream order sites where the streambed sediments were dominated by sand size particles, as was expected from the bedload fining associated with higher stream orders, due to the streambed mix of gravel and sand size particles.

Table 4.1. Study site characteristics. Study reach sampling date, stream order, discharge (m^3/s), stream depth (m), width (m), cross-sectional area (m^2), estimated mixing length (km), study reach length (km), porosity (%), mean water temperature ($°C$), and elevation above sea level (km) for the 2015 and 2016 sampling campaigns.

Sampling Date	Stream Order	Discharge (m^3/s)	Stream Depth (m)	Stream Width (m)	Cross-Sectional Area (m^2)	Mixing Length (km)	Reach Length (km)	Porosity (%)	Mean Water Temp. (C°)	Elevation (km)
2015	***Baseflow***	***(Dry Season)***				**Inj-A**	**A-B**			
27-Jun	1	0.014	0.20	1.82	0.36	0.65	0.57	59	18.78	2.75
26-Jun	2	0.020	0.16	2.23	0.42	1.03	0.54	47	18.50	2.64
25-Jun	3	0.090	0.16	3.00	0.47	0.76	2.63	27	19.56	2.46
24-Jun	4	0.160	0.23	4.15	1.20	1.24	2.75	35	24.38	1.81
23-Jun	5	0.180	0.22	7.65	1.71	2.98	1.47	27	25.17	1.72
2016	***Receding***	***(Wet Season)***								
3-Jun	1	0.001	0.05	0.35	0.02	0.41	0.01	59	16.56	2.82
16-May	2	0.110	0.38	1.09	0.41	1.46	0.63	47	21.00	2.68
20-May	3	0.500	0.23	4.80	1.11	1.77	2.80	27	14.20	2.45
21-May	4	0.790	0.32	3.00	1.58	2.23	3.77	35	19.18	1.81

We co-injected bromide (Br^-) and resazurin (Raz) (Table 4.2). Raz is a redox-sensitive phenoxazine dye that can be used as a "smart" tracer to estimate microbiological activity associated with stream water-sediment interactions (González-Pinzón et al., 2012; Haggerty et al., 2008; Knapp et al., 2018). In the presence of mildly reducing conditions, Raz undergoes an irreversible reduction to its daughter product, Rru. This transformation from Raz to Rru can be used as a proxy of *in situ* aerobic metabolism (Argerich et al. 2011; González-Pinzón et al. 2012; González-Pinzón et al. 2014; González-Pinzón et al. 2015).

We sampled the breakthrough curves (BTCs) of Br^-, Raz, and the reaction product, Rru, at two stations (i.e., Site A and Site B) downstream of the injection site (Fig. 2b) for periods ranging between 4 to 10 hours after injection. Grab samples in the surface water were collected from the thalweg at each of the sampling stations. Surface water samples were collected at intervals ranging from every 1 to 30 minutes throughout our tracer BTCs using 60 mL plastic syringes and were filtered through 0.45 μm pore size Whatman Nylon filters (25-mm diameter). Filtered samples were immediately stored in the dark and on ice, and later refrigerated at 4 °C, until they were analyzed in the laboratory, always within 48 hours after sampling.

Table 4.2. Tracer masses, travel times, and recoveries. Injected tracer masses (g), initial travel time (h), reach travel time (h), simulated surface water bromide mass recoveries $(\%)$, simulated surface water resazurin mass recoveries $(\%)$, and the resazurin to bromide recovery ratio $(-)$ for the 2015 and 2016 sampling campaigns. The 2016 1st order stream was sampled but was not analyzed due to low conservative tracer mass recovery.

Sampling Date	Stream Order	Mass Inj. NaBr (g)	Mass Inj. Raz (g)	Reach Travel Time (h)	Reach Br- Recovery (%)	Reach Raz Recovery (%)	Raz/Br- Recovery Ratio
2015				A to B	A to B	A to B	
27-Jun	1	200	10	1.55	36	13	0.36
26-Jun	2	50	10	1.85	55	50	0.91
25-Jun	3	900	50	3.90	65	55	0.85
24-Jun	4	900	60	2.39	63	63	1.00
23-Jun	5	600	60	2.37	65	62	0.95
16-May	2	152	28	0.77	92	92	1.00
20-May	3	500	90	1.84	88	85	0.97
21-May	4	1400	133	1.77	84	84	1.00

Each water sample was aliquoted (~1 mL) and buffered to a pH 8.5 before fluorescence was read (Haggerty et al., 2008, 2009). All water samples were analyzed for Raz and Rru fluorescence signals with a spectroflurometer (Varian Cary Eclipse; Santa Clara, California) at excitation/emission wavelengths of 602/632 nm for Raz and 571/584 nm for Rru. Fluorescence readings were converted to concentrations with the help of calibration standards. The limit of quantification (LOQ) for Raz was 1.01 x 10^{-1} $mol\ L^{-1}$ and 1.67 x 10^{-3} $mol\ L^{-1}$ for Rru. The remainder of each sample was frozen at -20 °C and stored in the dark until they could be thawed and analyzed for Br^- with ion chromatography using a Dionex ICS-1000 Ion Chromatograph with AS23/AG23 analytical and guard columns, and a 1000-µl injection loop with a Br^- analytical limit of detection (LOD) of 1.67 x 10^{-3} $mol\ m^{-3}$ (Thermo Fisher Scientific Inc.; Sunnyvale, California).

The model used in this work describes the one-dimensional in-stream, reach-scale transport of the tracer compounds undergoing exchange with the hyporheic zone during the transit downstream with uniform and time-invariant coefficients (Fig. 4.2c). Except for the boundary condition of the instantaneous tracer injection, the model applied here is similar to the one utilized by Knapp et al. (2017). This model considers the hyporheic zone as a single, well-mixed, transient storage zone that undergoes linear exchange with the main channel, accounts for the compound specific behavior of Raz and Rru in the hyporheic zone, and estimates surface water dilution due to groundwater inflow between sampling stations (Runkel, 1998; Lemke et al., 2014). Model results yielded effective bulk estimates of streambed reactivity but did not provide information about the spatial distribution of these processes. The coupled governing equations for Br^- ($i = 0$), Raz ($i = 1$), and the reaction product Rru ($i = 2$) are:

$$\frac{\partial c_i}{\partial t} + \frac{A_s}{A} R_i \frac{\partial c_{hz,i}}{\partial t} + v \frac{\partial c_i}{\partial x} - D \frac{\partial^2 c_i}{\partial x^2} = \frac{A_s}{A} r_{hz,i} + q_{in}\left(c_{in,i} - c_i\right) \qquad (1)$$

$$R_i \frac{\partial c_{i,hz}}{\partial t} = k\left(c_i - c_{hz,i}\right) + r_{hz,i} \quad (2)$$

subject to the following initial and boundary conditions:

$$c_i(x, t = 0) = c_{hz,i}(x, t = 0) = 0 \; \forall x \quad (3)$$

$$v c_i - D \frac{\partial c_i}{\partial x}|_{x=0} = \frac{M_i}{A}\delta(t) \quad (4)$$

$$\lim_{x \to \infty} c_i(x, t) = 0 \; \forall \; t \quad (5)$$

in which c_i $[mol{\cdot}m^{-3}]$ denotes the compound concentration in the main channel; $c_{hz,i}$ $[mol{\cdot}m^{-3}]$ represents the compound concentration in the transient storage zone; the in-stream advective velocity is given by v $[m\, s^{-1}]$; D $[m^2\, s^{-1}]$ represents the dispersion coefficient; A_s/A, $[-]$ represents the ratio of the cross-sectional area of the storage zone A_s $[m^2]$ to that of the stream A $[m^2]$; the reaction rate is given by $r_{hz,i}$ $[mol\, m^{-3}\, s^{-1}]$; q_{in} represents the dilution factor $[s^{-1}]$; $c_{in,i}$ denotes the groundwater inflow, where $c_{in,i} = 0$; the first order mass-transfer rate coefficient for exchange with the storage zone is given by k $[s^{-1}]$; and M_i $[mol]$ represents the injected tracer mass, except for resorufin where $M_2 = 0$.

The equilibrium sorption coefficient of the compound i in the hyporheic zone is represented by R_i $[-]$, assuming linear sorption at local equilibrium. Since bromide is a conservative tracer that neither undergoes sorption or transformation, we set

$$R_0 = 1 \text{ and } r_{hz,0} = 0$$

whereas both resazurin and resorufin may sorb in the streambed ($R_1 \geq 1;\; R_2 \geq 1$). Raz and Rru streambed chemical transformation were assumed to follow first-order kinetics (González-Pinzón and Haggerty, 2013), resulting in the following reactions rates:

$$r_{hz,1} = -\lambda_1 c_{hz,1} \quad (6)$$

$$r_{hz,2} = \lambda_{12} c_{hz,1} - \lambda_2 c_{hz,2} \quad (7)$$

in which λ_1 $[s^{-1}]$ is the total Raz transformation rate coefficient; λ_{12} $[s^{-1}]$ is the Raz-to-Rru transformation rate coefficient, with $\lambda_{12} \leq \lambda_1$ since the transformation of Raz to Rru cannot exceed the total transformation of Raz; and λ_2 $[s^{-1}]$ is the Rru transformation rate coefficient. The previous equations were solved in the Laplace domain and back-transformed numerically (Hollenbeck, 1998; Knapp et al., 2017). Details on the model calibration procedure are presented in the Supporting Information (Text S1). Briefly, model parameter estimation was completed using the *Differential Evolution Adaptive Metropolis* (DREAM (ZS)) algorithm (Vrugt et al., 2009). Parameters for Br^- and Raz were jointly estimated in a first step of 100,000 model generations. Rru-specific parameters were estimated separately from an additional 100,000 generations while all parameters related to Br^- and Raz were sampled from their previously determined distributions. Model convergence was assessed using Gelman and Rubin (1992) $\hat{R}$ statistics, and the agreement between measured and simulated BTCs was quantified through the calculation of the residual sum of squares, (*nRSS*) $[-]$, normalized by the squared theoretical peak tracer concentrations of each tracer BTC of the respective tracer at the given location. The median of the best 1,000 model simulations were used to assess the agreement between our final model fits and a subset of possible curve fits.

Tracer recoveries in Table 4.2 were quantified using an analysis of the zeroth temporal moments of the simulated BTCs (Harvey and Gorelick, 1995). The zeroth temporal moments at Site A, $\mu_0(x_A)$ $[mol.s.m^{-3}]$, and Site B, $\mu_0(x_B)$, over time t $[s]$ for Br^- $(i = 0)$ and Raz $(i = 1)$ were defined as:

$$\mu_{0,i}(x_A) = \int_0^\infty c_i(x_A, t)dt \tag{8}$$

$$\mu_{0,i}(x_B) = \int_0^\infty c_i(x_B, t)dt. \tag{9}$$

Mean reach travel times, $\tau\ [h]$, were calculated from the normalized 1st temporal moments (Harvey and Gorelick 1995; Lemke et al. 2013) of the simulated conservative tracer at Site A, $m_1(x_A)\ [h]$, and Site B, $m_1(x_B)[h]$:

$$m_1(x_A) = \frac{1}{\mu_{0,0}(x_A)} \int_0^\infty c_0(x_A, t)t\ dt \tag{10}$$

$$m_1(x_B) = \frac{1}{\mu_{0,0}(x_B)} \int_0^\infty c_0(x_B, t)t\ dt. \tag{11}$$

$$\tau = m_1(x_B) - m_1(x_A). \tag{12}$$

Tracer mass recovery, $r_i\ [-]$, along each stream reach was calculated as follows from the simulated BTCs:

$$r_i = \frac{\mu_{0,i}(x_B)}{\mu_{0,i}(x_A)}. \tag{13}$$

For Br- we expect recovery < 1 if discharge increased between A and B due to the dilution of the tracer, whereas the recovery of Raz at Site B was expected to be reduced by both dilution and reaction. We thus determined the relative recovery of Raz to Br^- by $\frac{r_1}{r_0}$.

The reach-scale hyporheic exchange rate coefficient, $q_{he,}\ [s^{-1}]$, represents the volume of water exchanged with the subsurface per time and river volume, and was evaluated using parameters from the above transient storage model (Liao and Cirpka, 2011; Knapp et al., 2017):

$$q_{he} = \frac{A_s}{A} k. \tag{14}$$

The apparent depth of the hyporheic zone, $d_{hz}\ [cm]$, was calculated from the relative size of the transient storage zone and measured field parameters:

$$d_{hz} = \frac{A_s}{A} A_{meas} \frac{1}{w_{hz}\theta} \tag{15}$$

where $A_{meas}\ [cm^2]$ was the measured cross-sectional area of the stream, $w_{hz}\ [cm]$ was the width of the hyporheic zone, and porosity, $\theta\ [-]$. Additionally, the mean hyporheic zone

residence times, τ_{hz} $[s]$, were determined from the inverse of the fitted transient storage model first-order exchange rate coefficient, k $[s^{-1}]$:

$$\tau_{hz} = \frac{1}{k}. \quad (16)$$

Reach-scale Damköhler numbers, Da $[-]$, were calculated for each reach using the following equation:

$$Da = \tau_{hz}\lambda_1 \ . \quad (17)$$

Damköhler numbers quantify the time-scale of the residence and reaction along hyporheic flow paths (Harvey and Fuller, 1998; Ensign and Doyle, 2005; Harvey et al., 2013; Oldham et al., 2013), providing insight into the factors limiting reaction progress in the hyporheic zone (Harvey et al., 2005; Ocampo et al., 2006). Values of Da near one indicate a relative balance between transport and reaction time-scales, which theoretically result in maximal hyporheic zone reactivity. When Da is significantly smaller than one, processing is reaction-limited and subzones of inactivity are created along hyporheic flow paths. During conditions where Da is greater than one, streambed substrates become transport-limited, and inactive hyporheic zone sections contribute to additional storage time but do not support additional reactions (Wagner and Harvey, 1997; González-Pinzón and Haggerty, 2013; Harvey et al., 2013).

Results and Discussion

We obtained ten unique, best-fit transient storage model parameters for each stream reach from the analysis of 54 surface water BTCs in total (Appendix 4.22). Plots of the resulting parameter estimates can be found in Figure 4.3. The measured and modeled tracer BTCs are shown in Figure 4.4 (for the 4th order stream) and in the Appendix 4.3 – Appendix 4.6 (for the rest). Table 4.2 presents temporal moments estimated from the simulated BTC.

Each of our model parameter estimates resulted in an $\hat{R}$ statistic (Gelman and Rubin, 1992) that confirmed good parameter convergence. The quality of the presented simulations, as indicated by the *nRSS* values in Appendix 4.22, shows that our modeling approach provided a fairly robust method for describing in-stream transport and hyporheic exchange processing across five different stream orders, even with some misfits between measured and simulated data at the BTC peaks. The downstream Br^- fit in 2016 at the 1st stream order largely overestimated the Br^- peak and was thus removed from any subsequent analysis.

Moreover, the quality of the model fits was supported by the small parameter uncertainties from the joint fit of Br^- and Raz. Higher parameter uncertainties for the Rru-specific parameters, as indicated by larger $nRSS_{rru}$ values, are likely due to error propagation from the Br^- and Raz joint fit on to the Rru fit and uncertain or correlated parameters. This additional step amplifies any encountered uncertainties during the second fit. We chose to interpret hyporheic processes based on the transformation of Raz alone due to the higher Rru-related parameter uncertainties similar to Knapp et al. (2017). Rru measurements were used to confirm that the measured Rru BTCs could be simulated with the estimated model parameters. The general agreement between the final BTC simulations and the median simulation of the best 1,000 model generations support the use of our model parameter optimization (Fig. 4.4 and Appendix 4.3 – Appendix 4.6), as the results typically converged to the best attainable fit to the measured data with the given model results from 100,000 simulations.

We found greater uncertainty in the BTC tails, as indicated by the larger confidence intervals along the tails of our BTC plots, due to the lower tracer concentrations in these BTC regions (Payn et al., 2008). Although an exponential transit time distribution may not be an ideal

representation of hyporheic zone residence times (Haggerty, 2002; Wörman et al., 2002; Gooseff et al., 2005), we used it in an effort to obtain a parsimonious model.

The results of our parameter correlation analysis provided additional information about the reliability of our model parameters (Appendix 4.7 – Appendix 4.14). A sensitivity analysis indicated the sensitivity of the resulting Raz BTCs to different parameter values (Appendix 4.15 – Appendix 4.21), and revealed that the BTC tails were typically less sensitive to the parameter values than the BTC peaks. Raz BTCs were analyzed because they contain the same parameters that influence the Br^- model fit.

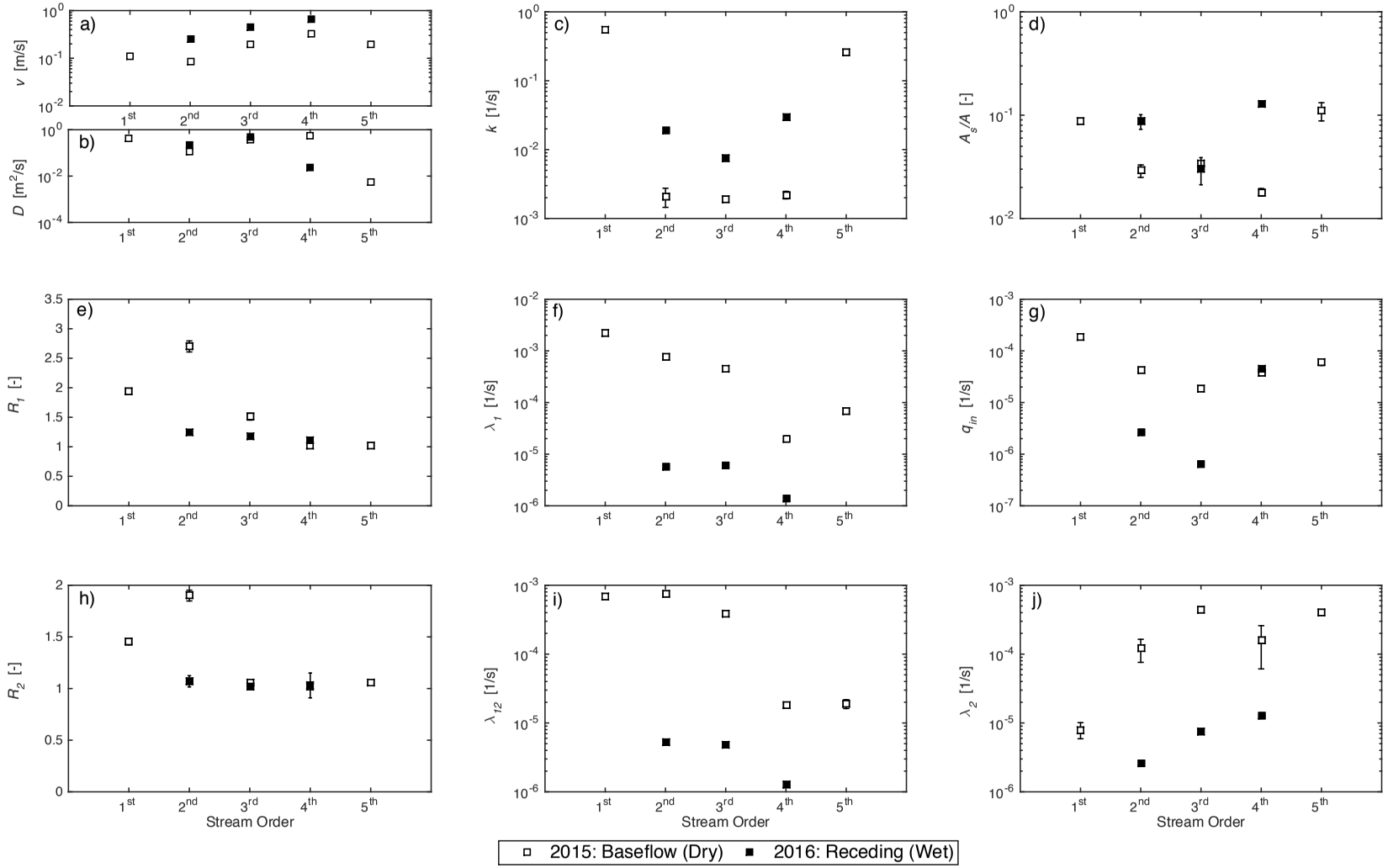
a)
b)
c)
d)
e)
f)
g)
h)
i)
j)
v [m/s]
D [m²/s]
k [1/s]
A_s/A [-]
R_1 [-]
λ_1 [1/s]
q_in [1/s]
R_2 [-]
λ_12 [1/s]
λ_2 [1/s]
1st
2nd
3rd
4th
5th
Stream Order
2015: Baseflow (Dry)
2016: Receding (Wet)

Figure 4.3. Model parameter outputs. Model parameters (± 1 σ) for the 2015 and 2016 sampling campaigns. v $[m\ s^{-1}]$ is in-stream advective velocity; D $[m^2\ s^{-1}]$ represents the dispersion coefficient; k $[s^{-1}]$ is the mass transfer rate coefficient; $A_s/A,\ [-]$ is the ratio of the cross-sectional area of the storage zone A_s $[m^2]$ to that of the stream A $[m^2]$; R_1 $[-]$ is the retardation factor of resazurin; λ_1 $[s^{-1}]$ is the total resazurin transformation rate coefficient; q_{in} $[s^{-1}]$ represents the dilution factor; R_2 $[-]$ is the retardation factor of resorufin; λ_{12} $[s^{-1}]$ is the transformation of resazurin to resorufin rate coefficient; and λ_2 $[s^{-1}]$ is the resorufin transformation rate coefficient. The 1st stream order from 2016 was excluded from these results due to poor model fits of the conservative tracer.

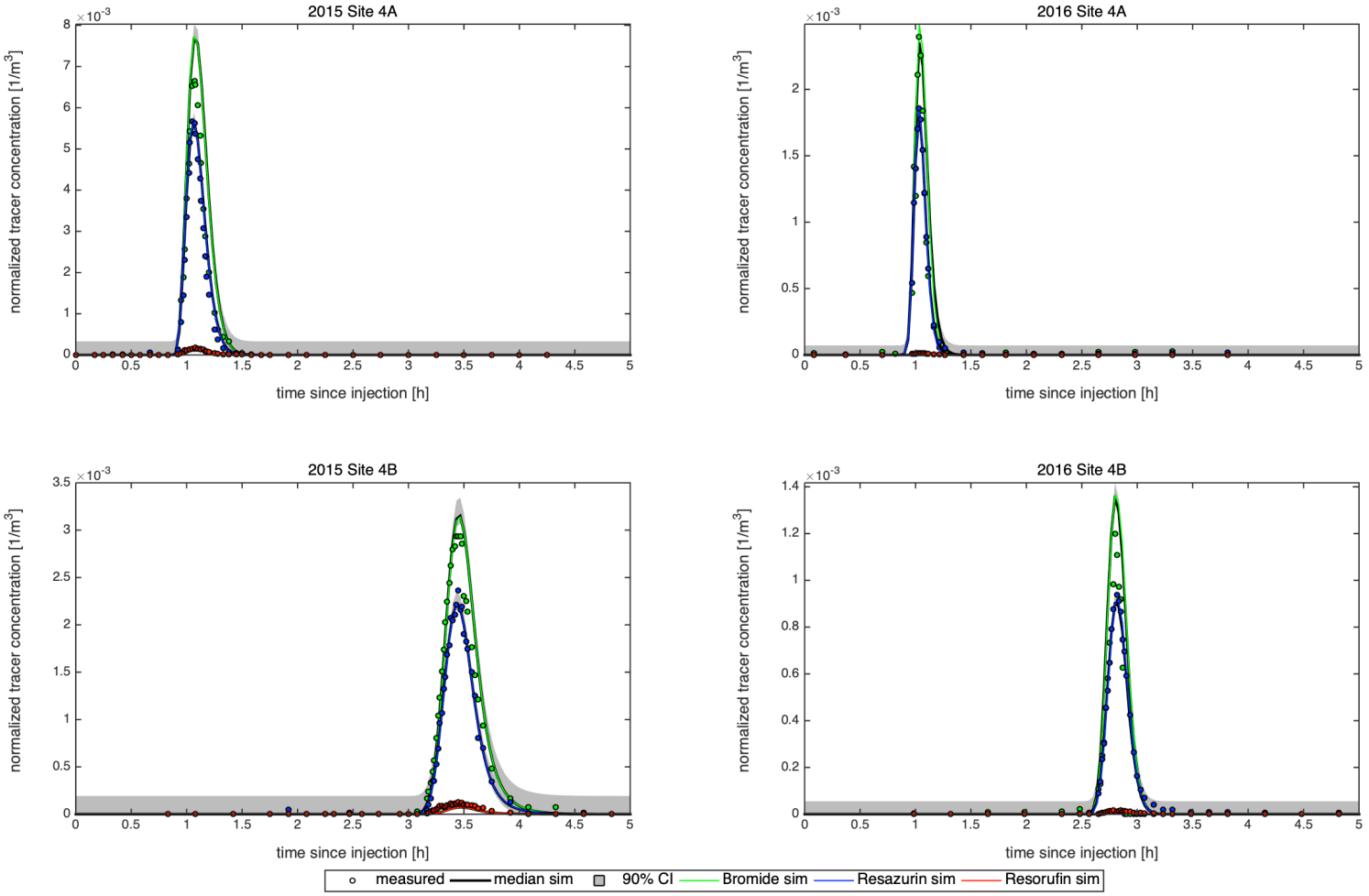
2015 Site 4A
2016 Site 4A
2015 Site 4B
2016 Site 4B
normalized tracer concentration [1/m3]
time since injection [h]
measured
median sim
90% CI
Bromide sim
Resazurin sim
Resorufin sim

Figure 4.4. Breakthrough curves for the 2015 and 2016 4th order stream reach. Measured (points), median of the best 1000 model simulations (black), and best modeled breakthrough curves for bromide (green), resazurin (blue), and resorufin (red), with the 90% confidence interval of the median curve from the last 1000 model simulations (grey) at the two downstream sampling stations (A: upstream; B: downstream) in the 4th order stream reach from the 2015 and 2016 sampling campaigns (Site 4). All plotted tracer concentrations were normalized by the number of injected moles to allow for better comparison across BTCs (Lemke et al. 2013).

For both flow regimes, we found that the total transformation coefficient of Raz, λ_1, and groundwater dilution coefficient, q_{in}, varied the most across reaches (3 orders of magnitude) and within comparable stream reaches (2 orders of magnitude). After λ_1 and q_{in}, dispersion, the mass transfer rate coefficient, k, varied by 2 orders of magnitude across reaches (Table 4.3). Other parameters such as velocity, the relative size of the storage zone, and the Raz retardation coefficient varied by ≤1 order of magnitude across all stream reaches. These results suggest that reactive transport processes are affected more strongly by spatial and temporal variability than conservative transport parameters.

The Raz total transformation rate coefficients, λ_1, typically decreased with stream order in both sampling years (Fig. 4.3f). However, λ_1 displayed a strong seasonal control, as the values in 2015 were higher than 2016. Although increases in stream order were associated with increases in stream temperature in 2015, reaction rate coefficients generally decreased with increasing stream order, suggesting that surface water temperature did not influence reactivity during baseflow conditions. These results agree with those found by Gonzalez-Pinzon et al. (2016) in a stream in Catalonia, which suggested that correcting hyporheic reaction rates based on surface water temperatures may be misleading due to drastic temperature differences between those two stream compartments.

Dilution coefficients, q_{in}, displayed similar patterns with increasing stream order to λ_1 during both sampling years, with the exception of the 4th stream order in 2016 where q_{in} increased by 2 orders of magnitude from the 3rd order stream that year (Fig. 4.3g). The variability of q_{in} values indicates that the groundwater dilution coefficient was independent of season. However, it is important to keep in mind that q_{in} is a correction term used to account for dilution of the conservative tracer.

Mass transfer rate coefficients, k, displayed greater variability during the drier conditions of 2015 (2 orders of magnitude vs. 1 order of magnitude in 2016) (Fig. 4.3c). Our results indicate that k did not always decrease with increasing stream order and was independent of season. These magnitudes of the obtained mass transfer rate coefficients are within the range of mass transfer rate coefficients found in other studies (Gooseff et al., 2005, 2013; Zarnetske et al., 2015; Knapp and Cirpka, 2018). Any differences in magnitude can be attributed to the hydrogeologic setting (i.e. stream order, time of year, and streambed substrate). Additionally, it is important to note that these studies utilized a range of reactive tracers and transient storage models to calculate k.

Based on our modeling results, for three (2^{nd}, 3^{rd} and 4^{th} order streams) of the four stream orders where we had comparable data (i.e., excluding the 5^{th} where only data for 2015 was available and excluding the 1^{st} order where the model simulation for 2016 only produced highly uncertain parameter estimates), mass transfer rates were higher and transformation rates were lower during higher flow conditions. However, these trends cannot be easily predicted from other model parameters or combination of parameters.

Table 4.3. Model parameter variability. Parameter variability across and within reaches is shown by the orders of magnitude difference across all studied stream reaches and within all pairs of studied stream reaches. The term "min" is equivalent to the minimum difference between the group of considered stream orders whereas "max" denotes the maximum difference between the group of considered stream orders. If the order of magnitude difference within a pair of stream orders was greater than or equal to one, it was noted in parentheses, thus highlighting where the greatest parameter variability occurred by sampling season.

Parameter	Orders of magnitude difference across reaches		Orders of magnitude difference within reaches (stream order with maximum value, if ≥1)	
	min	max	min	max
v [m/s]	<1	1	<1	1 (2^{nd})
D [m^2/s]	<1	2	<1	1 (4^{th})
k [1/s]	<1	2	<1	1 (2^{nd}, 4^{th})
A_s/A [-]	<1	1	<1	1 (4^{th})
R_1 [-]	<1	<1	<1	<1
λ_1 [1/s]	<1	3	1 (4^{th})	2 (2^{nd}, 3^{rd})
q_{in} [1/s]	<1	3	<1	2 (3^{rd})

For both flow regimes, we found that the Damköhler number, Da, varied the most across reaches (4 orders of magnitude) and within reaches (3 orders of magnitude). After Da, the reach-scale hyporheic exchange rate coefficient, q_{he}, varied 3 and 2 orders of magnitude across and within reaches, followed by the hyporheic zone residence time, τ_{hz}, which varied 2 and 1 orders of magnitude across and within reaches (Table 4.4). The hyporheic zone depth, d_{hz}, varied ≤1 order of magnitude.

In 2015, q_{he} decreased from the 1st to the 4th stream order before increasing in the 5th order stream. During this drier sampling period, the 5th order stream reach had a q_{he} value that was similar to that of the 1st order stream. In 2016, q_{he} was highest in the 2nd stream order and did not follow a consistent pattern further downstream.

When we normalize our q_{he} values by modeled in-stream velocity, we can compare them to other studies that also evaluated hyporheic exchange contributions throughout fluvial networks on a per meter basis (Appendix 4.23). This normalization process shows the relative proportion of hyporheic contribution to riverine processing and provides trends comparable to those reported in Wondzell (2011) regarding hyporheic contributions across spatial gradients. Our results from both sampling seasons indicated decreasing hyporheic contributions per meter with increasing stream order, which aligns with other studies (e.g., Boulton et al., 1998; Patil et al., 2013; Ward et al., 2013) that found decreasing hyporheic contributions with increasing discharge. However, under baseflow conditions, the value of normalized q_{he} increases in the 5th stream order to a value that is similar to the 1st order stream. Interestingly, the reemergence of a higher stream order in contributing to a greater proportion of hyporheic exchange flow is different than Wondzell's (2011) conceptual model and our expectations from our q_{he} values, where we would expect higher discharge values in larger stream orders to mask hyporheic

contributions. Thus, when normalized by a factor related to stream flow, larger stream order hyporheic contributions to riverine processing may be higher than expected due variable flow conditions throughout the year and have implications for large-scale predictions. Our findings agree with those of Ward et al. (in review, 2019), who utilized a 5th order fluvial network to systematically evaluate Wondzell's (2011) conceptual model and found that the predicted local hyporheic potential did not always decrease with increasing stream order. When taken together, the results from Ward et al. (in review, 2019) and our study suggest that spatiotemporal variability may play a larger role in catchment-wide hyporheic contributions.

Our values of d_{hz} were within expected ranges compared to other hyporheic zone studies (Harvey et al., 2012; Knapp et al., 2017). d_{hz} was roughly the same from the 1st to 4th order, but very different between the two sampling depths, indicating that discharge had a strong effect than stream order on hyporheic zone extent. The deepest d_{hz} was in the 5th order stream in 2015 and 4th stream order in 2016. It was interesting that the d_{hz} increased between the 4th and 5th order reaches in 2015. Based on the conceptual model proposed by Wondzell (2011), we would have expected a much shallower d_{hz} along this 5th order reach, therefore we can conclude that larger stream order reaches may not always follow expected patterns of decreasing hyporheic exchange contributions with increasing stream order. While there was no clear pattern of d_{hz} with stream order in both sampling years, the d_{hz} during the wetter sampling period were deeper than their baseflow counterparts, which is to be expected with greater hydraulic gradients during higher flow periods. The higher d_{hz} in the 5th order stream was expected, even during baseflow conditions, due to the relatively larger volume of water traveling though this larger order reach.

The lower limit of our range of τ_{hz} values was smaller than other reach-scale studies (Harvey and Fuller, 1998; Knapp et al., 2017; Knapp and Cirpka, 2017). In 2015, τ_{hz} values

were two orders of magnitude shorter in 1st and 5th order streams compared to the other sites. In 2016, the 2nd order stream had a τ_{hz} up to 2 orders of magnitude higher than τ_{hz} across all reaches (Table 4.4).

Table 4.4. Hyporheic zone metrics. Calculated hyporheic exchange rate coefficient, $q_{he} \pm 1\ \sigma\ (s^{-1})$, hyporheic zone depth, $d_{hz} \pm 1\ \sigma\ (cm)$, residence time, $\tau_{hz} \pm 1\ \sigma\ (min)$, and Damköhler number $(-)$ based on the reach-scale model results in 2015 and 2016.

Year	Stream Order	q_{he} (1/s)	d_{hz} (cm)	τ_{hz} (min)	Da (-)
2015	1	4.9e-2 ± 1.6e-3	3.3 ± 0.1	3.0e-2 ± 9.0e-6	3.9e-3 ± 7.4e-5
2015	2	6.1e-5 ± 2.8e-5	1.1 ± 0.2	7.9 ± 2.5	3.6e-1 ± 1.2e-1
2015	3	6.5e-5 ± 4.8e-6	2.2 ± 0.1	8.8 ± 0.2	2.4e-1 ± 1.9e-2
2015	4	4.0e-5 ± 8.2e-6	1.0 ± 0.1	7.6 ± 0.9	9.1e-3 ± 2.1e-2
2015	5	2.9e-2 ± 7.3e-3	9.4 ± 1.9	6.4e-2 ± 3.5e-3	2.6e-4 ± 4.6e-5
2016	2	1.7e-3 ± 2.3e-3	6.7 ± 1.1	0.9 ± 1.1	3.0e-4 ± 7.8e-4
2016	3	5.4e-4 ± 1.0e-4	7.0 ± 0.9	2.3 ± 0.2	8.0e-4 ± 1.2e-4
2016	4	3.9e-3 ± 4.0e-4	8.2 ± 0.4	5.6e-1 ± 3.0e-2	4.7e-5 ± 1.9e-4

Our Da values were within a range similar to other studies (Wagner and Harvey, 1997; Ocampo et al., 2006; Gooseff et al., 2013; Harvey et al., 2013; Zaramella et al., 2016). For all sites and flow regimes, Da<1 indicated the prevalence of reaction-limited conditions (Figure 4.5). These conditions occur when mass transfer rate coefficients are greater than reaction rate coefficients, suggesting that: 1) if more biomass is present, more processing could occur for the substrates being delivered to bioactive zones (biomass limitation), or 2) even though plentiful substrate supply and biomass are available, stoichiometric imbalances could be limiting reactions (substrate co-limitation). During the baseflow conditions, Da values increased between the 1st and 2nd order streams and for both flow regimes, decreased with increasing stream order. The 2nd and 3rd order stream reaches in 2015 had values of Da that were closer to 1, which represented a balance between transport and reaction timescales during baseflow, but still reaction-limited.

The reach-scale results displayed in Figure 4.5 show that the net functional behavior of the Jemez River is spatially and temporally dynamic. While this figure suggests a trend toward more reaction-limited conditions as discharge increases, we do not observe any consistent patterns of Da increase or decrease with respect to stream orders. As stated before, the main pattern is that all of the study reaches were reaction-limited for both flow conditions. This suggests that besides establishing a rough classification of reaction- vs. transport-limited conditions, the knowledge gained on hyporheic processing in one stream order is not readily transferable to other stream orders because unique transport and reaction dynamics seem to take place along the fluvial network.

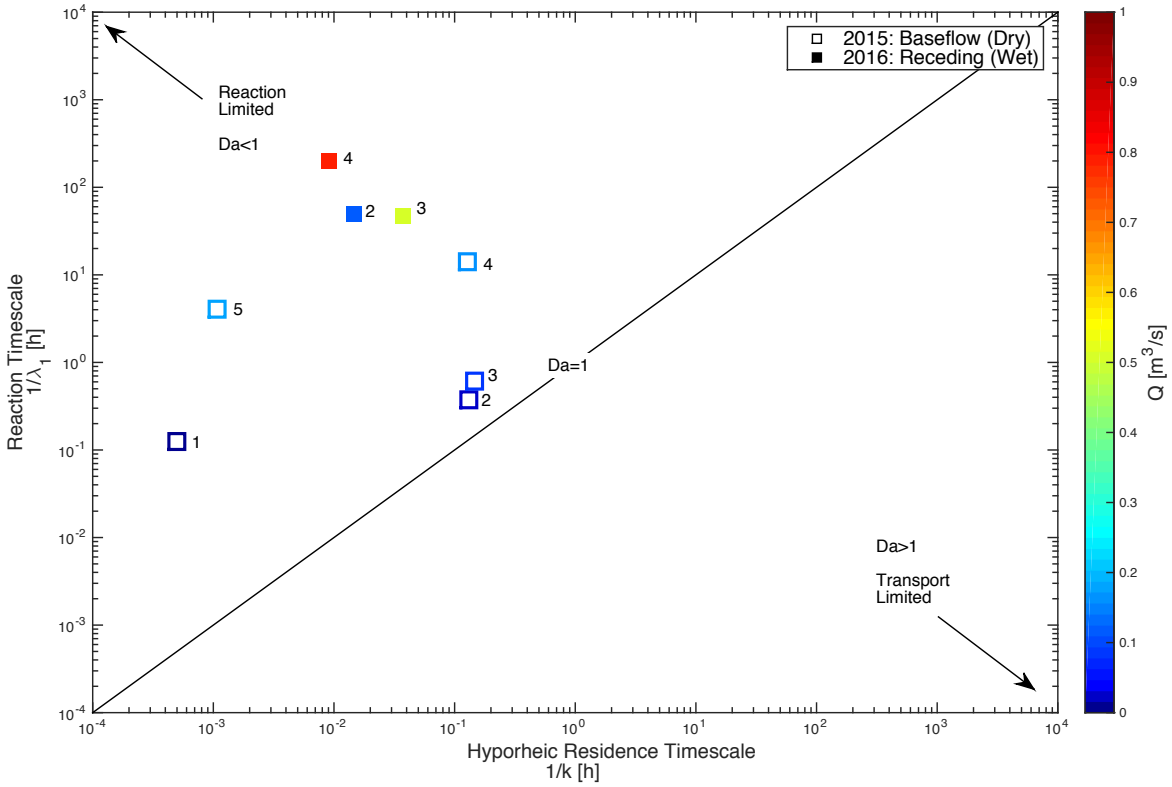

Figure 4.5. Damköhler scaling of bulk hyporheic zone activity. Dimensionless Damköhler scaling of bulk hyporheic zone reactivity. Reaction timescales, ${\lambda_{12}}^{-1}\ (h)$, increased during receding conditions while hyporheic residence timescales, $\tau_{hz} = 1/k\ (h)$, varied in response to wetter conditions. Receding conditions created more reaction limited conditions in the 4th order stream reach while greatly increasing the magnitude of reaction limited conditions remaining order stream reaches. The 2nd and 3rd order stream reach timescales moved from near-balanced conditions to reaction limited due to wetter conditions. Measured discharge, $Q\ (m^3/s)$, is indicated by the color bar scale.

It is important to note that the Da uncertainties were high due to the additive uncertainties in the residence time calculations and transformation rate coefficient of Raz to Rru, which indicates that these stream order reaches may not be strictly transport- or reaction-limited. However, we believe that Da, even with higher uncertainties, provide a useful way to look at patterns in hyporheic exchange from a non-dimensional perspective. The use of a generalized approach to classify riverine processing across different spatial scales is supported in the literature (Ocampo et al., 2006; Harvey et al., 2013; Pinay et al., 2015; Krause et al., 2017). For example, Oldham et al. (2013) suggested the use of Da as a tool to characterize material processing and study the scale-dependence of material processing within hydrologic systems. The focus on characterizing catchment hydrological elements provides a framework for moving towards a classification system that can make for easier cross-site comparisons. The use of Da, even with its associated uncertainties, provides an opportunity to explore hyporheic exchange scaling within and across different catchments.

Conclusions

We used a conservative tracer, Br^-, and a reactive tracer, Raz (and its daughter product Rru), to infer variability in hyporheic zone processing along a 1st-5th order fluvial network during low and high flow regimes in two consecutive years. Our work provides a standardized approach to comparing hyporheic zone behavior along fluvial networks and relates to other studies that have evaluated transient storage across several stream orders (e.g. Ensign and Doyle 2006; Briggs et al. 2010; Covino 2012; Gooseff et al. 2013).

Our results indicate that hyporheic zone processing throughout the Jemez River is both spatially and temporally dynamic. We found that the parameters associated with reactive transport (e.g., mass transfer and transformation rate coefficients) had more variability than those that could result from conservative transport (e.g., advection, dispersion, and groundwater input). Since some reactive transport parameters varied up to 3 orders of magnitude across reaches and other parameters only varied 1 or <1 orders of magnitude, we focused our analyses on highly varying parameters (cf. Tables 4.3 and 4.4).

Our modeling results suggest that for two (3rd and 4th order streams) of the four stream orders where we had paired data, mass transfer rates were higher and transformation rates were lower during higher flow conditions. However, these trends cannot be easily predicted from other model parameters or combination of parameters, suggesting the need to study hyporheic zone processing in different stream orders and under a variety of flow conditions. The more information we have about transport and reactive hyporheic zone processes are influenced by spatiotemporal variability, the better predictions we can make outside of headwater streams and target water resource management needs across the watershed. Additional information about how

these process scale can help fill knowledge gaps noted by Ward (2016) and inform hyporheic zone conceptual frameworks similar to those proposed by Magliozzi et al. (2018).

Using mass transfer and transformation rate coefficients, we calculated Damköhler numbers, Da, that helped us classify reaction- and transport-limited patterns in space, across stream orders, and time, for two different years with contrasting flow regimes. We found that all sites and flow regimes had $Da<1$, indicating that reaction-limited conditions are more prevalent. Such conditions may arise when microbial activity or biomass stocks are out of sync with substrate supply, or when stoichiometric imbalances limit reactions in the hyporheic zone, neither of which our study design could tell apart.

While we found a trend toward more reaction-limited conditions with increasing discharge, we did not observe consistent patterns of Da variation with respect to stream orders. Our data-based findings suggest that knowledge transferability of hyporheic zone processing along fluvial networks remains elusive. Therefore, network-scale modeling approaches may systematically over or underestimate actual processing. Either of those cases may result in improper management of water quality issues at the watershed scale.

Acknowledgements

Funding for this work was supported by the following: NSF (HRD-1345169) to RGP; CUASHI Pathfinder Fellowship and a GSA Grant-in-Aid (RG 1407-16) to KSG; the University of North Carolina at Chapel Hill; the University of New Mexico; the Pueblo of Jemez Department of Natural Resources; and funding from the European Union's Seventh Framework Program (Grant Agreement 608881) through an ETH Zurich Postdoctoral Fellowship to JK. The authors wish to thank Betsy Summers, James S. Fluke, Fabian Carbajal, Kathryn Bebe, and Justin Nichols, for their assistance in the New Mexico fieldwork and lab analyses, and Charlotte Hopson, Alexander Smith, Drew Hoag, and Savannah Swinea for their lab analysis assistance in North Carolina.

REFERENCES

Abbott, B. W., Baranov, V., Mendoza-Lera, C., Nikolakopoulou, M., Harjung, A., Kolbe, T., et al. (2016). Using multi-tracer inference to move beyond single-catchment ecohydrology. Earth-Science Reviews, 160, 19–42. https://doi.org/10.1016/j.earscirev.2016.06.014

Alexander, R. B., Boyer, E. W., Smith, R. A., Schwarz, G. E., and Moore, R. B. (2007). The role of headwater streams in downstream water quality. Journal of the American Water Resources Association, 43(1), 41–59. https://doi.org/10.1111/j.1752-1688.2007.00005.x

Argerich, A., Haggerty, R., Martí, E., Sabater, F., and Zarnetske, J. (2011). Quantification of metabolically active transient storage (MATS) in two reaches with contrasting transient storage and ecosystem respiration. Journal of Geophysical Research: Biogeosciences, 116(3), 1–14. https://doi.org/10.1029/2010JG001379

Bencala, K. E., and Walters, R. A. (1983). Simulation of solute transport in a mountain pool-and-riffle stream with a kinetic mass transfer model for sorption. Water Resources Research, 19(3), 732–738. https://doi.org/10.1029/WR019i003p00732

Beven, K. J. (2000). Uniqueness of place hydrological models. Hydrology and Earth System Sciences, 4(2), 2013–213. https://doi.org/https://doi.org/10.5194/hess-4-203-2000

Boano, F., Harvey, J. W., Marion, A., Packman, A. I., Revelli, R., Ridolfi, L., and Wörman, A. (2014). Hyporheic flow and transport processes: Mechanisms, models, and biogeochemical implications. Reviews of Geophysics, 52, 603–679. https://doi.org/10.1002/2012RG000417

Boulton, A. J., Findlay, S., Marmonier, P., Stanley, E. H., and Valett, H. M. (1998). The Functional Significance of the Hyporheic Zone in Streams and Rivers. Annual Review of Ecology and Systematics, 29(1), 59–81. https://doi.org/10.1146/annurev.ecolsys.29.1.59

Briggs, M. A., Gooseff, M. N., Peterson, B. J., Morkeski, K., Wollheim, W. M., and Hopkinson, C. S. (2010). Surface and hyporheic transient storage dynamics throughout a coastal stream network. Water Resources Research, 46(6). https://doi.org/10.1029/2009WR008222

Brunke, M., and Gonser, T. (1997). The ecological significance of exchange processes between rivers and groundwater. Freshwater Biology, 37, 1–33. https://doi.org/https://doi.org/10.1046/j.1365-2427.1997.00143.x

Cibils, A. F., Miller, J. A., Encinias, A. M., Boykin, K. G., and Cooper, B. F. (2008). Monitoring Heifer Grazing Distribution at the Valles Caldera National Preserve. Rangelands, 30(6), 19–23. https://doi.org/10.2111/1551-501X-30.6.19

Coop, J. D., and Givnish, T. J. (2007). Gradient analysis of reversed treelines and grasslands of the Valles Caldera, New Mexico. Journal of Vegetation Science, 18(1), 43–54. https://doi.org/https://doi.org/10.1111/j.1654-1103.2007.tb02514.x

Covino, T. P. (2012). The Role of Stream Network Nutrient Uptake Kinetics and Groundwater Exchange in Modifying the Timing, Magnitude, and Form of Watershed Export.

Craig, SD. 1992, Water Resources on the Pueblos of Jemez, Zia, and Santa Ana, Sandoval County, New Mexico. Water Resources Investigations Report 89-4091. Denver, Colorado: U.S. Department of the Interior U.S. Geological Survey.

Doyle, M. W. (2005). Incorporating hydrologic variability into nutrient spiraling. Journal of Geophysical Research, 110(G1), G01003. https://doi.org/10.1029/2005JG000015

Ensign, S. H., and Doyle, M. W. (2005). In-channel transient storage and associated nutrient retention: Evidence from experimental manipulations. Limnology and Oceanography, 50(6), 1740–1751. https://doi.org/10.4319/lo.2005.50.6.1740

Ensign, S. H., and Doyle, M. W. (2006). Nutrient spiraling in streams and river networks. Journal of Geophysical Research, 111(G4). https://doi.org/10.1029/2005JG000114

Fetter, C. W. 1. (2001). Applied hydrogeology. 4th ed. Upper Saddle River, N.J.: Prentice Hall.

Fischer, H., Kloep, F., Wilzcek, S., and Pusch, M. T. (2005). A River's Liver: Microbial Processes within the Hyporheic Zone of a Large Lowland River. Biogeochemistry, 76(2), 349–371. https://doi.org/10.1007/sl0533-005-6896-y

Freeman, M. C., Pringle, C. M., and Jackson, C. R. (2007). Hydrologic Connectivity and the Contribution of Stream Headwaters to Ecological Integrity at Regional Scales. Journal of the American Water Resources Association, 43(1), 5–14. https://doi.org/10.1111/j.1752-1688.2007.00002.x

Gelman, A., Rubin, D. B., Gelman, A., and Rubin, D. B. (1992). Inference from Iterative Simulation Using Multiple Sequences Linked references are available on JSTOR for this article: Inference from Iterative Simulation Using Multiple Sequences. Statistical Science, 7(4), 457–472. https://doi.org/10.1214/ss/1177011136

Gomez-Velez, J. D., and Harvey, J. W. (2014). A hydrogeomorphic river network model predicts where and why hyporheic exchange is important in large basins. Geophysical Research Letters, 41(18), 6403–6412. https://doi.org/10.1002/2014GL061099

Gomez-Velez, J. D., Harvey, J. W., Cardenas, M. B., and Kiel, B. (2015). Denitrification in the Mississippi River network controlled by flow through river bedforms. Nature Geoscience, 8(October). https://doi.org/10.1038/ngeo2567

González-Pinzón, R., and Haggerty, R. (2013). An efficient method to estimate processing rates in streams. Water Resources Research, 49, 6096–6099. https://doi.org/10.1002/wrcr.20446

González-Pinzón, R., Haggerty, R., and Myrold, D. D. (2012). Measuring aerobic respiration in stream ecosystems using the resazurin-resorufin system. Journal of Geophysical Research,

117(January), G00N06. https://doi.org/10.1029/2012JG001965

González-Pinzón, R., Haggerty, R., and Argerich, A. (2014). Quantifying spatial differences in metabolism in headwater streams. Freshwater Science, 33(3), 798–811. https://doi.org/10.1086/677555.

González-Pinzón, R., Ward, A. S., Hatch, C. E., Wlostowski, A. N., Singha, K., Gooseff, M. N., et al. (2015). A field comparison of multiple techniques to quantify groundwater – surface-water interactions. Freshwater Science, 34(August 2014), 139–160. https://doi.org/10.1086/679738.

González-Pinzón, R., Mortensen, J., and Van Horn, D. (2015). Comment on "solute-specific scaling of inorganic nitrogen and phosphorus uptake in streams" by Hall et al. (2013). Biogeosciences, 12(18), 5365–5369. https://doi.org/10.5194/bg-12-5365-2015

González-Pinzón, R., Peipoch, M., Haggerty, R., Martí, E., and Fleckenstein, J. H. (2015). Nighttime and daytime respiration in a headwater stream. Ecohydrology, n/a-n/a. https://doi.org/10.1002/eco.1615

González-Pinzón, R., Peipoch, M., Haggerty, R., Martí, E., and Fleckenstein, J. H. (2016). Nighttime and daytime respiration in a headwater stream. Ecohydrology, 9(1), 93–100. https://doi.org/10.1002/eco.1615

Gooseff, M. N. (2010). Defining Hyporheic Zones - Advancing Our Conceptual and Operational Definitions of Where Stream Water and Groundwater Meet. Geography Compass, 4(8), 945–955. https://doi.org/10.1111/j.1749-8198.2010.00364.x

Gooseff, M. N., Bencala, K. E., Scott, D. T., Runkel, R. L., and McKnight, D. M. (2005). Sensitivity analysis of conservative and reactive stream transient storage models applied to field data from multiple-reach experiments. Advances in Water Resources, 28(5), 479–492. https://doi.org/http://dx.doi.org/10.1016/j.advwatres.2004.11.012

Gooseff, M. N., Briggs, M. A., Bencala, K. E., McGlynn, B. L., and Scott, D. T. (2013). Do transient storage parameters directly scale in longer, combined stream reaches? Reach length dependence of transient storage interpretations. Journal of Hydrology, 483(0), 16–25. https://doi.org/http://dx.doi.org/10.1016/j.jhydrol.2012.12.046

Graf, W. L. (2001). age Control: Restoring the Physical Integrity of America's Rivers. Annals of the Association of American Geographers, 91(1), 1–27. https://doi.org/10.1111/0004-5608.00231

Groffman, P. M., Butterbach-Bahl, K., Fulweiler, R. W., Gold, A. J., Morse, J. L., Stander, E. K., et al. (2009). Challenges to incorporating spatially and temporally explicit phenomena (hotspots and hot moments) in denitrification models. Biogeochemistry, 93(1–2), 49–77. https://doi.org/10.1007/s10533-008-9277-5

Haggerty, R. (2002). Power-law residence time distribution in the hyporheic zone of a 2nd-order mountain stream. Geophysical Research Letters, 29(13), 1640. https://doi.org/10.1029/2002GL014743

Haggerty, R., Argerich, A., and Martí, E. (2008). Development of a "smart" tracer for the assessment of microbiological activity and sediment-water interaction in natural waters: The resazurin-resorufin system. Water Resources Research, 44(4), n/a-n/a. https://doi.org/10.1029/2007WR006670

Haggerty, R., Martí, E., Argerich, A., von Schiller, D., and Grimm, N. B. (2009). Resazurin as a "smart" tracer for quantifying metabolically active transient storage in stream ecosystems. Journal of Geophysical Research, 114(G3), G03014. https://doi.org/10.1029/2008JG000942

Hall, R. O., Baker, M. A., Rosi-Marshall, E. J., Tank, J. L., and Newbold, J. D. (2013). Solute-specific scaling of inorganic nitrogen and phosphorus uptake in streams. Biogeosciences, 10(11), 7323–7331. https://doi.org/10.5194/bg-10-7323-2013

Harvey, C. F., and Gorelick, S. M. (1995). Mapping hydraulic conductivity: Sequential conditioning with measurements of solute arrival time, hydraulic head, and local conductivity. Water Resources Research, 31(7), 1615–1626. https://doi.org/10.1029/95WR00547

Harvey, J. W., and Fuller, C. C. (1998). Effect of enhanced manganese oxidation in the hyporheic zone on basin-scale geochemical mass balance. Water Resources Research, 34(4), 623. https://doi.org/10.1029/97WR03606

Harvey, J. W., and Gooseff, M. N. (2015). River corridor science: Hydrologic exchange and ecological consequences from bedforms to basins. Water Resources Research, 51, 6893–6922. https://doi.org/10.1002/2015WR017617

Harvey, J. W., Saiers, J. E., and Newlin, J. T. (2005). Solute transport and storage mechanisms in wetlands of the Everglades, south Florida. Water Resources Research, 41(5), 1–14. https://doi.org/10.1029/2004WR003507

Harvey, J. W., Drummond, J. D., Martin, R. L., McPhillips, L. E., Packman, A. I., Jerolmack, D. J., et al. (2012). Hydrogeomorphology of the hyporheic zone: Stream solute and fine particle interactions with a dynamic streambed. Journal of Geophysical Research: Biogeosciences, 117(4), 1–20. https://doi.org/10.1029/2012JG002043

Harvey, J. W., Böhlke, J. K., Voytek, M. A., Scott, D., and Tobias, C. R. (2013). Hyporheic zone denitrification: Controls on effective reaction depth and contribution to whole-stream mass balance. Water Resources Research, 49(10), 6298–6316. https://doi.org/10.1002/wrcr.20492

Heathwaite, A. L. (2010). Multiple stressors on water availability at global to catchment scales: Understanding human impact on nutrient cycles to protect water quality and water availability in the long term. Freshwater Biology, 55(SUPPL. 1), 241–257.

https://doi.org/10.1111/j.1365-2427.2009.02368.x

Hester, E. T., Cardenas, M. B., Haggerty, R., and Apte, S. V. (2017). The importance and challenge of hyporheic mixing. Water Resources Research, 53, 3565–3575. https://doi.org/10.1002/2016WR020005

Hollenbeck, K. (1998). INVLAP. M: A MATLAB function for numerical inversion of Laplace transforms by the de Hoog algorithm. Retrieved from https://www.mathworks.com/matlabcentral/answers/uploaded_files/1034/invlap.m

Homer, C.G., Dewitz, J.A., Yang, L., Jin, S., Danielson, P., Xian, G., Coulston, J., Herold, N.D., Wickham, J.D., and Megown, K., 2015, Completion of the 2011 National Land Cover Database for the conterminous United States-Representing a decade of land cover change information. Photogrammetric Engineering and Remote Sensing, v. 81, no. 5, p. 345-354

Kirchner, J. W. (2006). Getting the right answers for the right reasons: Linking measurements, analyses, and models to advance the science of hydrology. Water Resources Research, 42(3), 1–5. https://doi.org/10.1029/2005WR004362

Knapp, J. L. A., and Cirpka, O. A. (2017). Determination of Hyporheic Travel-Time Distributions and other Parameters from Concurrent Conservative and Reactive Tracer Tests by Local-in-Global Optimization. Water Resources Research, 53. https://doi.org/10.1002/2017WR020734

Knapp, J. L. A., and Cirpka, O. A. (2018). A Critical Assessment of Relating Resazurin-Resorufin Experiments to Stream Metabolism in Lowland Streams, 1–35. https://doi.org/10.1029/2018JG004797

Knapp, J. L. A., González-Pinzón, R., Drummond, J. D., Larsen, L. G., Cirpka, O. A., and Harvey, J. W. (2017). Tracer-based characterization of hyporheic exchange and benthic biolayers in streams. Water Resources Research, 53. https://doi.org/10.1002/2013WR014979

Knapp, J. L. A., González-Pinzón, R., and Haggerty, R. (2018). The Resazurin-Resorufin System: Insights from a Decade of "Smart" Tracer Development for Hydrologic Applications. Water Resources Research, 54(9), 6877–6889. https://doi.org/10.1029/2018WR023103

Krause, S., Hannah, D. M., Fleckenstein, J. H., Heppell, C. M., Kaeser, D., Pickup, R., et al. (2011). Inter-disciplinary perspectives on processes in the hyporheic zone. Ecohydrology, 4, 481–499. https://doi.org/10.1002/eco

Krause, S., Lewandowski, J., Grimm, N. B., Hannah, D. M., Pinay, G., McDonald, K., et al. (2017). Ecohydrological interfaces as hot spots of ecosystem processes. Water Resources Research, 53(8), 6359–6376. https://doi.org/10.1002/2016WR019516

Lemke, D., Liao, Z., Wöhling, T., Osenbrück, K., and Cirpka, O. A. (2013). Concurrent conservative and reactive tracer tests in a stream undergoing hyporheic exchange. Water Resources Research, 49(5), 3024–3037. https://doi.org/10.1002/wrcr.20277

Lemke, D., González-Pinzón, R., Liao, Z., Wöhling, T., Osenbrück, K., Haggerty, R., and Cirpka, O. A. (2014). Sorption and transformation of the reactive tracers resazurin and resorufin in natural river sediments. Hydrology and Earth System Sciences, 18(8), 3151–3163. https://doi.org/10.5194/hess-18-3151-2014

Liao, Z., and Cirpka, O. A. (2011). Shape-free inference of hyporheic travel time distributions from synthetic conservative and "smart" tracer tests in streams. Water Resources Research, 47(7), 1–14. https://doi.org/10.1029/2010WR009927

Liao, Z., Lemke, D., Osenbrück, K., and Cirpka, O. A. (2013). Modeling and inverting reactive stream tracers undergoing two-site sorption and decay in the hyporheic zone. Water Resources Research, 49(6), 3406–3422. https://doi.org/10.1002/wrcr.20276

Magliozzi, C., Grabowski, R., Packman, A. I., and Krause, S. (2018). Toward a conceptual framework of hyporheic exchange across spatial scales. Hydrology and Earth System Sciences, 22(May), 6163–6185. https://doi.org/10.5194/hess-2018-268

McClain, M. E., Boyer, E. W., Dent, C. L., Gergel, S. E., Grimm, N. B., Groffman, P. M., et al. (2003). Biogeochemical Hot Spots and Hot Moments at the Interface of Terrestrial and Aquatic Ecosystems. Ecosystems, 6(4), 301–312. https://doi.org/10.1007/s10021-003-0161-9

McDonnell, J. J., Sivapalan, M., Vaché, K., Dunn, S., Grant, G., Haggerty, R., et al. (2007). Moving beyond heterogeneity and process complexity: A new vision for watershed hydrology. Water Resources Research, 43(7). https://doi.org/10.1029/2006WR005467

New Mexico Climate Center. Cooperative Observer Program Stations. 2018 Jul [accessed 2018 Jul]. https://weather.nmsu.edu/coop/

Nowinski, J. D., Cardenas, M. B., and Lightbody, A. F. (2011). Evolution of hydraulic conductivity in the floodplain of a meandering river due to hyporheic transport of fine materials. Geophysical Research Letters, 38(1), n/a-n/a. https://doi.org/10.1029/2010GL045819

Ocampo, C. J., Oldham, C. E., and Sivapalan, M. (2006). Nitrate attenuation in agricultural catchments: Shifting balances between transport and reaction. Water Resources Research, 42(1), 1–16. https://doi.org/10.1029/2004WR003773

Oldham, C. E., Farrow, D. E., and Peiffer, S. (2013). A generalized Damköhler number for classifying material processing in hydrological systems. Hydrology and Earth System Sciences, 17(3), 1133–1148. https://doi.org/10.5194/hess-17-1133-2013

Orghidan, T. (1959). A new habitat of subsurface waters: the hyporheic biotope. Fundamental and Applied Limnology / Archiv Für Hydrobiologie, 176(4), 291–302. https://doi.org/10.1127/1863-9135/2010/0176-0291

Patil, S., Covino, T. P., Packman, A. I., McGlynn, B. L., Drummond, J. D., Payn, R. A., and Schumer, R. (2013). Intrastream variability in solute transport: Hydrologic and geomorphic controls on solute retention. Journal of Geophysical Research: Earth Surface, 118(2), 413–422. https://doi.org/10.1029/2012JF002455

Payn, R. A., Gooseff, M. N., Benson, D. A., Cirpka, O. A., Zarnetske, J. P., Bowden, W. B., et al. (2008). Comparison of instantaneous and constant-rate stream tracer experiments through non-parametric analysis of residence time distributions. Water Resources Research, 44(6), 1–10. https://doi.org/10.1029/2007WR006274

Pinay, G., Peiffer, S., De Dreuzy, J. R., Krause, S., Hannah, D. M., Fleckenstein, J. H., et al. (2015). Upscaling Nitrogen Removal Capacity from Local Hotspots to Low Stream Orders' Drainage Basins. Ecosystems, 18(6), 1101–1120. https://doi.org/10.1007/s10021-015-9878-5

Runkel, R. L. (1998). One-dimensional transport with inflow and storage (OTIS): a solute transport model for streams and rivers. Water-Resources Investigations Report 98-4018, 0–80. https://doi.org/https://doi.org/10.3133/wri984018

Small, E. E., and McConnell, J. R. (2008). Comparison of soil moisture and meteorological controls on pine and spruce transpiration. Ecohydrology, 1, 205–214. https://doi.org/10.1002/eco

Smith, R.L., Bailey, R.A. and Ross, C. S. (1970). Geologic Map of the Jemez Mountains, New Mexico. Miscellaneous Geologic Investigations Map I-571. USGS, Reston, VA, US.

Stonedahl, S. H., Harvey, J. W., and Packman, A. I. (2013). Interactions between hyporheic flow produced by stream meanders, bars, and dunes. Water Resources Research, 49(9), 5450–5461. https://doi.org/10.1002/wrcr.20400

Strahler, A. N. (1952). Hypsometric (Area - Altitude) Analysis of Erosional Topography. Geological Society of America Bulletin, 63(11), 1117–1142. https://doi.org/10.1130/0016-7606(1952)63

Stream Solute Workshop. (1990). Concepts and Methods for Assessing Solute Dynamics in Stream Ecosystems. Journal of the North American Benthological Society, 9(2), 95–119.

Tank, J. L., Rosi-Marshall, E. J., Baker, M. A., and Hall, Jr., R. O. (2008). Are Rivers Just Big Streams? A Pulse Method to Quantify Nitrogen Demand in a Large River. Ecology, 89(10), 2935–2945. https://doi.org/https://doi.org/10.1890/07-1315.1

United States Geological Survey. National Water Information Systems. Site Map for New

Mexico. 7/18 [accessed 7/18]. https://waterdata.usgs.gov/nm/nwis/nwismap/?site_no=08328950andagency_cd=USGS

Vomocil, J. A. (1965). Porosity. In C. A. Black (Ed.), Methods of Soil Analysis (pp. 299–314). Madison, Wisconsin: American Society of Agronomy.

Wagner, B. J., and Harvey, J. W. (1997). Experimental design for estimating parameters of rate-limited mass transfer: Analysis of stream tracer studies. Water Resources Research, 33(7), 1731. https://doi.org/10.1029/97WR01067

Ward, A. S. (2016). The evolution and state of interdisciplinary hyporheic research. Wiley Interdisciplinary Reviews: Water, 3(January/February), 83–103. https://doi.org/10.1002/wat2.1120

Ward, A. S., Payn, R. A., Gooseff, M. N., McGlynn, B. L., Bencala, K. E., Kelleher, C. A., et al. (2013). Variations in surface water-ground water interactions along a headwater mountain stream: Comparisons between transient storage and water balance analyses. Water Resources Research, 49(6), 3359–3374. https://doi.org/10.1002/wrcr.20148

Ward, A. S., Wondzell, B. S. M., Schmadel, N. M., Herzog, S., Zarnetske, J. P., Baranov, V., et al. (in review, 2019). Spatial and temporal variation in river corridor exchange across a 5th order mountain stream network. *Hydrology and Earth System Sciences*, (April), 1–39. https://doi.org/https://doi.org/10.5194/hess-2019-108

Woessner, W. W. (2000). Stream and fluvial plain ground water interactions: Rescaling hydrogeologic thought. Ground Water, 38(3), 423–429. https://doi.org/https://doi.org/10.1111/j.1745-6584.2000.tb00228.x

Wohl, E. (2015). Legacy Effects on Sediments in River Corridors. Earth-Science Reviews, 147, 30–53. https://doi.org/10.1016/j.earscirev.2015.05.001

Wollheim, W. M., Vörösmarty, C. J., Peterson, B. J., Seitzinger, S. P., and Hopkinson, C. S. (2006). Relationship between river size and nutrient removal. Geophysical Research Letters, 33(6), 2–5. https://doi.org/10.1029/2006GL025845

Wondzell, S. M. (2011). The role of the hyporheic zone across stream networks. Hydrological Processes, 25(22), 3525–3532. https://doi.org/10.1002/hyp.8119

Wörman, A., Packman, A. I., Johansson, H., and Jonsson, K. (2002). Effect of flow-induced exchange in hyporheic zones on longitudinal transport of solutes in streams and rivers. Water Resources Research, 38(1), 2-1-2–15. https://doi.org/10.1029/2001WR000769

Wroblicky, G. J., Campana, M. E., Valett, H. M., and Dahm, N. (1998). Seasonal variation in surface-subsurface water exchange and lateral hyporheic area of two stream-aquifer systems. Water Resources Research, 34(3), 317–328. https://doi.org/https://doi.org/10.1029/97WR03285

Xie, X., and Zhang, D. (2010). Data assimilation for distributed hydrological catchment modeling via ensemble Kalman filter. Advances in Water Resources, 33(6), 678–690. https://doi.org/10.1016/j.advwatres.2010.03.012

Xie, Y., Cook, P. G., Shanafield, M., Simmons, C. T., and Zheng, C. (2016). Uncertainty of natural tracer methods for quantifying river-aquifer interaction in a large river. Journal of Hydrology, 535, 135–147. https://doi.org/10.1016/j.jhydrol.2016.01.071

Zaramella, M., Marion, A., Lewandowski, J., and Nützmann, G. (2016). Assessment of transient storage exchange and advection-dispersion mechanisms from concentration signatures along breakthrough curves. Journal of Hydrology, 538, 794–801. https://doi.org/10.1016/j.jhydrol.2016.05.004

Zarnetske, J. P., Haggerty, R., and Wondzell, S. M. (2015). Coupling multiscale observations to evaluate hyporheic nitrate removal at the reach scale. Freshwater Science, 34(1), 172–186. https://doi.org/10.1086/680011

CHAPTER 5. - CONCLUSION.

Overall Conclusions

The goal of this dissertation was to quantify hyporheic exchange spatial and temporal heterogeneity, from multiple perspectives, to increase our hyporheic zone process knowledge and better meet riverine materials processing demands. The research challenges described in Chapter 1 are driven by the dynamic nature of hyporheic zones, coupled with difficulties stemming from the lack of a unifying conceptual model that describes how hyporheic exchange scales from individual study sites to entire fluvial networks. Chapters 2, 3, and 4 each focused on unique hyporheic zone spatiotemporal scales and the insights generated from each study help increase our understanding of hyporheic zone dynamics. As a whole, the results of my research will provide a foundation for further study and development of hyporheic exchange scaling relationships throughout the river continuum, as they pertain to riverine materials processing and controls on water quality.

Chapter 2 demonstrated that hyporheic zones respond variability to a series of fine particle disturbances. This study was designed to evaluate how fine particle disturbances influence the water column and streambed in a recirculating laboratory flume over the course of several days. We observed both fine particle infiltration and resuspension throughout our experiments. This suggests that individual and recursive disturbance events are associated with cycles of streambed clogging and recovery that have unique impacts on hyporheic exchange at the sediment-water interface. These results also support expanding the application of temperature

time series data to improve our understanding of streambed clogging responses in model systems and field environments, while informing possible water quality outcomes.

Chapter 3 confirmed that not all portions of the hyporheic zone contribute equally to riverine materials processing throughout a single stream reach and that subsurface reactivity does not always scale as expected with increasing stream order. Tracer breakthrough curves were sampled directly from the pore waters at two sampling locations in three unique stream orders. We utilized a previously developed subsurface transient storage model to evaluate hyporheic zone processing along vertical, downwelling flowpaths within each stream order. These results suggest that intra-reach and inter-reach heterogeneity play variable roles in hyporheic contributions to overall fluvial network processing and related water quality outcomes.

Chapter 4 revealed that knowledge transferability of hyporheic zone processing along fluvial networks still remains elusive, as reach-scale hyporheic zone contributions to riverine processing did not vary longitudinally and seasonally as excepted from current scaling relationship theories. We explored hyporheic exchange dynamics from spatial and temporal perspectives with the transient storage modeling of nine unique reactive tracer tests that were performed in two different years. Our findings suggest that network-scale modeling approaches may systematically misestimate actual hyporheic zone processing, resulting in an improper management of water quality issues at the watershed scale.

Future Research Directions

While this dissertation provides an understanding of hyporheic zone spatial variability, ranging from the sediment-water interface to a 5th order fluvial network, and temporal variability, ranging from hours to seasons, a number of interesting questions remain unanswered. For

example, the streambed clogging response study presented in Chapter 2 was completed in a recirculating laboratory flume, which reduced exchange to a vertical flux between the surface water and streambed, under an assumed steady streamflow. In reality, exchanges between surface waters and streambed environments vary with stream discharge and groundwater inflow. Quantifying the effects of variable streamflow, especially gaining and losing conditions, on streambed clogging dynamics would add to the applicability of this study to clogging dynamics in stream environments similar to the work of Karwan and Saiers (2009), Arnon, et al. (2010), and Fox et al. (2016). Additionally, the use of heat differential to evaluate *in situ* hyporheic zone disturbance responses can be easily applied to a number of field studies and take advantage of naturally occurring diurnal streambed temperature patterns (Briggs et al., 2012; Gordon et al., 2013; Irvine et al., 2017). The addition of longer-term streambed temperature data before, during, and after future field studies can contribute to clarifying hyporheic exchange disturbance-response behaviors while expanding our understanding the drivers of spatiotemporal heterogeneity related to riverine materials processing.

Chapters 3 and 4 utilized reactive tracers to better understand spatiotemporal differences in streambed reactivity and how potential hyporheic zone contributions vary with depth and throughout a fluvial network. The results from Chapter 3 support the concept of a benthic biolayer, where streambed reactivity is highest near the streambed surface, in addition to intra- and inter-reach processing variability (O'Connor et al., 2012; Arnon et al., 2013; Knapp et al., 2017). Chapter 4 took advantage of tracer studies that were performed under two unique flow regimes and the results suggest that hyporheic zone processing contributions vary longitudinally and seasonally (Ensign & Doyle, 2006; Tank et al., 2008; González-Pinzón et al., 2013; Bernhardt et al., 2017). However, both studies show that hyporheic zone contributions to riverine

materials processing do not always follow excepted patters of decreasing with increasing stream order. These findings suggest that more work is needed to quantify streambed reactivity throughout fluvial networks that include larger stream order reaches, in addition to well-studied headwater streams. Additional streambed reactivity data from a variety of fluvial networks can improve our riverine scaling relationships and advance our hyporheic zone process knowledge towards a clearer, conceptual framework of hyporheic exchange across spatiotemporal scales (Ward, 2016; Boano et al., 2014; Harvey, 2016; Magliozzi et al., 2018).

After completing the research for each of these chapters, I believe there is more work to do with regards to improving our understanding of hyporheic exchange spatiotemporal variability. While additional laboratory, modeling, and field studies can generate the data needed to improve our predictions of hyporheic contributions throughout the river continuum, I see the wealth of existing hyporheic exchange knowledge as an opportunity to address these challenges. Synthesis of existing data can provide a path forward to addressing the known hyporheic zone research challenges. A detailed metanalysis of existing field studies that evaluate hyporheic zone properties, including metrics such as depth and hyporheic exchange rate, from a variety of catchments can help us quantify hyporheic contributions relative to riverine materials processing. Results from this analysis can inform hyporheic exchange scaling relationships and improve riverine conceptual models that account for hyporheic properties. Additionally, a metanalysis can further support the use of summary riverine processing metrics, such as Damköhler numbers and the reaction significance factor, that may help us better elucidate spatiotemporal patterns in streambed reactivity and water quality dynamics (Ocampo et al., 2006; Oldham et al., 2013; Pinay et al., 2015; Abbott et al., 2016; Harvey et al., 2018).

Final Thoughts

Although the hyporheic zone is relatively small in size when compared to other hydrologic components, it plays a major role in riverine ecosystem process-based, biogeochemical, and ecological functioning (Orghidan, 1959; Brunke & Gonser, 1997; Boulton et al., 1998; Krause et al., 2011; Cardenas, 2015). Streambed hyporheic exchange creates a predictable vector for dissolved constituents to travel between surface water and groundwater environments (Hester & Gooseff, 2010; Boano et al., 2014). The development and maintenance of the hyporheic zone is governed by this bidirectional water exchange. Hyporheic exchange has the potential to significantly impact stream ecosystems at all scales ranging from interstitial pore spaces to larger fluvial networks (Findlay, 1995; Boulton et al., 2010; Hartwig & Borchardt, 2015). As such, hyporheic zone integrity can play important roles in stream biogeochemical cycling, water quality, streambed organism life cycles, and provide a foundation for higher trophic levels (Nogaro et al., 2010; Descloux et al., 2014).

Understanding hyporheic zone dynamics and how controls on riverine materials processing scale, must be at the forefront of scientific exploration and catchment management for hyporheic zone process knowledge to meet the current demand for predictions of larger scale water quality outcomes (Krause et al., 2011; Abbott et al., 2016). As such, the associated challenges and knowledge gaps can be met with continued data collection, the use of innovated technologies, careful evaluation of our current knowledge base, and further scientific collaboration (Woessner, 2000; Sophocleous, 2002; Marmonier et al., 2012; Boano et al., 2014). Strengthening interdisciplinary cooperation between hyporheic zone researchers is needed as we seek to fully articulate the effects of hyporheic exchange spatiotemporal variability on riverine ecosystem functions and better inform riverine ecosystem management.

REFERENCES

Abbott, B. W., Baranov, V., Mendoza-Lera, C., Nikolakopoulou, M., Harjung, A., Kolbe, T., et al. (2016). Using multi-tracer inference to move beyond single-catchment ecohydrology. *Earth-Science Reviews*, *160*, 19–42. https://doi.org/10.1016/j.earscirev.2016.06.014

Arnon, S., Marx, L. P., Searcy, K. E., & Packman, A. I. (2010). Effects of overlying velocity, particle size, and biofilm growth on stream-subsurface exchange of particles. *Hydrological Processes*, *24*, 108–114. https://doi.org/10.1002/hyp

Arnon, S., Yanuka, K., & Nejidat, A. (2013). Impact of overlying water velocity on ammonium uptake by benthic biofilms. *Hydrological Processes*, *27*(4), 570–578. https://doi.org/10.1002/hyp.9239

Bernhardt, E. S., Blaszczak, J. R., Ficken, C. D., Fork, M. L., Kaiser, K. E., & Seybold, E. C. (2017). Control Points in Ecosystems: Moving Beyond the Hot Spot Hot Moment Concept. *Ecosystems*, *20*(4), 665–682. https://doi.org/10.1007/s10021-016-0103-y

Boano, F., Harvey, J. W., Marion, A., Packman, A. I., Revelli, R., Ridolfi, L., & Wörman, A. (2014). Hyporheic flow and transport processes: Mechanisms, models, and biogeochemical implications. *Reviews of Geophysics*, *52*, 603–679. https://doi.org/10.1002/2012RG000417

Boulton, A. J., Findlay, S., Marmonier, P., Stanley, E. H., & Valett, H. M. (1998). The Functional Significance of the Hyporheic Zone in Streams and Rivers. *Annual Review of Ecology and Systematics*, *29*(1), 59–81. https://doi.org/10.1146/annurev.ecolsys.29.1.59

Boulton, A. J., Datry, T., Kasahara, T., Mutz, M., & Stanford, J. A. (2010). Ecology and management of the hyporheic zone: stream–groundwater interactions of running waters and their floodplains. *Journal of the North American Benthological Society*, *29*(1), 26–40. https://doi.org/10.1899/08-017.1

Briggs, M. A., Lautz, L. K., McKenzie, J. M., Gordon, R. P., & Hare, D. K. (2012). Using high-resolution distributed temperature sensing to quantify spatial and temporal variability in vertical hyporheic flux. *Water Resources Research*, *48*(2), 1–16. https://doi.org/10.1029/2011WR011227

Brunke, M., & Gonser, T. (1997). The ecological significance of exchange processes between rivers and groundwater. *Freshwater Biology*, *37*, 1–33. https://doi.org/https://doi.org/10.1046/j.1365-2427.1997.00143.x

Cardenas, M. B. (2015). Hyporheic zone hydrologic science: A historical account of its emergence and a prospectus. *Water Resources Research*, *6*(4), 446. https://doi.org/10.1016/0022-1694(68)90080-2

Descloux, S., Datry, T., & Usseglio-Polatera, P. (2014). Trait-based structure of invertebrates along a gradient of sediment colmation: Benthos versus hyporheos responses. *Science of the*

Total Environment, *466–467*, 265–276. https://doi.org/10.1016/j.scitotenv.2013.06.082

Ensign, S. H., & Doyle, M. W. (2006). Nutrient spiraling in streams and river networks. *Journal of Geophysical Research*, *111*(G4). https://doi.org/10.1029/2005JG000114

Findlay, S. (1995). Importance of surface-subsurface exchange in stream ecosystems: The hyporheic zone. *Limnology and Oceanography*, *40*(1), 159–164. https://doi.org/10.4319/lo.1995.40.1.0159

Fox, A., Laube, G., Schmidt, C., Fleckenstein, J. H., & Arnon, S. (2016). The effect of losing and gaining flow conditions on hyporheic exchange in heterogeneous streambeds. *Water Resources Research*, *52*(9), 7460–7477. https://doi.org/10.1002/2016WR018677

González-Pinzón, R., Haggerty, R., & Dentz, M. (2013). Scaling and predicting solute transport processes in streams. *Water Resources Research*, *49*(7), 4071–4088. https://doi.org/10.1002/wrcr.20280

Gordon, R. P., Lautz, L. K., & Daniluk, T. L. (2013). Spatial patterns of hyporheic exchange and biogeochemical cycling around cross-vane restoration structures: Implications for stream restoration design. *Water Resources Research*, *49*(4), 2040–2055. https://doi.org/10.1002/wrcr.20185

Hartwig, M., & Borchardt, D. (2015). Alteration of key hyporheic functions through biological and physical clogging along a nutrient and fine-sediment gradient. *Ecohydrology*, *975*(November 2014), n/a-n/a. https://doi.org/10.1002/eco.1571

Harvey, J., Gomez-Velez, J., Schmadel, N., Scott, D., Boyer, E., Alexander, R., et al. (2018). How Hydrologic Connectivity Regulates Water Quality in River Corridors. *Journal of the American Water Resources Association*, *55*(2), 369–381. https://doi.org/10.1111/1752-1688.12691

Harvey, J. W. (2016). Hydrologic Exchange Flows and Their Ecological Consequences in River Corridors. In B. Jones, Jeremy & E. Stanley (Eds.), *Stream Ecosytems in a Changing Environment* (pp. 1–83). Academic Press.

Hester, E. T., & Gooseff, M. N. (2010). Moving Beyond the Banks : Hyporheic Restoration Is Fundamental to Restoring Ecological Services and Functions of Streams. *Enivronmental Science and Technology*, *44*, 1521–1525.

Irvine, D. J., Briggs, M. A., Cartwright, I., Scruggs, C. R., & Lautz, L. K. (2017). Improved Vertical Streambed Flux Estimation Using Multiple Diurnal Temperature Methods in Series. *Groundwater*, *55*(1), 73–80. https://doi.org/10.1111/gwat.12436

Karwan, D. L., & Saiers, J. E. (2009). Influences of seasonal flow regime on the fate and transport of fine particles and a dissolved solute in a New England stream. *Water Resources Research*, *45*(11), 1–9. https://doi.org/10.1029/2009WR008077

Knapp, J. L. A., González-Pinzón, R., Drummond, J. D., Larsen, L. G., Cirpka, O. A., & Harvey,

J. W. (2017). Tracer-based characterization of hyporheic exchange and benthic biolayers in streams. *Water Resources Research*, *53*. https://doi.org/10.1002/2013WR014979

Krause, S., Hannah, D. M., Fleckenstein, J. H., Heppell, C. M., Kaeser, D., Pickup, R., et al. (2011). Inter-disciplinary perspectives on processes in the hyporheic zone. *Ecohydrology*, *4*, 481–499. https://doi.org/10.1002/eco

Magliozzi, C., Grabowski, R., Packman, A. I., & Krause, S. (2018). Toward a conceptual framework of hyporheic exchange across spatial scales. *Hydrology and Earth System Sciences*, *22*(May), 6163–6185. https://doi.org/10.5194/hess-2018-268

Marmonier, P., Archambaud, G., Belaidi, N., Bougon, N., Breil, P., Chauvet, E., et al. (2012). The role of organisms in hyporheic processes: gaps in current knowledge, needs for future research and applications. *Annales de Limnologie - International Journal of Limnology*, *48*(3), 253–266. https://doi.org/10.1051/limn/2012009

Nogaro, G., Datry, T., Mermillod-Blondin, F., Descloux, S., & Montuelle, B. (2010). Influence of streambed sediment clogging on microbial processes in the hyporheic zone. *Freshwater Biology*, *55*(6), 1288–1302. https://doi.org/10.1111/j.1365-2427.2009.02352.x

O'Connor, B. L., Harvey, J. W., & McPhillips, L. E. (2012). Thresholds of flow-induced bed disturbances and their effects on stream metabolism in an agricultural river. *Water Resources Research*, *48*(8), n/a-n/a. https://doi.org/10.1029/2011WR011488

Ocampo, C. J., Oldham, C. E., & Sivapalan, M. (2006). Nitrate attenuation in agricultural catchments: Shifting balances between transport and reaction. *Water Resources Research*, *42*(1), 1–16. https://doi.org/10.1029/2004WR003773

Oldham, C. E., Farrow, D. E., & Peiffer, S. (2013). A generalized Damköhler number for classifying material processing in hydrological systems. *Hydrology and Earth System Sciences*, *17*(3), 1133–1148. https://doi.org/10.5194/hess-17-1133-2013

Orghidan, T. (1959). A new habitat of subsurface waters: the hyporheic biotope. *Fundamental and Applied Limnology / Archiv Für Hydrobiologie*, *176*(4), 291–302. https://doi.org/10.1127/1863-9135/2010/0176-0291

Pinay, G., Peiffer, S., De Dreuzy, J. R., Krause, S., Hannah, D. M., Fleckenstein, J. H., et al. (2015). Upscaling Nitrogen Removal Capacity from Local Hotspots to Low Stream Orders' Drainage Basins. *Ecosystems*, *18*(6), 1101–1120. https://doi.org/10.1007/s10021-015-9878-5

Sophocleous, M. (2002). Interactions between groundwater and surface water: the state of the science. *Hydrogeology Journal*, *10*(1), 52–67. https://doi.org/10.1007/s10040-001-0170-8

Tank, J. L., Rosi-Marshall, E. J., Baker, M. A., & Hall, Jr., R. O. (2008). Are Rivers Just Big Streams ? A Pulse Method To Quantify Nitrogen Demand in a Large River. *Ecology*,

89(10), 2935–2945. https://doi.org/https://doi.org/10.1890/07-1315.1

Ward, A. S. (2016). The evolution and state of interdisciplinary hyporheic research. *Wiley Interdisciplinary Reviews: Water*, *3*(January/February), 83–103. https://doi.org/10.1002/wat2.1120

Woessner, W. W. (2000). Stream and fluvial plain ground water interactions: Rescaling hydrogeologic thought. *Ground Water*, *38*(3), 423–429. https://doi.org/https://doi.org/10.1111/j.1745-6584.2000.tb00228.x

APPENDIX A: CHAPTER 3 SUPPLEMENTAL INFORMATION.

Appendix 3.1: Table of model parameters

Calibrated parameters (± 1 σ) and goodness of fit metrics for each stream order and sampling depth[a]. Normalized residual sum of squares for bromide, $nRSS_{br}$ (-), resazurin, $nRSS_{raz}$ (-), and resorufin, $nRSS_{rru}$ (-) represent the sum of squared residuals normalized by the squared theoretical peak tracer concentrations. [a]n.d. indicate that tracer breakthrough curves were not sampled at these additional depths.

Stream Order Sampling Station	Description	2 A	2 B	3 A	3 B	4 A	4 B
Depth 1		3 cm	3 cm	4 cm	3 cm	3 cm	3 cm
v_z [m/s]	Advective velocity	1.6e-4 ± 7.5e-6	4.5e-3 ± 2.6e-4	1.2e-6 ± 1.1e-6	2.9e-4 ± 8.1e-6	3.4e-5 ± 6.7e-7	3.1e-6 ± 2.5e-7
D_z [m^2/s]	Dispersion coefficient	4.9e-7 ± 2.6e-8	4.7e-4 ± 2.4e-5	1.4e-6 ± 6.5e-8	2.3e-6 ± 1.8e-7	8.4e-7 ± 1.7e-8	3.3e-7 ± 6.4e-9
q_{in} [1/s]	Groundwater dilution rate coefficient	4.6e-4 ± 9.6e-5	1.3e-1 ± 4.8e-3	1.2e-4 ± 5.0e-5	5.5e-4 ± 3.7e-5	1.7e-4 ± 9.5e-6	8.0e-4 ± 2.0e-5
R_1 [-]	Resorufin retardation coefficient	2.052 ± 9.6e-2	1.15 ± 1.7e-1	1.31 ± 5.6e-2	1.80 ± 4.5e-2	1.32 ± 2.5e-2	1.29 ± 2.4e-2
λ_1 [1/s]	Resazurin total transformation coefficient	9.0e-4 ± 5.3e-5	4.7e-3 ± 2.6e-4	1.1e-3 ± 5.2e-5	1.3e-4 ± 6.0e-5	1.6e-5 ± 1.2e-5	1.4e-5 ± 1.3e-5
R_2 [-]	Resorufin retardation coefficient	2.15 ± 3.3e-2	1.66 ± 3.7e-2	1.01 ± 4.9e-3	1.04 ± 1.9e-3	1.01 ± 1.1e-2	1.02 ± 7.7e-4
λ_{12} [1/s]	Resazurin to resorufin transformation coefficient	3.3e-4 ± 1.1e-5	4.0e-3 ± 9.5e-5	3.2e-5 ± 6.4e-7	1.3e-4 ± 1.5e-7	1.6e-5 ± 3.2e-8	1.4e-5 ± 2.6e-8
λ_2 [1/s]	Resorufin transformation coefficient	4.5e-3 ± 2.4e-4	2.7e-4 ± 1.7e-5	1.2e-5 ± 2.5e-6	9.9e-4 ± 1.0e-5	3.1e-6 ± 1.3e-6	2.6e-6 ± 4.2e-6
$nRSS_{br}$	Normalized RSS for bromide	0.41	1.94	1.12	1.93	15.62	1.53
$nRSS_{raz}$	Normalized RSS for resazurin	0.47	0.63	1.34	1.70	0.42	0.76
$nRSS_{rru}$	Normalized RSS for resorufin	0.94	2.84	3.76	18.66	12.22	184.63
Depth 2		6 cm	5 cm	10 cm	7 cm	9 cm	n.d.
v_z [m/s]	Advective velocity	9.6e-5 ± 4.4e-6	1.3e-4 ± 3.8e-6	2.7e-5 ± 4.7e-7	4.4e-7 ± 3.2e-7	2.6e-5 ± 3.6e-7	
D_z [m^2/s]	Dispersion coefficient	1.0e-4 ± 4.4e-7	4.6e-7 ± 2.0e-8	2.7e-7 ± 5.4e-9	3.0e-6 ± 1.2e-7	8.1e-8 ± 1.5e-9	
q_{in} [1/s]	Groundwater dilution rate coefficient	1.5e-4 ± 8.2e-5	1.6e-4 ± 1.4e-4	1.9e-6 ± 1.1e-6	5.0e-3 ± 2.5e-4	1.6e-4 ± 1.2e-5	
R_1 [-]	Resorufin retardation coefficient	1.01 ± 5.5e-3	3.88 ± 1.2e-1	1.45 ± 2.6e-2	3.78 ± 1.6e-1	1.30 ± 1.8e-2	
λ_1 [1/s]	Resazurin total transformation coefficient	1.7e-4 ± 8.3e-5	2.7e-3 ± 1.4e-4	1.4e-4 ± 3.0e-6	7.4e-4 ± 1.8e-4	2.8e-4 ± 1.0e-5	
R_2 [-]	Resorufin retardation coefficient	1.09 ± 1.4e-1	1.96 ± 1.3e-2	1.32 ± 1.8e-2	1.03 ± 2.2e-2	1.29 ± 1.2e-2	
λ_{12} [1/s]	Resazurin to resorufin transformation coefficient	6.1e-6 ± 9.6e-7	5.1e-5 ± 3.0e-6	3.2e-5 ± 7.5e-7	7.9e-5 ± 2.2e-6	1.4e-5 ± 2.8e-7	
λ_2 [1/s]	Resorufin transformation coefficient	5.0e-3 ± 3.4e-5	1.4e-4 ± 2.0e-5	8.0e-6 ± 4.3e-6	1.3e-4 ± 1.9e-5	2.7e-5 ± 1.3e-6	
$nRSS_{br}$	Normalized RSS for bromide	0.20	0.89	43.77	5.20	5.47	
$nRSS_{raz}$	Normalized RSS for resazurin	0.88	0.86	1.25	4.07	2.06	
$nRSS_{rru}$	Normalized RSS for resorufin	1.81	4.66	1.10	9.39	3.78	
Depth 3		n.d.	n.d.	n.d.	11 cm	n.d.	n.d.
v_z [m/s]	Advective velocity				3.1e-5 ± 2.3e-6		
D_z [m^2/s]	Dispersion coefficient				9.0e-6 ± 3.2e-8		
q_{in} [1/s]	Groundwater dilution rate coefficient				9.2e-6 ± 1.4e-5		
R_1 [-]	Resorufin retardation coefficient				1.00 ± 2.8e-3		
λ_1 [1/s]	Resazurin total transformation coefficient				1.0e-5 ± 2.3e-5		
R_2 [-]	Resorufin retardation coefficient				1.00 ± 4.3e-3		
λ_{12} [1/s]	Resazurin to resorufin transformation coefficient				1.0e-5 ± 4.4e-8		
λ_2 [1/s]	Resorufin transformation coefficient				1.4e-6 ± 1.3e-6		
$nRSS_{br}$	Normalized RSS for bromide				4.37		
$nRSS_{raz}$	Normalized RSS for resazurin				6.38		
$nRSS_{rru}$	Normalized RSS for resorufin				21.70		

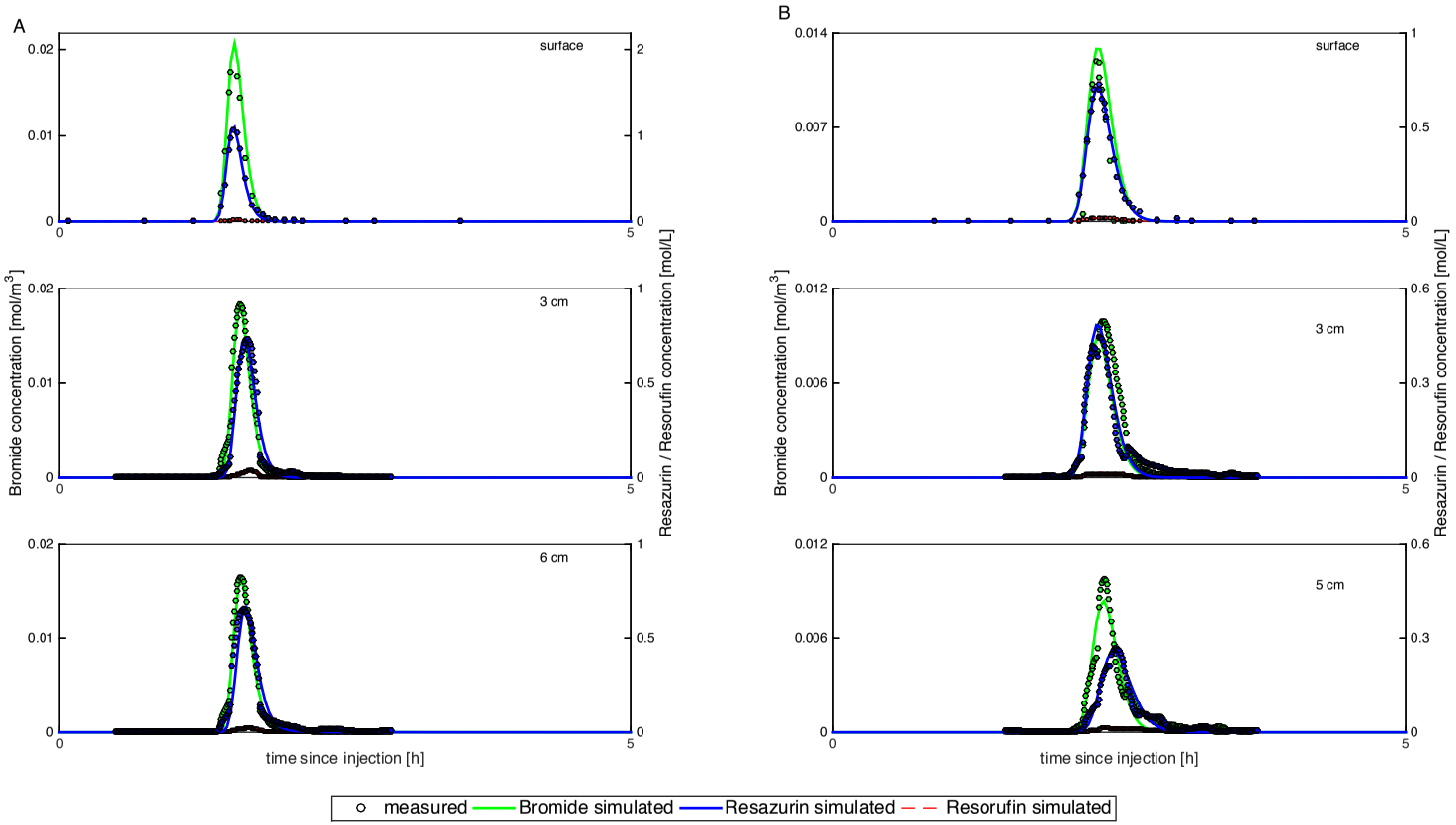
A
B
surface
3 cm
6 cm
5 cm
Bromide concentration [mol/m3]
Resazurin / Resorufin concentration [mol/L]
time since injection [h]
measured
Bromide simulated
Resazurin simulated
Resorufin simulated

Appendix 3.2: Breakthrough curves for the 2nd order stream

Measured (points) and best modeled breakthrough curves for bromide (green), resazurin (blue), and resorufin (red) at the two downstream sampling stations (A: upstream; B: downstream) for depths sampled in the 2nd order stream.

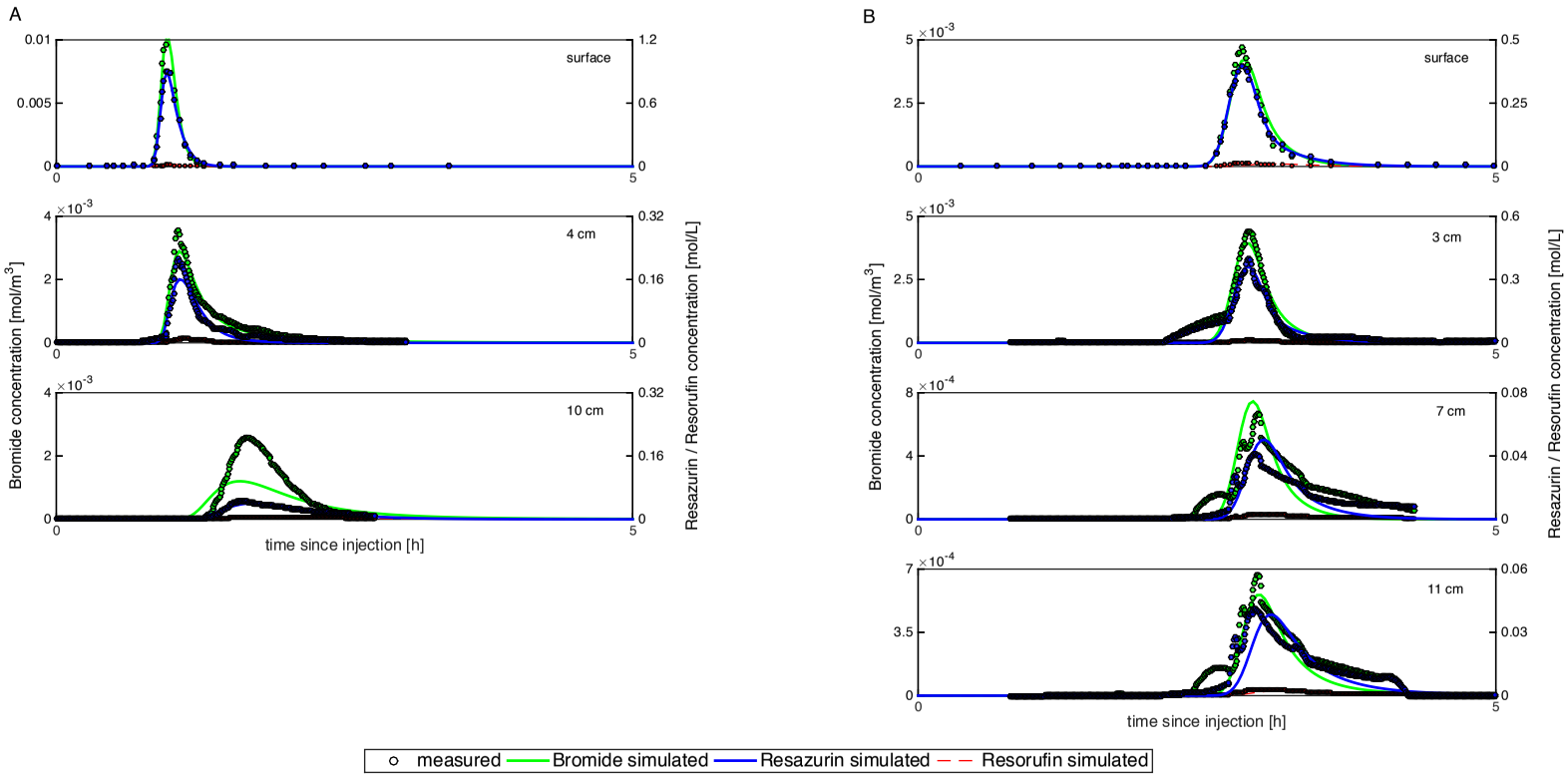
A
B
surface
4 cm
10 cm
3 cm
7 cm
11 cm
Bromide concentration [mol/m3]
Resazurin / Resorufin concentration [mol/L]
time since injection [h]
measured
Bromide simulated
Resazurin simulated
Resorufin simulated

Appendix 3.3: Breakthrough curves for the 3rd order stream

Measured (points) and best modeled breakthrough curves for bromide (green), resazurin (blue), and resorufin (red) at the two downstream sampling stations (A: upstream; B: downstream) for depths sampled in the 3rd order stream.

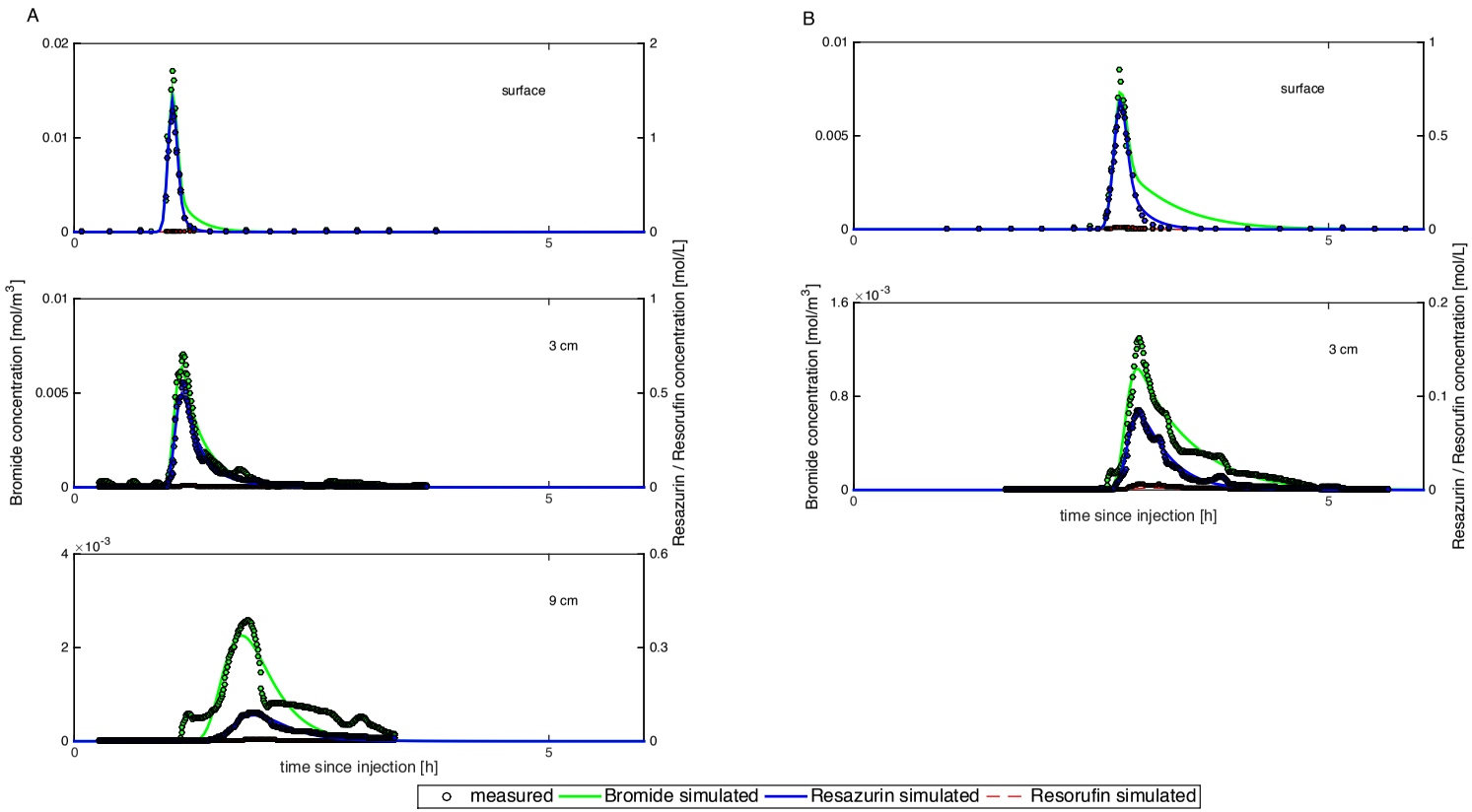
A
B
surface
3 cm
9 cm
Bromide concentration [mol/m3]
Resazurin / Resorufin concentration [mol/L]
time since injection [h]
measured
Bromide simulated
Resazurin simulated
Resorufin simulated

Appendix 3.4: Breakthrough curves for the 4th order stream

Measured (points) and best modeled breakthrough curves for bromide (green), resazurin (blue), and resorufin (red) at the two downstream sampling stations (A: upstream; B: downstream) for depths sampled in the 4th order stream.

Appendix 3.5: Simulated breakthrough curve zeroth temporal moments

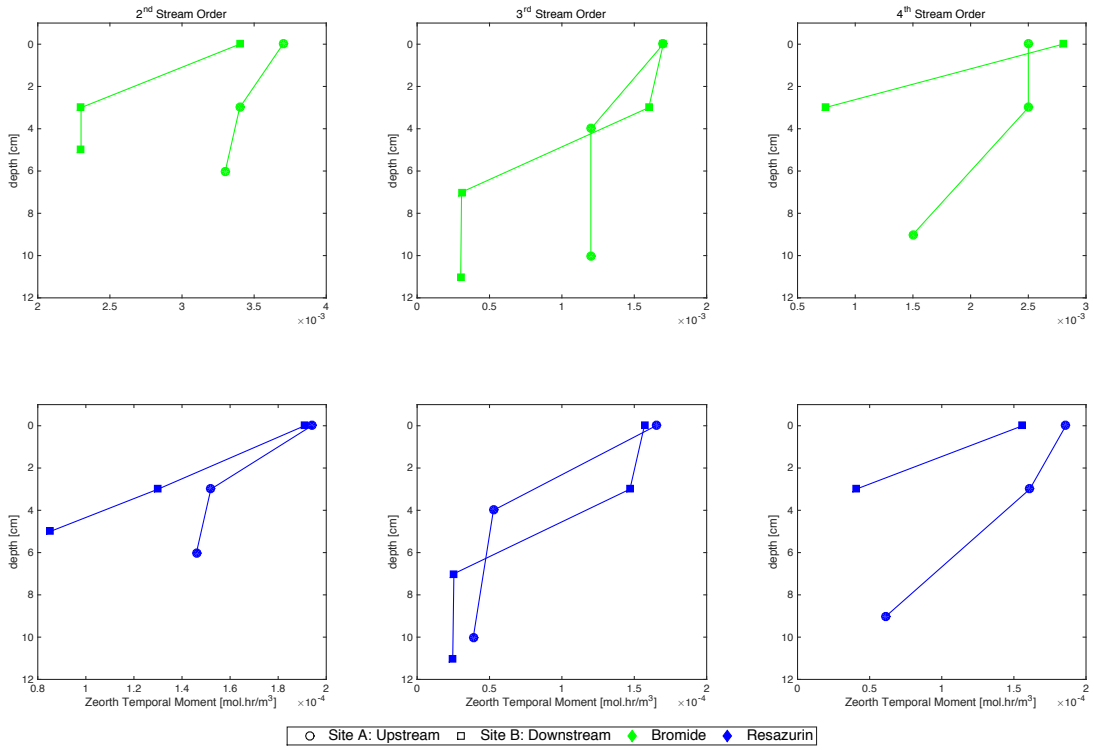

Simulated breakthrough curve zeroth temporal moments (mol.hr/m^3) for bromide (green) and resazurin (blue).

Appendix 3.6: Simulated breakthrough curve fraction of tracer recovery

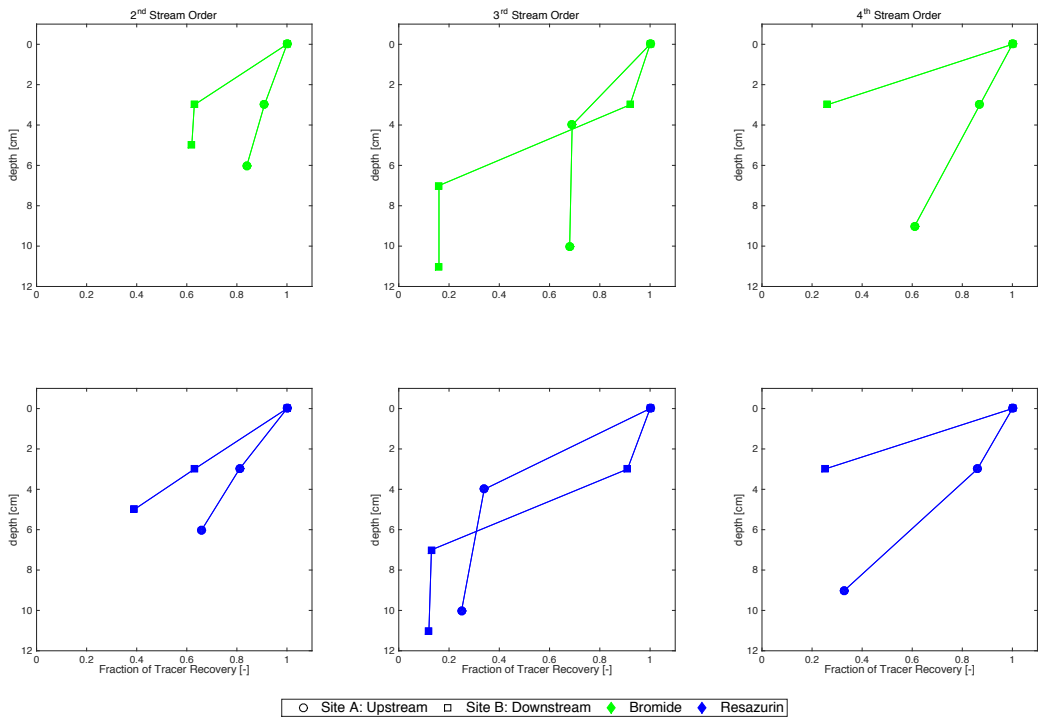

Fraction of tracer recovery, as derived from X_{rec}^{br} and X_{rec}^{raz} (Knapp et al., 2017), from the surface water as a function of depth for bromide (green) and resazurin (blue).

Appendix 3.7: Density plots for the 2nd order stream Site A depth 1

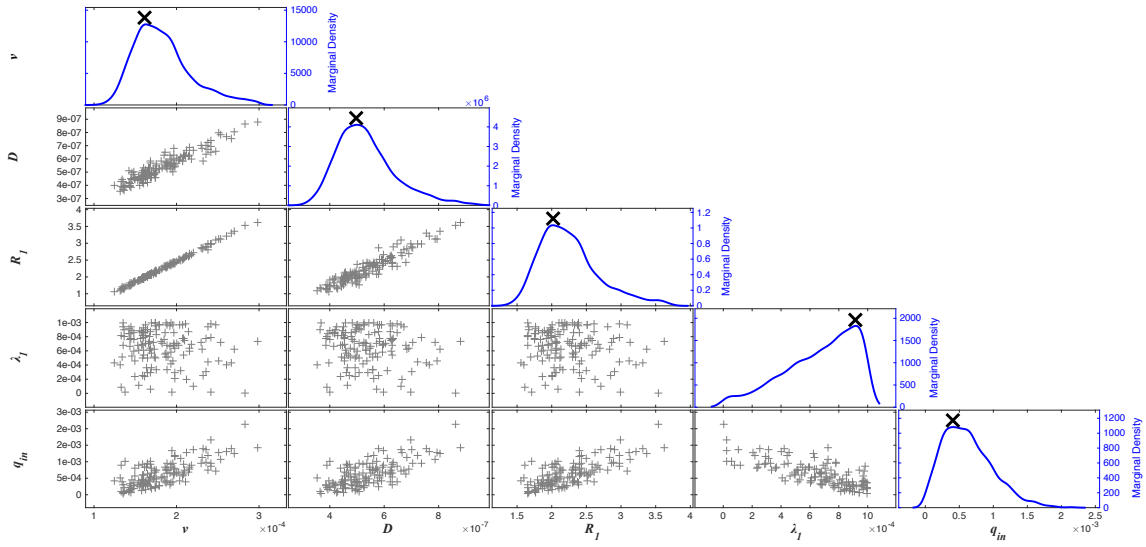

Marginal distribution and two-dimensional correlation plots of posterior parameter samples from the bromide/resazurin joint fit for the 2nd order upstream Site A depth 1 (3 cm).

Appendix 3.8: Density plots for the 2nd order stream Site A depth 2

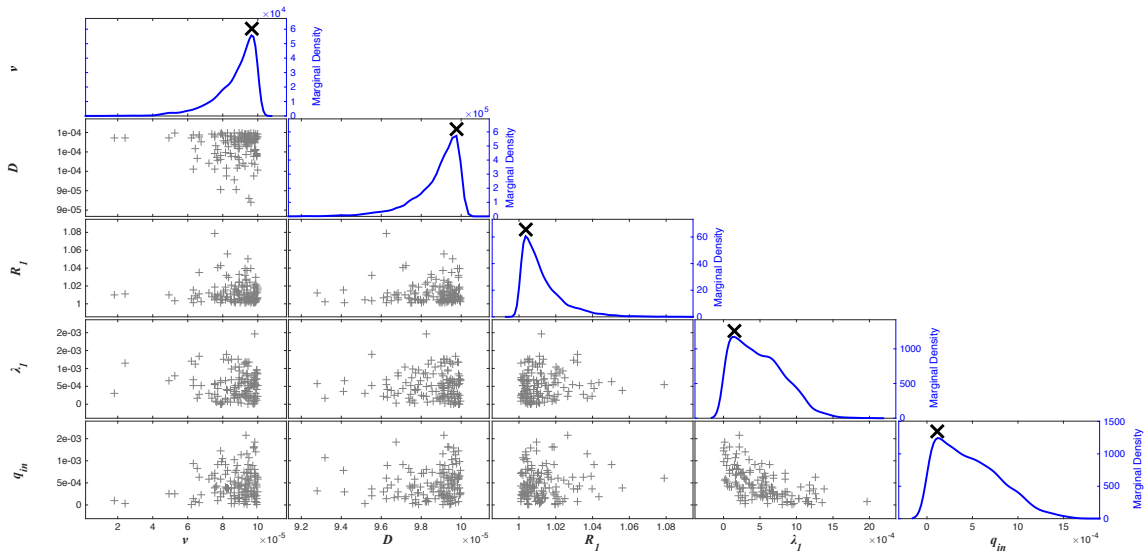

Marginal distribution and two-dimensional correlation plots of posterior parameter samples from the bromide/resazurin joint fit for the 2nd order upstream Site A depth 2 (6 cm).

Appendix 3.9: Density plots for the 2nd order stream Site B depth 1

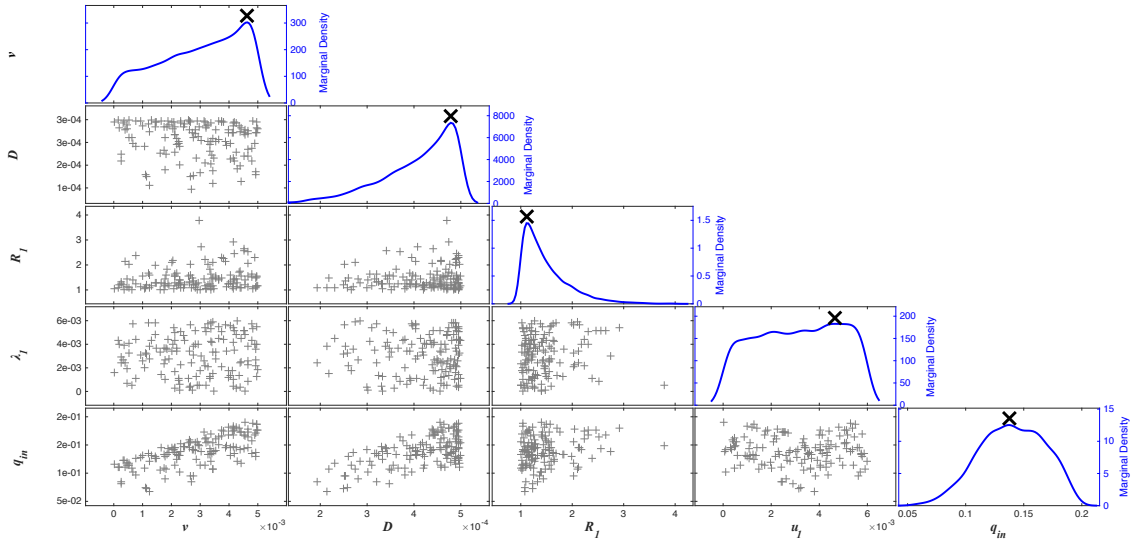

Marginal distribution and two-dimensional correlation plots of posterior parameter samples from the bromide/resazurin joint fit for the 2nd order downstream Site B depth 1 (3 cm).

Appendix 3.10: Density plots for the 2nd order stream Site B depth 2

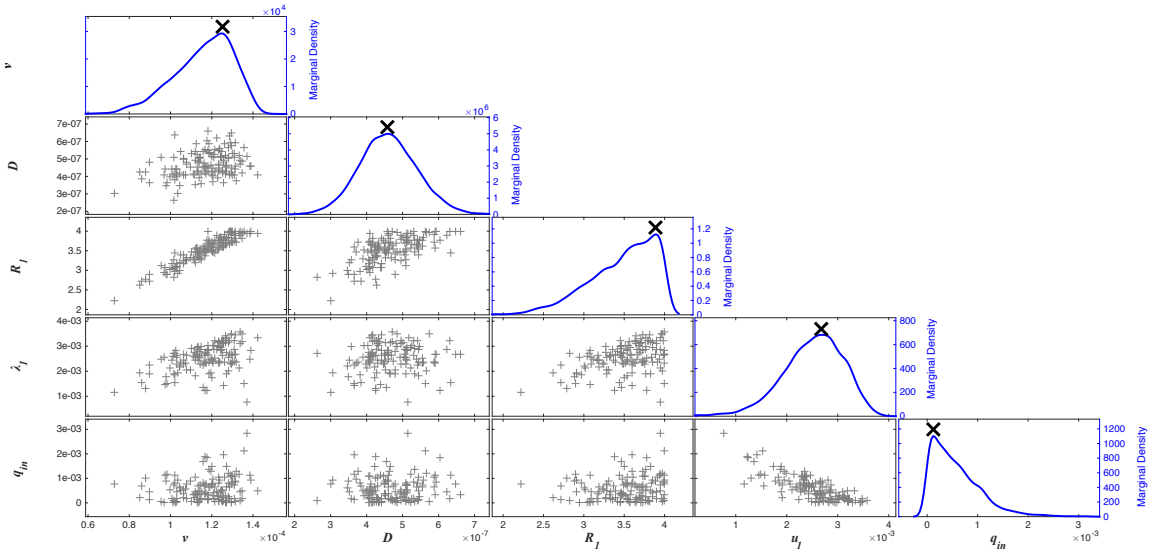

Marginal distribution and two-dimensional correlation plots of posterior parameter samples from the bromide/resazurin joint fit for the 2nd order downstream Site B depth 2 (5 cm).

Appendix 3.11: Density plots for the 3rd order stream Site A depth 1

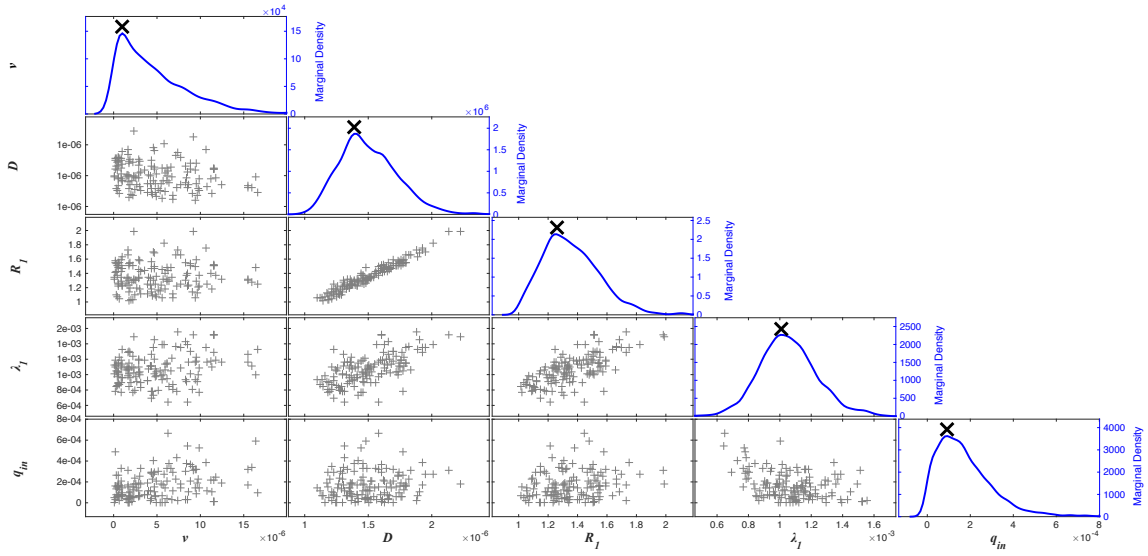

Marginal distribution and two-dimensional correlation plots of posterior parameter samples from the bromide/resazurin joint fit for the 3rd order upstream Site A depth 1 (4 cm).

Appendix 3.12: Density plots for the 3rd order stream Site A depth 2

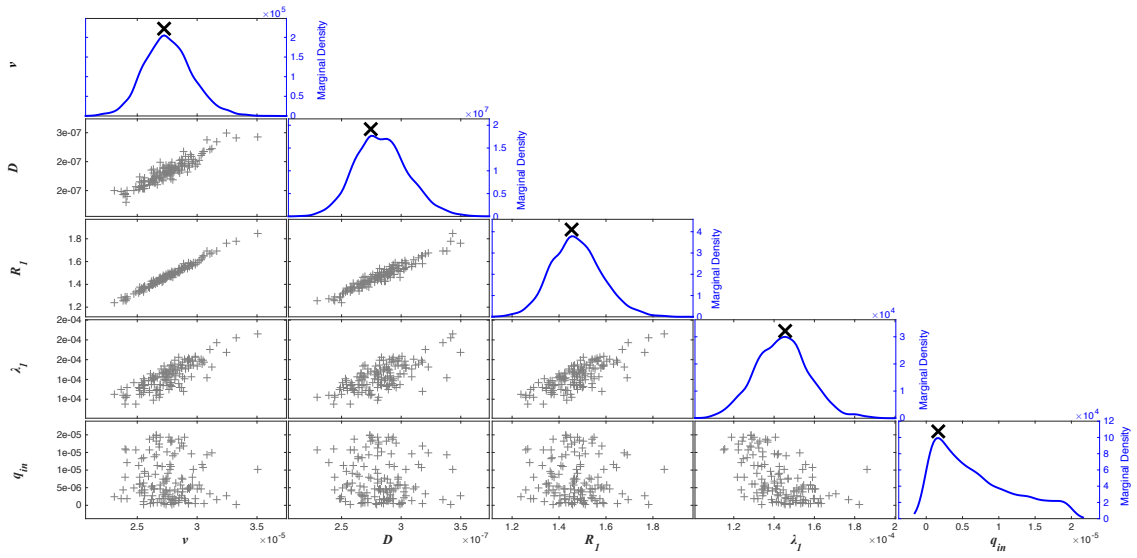

Marginal distribution and two-dimensional correlation plots of posterior parameter samples from the bromide/resazurin joint fit for the 3rd order upstream Site A depth 2 (10 cm).

Appendix 3.13: Density plots for the 3rd order stream Site B depth 1

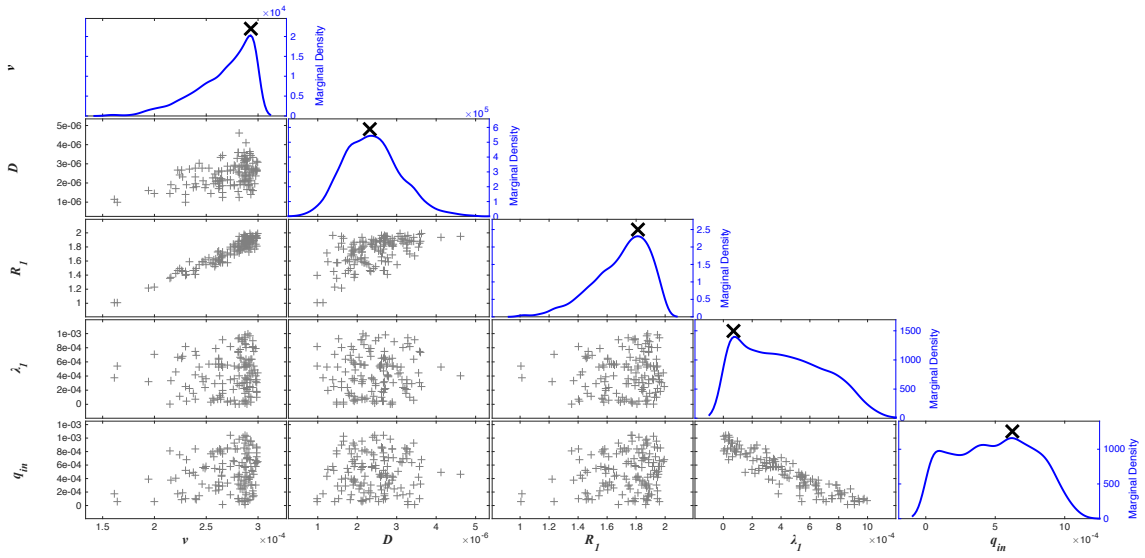

Marginal distribution and two-dimensional correlation plots of posterior parameter samples from the bromide/resazurin joint fit for the 3rd order downstream Site B depth 1 (3 cm).

Appendix 3.14: Density plots for the 3rd order stream Site B depth 2

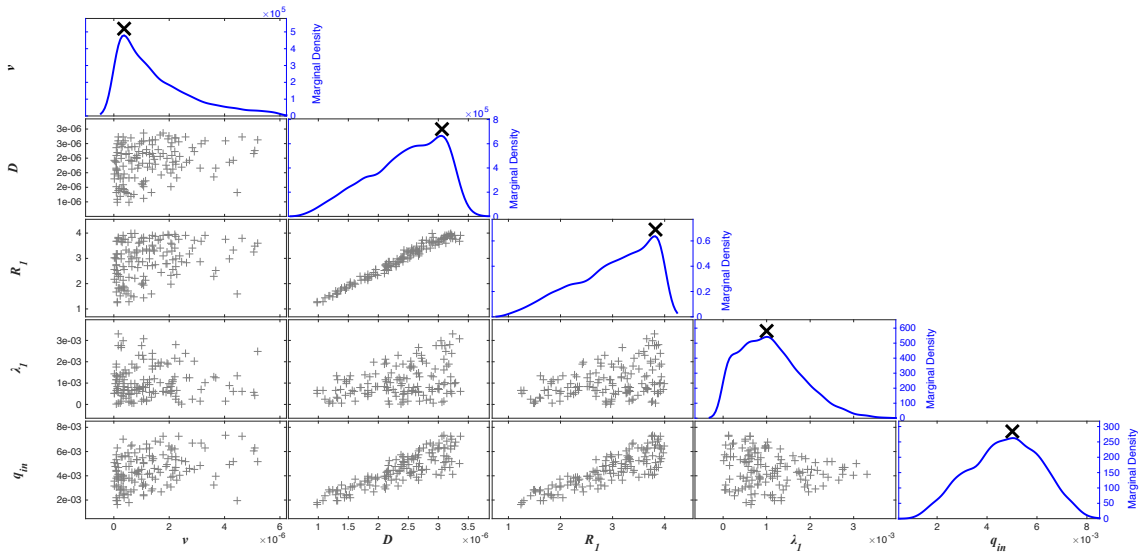

Marginal distribution and two-dimensional correlation plots of posterior parameter samples from the bromide/resazurin joint fit for the 3rd order downstream Site B depth 2 (7 cm).

Appendix 3.15: Density plots for the 3rd order stream Site B depth 3

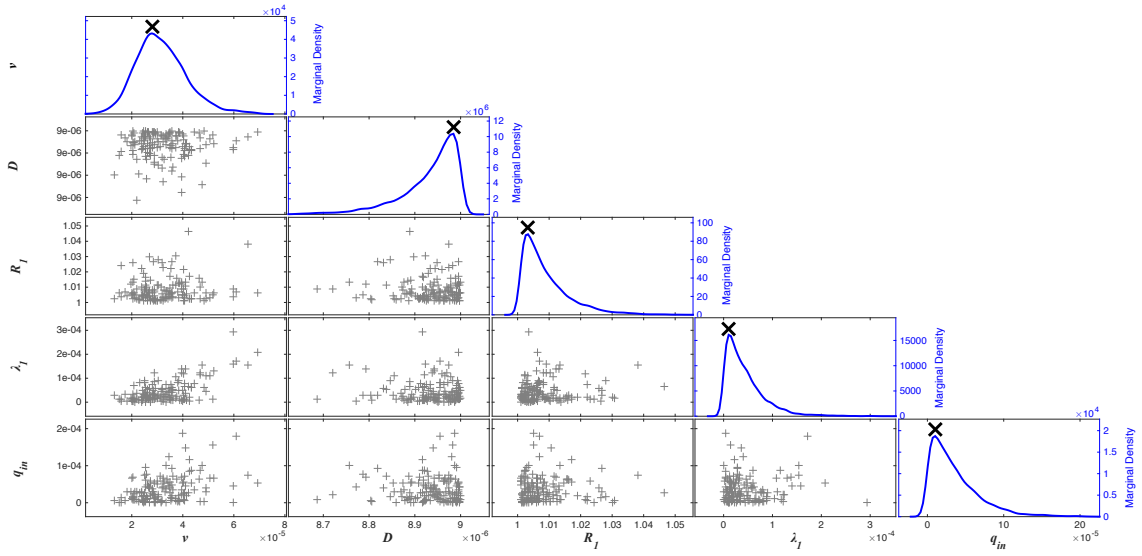

Marginal distribution and two-dimensional correlation plots of posterior parameter samples from the bromide/resazurin joint fit for the 3rd order downstream Site B depth 3 (11 cm).

Appendix 3.16: Density plots for the 4th order stream Site A depth 1

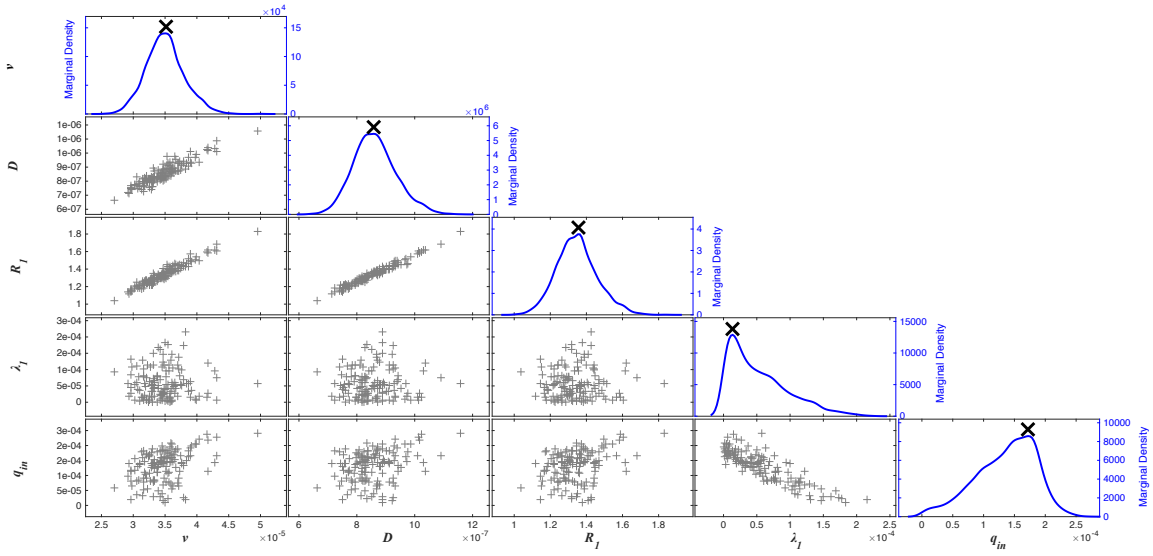

Marginal distribution and two-dimensional correlation plots of posterior parameter samples from the bromide/resazurin joint fit for the 4th order upstream Site A depth 1 (3 cm).

Appendix 3.17: Density plots for the 4th order stream Site A depth 2

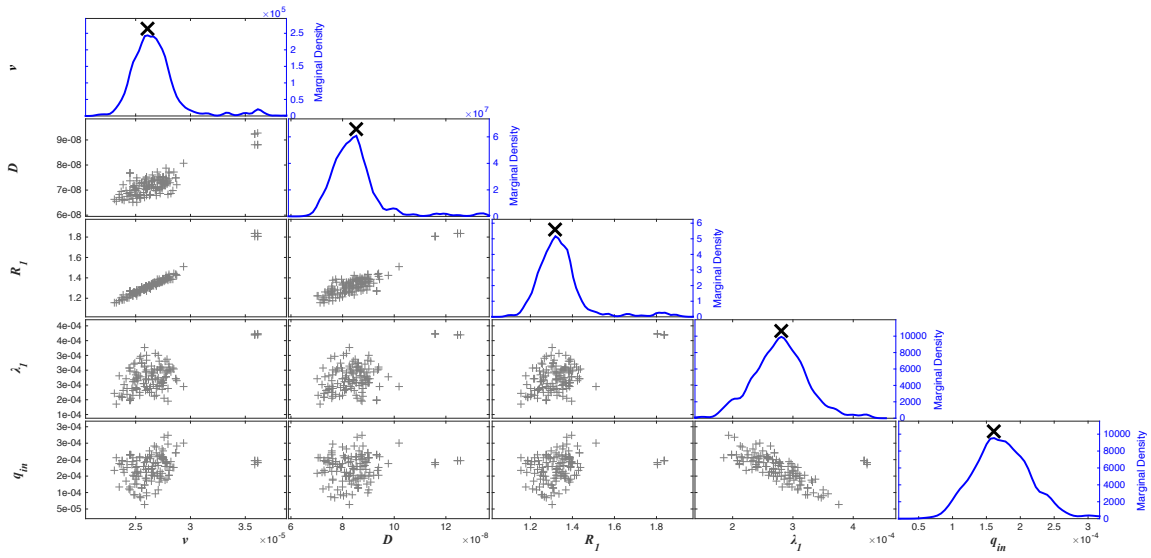

Marginal distribution and two-dimensional correlation plots of posterior parameter samples from the bromide/resazurin joint fit for the 4th order upstream Site A depth 2 (9 cm).

Appendix 3.18: Density plots for the 4th order stream Site B depth 1

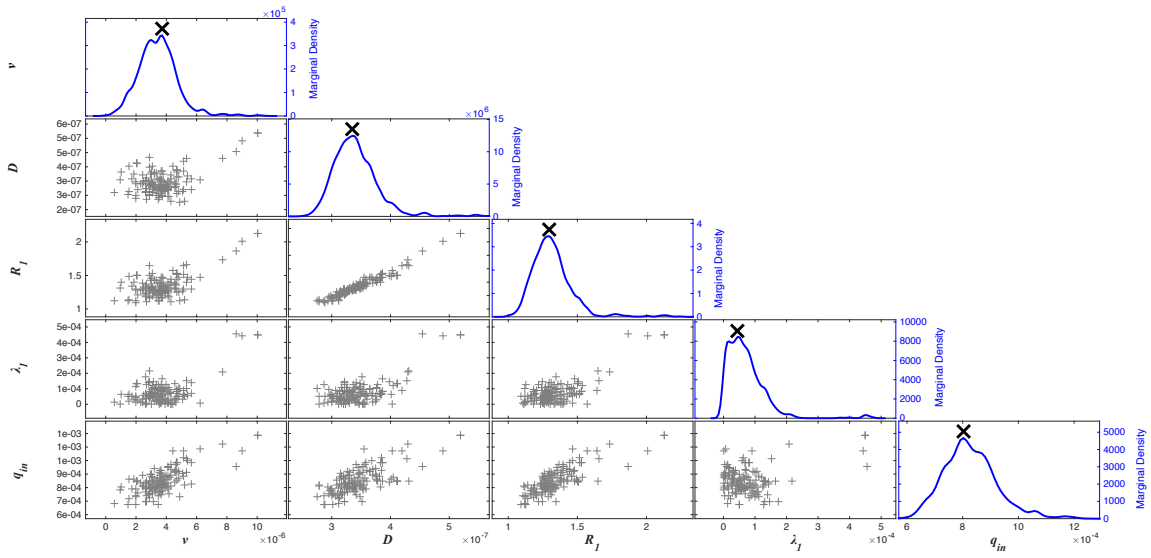

Marginal distribution and two-dimensional correlation plots of posterior parameter samples from the bromide/resazurin joint fit for the 4th order downstream Site B depth 1 (3 cm).

Appendix 3.19: Table of hyporheic zone metrics

Calculated mean hyporheic zone residence time $\tilde{\tau}_{hz}[cm]$, mean hyporheic zone residence time of resazurin, $\tilde{\tau}_{reac}[cm]$, mean hyporheic zone depth, $\tilde{d}_{hz}\ [cm]$, of bromide, mean hyporheic zone depth, $\tilde{d}_{raz}\ [cm]$, of resazurin, highest resazurin decay coefficient, $\lambda_{1\ max}\ (1/s)$, and hyporheic exchange rates at the sediment-water interface, $q_{he}\ (1/s)$.

Sampling Date	Stream Order	Site	$\tilde{\tau}_{hz}$ (min)	$\tilde{\tau}_{reac}$ (min)	$\tilde{d}_{hz}$ (cm)	$\tilde{d}_{reac}$ (cm)	$\lambda_{1\ max}$ (1/s)	q_{he} (1/s)
16-May	2	A	16.91 ± 2.85	28.39 ± 2.85	23.13 ± 4.33	15.56 ± 1.74	9.04e-4 ± 5.26e-5	2.86e-4 ± 1.71e-5
16-May	2	B	10.89 ± 5.20	8.94 ± 0.48	10.21 ± 3.15	5.01 ± 0.08	4.70e-3 ± 3.00e-4	8.70e-3 ± 5.00e-4
20-May	3	A	284.01 ± 59.22	119.20 +17.24	64.86 ± 3.11	8.82 ± 0.85	1.10e-3 ± 1.00e-4	1.03e-6 ± 4.42e-6
20-May	3	B	99.49 ± 74.86	56.07 ± 17.47	15.57 ± 0.88	10.26 ± 0.51	7.37e-4 ± 1.77e-4	2.26e-4 ± 9.30e-6
21-May	4	A	83.16 ± 7.61	42.60 ± 7.67	15.47 ± 1.57	8.14 ± 0.43	2.81e-4 ± 1.01e-5	3.76e-5 ± 3.95e-6
21-May	4	B	10.77 ± 0.62	13.123 ± 0.76	2.39 ± 0.10	2.14 ± 0.09	1.43e-5 ± 1.28e-5	3.26e-6 ± 4.99e-6

APPENDIX B: CHAPTER 4 SUPPLEMENTAL INFORMATION.

Appendix 4.1: Model Calibration Information

Model parameter estimation was completed using the *Differential Evolution Adaptive Metropolis* (DREAM (ZS)) algorithm (Vrugt et al., 2009). DREAM (ZS) is a self-adaptive Markov chain Monte Carlo (MCMC) algorithm that automatically updates the scale and orientation of the parameter distribution during sampling (Vrugt et al., 2008; Laloy & Vrugt, 2012; Vrugt, 2016). DREAM (ZS) samples from an archive of past model parameter states to generate new parameters sets and provide correlated parameter uncertainties (Knapp et al., 2017; Knapp & Cirpka, 2017). Using this approach allowed us to overcome the typical problem of gradient-based search algorithms of running into local minima (Lemke et al. 2013). Thus, we were able to avoid an estimated parameter dependence on their initial values since DREAM (ZS) searches the entire parameter space for multiple parameters simultaneously. The parameters for the in-stream processing, mass transfer, and transformation coefficients were constrained to be non-negative, whereas the reactive tracer retardation coefficients parameter lower limits were set to 1. All upper parameter limits were guided by previously published values (Haggerty et al. 2008; Haggerty et al. 2009; Lemke et al. 2013; Knapp et al. 2017; Knapp and Cirpka 2017).

Parameters for bromide, Br^-, and resazurin, Raz, were jointly estimated in a first step. We normalized the residuals by the peak concentrations of the individual tracer to optimize fit for both tracers simultaneously, since our concentrations of Br^- and Raz differed by multiple orders of magnitude. Afterwards, parameters specific to resorufin, Rru, were estimated separately while all parameters related to Br^- and Raz were sampled from their previously determined distributions. The resulting simulated BTCs represent the best fitting parameters obtained from a forward run after the burn-in period evaluations were discarded. Goodness of fit was assessed

using a normalized residual sum of squares (*nRSS*) $[-]$, where the sum of squared residuals was normalized by the squared theoretical peak tracer concentrations of each tracer BTC. As such, lower *nRSS* values indicated a more reliable model fit.

During all optimization runs, a thinning rate of 10 was applied to the estimated parameter sets to reduce autocorrelation between successively stored parameter chains. Sampled chain convergence was monitored using the Gelman and Rubin (1992) $\hat{R}$ statistic with a desired threshold of 1.2. For more information on this process, please see the supporting information of Knapp et al. (2017). Parameter density distributions and the resulting correlations can be found in Appendix 4.7 - Appendix 4.14.

We used the median of the best 1,000 model simulations to assess the agreement between our final model fits and a subset of possible curve fits resulting from the end of each DREAM(ZS) run. The best model fits were determined from an ordered list of parameter values that were sorted by their objective function values, where the higher values indicated better model fits. Since our final model fits were based on the maximum values of each parameter density distribution, there was a possibility that these values are only marginally better than other possible parameter combinations within the set parameter space. This model fit assessment allowed us to evaluate if our resulting parameter sets accurately represented the best possible model fits.

Model sensitivity was determined by adjusting each model parameter from the first joint fit by 10-50% to determine which portions of the Raz BTCs were sensitive to certain model parameters (Appendix 4.15 - Appendix 4.21). We chose to evaluate the Raz BTC sensitivity because it is representative of hydrologic processes that influence hyporheic exchange and potential streambed reactivity. Model parameter interactions were analyzed with the

DREAM(ZS) postprocessing toolbox to determine parameter correlations (Vrugt et al., 2009). The resulting marginal distributions and two-dimensional correlations of the posterior parameter samples of the joint-fit can be found in the Supplemental Information. The second Rru-fit was used to confirm that the measured Rru BTCs could be simulated with the model parameters from the joint fit of Br^-/Raz.

Appendix 4.2: Model Calibration Information Reference List

Gelman, A., Rubin, D. B., Gelman, A., & Rubin, D. B. (1992). Inference from Iterative Simulation Using Multiple Sequences Linked references are available on JSTOR for this article : Inference from Iterative Simulation Using Multiple Sequences. *Statistical Science*, *7*(4), 457–472. https://doi.org/10.1214/ss/1177011136

Haggerty, R., Argerich, A., & Martí, E. (2008). Development of a "smart" tracer for the assessment of microbiological activity and sediment-water interaction in natural waters: The resazurin-resorufin system. *Water Resources Research*, *44*(4), n/a-n/a. https://doi.org/10.1029/2007WR006670

Haggerty, R., Martí, E., Argerich, A., von Schiller, D., & Grimm, N. B. (2009). Resazurin as a "smart" tracer for quantifying metabolically active transient storage in stream ecosystems. *Journal of Geophysical Research*, *114*(G3), G03014. https://doi.org/10.1029/2008JG000942

Kasahara, T., & Wondzell, S. M. (2003). Geomorphic controls on hyporheic exchange flow in mountain streams. *Water Resources Research*, *39*(1), SBH 3-1-SBH 3-14. https://doi.org/10.1029/2002wr001386

Knapp, J. L. A., & Cirpka, O. A. (2017). Determination of Hyporheic Travel-Time Distributions and other Parameters from Concurrent Conservative and Reactive Tracer Tests by Local-in-Global Optimization. *Water Resources Research*, *53*. https://doi.org/10.1002/2017WR020734

Knapp, J. L. A., González-Pinzón, R., Drummond, J. D., Larsen, L. G., Cirpka, O. A., & Harvey, J. W. (2017). Tracer-based characterization of hyporheic exchange and benthic biolayers in streams. *Water Resources Research*, *53*. https://doi.org/10.1002/2013WR014979

Laloy, E., & Vrugt, J. A. (2012). High-dimensional posterior exploration of hydrologic models using multiple-try DREAM(ZS) and high-performance computing. *Water Resources Research*, *48*(1), 1–18. https://doi.org/10.1029/2011WR010608

Lemke, D., Liao, Z., Wöhling, T., Osenbrück, K., & Cirpka, O. A. (2013). Concurrent conservative and reactive tracer tests in a stream undergoing hyporheic exchange. *Water Resources Research*, *49*(5), 3024–3037. https://doi.org/10.1002/wrcr.20277

Vrugt, J. A. (2016). Markov chain Monte Carlo simulation using the DREAM software package: Theory, concepts, and MATLAB implementation. *Environmental Modelling and Software*, *75*(January), 273–316. https://doi.org/10.1016/j.envsoft.2015.08.013

Vrugt, J. A., ter Braak, C. J. F., Clark, M. P., Hyman, J. M., & Robinson, B. A. (2008). Treatment of input uncertainty in hydrologic modeling: Doing hydrology backward with Markov chain Monte Carlo simulation. *Water Resources Research*, *44*(12), 1–15. https://doi.org/10.1029/2007WR006720

Vrugt, J. A., ter Braak, C. J. F., Diks, C. G. H., Robinson, B. A., Hyman, J. M., & Higdon, D. (2009). Accelerating Markov Chain Monte Carlo Simulation by Differential Evolution with Self-Adaptive Randomized Subspace Sampling. *International Journal of Nonlinear Sciences and Numerical Simulation*, *10*(3). https://doi.org/10.1515/IJNSNS.2009.10.3.273

Wondzell, S. M. (2006). Effect of morphology and discharge on hyporheic exchange flows in two small streams in the Cascade Mountains of Oregon, USA. *Hydrological Processes*, *20*(2), 267–287. https://doi.org/10.1002/hyp.5902

Wondzell, S. M. (2011). The role of the hyporheic zone across stream networks. *Hydrological Processes*, *25*(22), 3525–3532. https://doi.org/10.1002/hyp.8119

Wondzell, S. M., & Swanson, F. J. (1996). Seasonal and Storm Dynamics of the Hyporheic Zone of a 4th-Order Mountain Stream . I : Hydrologic Processes. *Journal of North American Benthological Society*, *15*(1), 3–19.

Appendix 4.3: Measured and simulated results for the 1st order stream

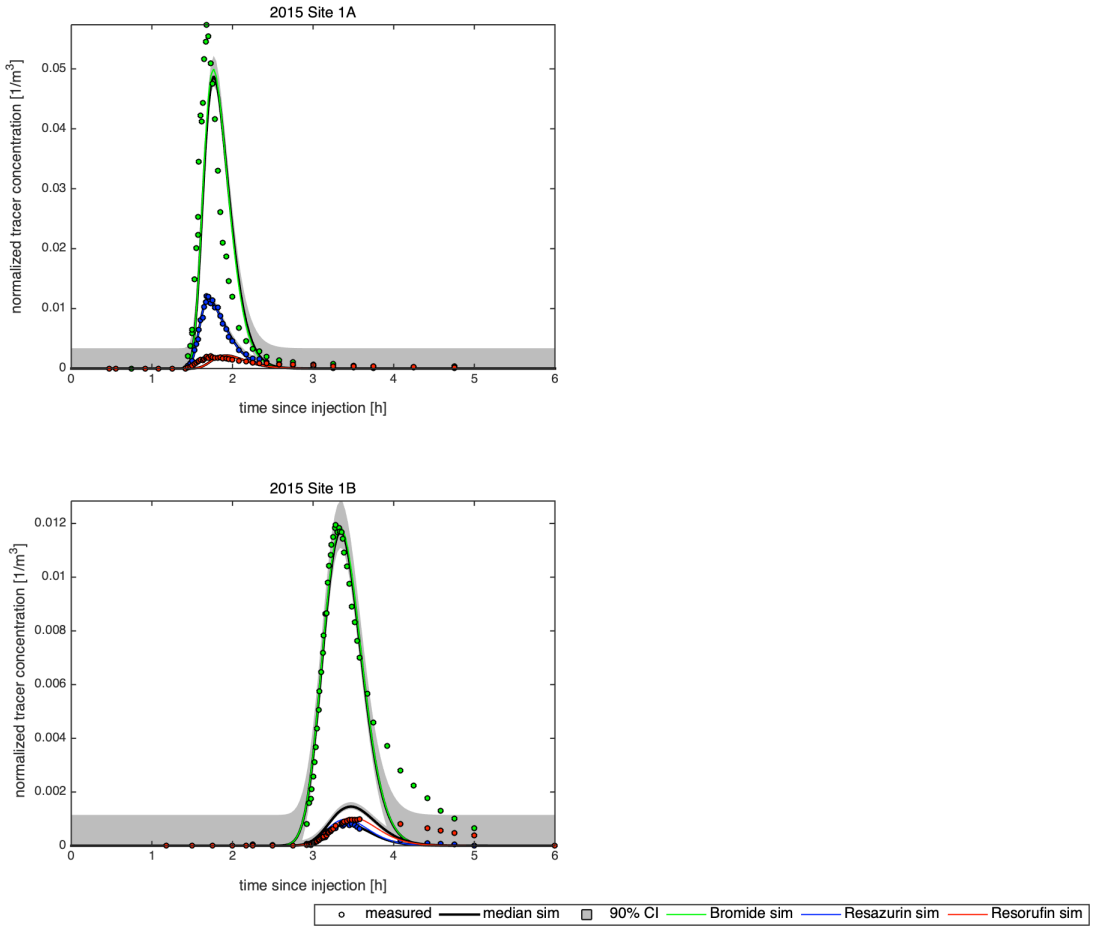

Measured (points), median of the best 1000 model simulations (black), and best modeled breakthrough curves for bromide (green), resazurin (blue), and resorufin (red), with the 90% confidence interval of the median curve from the last 1000 model simulations (grey) at the two downstream sampling stations (A: upstream; B: downstream) in the 1st order stream from the 2015 sampling campaign (Site 1). All plotted tracer concentrations were normalized by the number of injected moles to allow for better comparison across BTCs (Lemke et al. 2013).

Appendix 4.4: Measured and simulated results for the 2nd order stream

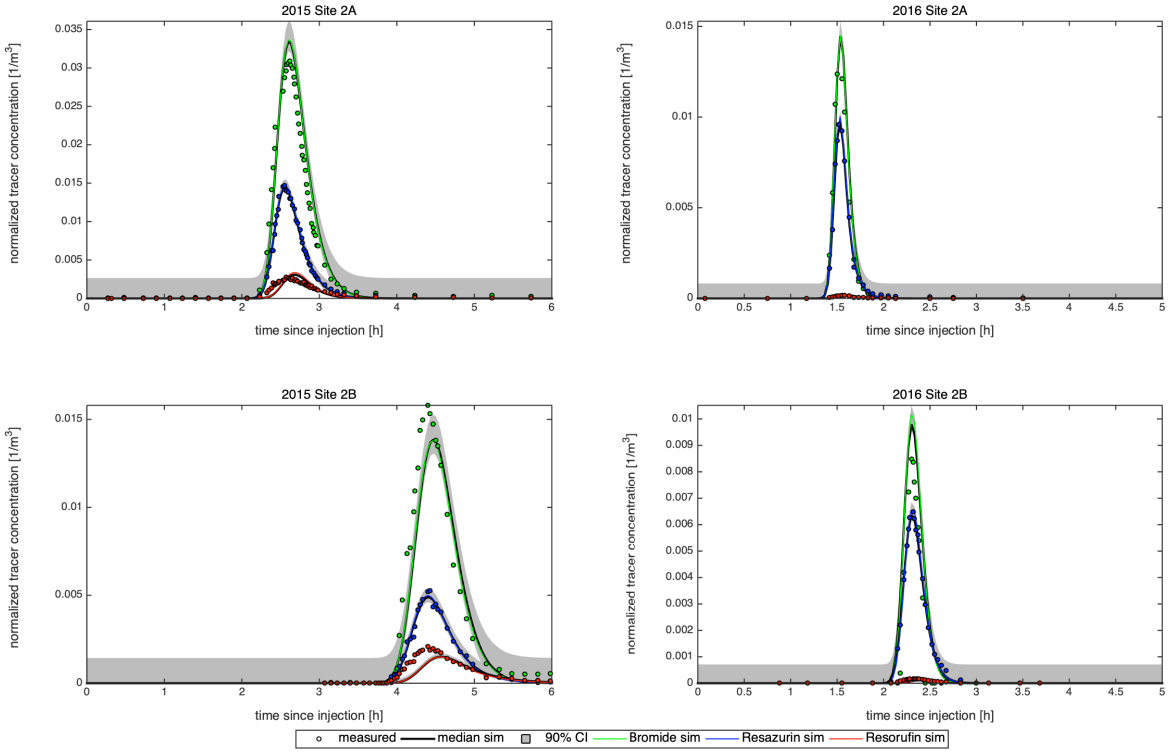

Measured (points), median of the best 1000 model simulations (black), and best modeled breakthrough curves for bromide (green), resazurin (blue), and resorufin (red), with the 90% confidence interval of the median curve from the last 1000 model simulations (grey) at the two downstream sampling stations (A: upstream; B: downstream) in the 2nd order stream from the 2015 and 2016 sampling campaigns (Site 2). All plotted tracer concentrations were normalized by the number of injected moles to allow for better comparison across BTCs (Lemke et al. 2013).

Appendix 4.5: Measured and simulated results for the 3rd order stream

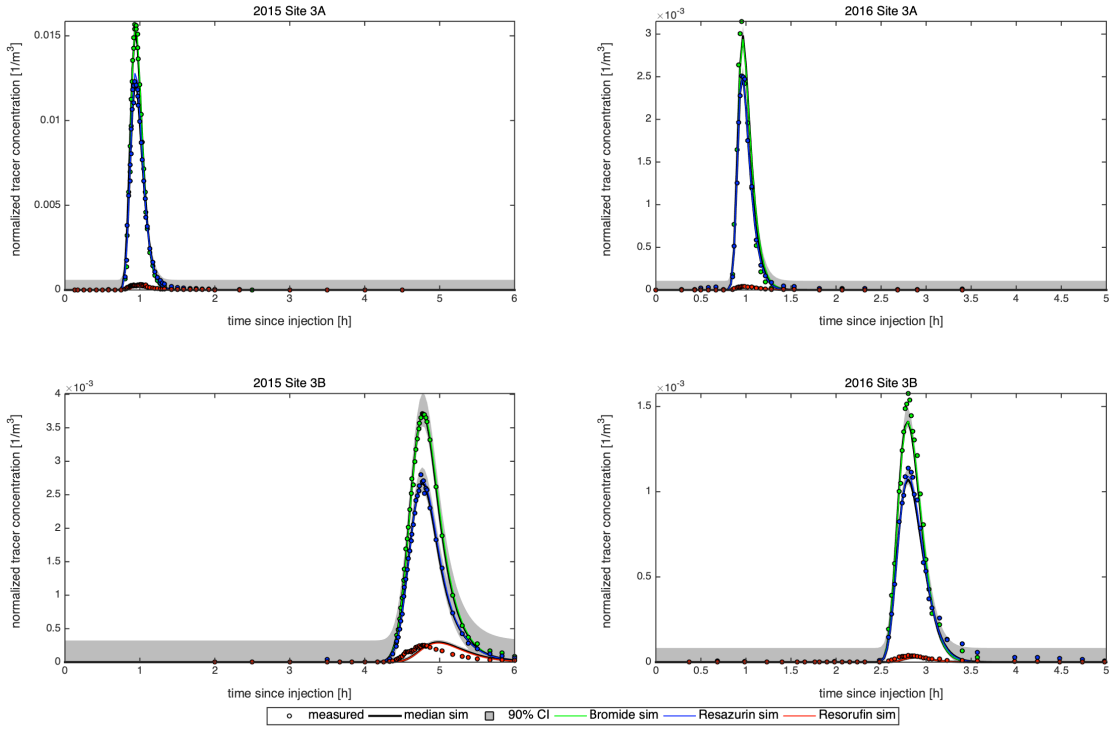

Measured (points), median of the best1000 model simulations (black), and best modeled breakthrough curves for bromide (green), resazurin (blue), and resorufin (red), with the 90% confidence interval of the median curve from the last 1000 model simulations (grey) at the two downstream sampling stations (A: upstream; B: downstream) in the 3rd order stream from the 2015 and 2016 sampling campaigns (Site 3). All plotted tracer concentrations were normalized by the number of injected moles to allow for better comparison across BTCs (Lemke et al. 2013).

Appendix 4.6: Measured and simulated results for the 5th order stream

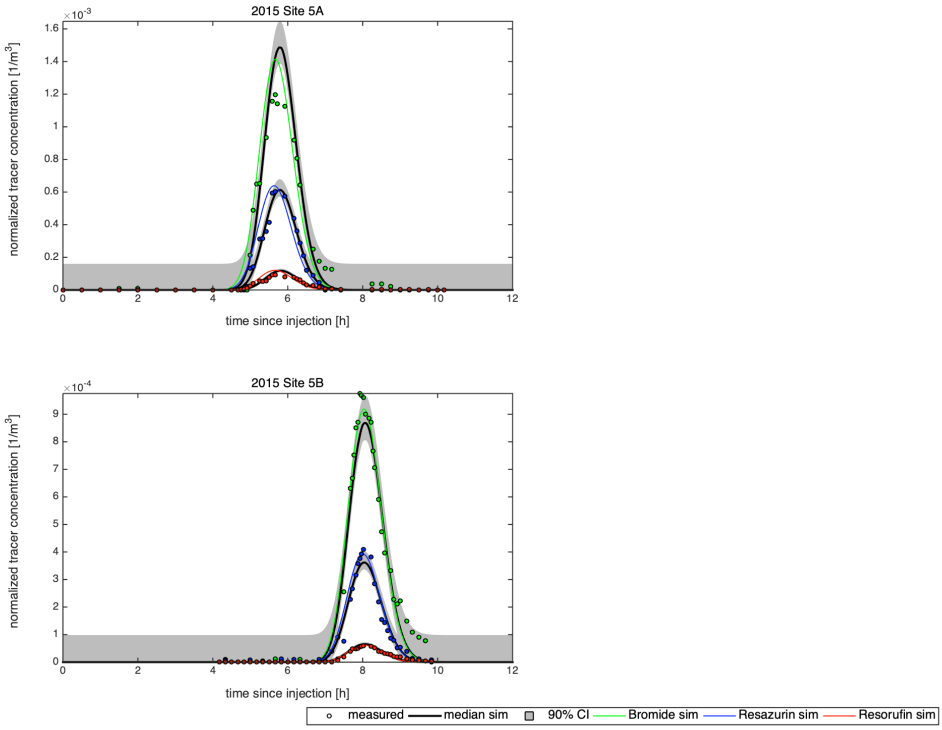

Measured (points), median of the best 1000 model simulations (black), and best modeled breakthrough curves for bromide (green), resazurin (blue), and resorufin (red), with the 90% confidence interval of the median curve from the last 1000 model simulations (grey) at the two downstream sampling stations (A: upstream; B: downstream) in the 5th order stream from the 2015 sampling campaign (Site 5). All plotted tracer concentrations were normalized by the number of injected moles to allow for better comparison across BTCs (Lemke et al. 2013).

Appendix 4.7: Density plots for the 2015 1st order stream

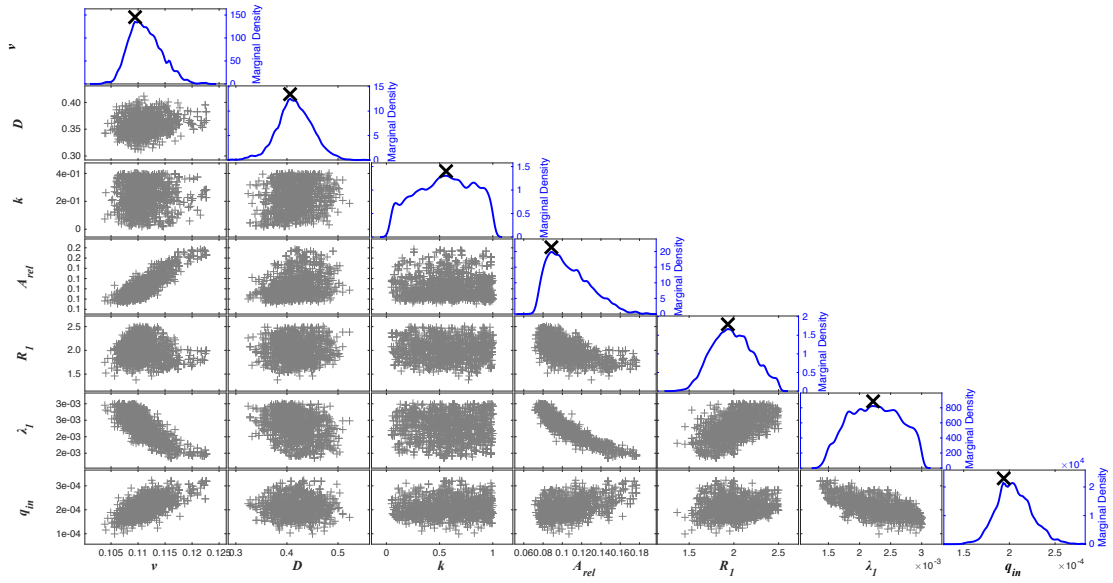

Marginal distribution and two-dimensional correlation plots of posterior parameter samples from the bromide/resazurin joint fit for the 2015 1st order stream reach.

Appendix 4.8: Density plots for the 2015 2nd order stream

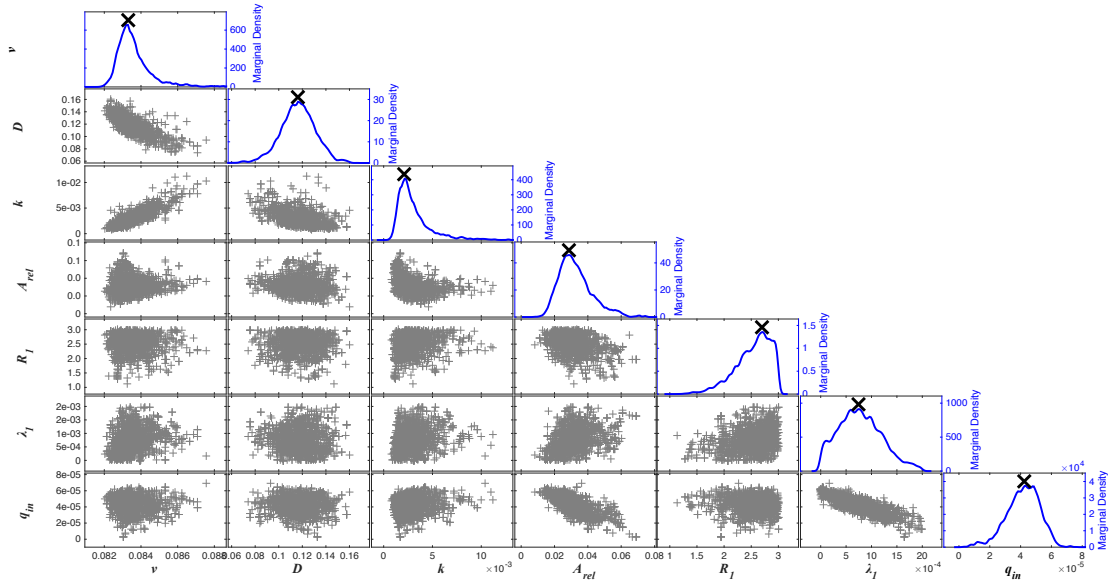

Marginal distribution and two-dimensional correlation plots of posterior parameter samples from the bromide/resazurin joint fit for the 2015 2nd order stream reach.

Appendix 4.9: Density plots for the 2015 3rd order stream

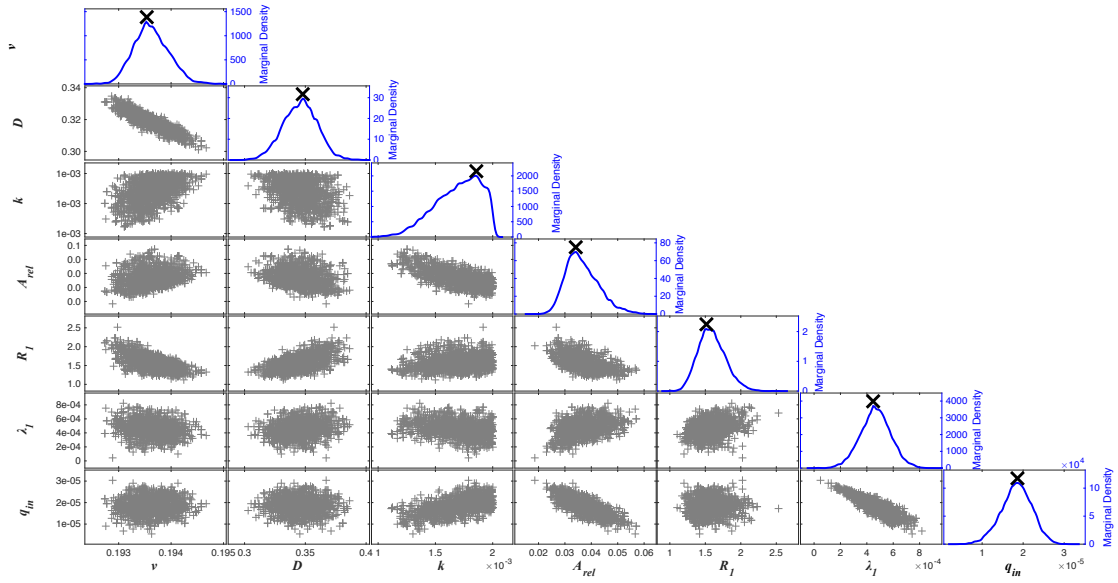

Marginal distribution and two-dimensional correlation plots of posterior parameter samples from the bromide/resazurin joint fit for the 2015 3rd order stream reach.

Appendix 4.10: Density plots for the 2015 4th order stream

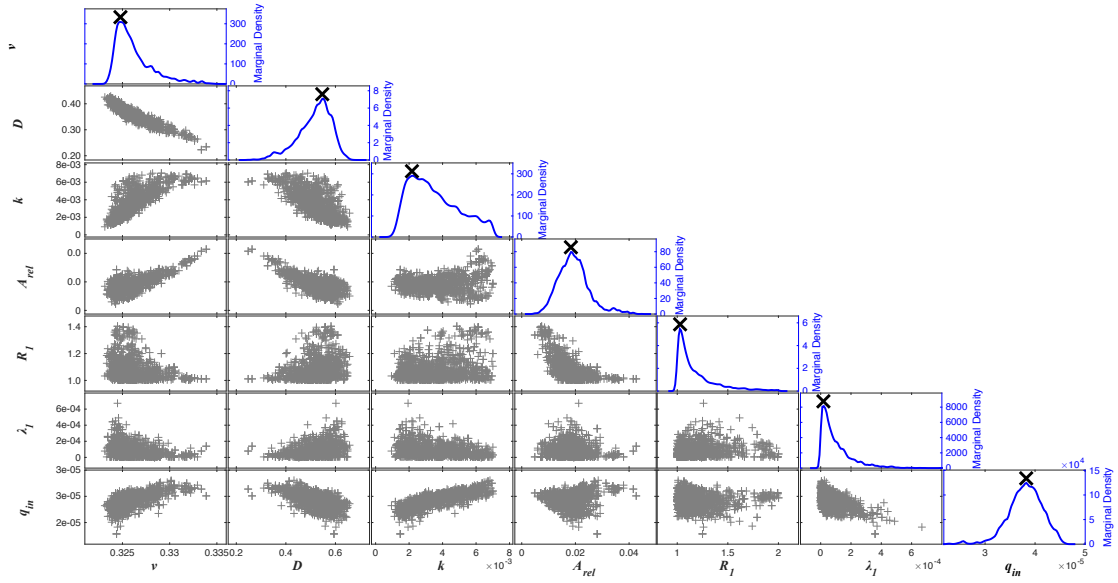

Marginal distribution and two-dimensional correlation plots of posterior parameter samples from the bromide/resazurin joint fit for the 2015 4th order stream reach.

Appendix 4.11: Density plots for the 2015 5th order stream

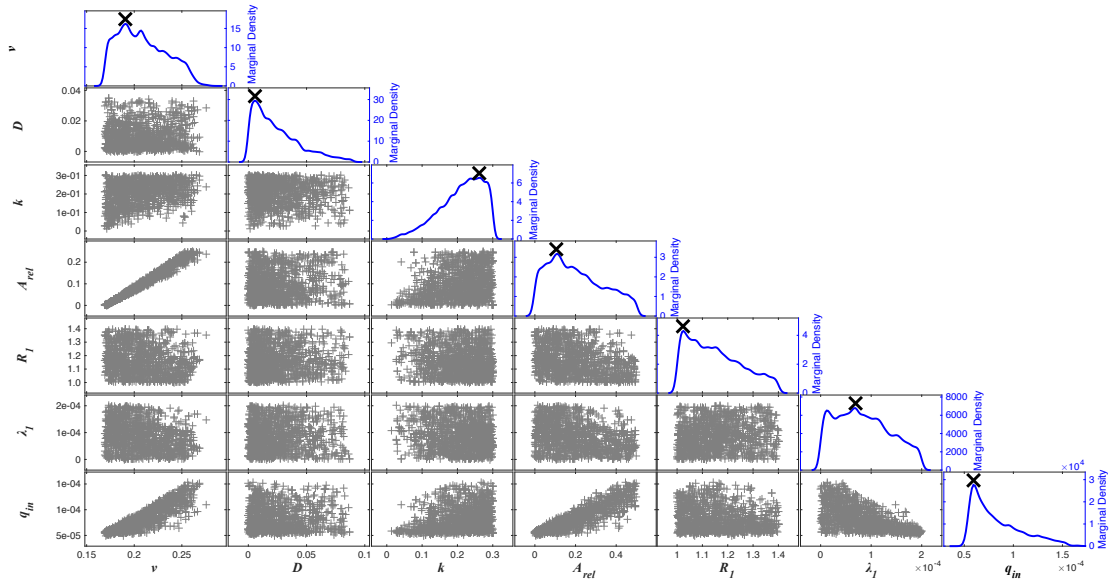

Marginal distribution and two-dimensional correlation plots of posterior parameter samples from the bromide/resazurin joint fit for the 2015 5th order stream reach.

Appendix 4.12: Density plots for the 2016 2nd order stream

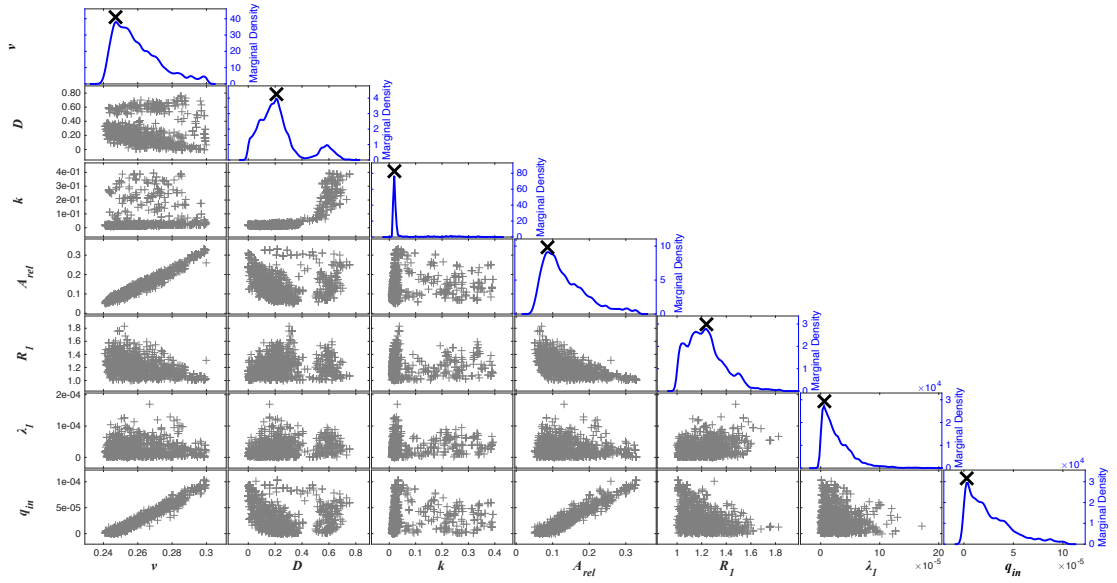

Marginal distribution and two-dimensional correlation plots of posterior parameter samples from the bromide/resazurin joint fit for the 2016 2nd order stream reach.

Appendix 4.13: Density plots for the 2016 3rd order stream

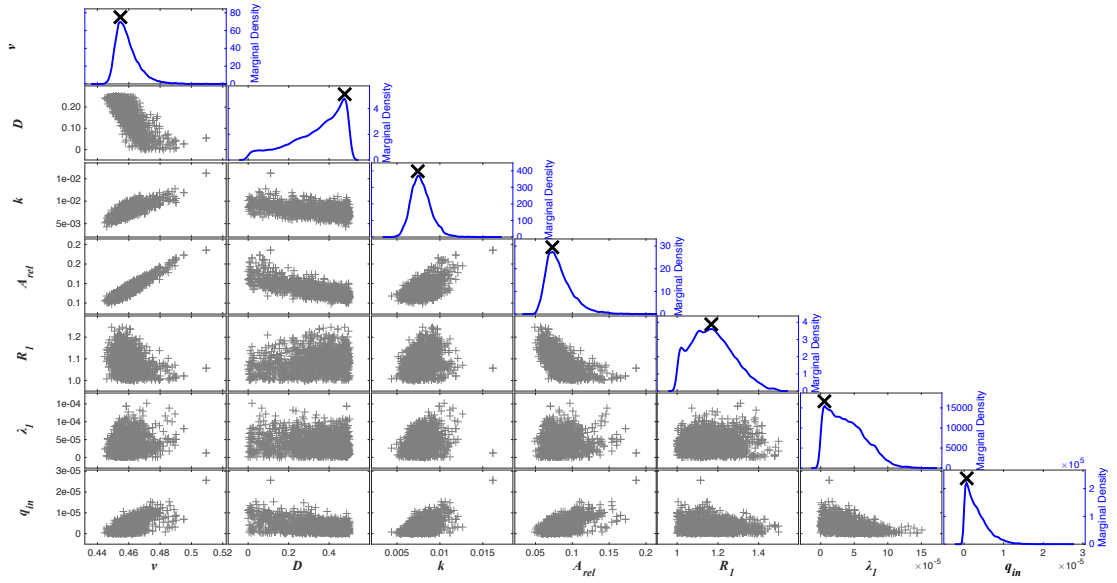

Marginal distribution and two-dimensional correlation plots of posterior parameter samples from the bromide/resazurin joint fit for the 2016 3rd order stream reach.

Appendix 4.14: Density plots for the 2016 4th order stream

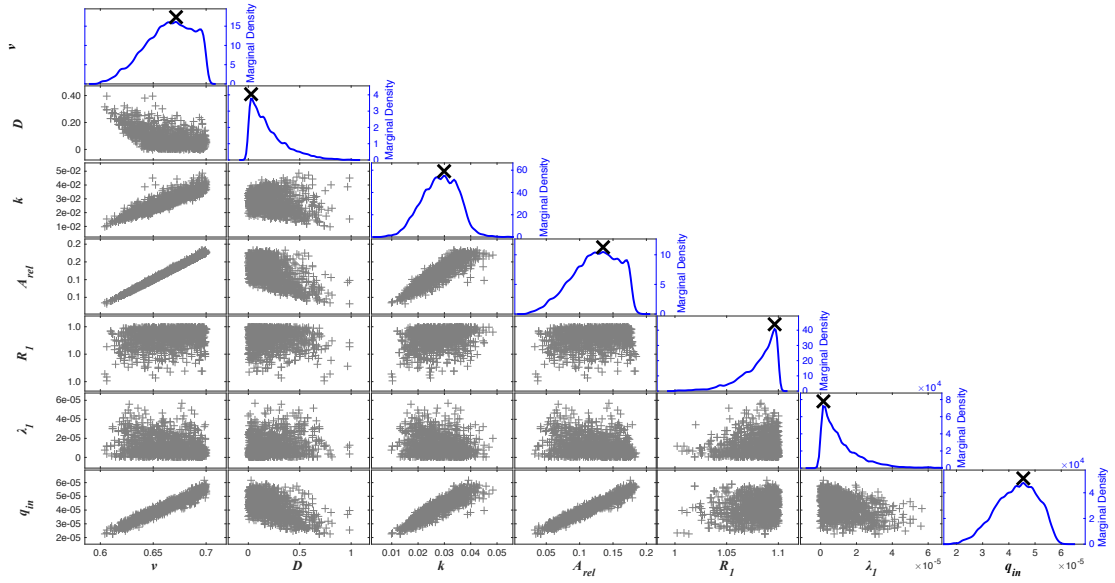

Marginal distribution and two-dimensional correlation plots of posterior parameter samples from the bromide/resazurin joint fit for the 2016 4th order stream reach.

Appendix 4.15: 2015 3rd order stream sensitivity analysis for velocity

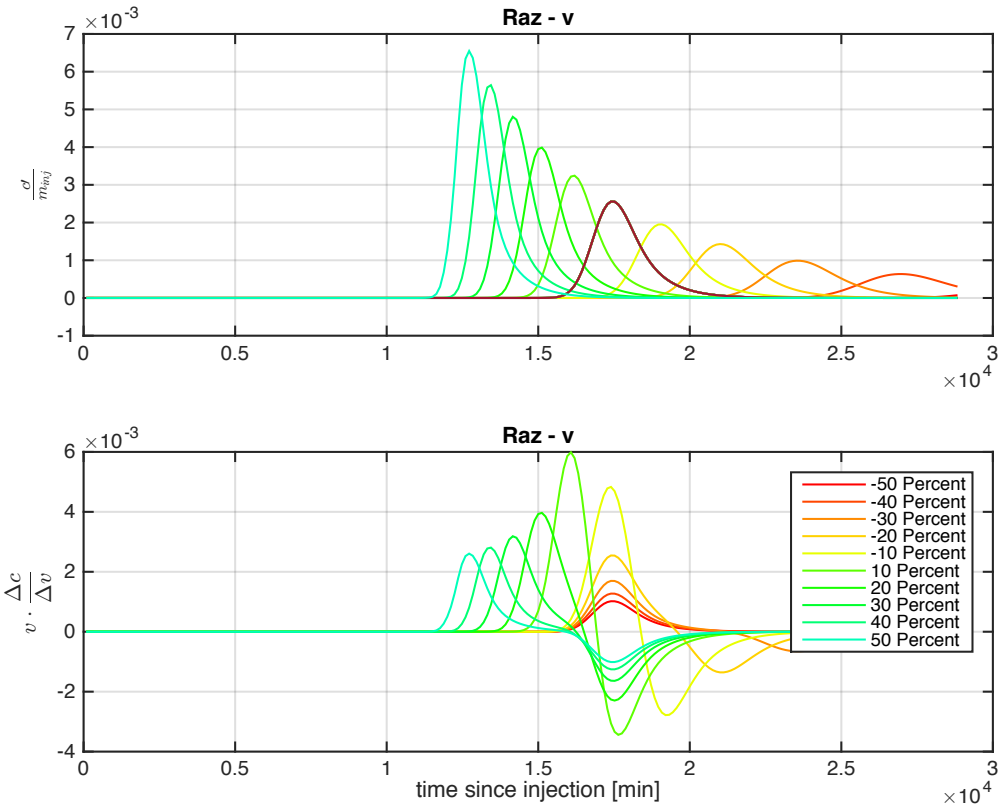

Example sensitivity analysis for advective velocity from the 2015 3rd order stream reach. Each curve represents +/- 10 – 50% change in the parameter of interest of the resazurin breakthrough curve.

Appendix 4.16: 2015 3rd order stream sensitivity analysis for dispersion

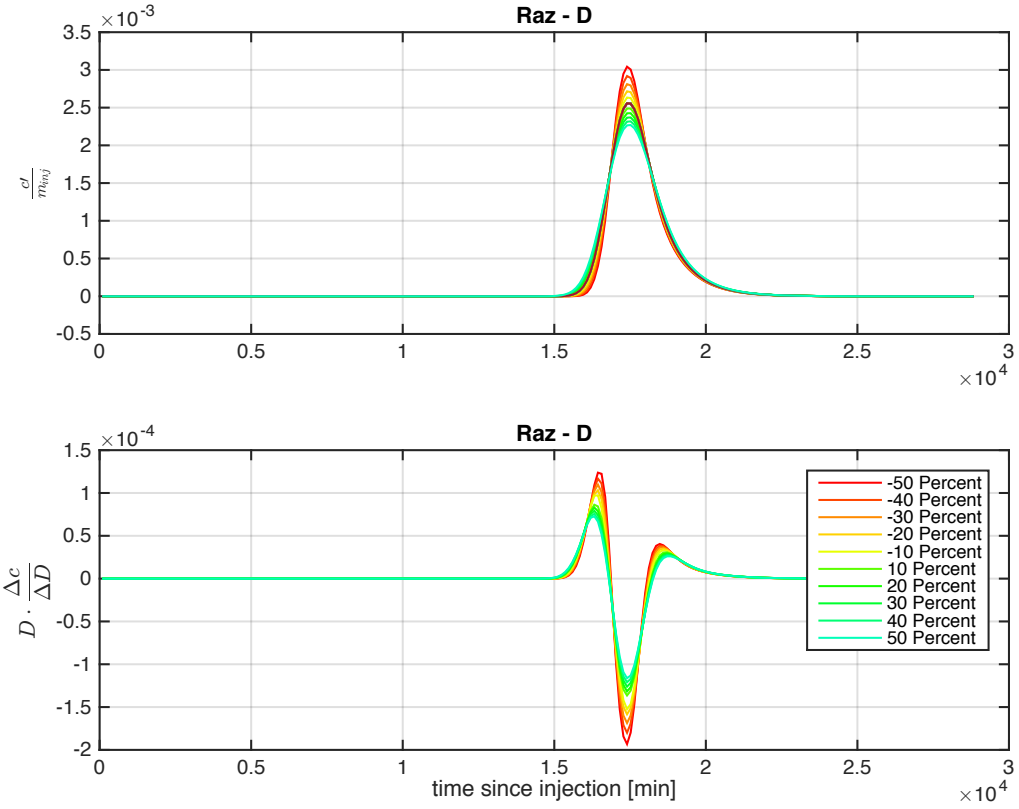

Example sensitivity analysis for the dispersion coefficient from the 2015 3rd order stream reach. Each curve represents +/- 10 – 50% change in the parameter of interest of the resazurin breakthrough curve.

Appendix 4.17: 2015 3rd order stream sensitivity analysis for the mass transfer rate

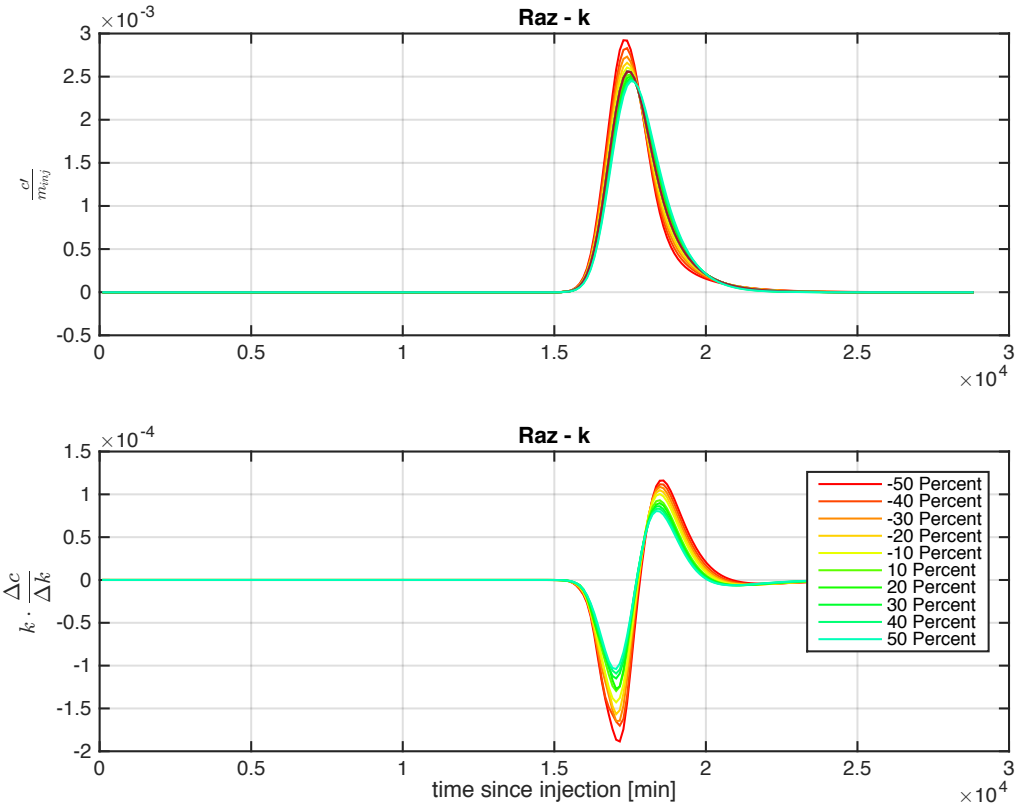

Example sensitivity analysis for the first-order mass transfer rate coefficient from the 2015 3rd order stream reach. Each curve represents +/- 10 – 50% change in the parameter of interest of the resazurin breakthrough curve.

Appendix 4.18: 2015 3rd order stream sensitivity analysis for the size of the storage zone

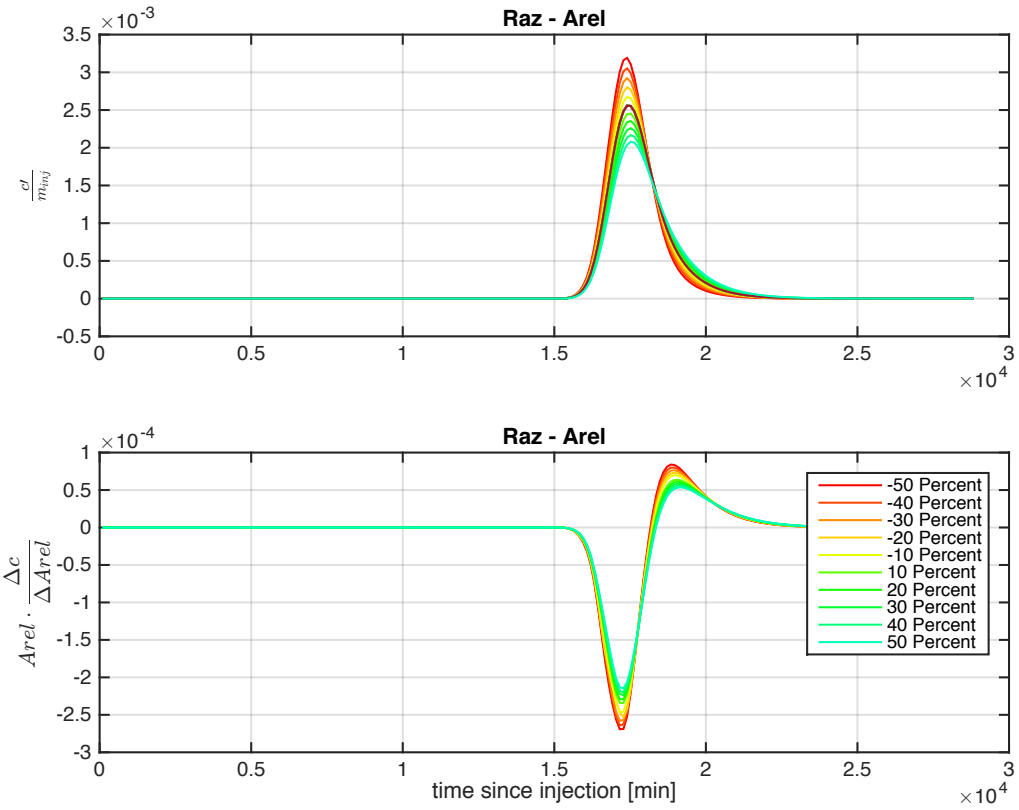

Example sensitivity analysis for the relative size of the storage zone from the 2015 3rd order stream reach. Each curve represents +/- 10 – 50% change in the parameter of interest of the resazurin breakthrough curve.

Appendix 4.19: 2015 3rd order stream sensitivity analysis for the Raz retardation factor

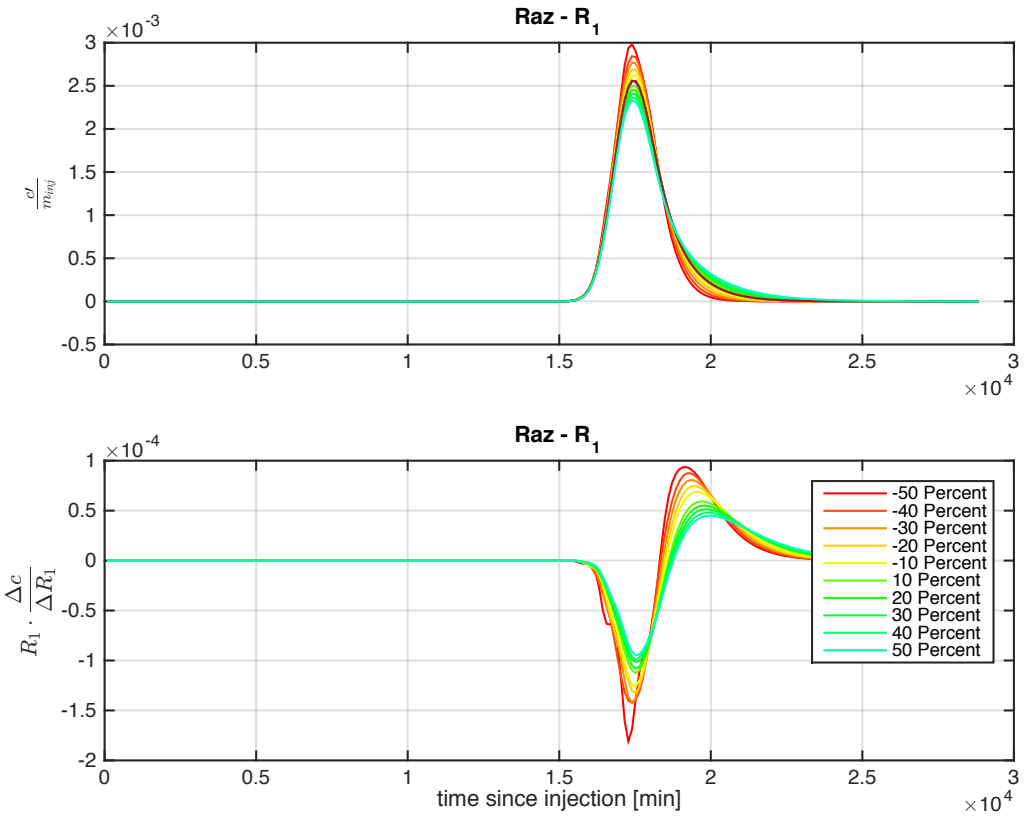

Example sensitivity analysis for the resazurin retardation factor from the 2015 3rd order stream reach. Each curve represents +/- 10 – 50% change in the parameter of interest of the resazurin breakthrough curve.

Appendix 4.20: 2015 3rd order stream sensitivity analysis for the Raz transformation

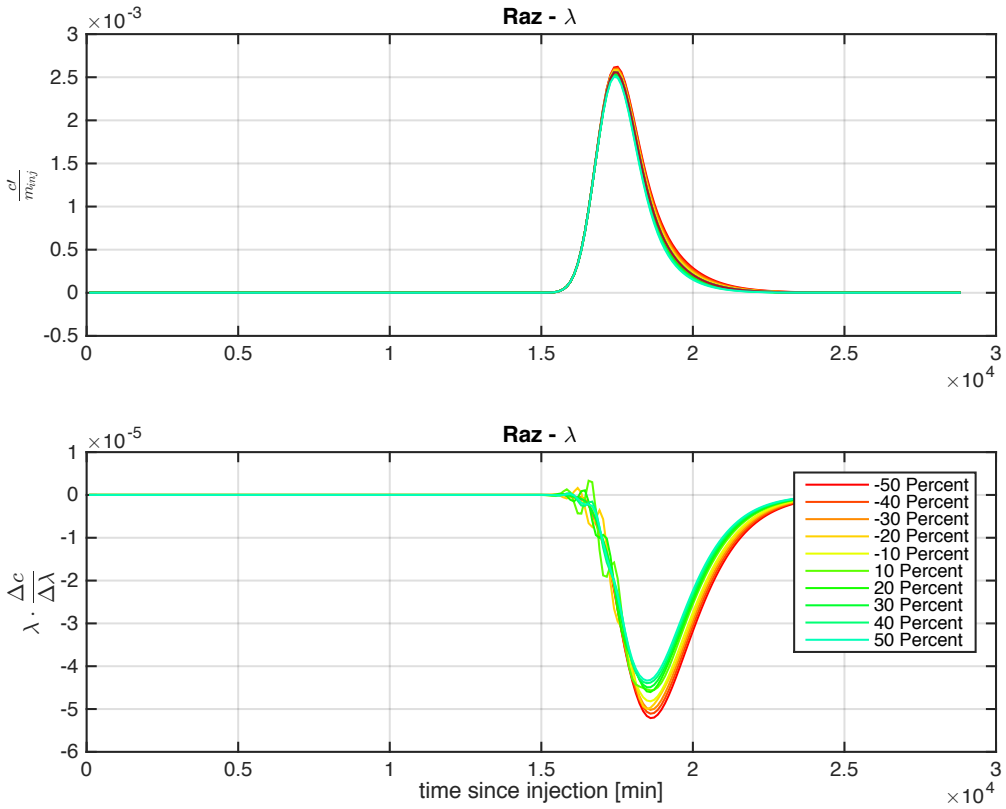

Example sensitivity analysis for the resazurin total transformation coefficient from the 2015 3rd order stream reach. Each curve represents +/- 10 – 50% change in the parameter of interest of the resazurin breakthrough curve.

Appendix 4.21: 2015 3rd order stream sensitivity analysis for groundwater dilution

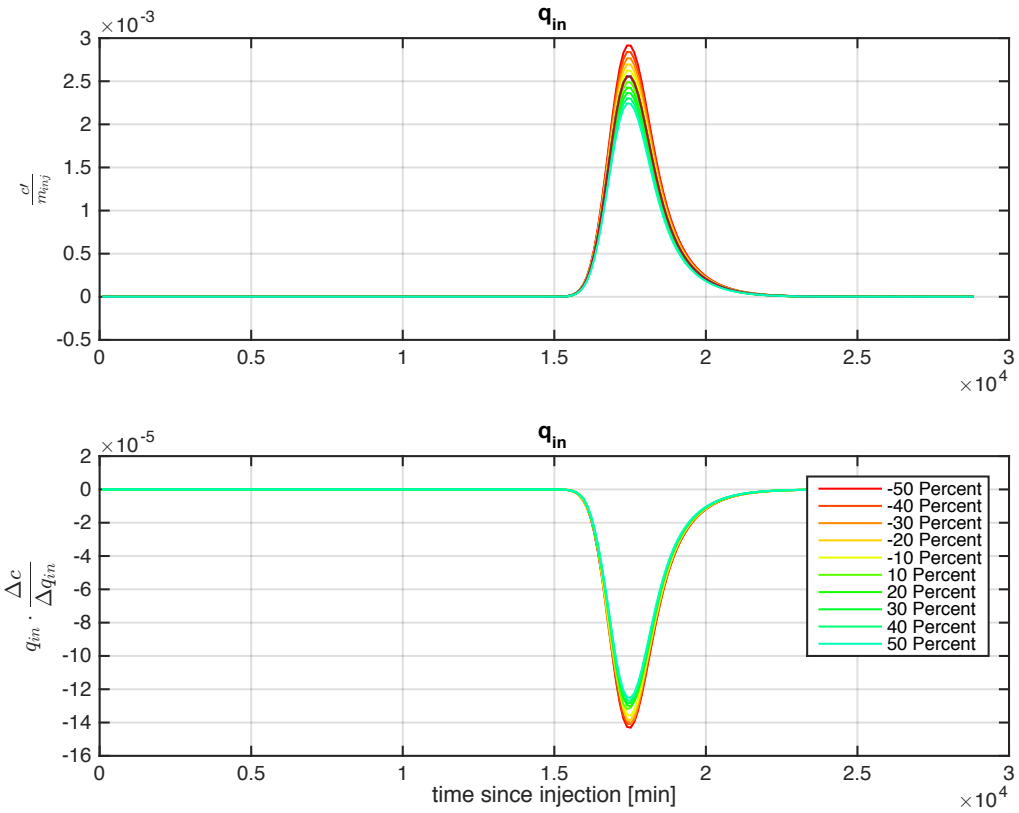

Example sensitivity analysis for the groundwater dilution rate coefficient from the 2015 3rd order stream reach. Each curve represents +/- 10 – 50% change in the parameter of interest of the resazurin breakthrough curve.

Appendix 4.22: Model parameters

Calibrated parameters (± 1 σ) and goodness of fit metrics for the 2015 and 2016 sampling campaigns. Normalized residual sum of squares for bromide, $nRSS_{br}$ (-), resazurin, $nRSS_{raz}$ (-), and resorufin, $nRSS_{rru}$ (-) represent the sum of squared residuals normalized by the squared theoretical peak tracer concentrations. In 2016, reactive tracer tests with resazurin were not performed in the 5th order stream. The 1st stream results from 2016 were not analyzed due to a poor conservative tracer fit.

2015 Model Fit:	Description	Stream Order 1	2	3	4	5
v [m/s]	Advective velocity	1.1e-1 ± 5.9e-4	8.3e-2 ± 4.2e-4	1.9e-1 ± 8.7e-5	3.2e-1 ± 5.8e-4	1.9e-1 ± 5.2e-3
D [m^2/s]	Dispersion coefficient	4.1e-1 ± 1.1e-2	1.2e-1 ± 4.2e-3	3.5e-1 ± 3.4e-3	5.5e-1 ± 1.7e-2	5.4e-3 ± 5.0e-3
k [1/s]	First-order mass transfer rate coefficient	5.6e-1 ± 1.7e-4	2.1e-3 ± 6.5e-4	1.9e-3 ± 5.1e-5	2.2e-3 ± 2.7e-4	2.6e-1 ± 1.4e-2
A_s/A [-]	Relative size of the storage zone	8.8e-2 ± 2.9e-3	2.9e-2 ± 4.0e-3	3.4e-2 ± 1.6e-3	1.8e-2 ± 1.5e-3	1.1e-1 ± 2.2e-2
R_1 [-]	Resazurin retardation factor	1.94 ± 3.7e-2	2.70 ± 9.3e-2	1.51 ± 5.7e-2	1.03 ± 5.8e-2	1.03 ± 2.2e-2
λ_1 [1/s]	Resazurin total transformation coefficient	2.2e-3 ± 4.0e-5	7.5e-4 ± 7.2e-5	4.5e-4 ± 3.0e-5	2.0e-5 ± 4.6e-5	6.8e-5 ± 7.5e-6
q_{in} [1/s]	Groundwater dilution rate coefficient	1.9e-4 ± 5.7e-6	4.3e-5 ± 2.5e-6	1.9e-5 ± 9.3e-7	3.8e-5 ± 8.9e-7	5.9e-5 ± 7.0e-6
R_2 [-]	Resorufin retardation coefficient	1.45 ± 2.7e-2	1.90 ± 5.2e-2	1.06 ± 3.4e-3	1.02 ± 1.8e-3	1.06 ± 7.6e-3
λ_{12} [1/s]	Resazurin to resorufin transformation coefficient	6.8e-4 ± 2.3e-5	7.5e-4 ± 9.3e-6	3.8e-4 ± 7.1e-6	1.8e-5 ± 1.0e-6	1.9e-5 ± 2.8e-6
λ_2 [1/s]	Resorufin transformation coefficient	8.0e-6 ± 2.1e-6	1.2e-4 ± 4.4e-5	4.4e-4 ± 2.5e-5	1.6e-4 ± 9.9e-5	4.0e-4 ± 2.2e-5
$nRSS_{br}$	Normalized RSS for bromide	0.252	0.337	0.016	0.258	0.129
$nRSS_{raz}$	Normalized RSS for resazurin	0.817	0.055	0.018	0.025	0.259
$nRSS_{rru}$	Normalized RSS for resorufin	1.544	2.097	3.034	3.329	0.253

2016 Model Fit:	Description	Stream Order 1	2	3	4	5
v [m/s]	Advective velocity	n.d.	2.5e-1 ± 3.0e-3	4.5e-1 ± 3.7e-3	6.7e-1 ± 4.1e-3	n.d.
D [m^2/s]	Dispersion coefficient		2.1e-1 ± 3.1e-2	4.8e-1 ± 2.8e-2	2.5e-2 ± 5.8e-2	
k [1/s]	First-order mass transfer rate coefficient		1.9e-2 ± 2.3e-2	7.4e-3 ± 4.9e-4	3.0e-2 ± 1.6e-3	
A_s/A [-]	Relative size of the storage zone		8.7e-2 ± 1.4.e-2	7.3e-2 ± 8.8e-3	1.3e-1 ± 6.4e-3	
R_1 [-]	Resazurin retardation factor		1.24 ± 3.8e-2	1.17 ± 1.9e-2	1.10 ± 5.7e-3	
λ_1 [1/s]	Resazurin total transformation coefficient		5.7e-6 ± 1.3e-5	5.9e-6 ± 9.1e-6	1.4e-6 ± 5.8e-6	
q_{in} [1/s]	Groundwater dilution rate coefficient		2.7e-6 ± 6.1e-6	6.6e-7 ± 1.5e-6	4.6e-5 ± 1.6e-6	
R_2 [-]	Resorufin retardation coefficient		1.07 ± 5.4e-2	1.02 ± 1.0e-2	1.03 ± 1.2e-1	
λ_{12} [1/s]	Resazurin to resorufin transformation coefficient		5.3e-6 ± 3.1e-7	4.9e-6 ± 2.5e-7	1.3e-6 ± 7.6e-8	
λ_2 [1/s]	Resorufin transformation coefficient		2.6e-6 ± 7.6e-5	7.5e-6 ± 4.2e-7	1.3e-5 ± 5.8e-5	
$nRSS_{br}$	Normalized RSS for bromide		0.975	0.052	2.199	
$nRSS_{raz}$	Normalized RSS for resazurin		0.018	0.039	0.021	
$nRSS_{rru}$	Normalized RSS for resorufin		2.309	1.815	2.828	

Appendix 4.23: Study comparison metrics

Mean hyporheic exchange, q_{he}, normalized by velocity, v, from this study and predicted hyporheic exchange flow normalized by discharge, Q_{HEF}/Q, from Wondzell (2011) Table 1.

Study	Stream Order	Flow Condition	Discharge (m^3/s)	Normalized Discharge (1/m)
This Study	1st	Baseflow	0.01	4.5e-1
Kasahara and Wondzell (2003); Wondzell (2006)	1st	Low, baseflow	0.02	1.9e-2
Kasahara and Wondzell (2003); Wondzell (2006)	1st	High, baseflow	0.09	4.8e-3
Kasahara and Wondzell (2003); Wondzell (2006)	1st	Low, baseflow	0.16	1.3e-2
Kasahara and Wondzell (2003); Wondzell (2006)	1st	High, baseflow	0.18	3.7e-3
This Study	2nd	Baseflow	0.11	7.4e-4
This Study	2nd	Receding snowmelt	0.50	6.8e-3
This Study	3rd	Baseflow	0.79	3.4e-4
This Study	3rd	Receding snowmelt	1.22	1.2e-3
This Study	4th	Baseflow	4.67	1.3e-4
This Study	4th	Receding snowmelt	3.23	5.9e-3
Wondzell and Swanson (1996)	4th	Low, baseflow	11.46	1.1e-4
Wondzell and Swanson (1996)	4th	High, baseflow	117	3.0e-5
Wondzell and Swanson (1996)	4th	Stormflow	590	1.0e-5
This Study	5th	Baseflow	2400	1.5e-1
Kasahara and Wondzell (2003)	5th	Baseflow	308	6.9e-4
Kasahara and Wondzell (2003)	5th	Baseflow	873	2.0e-5